Achieving High Stereoselectivity in Ruthenium-Catalyzed Olefin Metathesis Reactions for Organic and Polymer Synthesis

Thesis by

Tonia Sarah Ahmed

In Partial Fulfillment of the Requirements for the

Degree of

Doctor of Philosophy

Caltech

CALIFORNIA INSTITUTE OF TECHNOLOGY

Pasadena, California

2018

(Defended May 29, 2018)

Tonia Sarah Ahmed

ORCID: 0000-0001-9407-0250

For my mother, sisters,

and in memory of my father (February 13, 1954 – January 11, 2012)

Acknowledgments

The people in my life have put a remarkable amount of time and energy into this thesis. Without them, the work described herein would not have been possible. I really can't thank them enough, but I'll try my best in the next few pages.

I would first like to thank my advisor, Bob Grubbs. Bob has been a truly exceptional advisor throughout my graduate studies. He has promoted my development as an independent researcher by letting me pursue my own project ideas. This allowed me to both succeed and fail, and Bob was always there to provide advice during times of failure. I will forever be grateful for his guidance and for the experiences I have had in his lab. I would like to thank him for his unwavering support, which I know will continue in the future.

Next I would like to thank the members of my thesis committee, Theo Agapie, Harry Gray, Sarah Reisman, and Dave Tirrell, for all of the advice they have given me throughout my studies. Aside from our yearly meetings, they have always made time to meet with me whenever I needed perspective, regardless of their remarkably busy schedules. I hope to continue to learn and gain advice from them even after I leave Caltech.

My time at Caltech actually began before the start of my graduate studies. I had the opportunity to work in John Bercaw's lab as a Summer Undergraduate Research Fellow (SURF) in 2011 and 2012. I honestly can't thank John enough for his support and guidance throughout my undergraduate and graduate studies. Even when I was an undergraduate student, he made sure that I felt comfortable enough to consult him for any guidance. Thank you so much for following my career and always providing me with the

opportunity to gain wisdom from you. In the Bercaw lab, I had the pleasure of working with two great co-mentors, Ian Tonks and Rachel Klet. I want to thank both of them (and the remainder of the group) for their guidance and for molding me into the scientist that I am. Also thanks to Pat Anderson for always being awesome. I would furthermore like to extend a special thanks to Caltech undergraduates I became close friends with during my SURF: Prastuti Singh, Max Horton, Samantha Piszkiewicz, Sevan Shanakian, Misha Raffiee, and Brooklyn Schlamp.

Next I would also like to thank the members of the Grubbs group. I have been quite fortunate to work with many great people. I would like to extend a special thank you to Linda Syme, who has always kept the lab together (and me together) and has been a great person to chat with. I would like to thank Brendan Quigley, Melanie Pribisko Yen, and Myles Herbert for helping me through my first year (and of course, subsequent years) and keeping me sane. I am very grateful for your continuing friendships even after you have moved on to other jobs. My past and present office mates of 219 Church (the best office) have all become very close friends of mine. I don't even know how to accurately describe Chris Bates, but he was (and continues to be) a great source of laughter. Because he was a health nut, I was often regifted chocolate and other sweets that were given to him, so I should thank him for that as well. Noah Fine Nathel and I share a love for eating chips, sending each other ridiculous news stories, and looking at pictures of Sonic. I'm very much looking forward to hanging out with him again in Boston. Willie Wolf and I are like two peas in a pod ("if one pea really hates the other pea," he clarifies). We like giving each other a hard time, and I have thoroughly enjoyed our (best) friendship since he joined the lab, even if he tells "long rib" jokes. June has

Miyake, Bill Morandi, Victoria Piunova, Shunsuke Sato, Jacob Sertich, Benjamin Sveinbjörnsson, Michael Schulz, Anton Toutov, Robert Tuba, Ray Weitekamp, Zach Wickens, and Daniel Ziegler. I would like to also thank Materia, Inc. for the great people I've had the opportunity to work with (Adam Johns, Dick Pederson, John Phillips, Daryl Allen) and for the supplies of catalyst that they generously give us.

Next I would like to thank all of my other close friends at Caltech. First and foremost, Rebekah Silva has been a remarkable friend/roommate. In particular, I would like to thank her for helping me down the stairs when I had vertigo, and for subsequently helping me when I threw up when we reached the bottom of the stairs and also on the way back from the doctor's office. I would also like to thank her for providing me with company and food on days when I was working late in lab. I really can't thank her enough in this space, so I hope she knows how much I "preeschiateher." Even though we will be friends for forever even at a distance, she better continue looking for postdoctoral positions in Boston in the future. I would also like to thank Jessica Sampson for her friendship. Jess and I have dinner together regularly, and with her I've had the opportunity to explore food options in the LA area. I truly appreciate our times commiserating together. Kelsey Boyle and I became close friends when we worked together on seemingly endless problem sets in our first year while listening to Beyoncé and Chingy and while eating Domino's Pizza, Du-Par's, or Which Wich. Thanks for letting me hang out with your cat (the cutest cat, obviously) and for being on my team when picking movies even when Bekah doesn't agree. I would also like to thank my friends Samuel Ho, Stephanie Threatt, Matthew Chalkley, Marcus Low, Annet Blom, Denise Grünenfelder, Sarah Del Ciello, Bryce Jarman, Daniel Torelli, Heui-Beom Lee,

Joe Ahn, Trixia Buscugan, Jeremy Tran, Blake Daniels, and Catie Blunt. I also would like to thank the Agapie and Barton groups for being my "labs away from lab."

Next I would like to thank David VanderVelde for always being excited to help me with my NMR studies. I wouldn't have been able to fully characterize all the compounds I've made without the help of Naseem Torian and Mona Shahgholi in the mass spectrometry laboratory. Larry Henling and Mike Takase in the X-ray facility have been super helpful each time I grew crystals for diffraction. I would like to also thank Rick Gerhart and Brian Markowicz for being excellent glassblowers and great people to chat with. Furthermore, I would like to thank Agnes Tong, Alison Ross, Joe Drew, and Steve Gould for keeping everything running smoothly.

Of course, this work would not have been possible without support from home. I want to thank all of my friends and my team at West Virginia University for continuing to support me throughout my graduate studies. In particular, I would like to thank my friends, Madeline Vandevender, Nathan Tauger, and Billy Hardy, who came out to visit me during my time in Pasadena. Madeline is my best friend and is always there when I need her. I know that I will continue to receive her support throughout the entirety of my life. I would like to thank Nathan and Billy for always having my back through the tough times. My professors at WVU have continued to be supportive of me throughout my graduate studies. In particular, Jeffrey Petersen, Michael Shi, and George O'Doherty have made me the scientist that I am today.

Last, but not least, I would like to thank my family for all of their love and support. My parents were both chemists, and provided me with a passion for the sciences while I was growing up. My father was the strongest man I knew, and he equipped me

Abstract

Transition metal-catalyzed olefin metathesis has emerged as a powerful tool for constructing C−C double bonds. This thesis delineates the development of Ru-based catalysts for the stereoselective formation of olefins and mechanistic studies used to examine how catalyst structure influences selectivity and activity.

Chapter 2 details the synthesis of *Z*-selective, cyclometalated catalysts bearing nitrite X-ligands. The activity and selectivity of these catalysts were examined in an array of ring-opening metathesis polymerization and cross metathesis reactions. Comparison of these catalysts with their nitrate-bound analogues is described.

Chapter 3 describes the examination of several *Z*-selective, cyclometalated catalysts in ring-opening metathesis polymerizations. The polymerizations of a variety of norbornene and norbornene derivatives were examined to determine the tacticity and microstructure of the resulting polymer. Computational studies were used to examine the mechanism of the polymerization reactions.

Chapter 4 examines the decomposition of Fischer carbene complexes derived from cyclometalated catalysts. In-depth NMR studies are used to determine the identity of the decomposition product, and the decomposition pathway is examined through computational studies.

Chapter 5 describes the first example of highly *E*-selective cross metathesis through kinetic control using stereoretentive, Ru-based catalysts bearing dithiolate catalysts. The preparation of additional stereoretentive catalysts is described for increasing catalyst activity while maintaining or increasing selectivity. A model for the observed stereoselectivity is proposed.

Chapter 6 delineates the preparation of a series of fast initiating, stereoretentive catalysts. These catalysts are assessed in an array of cross metathesis reactions, and significantly enhanced activity is observed in *E*-selective reactions. The examination of the relationships between the structure of a catalyst and its selectivity and activity is described.

Chapter 7 examines the use of stereoretentive catalysts in the synthesis of *Z*-macrocycles from diene starting materials bearing a *Z*-olefin and a terminal olefin. Initiation rate studies are conducted to examine the activity of these catalysts compared to previously reported cyclometallated catalysts used in this ring-closing metathesis reaction. The synthesis of twelve- to seventeen-membered rings with high *Z*-selectivity is described.

Chapter 8 explores the use of fast-initiating, stereoretentive catalysts for synthesizing *E*-macrocycles. The preparation of diene starting materials containing two *E*-olefins is described. Using these catalysts, twelve- to eighteen-membered rings are constructed with high *E*-selectivity.

Published Content and Contributions

Pribisko, M. A.; Ahmed, T. S; Grubbs, R. H. "Z-Selective Ruthenium Metathesis Catalysts: Comparison of Nitrate and Nitrite X-type Ligands." *Polyhedron* **2014**, *84*, 144–149.   doi:10.1016/j.poly.2014.06.055
T.S.A. helped synthesize catalysts, perform cross metathesis and ring-opening metathesis polymerization reactions, prepare data, and write the manuscript.

Rosebrugh. L. E.; Ahmed, T. S.; Marx, V. M.; Hartung, J.; Liu, P.; López, J. G.; Liu, P.; Houk, K. N.; Grubbs, R. H. "Probing Stereoselectivity in Ring-Opening Metathesis Polymerization Mediated by Cyclometalated Ruthenium-Based Catalysts: A Combined Experimental and Computational Study." *J. Am. Chem. Soc.* **2016***, 138,* 1394–1405. doi: 10.1021/jacs.5b12277
T.S.A. synthesized catalysts to be tested, performed almost all ring-opening metathesis polymerization reactions, and assisted in editing the manuscript.

Ahmed, T. S.; Grandner, J. M.; Taylor, B. L. H.; Herbert, M. B.; Houk, K. N.; Grubbs, R. H. "Metathesis and Decomposition of Fischer Carbenes of Cyclometalated *Z*-Selective Ruthenium Metathesis Catalysts" Submitted.

Johns, A. M.; Ahmed, T. S; Jackson, B. W.; Grubbs, R. H.; Pederson, R. L. "High *Trans* Kinetic Selectivity in Ruthenium-Based Olefin Cross-Metathesis through Stereoretention." *Org. Lett.* **2016**, *18*, 772. doi: 10.1021/acs.orglett.6b00031
T.S.A. helped perform cross metathesis reactions and contributed to the writing of the manuscript.

Ahmed, T. S; Grubbs, R. H. "Fast-Initiating, Ruthenium-based Catalysts for Improved Activity in Highly *E*-Selective Cross Metathesis." *J. Am. Chem. Soc.* **2017**, *139*, 1532–1537. doi: 10.1021/jacs.6b11330
T.S.A. conceived of all ideas, performed all experimental work, and wrote the manuscript.

Ahmed, T. S; Grubbs, R. H. "A Highly Efficient Synthesis of *Z*-Macrocycles using Stereoretentive, Ruthenium-Based Metathesis Catalysts." *Angew. Chem. Int. Ed.* **2017**, *56*, 11213–11216. doi: 10.1002/anie.201704670.
T.S.A. conceived of all ideas, performed all experimental work, and wrote the manuscript.

Ahmed, T. S.; Montgomery, T. P.; Grubbs, R. H. "Using Stereoretention for the Synthesis of *E*-Macrocycles with Ruthenium-based Olefin Metathesis Catalysts." *Chem. Sci.* **2018**, *9*, 3580
doi: 10.1039/C8SC00435H
T.S.A. conceived of all ideas, performed the majority of the experimental work, and wrote the manuscript.

Table of Contents

Chapter 1

Introduction

Introduction

Olefin metathesis is a reaction that involves the breaking, redistribution, and recombination of carbon−carbon double bonds.[1] This transformation has become an increasingly powerful method for the construction of C−C double bonds in the synthesis of desirable products. It has thus seen applications in an array of fields including materials science,[2] organic synthesis,[3] pharmaceuticals,[4] biochemistry,[5] and green chemistry.[6] Further development of new olefin metathesis catalysts will continue to expand the employment of this transformation in a number of research areas.

Olefin metathesis was first discovered serendipitously during studies of Ziegler-Natta polymerization catalysts conducted by DuPont in the 1950s.[7] Using the heterogeneous mixture $TiCl_4/Li[Al(n\text{-}C_7H_{15})_4]$ as an ill-defined catalyst, the polymerization of norbornene to polynorbornene was observed (Scheme 1.1a). The disproportionation of propylene to ethylene and 2-butene catalyzed by $W(CO)_6$, $Mo(CO)_6$, and MoO_3 on alumina was then observed in 1964 by Phillips Petroleum Company.[8] In 1967, the Goodyear Tire and Rubber Company examined the reaction of 2-pentene with $WCl_6/EtAlCl_2/EtOH$ to produce 2-butene and 3-hexene, and coined the term "olefin metathesis" to describe this transformation (Scheme 1.1b).[9]
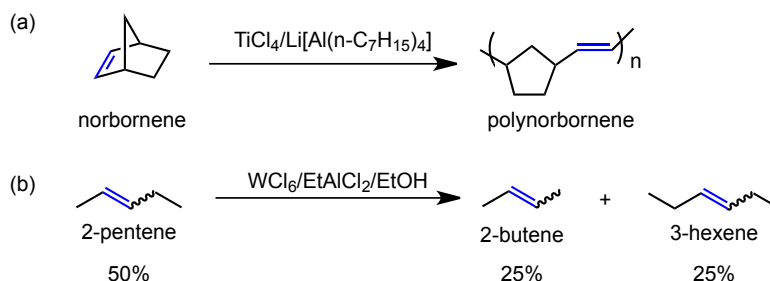
Scheme 1.1. (a) Polymerization of norbornene to polynorbornene observed by DuPont with $TiCl_4/Li[Al(n\text{-}C_7H_{15})_4]$ and (b) olefin metathesis of 2-pentene to give 2-butene and 3-hexene observed by the Goodyear Tire and Rubber Company with $WCl_6/EtAlCl_2/EtOH$.

In 1971, Yves Chauvin proposed the now widely accepted mechanism of olefin metathesis (Scheme 1.2).[10] He posited that the identity of the catalyst is a metal alkylidene, which reacts with an olefin in a [2+2] cycloaddition to give a metallacyclobutane intermediate. Subsequent cycloreversion gives a new alkylidene catalyst and an olefin product. Identification of the proposed metal alkylidene as the catalyst of this reaction allowed for the development of well-defined, homogeneous olefin metathesis catalysts.[11] Over the last few decades, early and late transitional metal-based alkylidenes have been synthesized for catalyzing olefin metathesis reactions (Figure 1.1).[12-15]
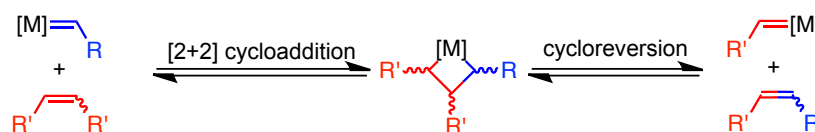
Scheme 1.2. Proposed Chauvin mechanism of olefin metathesis.
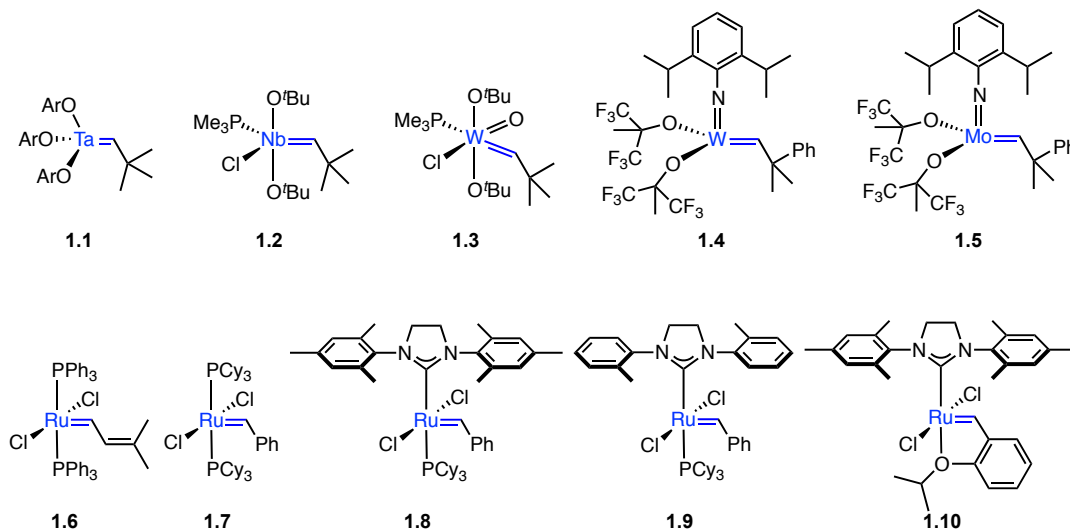
Figure 1.1. Early and late transition metal-based olefin metathesis catalysts.

Olefin metathesis can be categorized into a number of classes of transformations (Scheme 1.3). Cross metathesis, ring-opening cross metathesis, and ring-closing metathesis have been implemented in the generation of important molecules in organic

synthesis. Ring-opening metathesis polymerization and acyclic diene metathesis polymerization have been used for producing polymers with desired properties. Each of these reactions is thermodynamically controlled; cross metathesis, ring-closing metathesis, and acyclic diene metathesis polymerization reactions can be driven by the loss of gaseous byproducts, whereas ring-opening metathesis polymerization and ring-opening cross metathesis are driven by the ring strain of the starting materials.
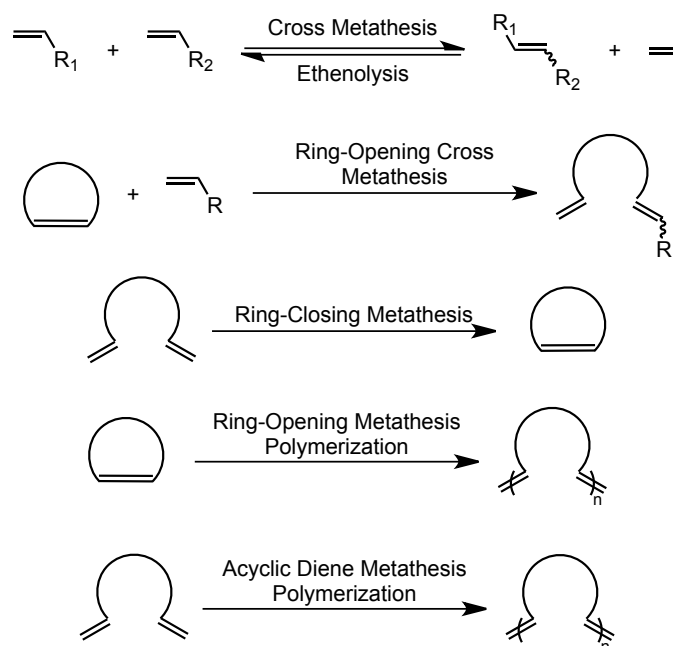
Scheme 1.3. Examples of common olefin metathesis reactions.

Catalyst Development

The work conducted in our group focuses on the development and use of well-defined, Ru-based olefin metathesis catalysts. In general, these catalysts have a wide functional group tolerance and are less sensitive to air and water than their early transition metal-based counterparts. During the last few decades, these catalysts have been tuned to attain higher activity, stability, and selectivity and to achieve wider reaction scopes. The first Ru-based catalysts contained PPh$_3$ ligands (**1.6**) and were used in ring-opening metathesis polymerizations. Exchange of these ligands with PCy$_3$ ligands (**1.7**)

4

and the subsequent replacement of one of these ligands with an *N*-heterocyclic carbene (NHC) ligand (**1.8**) showed significant improvements in catalyst activity. Implementing an *N*-*o*-tolyl group in place of the *N*-2,4,6-trimethylphenyl group of the NHC (**1.9**) allowed for the cross metathesis of hindered olefins. Replacement of the phosphine ligand with an isopropoxybenzylidene ligand to give **1.10** increased the stability of these catalysts under reaction conditions.

Stereoselectivity in Cross Metathesis

The properties of a molecule containing a disubstituted olefin can be dictated by the stereochemistry, *E* (*trans*) or *Z* (*cis*), of the C−C double bond. It is often difficult to separate *E* and *Z* isomers, and techniques used for their separation are not general. As such, it is important to develop catalysts that generate products with high stereoselectivity. The thermodynamically favored isomer is generally the *E*-product. First-generation, phosphine-based catalysts, such as **1.7**, often deliver cross metathesis products with ~4−5:1 *E*:*Z*-selectivity. NHC-based complexes **1.8** and **1.10** give products initially with 2:1 *E*:*Z*-selectivity. However, as conversion increases, secondary metathesis processes increase the amount of *E*-isomer in product mixtures to afford *E*:*Z* ratios of 11:1.

In 2009, Schrock and coworkers reported the first highly *Z*-selective catalysts **1.11** (>95% *Z*) based on Mo and W (Figure 1.2).[16] The Grubbs group then reported *Z*-selective (>95% *Z*), cyclometallated Ru-based catalyst **1.12** in 2011.[17] In 2013, the Jensen lab reported catalyst **1.13**, which generated products in up to 96% *Z*-selectivity.[18] In cross metathesis, each of these catalysts was capable of crossing terminal olefins to give the disubstituted *Z*-products. In 2015, Hoveyda and coworkers reported Ru-based catalyst

1.14, which was able to generate *Z*-products (up to 98% *Z*) from the cross metathesis of two *Z*-olefins or between a *Z*-olefin and a terminal olefin.[19] The surrounding ligand environment of all of these catalysts was manipulated so that generation of the *syn* metallacyclobutane was favored over the *anti* pathway (Figure 1.2). Cycloreversion of this *syn* intermediate gives the *Z*-product.
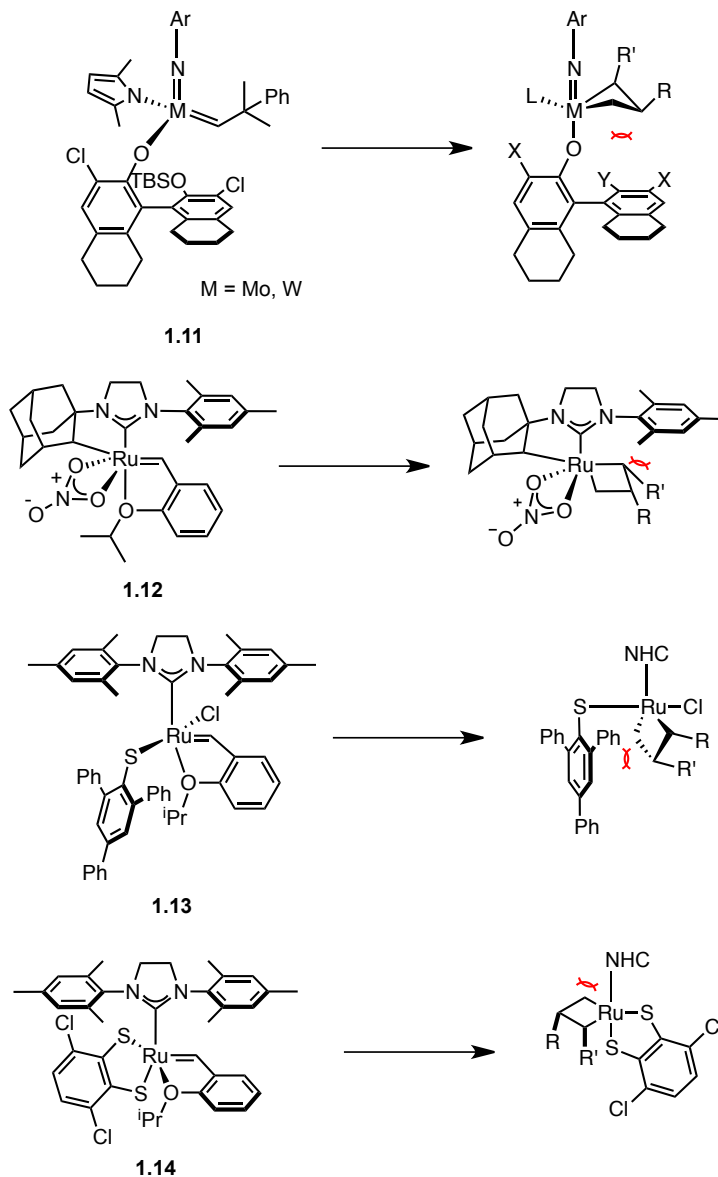
Figure 1.2. *Z*-Selective olefin metathesis catalysts.

In 2016, it was reported that **1.14** was also capable of performing highly *E*-selective cross metathesis (>98% *E*) from *E*-olefin starting materials.[20] This was the first report of kinetically controlled, highly *E*-selective metathesis. This has led to the further development of catalysts that are capable of performing this transformation with higher activity[21] and selectivity.[20,22] Furthermore, demonstration of the utility of these catalysts in the synthesis of useful molecules has been recently reported.[23,24]

Future Outlook

Over the last few decades, great strides have been made in the field of olefin metathesis, and catalysts have been tailored for employment in a large number of applications. However, there will always be a demand for the development of catalysts for specific research areas.

In particular, recent studies in our lab and by Hoveyda and coworkers have focused on the development of the first examples of high kinetic *E*-selectivity in cross metathesis. While this was a significant breakthrough in the field of metathesis, these catalysts readily decompose in the presence of terminal olefins.[20-22,24] Thus, studies of the decomposition pathways of these catalysts is necessary to develop *E*-selective catalysts that are capable of crossing terminal olefins to generate *E*-products with high selectivity. This will increase the utility of these catalysts in *E*-selective transformations.

In general, specific questions about the identity and the characteristics of intermediates in olefin metathesis remain to be answered for particular systems where catalyst decomposition is common, such as in the ring-opening metathesis polymerization reactions in the synthesis of functionalized materials. The synthesis of catalysts for these specific purposes will require a deeper understanding of the catalytic process, catalyst

decomposition routes, and the properties of the active catalyst under these reaction conditions. This knowledge could be used to expand the utilization of these catalysts in the various common metathesis reactions shown in Scheme 1.3.

Conclusions

Olefin metathesis has increasingly become a ubiquitous technique for generating C−C double bonds and has enjoyed wide employment in an array of fields. During the last several decades, significant progress has been made in the development of catalysts for this reaction. However, there still continues to be a need for new catalysts with greater selectivity, activity, and stability than those already developed. This will further expand the utility of olefin metathesis to an increasing number of applications.

References

1. Grubbs, R. H. Handbook of Metathesis, Wiley-VCH, Weinheim, 2003.

2. (a) Slugovc C. *Macromol. Rapid Commun*. **2004**, *25*, 1283. (b) Buchmeiser, M. R. *Chemical Reviews* **2000**, *100*, 1565.

3. Grubbs, R. H., O'Leary, D. J.; *Handbook of Metathesis, Vol. 2*: *Applications in Organic Synthesis*, 2nd ed.; Wiley- VCH: Weinheim, Germany, 2015.

4. Cossy, J.; Arseniyadis, S.; Meyer, C. *Metathesis in Natural Product Synthesis: Strategies, Substrates and Catalysts*.; Wiley-VCH: Weinheim, Germany, 2011.

5. Binder, J. B.; Raines, R. T. *Curr. Opin. Chem. Biol.* **2008**, *12*, 767.

6. Schrodi, Y.; Ung, T.; Vargas, A.; Mkrtumyan, G.; Lee, C. W.; Champagne, T. M.; Pederson, R. L.; Hong, S. H. *Clean: Soil, Air, Water*. **2008**, *36*, 669.

7. Truett, W. L.; Johnson, D. R.; Robinson, I. M.; Montague, B. A. *J. Am. Chem. Soc.* **1960**, *82*, 2337

8. Banks, R. L.; Bailey, G. C. *Ind. Eng. Chem. Prod. Res. Dev.* **1964**, *3*, 170.

9. Calderon, N; Chen, Hung Yu; Scott, Kenneth W. *Tetrahedron Lett.* **1967**, *8*, 3327.

10. Herisson, J.-L.; Chauvin, Y. *Makromol. Chem.* **1971**, *141*, 161.

11. Early Transition Metal-Based Catalysts: (a) Schrock, R. R. *J. Am. Chem. Soc.* **1974**, *96*, 6796. (b) Schrock, R. R.; Rocklage, S.; Wengrovious J.; Rupprecht, G.; Fellman, J. *J. Mol. Cat.* **1980**, *8*, 73. (c) Schrock, R. R.; DePue, R. T. Feldman, J.; Schaverien, C. J.; Dewan, J. C.; Liu, A. H. *J. Am. Chem. Soc.* **1988**, *110*, 1423. (d) Schrock, R. R.; Murdzek, J. S.; Bazan, G. C.; Robbins, J.; DiMare, M.; O'Regan, M. *J. Am. Chem. Soc.* **1990**, *112*, 3875. (e) Bazan, G. C.; Oskam, J. H.; Cho, H.-N.; Park, L. Y.; *J. Am. Chem. Soc.* **1991**, *113*, 6899. Late Transition Metal-Based Catalysts: (a) Nguyen, S. T.; Johnson, L. K.; Grubbs, R. H. *J. Am. Chem. Soc.* **1992**, *114*, 3974. (b) Schwab, P.; France, M. B.; Ziller, J. W.; Grubbs, R. H. *Angew. Chem. Int. Ed.* **1995**, *34*, 2039. (c) Scholl, M.; Trnka, T. M.; Morgan, J. P.; Grubbs, R. H. *Tetrahedron Lett.* **1999**, *40*, 2247. (d) Scholl, M.; Ding, S.; Lee, C. W.; Grubbs, R. H. *Org. Lett.* **1999**, *1*, 953. (e) Garber, S. B.; Kingsbury, J. S.; Gray, B. L.; Hoveyda, A. H. *J. Am. Chem. Soc.* **2000**, *122*, 8168.

12. Trnka, T. M.; Grubbs, R. H. *Acc. Chem. Res.*, **2001**, *34*, 18.

13. Schrock, R. R.; Hoveyda, A. H. *Angew. Chem. Int. Ed.* **2003**, *42*, 4592.

14. Stewart, I. C.; Ung, T.; Pletnev, A. A.; Berlin, J. M.; Grubbs, R. H.; Schrodi, Y. *Org. Lett.* **2007**, *9*, 1589.

15. (a) Gessler, S.; Randl, S.; Blechert, S. *Tetrahedron Lett.* **2000**, *41*, 9973. (b) Garber, S. B.; Kingsbury, J. S.; Gray, B. L.; Hoveyda, A. H. *J. Am. Chem. Soc.* **2000**, *122*, 8168.

16. (a) Jiang, A. J.; Zhao, Y.; Schrock, R. R.; Hoveyda, A. H. *J. Am. Chem. Soc.* **2009**, *131*, 16630. (b) Marinescu, S. C.; Schrock, R. R.; Müller, P.; Takase, M. K.; Hoveyda, A. H. *Organometallics* **2011**, *30*, 1780. (c) Meek, S. J.; O'Brien, R. V.; Llaveria, J.; Schrock, R. R.; Hoveyda, A. H. *Nature* **2011**, *471*, 461. (d) Marinescu, S. C.; Levine, D. S.; Zhao, Y.; Schrock, R. R.; Hoveyda, A. H. *J. Am. Chem. Soc.* **2011**, *133*, 11512.

17. (a) Endo, K.; Grubbs, R. H. *J. Am. Chem. Soc.* **2011**, *133*, 8525. (b) Keitz, B. K.; Endo, K.; Patel, P. R.; Herbert, M. B.; Grubbs, R. H. *J. Am. Chem. Soc.* **2012**, *134*, 693.

18. Occhipinti, G.; Hansen, F. R.; Törnroos, K. W.; Jensen, V. R. *J. Am. Chem. Soc.*, **2013**, *135*, 3331.

19. Koh, M. J.; Khan, R. K. M.; Torker, S.; Yu, M.; Mikus, M. S.; Hoveyda, A. H. *Nature* **2015**, *517*, 181.

20. Johns, A. M.; Ahmed, T. S.; Jackson, B. W.; Grubbs, R. H.; Pederson, R. L. *Org. Lett.* **2016**, *18*, 772.

21. (a) Nguyen, T. T.; Koh, M. J; Shen, X.; Romiti, F.; Schrock, R. R.; Hoveyda, A. R. *Science* **2016**, *352*, 569. (b) Shen, X.; Nguyen, T. T.; Koh, M. J; Xu, D.; Speed, A. W. H.; Schrock, R. R.; Hoveyda, A. R. *Nature*, **2017**, *541*, 380.

22. Ahmed, T. S.; Grubbs, R. H. *J. Am. Chem. Soc.*, **2017**, *139*, 1532.

23. Ahmed, T. S.; Grubbs, R. H. *Angew. Chem. Int. Ed.* **2017**, *56*, 11213.

24. Ahmed, T. S.; Montgomery, T. P.; Grubbs, R. H. *Chem. Sci.* **2018**, *9*, 3580.

Chapter 2

***Z*-Selective Ruthenium Metathesis Catalysts: Comparison of Nitrate
and Nitrite X-type Ligands**

Abstract

Two new Ru-based metathesis catalysts, **2.3** and **2.4**, have been synthesized for the purpose of comparing their catalytic properties to those of their *cis*–selective nitrate analogues, **2.1** and **2.2**. Although catalysts **2.3** and **2.4** exhibited slower initiation rates than **2.1** and **2.2**, they maintained remarkable *cis*–selectivity in homodimerization and ring–opening metathesis polymerization reactions. Furthermore, they displayed higher *cis*–selectivity than **2.2** for ring–opening metathesis polymerizations, and **2.4** delivered higher yields of polymer.

Introduction

With ever-greater control of stereo- and chemo-selectivity, transition metal–catalyzed olefin metathesis rapidly is becoming the preferred and ubiquitous method for constructing carbon–carbon double bonds.[1] This process has gained widespread applicability in a variety of fields including organic synthesis, biochemistry, and materials science.[2] Transition metal catalysts that could selectively produce the kinetically favored *cis*–products remained elusive until the discovery of Group VI–based systems by Schrock and Hoveyda.[3] *Cis*-selective Ru-based metathesis catalysts were developed soon thereafter, providing a stable and heteroatom-tolerant alternative to Mo- and W-based catalysts.[4] In these catalysts, an *N*-adamantyl substituent of the NHC has undergone C–H activation at Ru, which imposes unique geometrical constraints.[5] The resulting catalysts form side-bound ruthenacycles during olefin metathesis with the *N*-aryl NHC substituent dictating a *cis*-conformation of the metallacycle substituents, resulting in production of the corresponding *Z*-olefin.[6,7] Later *N*-adamantyl analogues with a bidentate nitrate ligand (catalysts **2.1** and **2.2**) displayed greater activity and

stability (Figure 2.1).[8,9] In 2013, the Jensen and Hoveyda groups independently reported cis-selective Ru-based metathesis catalysts with [H$_2$IMes$_2$] (H$_2$I = imidazolidinylidene, Mes = mesityl) NHC ligands, but different X-type ligands.[10,11]

In order to further probe the effect and role of the nitrate ligand in catalyst activity, stability and selectivity of the Grubbs' systems, herein is reported the synthesis of the nitrite analogues of these catalysts, **2.3** and **2.4**, and their reactivities for homodimerization and ring-opening metathesis polymerization reactions.[12]
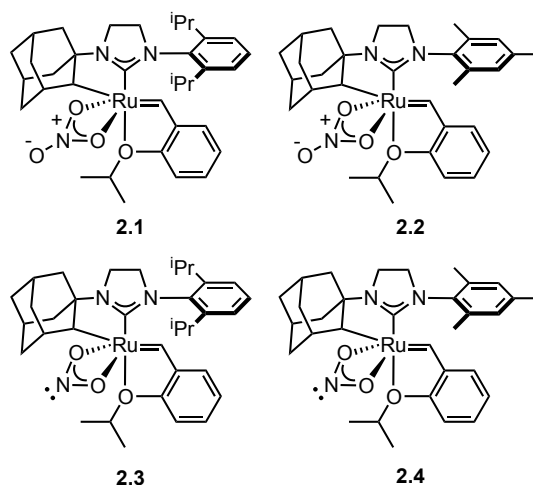
Figure 2.1. Catalysts **2.1**–**2.4** used for homodimerization and ring–opening metathesis polymerization reactions.

Results and Discussion

Synthesis

Previous studies demonstrated the nitrato X–type ligand on catalysts **2.1** and **2.2** exchanges to form the corresponding iodo complexes **2.5** and **2.6** (Scheme 2.1) upon exposure to excess NaI in THF. It was found that these iodo complexes could be readily converted to the corresponding nitrito complexes, **2.3** and **2.4**, using excess AgNO$_2$ in benzene. Trituration with pentane/ether was found to afford the pure catalysts. The ^{1}H NMR spectra of **2.3** and **2.4** were recorded in C$_6$D$_6$. Both complexes showed a

characteristic singlet at 14.82 ppm, which can be assigned to the benzylidene proton and is slightly, but distinctly, shifted from the corresponding benzylidene singlets of the nitrate catalysts **2.1** and **2.2** (15.22 ppm). The corresponding carbon is observed at 261.3 and 259.5 ppm for **2.3** and **2.4**, respectively, compared to 267.5 and 265.8 for the corresponding nitrato-ruthenium catalysts.

2.1, **2.2**   **2.5**, **2.6**   **2.3**, **2.4**

Ar = Mes, DIPP
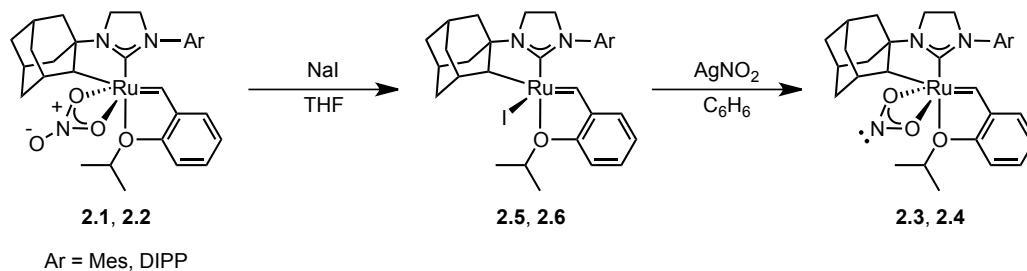
Scheme 2.1. Preparation of catalysts **2.3** and **2.4**.

Homodimerizations

In order to elucidate differences in reactivity and *Z*-selectivity between the nitrato and nitrito catalysts, we subjected them to a standard set of substrates. The homodimerization of allylbenzene (**2.7**) is a good benchmark to determine the activity and stability of olefin metathesis catalysts. Since allylbenzene homodimerization occurs quickly with catalysts **2.1** and **2.2**, a low catalyst loading of 0.1 mol% was used to differentiate the new nitrite–containing catalysts from the highly active and *Z*–selective nitrate catalysts (Figure 2.2). Both catalysts **2.3** and **2.4** proved to be slower than the nitrate analogues, achieving 88% and 78% conversion, respectively, at 3 h. In comparison, the reaction reached completion after approximately one hour with the nitrate catalysts. While slower, **2.3** and **2.4** are able to retain the high *Z*–selectivity seen in the nitrate catalysts. In the case of allylbenzene, catalyst **2.4** with the less bulky *N*-Mes substituent was found to achieve higher conversion over the course of the reaction

compared to catalyst **2.3** with the more sterically hindered *N*-DIPP substituent. Such a difference is not observed with the NO$_3$ catalysts.

[Ru]	Time (h)	Conversion (%)[a]	Z (%)[a]	2.8:2.9[b]
2.1	3	17	>95	22.2
2.2	3	24	>95	20.2
2.3	3	16	>95	31.6
2.4	3	47	>95	16.9
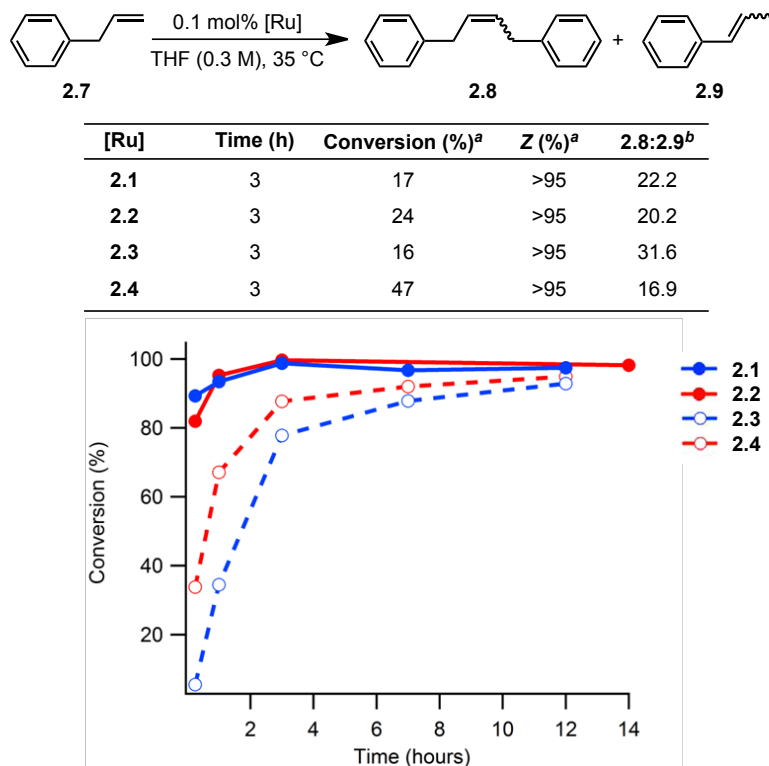
Figure 2.2. Plots of percent conversion versus time for the homodimerization reaction of allylbenzene using 0.1 mol% **2.1–2.4** at 35 °C. [a]Percent conversion and *Z*-selectivity were determined using ^{1}H NMR spectroscopy. [b]Cross:Isomerization ratio determined using ^{1}H NMR spectroscopy at 12 h.

Conversion to the olefin isomerization product **2.9** can be used as a measure of catalyst stability. At long time points when conversion of allylbenzene is complete or nearly complete, the ratio of **2.8** to **2.9** is comparable for all four of the catalysts. This supports our observation that the new nitrite-containing catalysts are stable metathesis catalysts. We plan to further investigate isomerization and decomposition pathways of these catalysts, particularly since the nitrite-containing catalyst **2.4** appears to promote less formation of the olefin isomerization product than **2.1**−**2.3**.

Two more challenging homodimerization substrates, methyl undecenoate (**2.10**) and allyl acetate (**2.12**), were tested to further examine the nitrite activity (Figure 2.3). At

3 h, both nitrate catalysts achieved high conversion to the methyl undecenoate homodimer (Figure 2.3). In contrast, catalyst **2.4** had a modest conversion of 63% whereas **2.3** only achieved minimal conversion (13%). At 12 h, **2.4** had a reasonable 81% conversion, while **2.3** had reached 61% conversion. Here, there is a clear difference in conversion between the DIPP–NHC catalyst **2.3** and the Mes–NHC catalyst **2.4** that is not apparent with the nitrato catalysts **2.1** and **2.2**. This observable differentiation may be

[Ru]	Time (h)	Conversion (%)^a	Z (%)^a
2.1	3	94	>95
2.2	3	96	>95
2.3	3	13	>95
2.4	3	63	>95

Figure 2.3. Plots of percent conversion versus time for the homodimerization reaction of methyl undecenoate using 0.1 mol% **2.1–2.4** at 35 °C. ^{a} Percent conversion and Z-selectivity were determined using ^{1}H NMR spectroscopy.

due more to an induction period before metathesis rather than less active catalysts. For all four catalysts, the Z-selectivity remained above 95% at all conversions of methyl undecenoate. For allyl acetate, which is a challenging substrate for metathesis catalysts, we observed lower conversion by catalysts **2.2–2.4** at 3 h, but by 5 h all catalysts were achieving comparable conversions, although the nitrito catalysts had slightly lower Z–

selectivity (Figure 2.4). There is no clear difference in the rate of conversion for catalysts **2.2**–**2.4** for allyl acetate. In contrast, the DIPP–NHC nitrato catalyst **2.1** maintains a similar rate of conversion across the time period monitored. This difference in behavior will be investigated further through initiation rate studies (*vide infra*).

[Ru]	Time (h)	Conversion (%)^a	Z (%)^a
2.1	3	43	>95
2.2	3	28	90
2.3	3	18	94
2.4	3	13	86

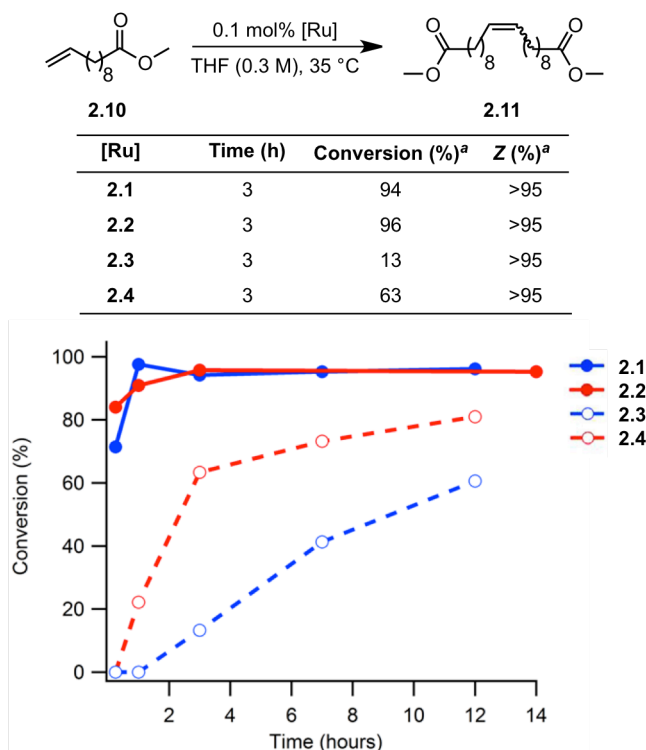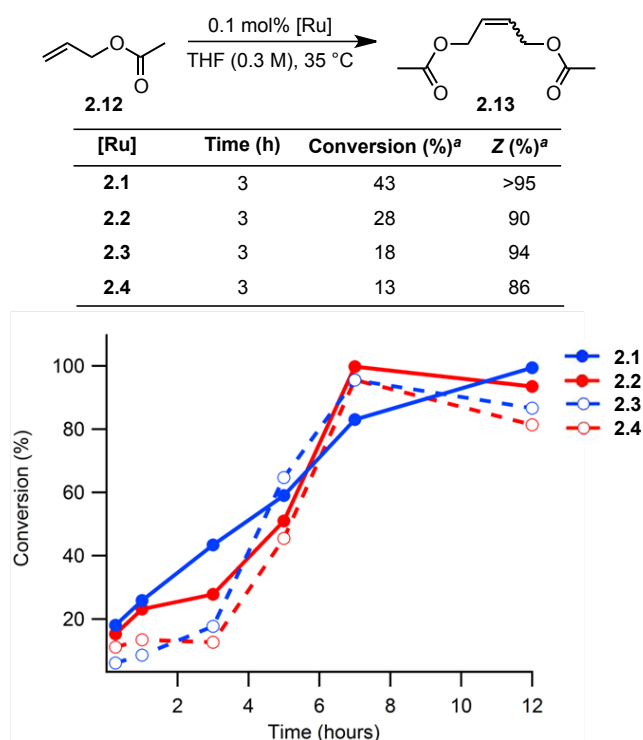**Figure 2.4.** Plots of percent conversion versus time for the homodimerization reaction of allyl acetate using 0.1 mol% **2.1**–**2.4** at 35 °C. ^{a} Percent conversion and *Z*-selectivity were determined using ^{1}H NMR spectroscopy.

With this obvious induction period where the nitrite-containing catalysts are initially slow but reach comparable overall conversion and similar *Z*-selectivity compared to catalysts **2.1** and **2.2**, we tested the initiation rate of catalyst reaction with butyl vinyl ether (BVE) substrate.[13] Consistent with the results of the homodimerizations, the DIPP–NHC catalyst **2.3** was much slower than catalysts **2.1**, **2.2** and **2.4** (Table 2.1). There is a clear trend that the DIPP–NHC catalysts have slower initiation when compared to the Mes–NHC catalysts and the nitrite–containing catalysts are slower to initiate than the

nitrato catalysts. The order of magnitude difference seen for **2.3** is somewhat greater than expected, particularly as this is an extremely active and productive metathesis catalyst.

Table 2.1. Initiation Rates of the Reaction of Catalysts **2.1–2.4** with Butyl Vinyl Ether as Determined by ^{1}H NMR Spectroscopy.
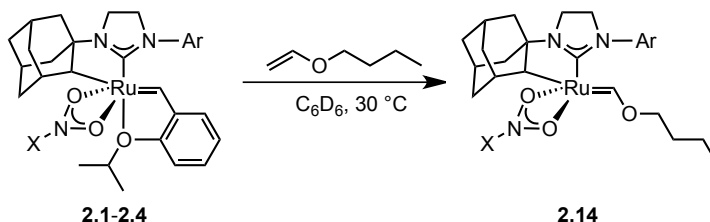
[Ru]	Initiation Rate (10^{-4} s^{-1})
2.1	5.25
2.2	8.40
2.3	0.44
2.4	3.21

In previous initiation rate studies, electron donating ligands such as 2,2 dimethoxypropanoate (**2.15**) imparted greater initiation rates compared to a pivalate (**2.16**) X–ligand (2.5×10^{-3} s^{-1} versus 0.87×10^{-3} s^{-1}, respectively) (Figure 2.5).[5a] Steric bulk also increased the rate; the much larger dicyclohexyl carboxylate group (**2.17**) has an initiation rate constant of 6.9×10^{-3} s^{-1} while the smaller methyl group (**2.18**) has a constant of 0.17×10^{-3} s^{-1}.[5a] Finally, the hapticity of this X–ligand plays a large role in the magnitude of initiation rate as monodentate X–ligands (**2.19**) required much longer times at elevated temperature (70 °C) to initiate. Recent theoretical studies predict the ability of nitrato and carboxylato ligands to convert between monodentate and bidentate conformations is critical for metallacycle stabilization. The inability of monodentate X-ligands to form multiple coordination modes may be the reason these catalysts often are slow to initiate and have negligible metathesis activity. The fact that **2.3** and **2.4** are metathesis active and stable supports a bidentate binding mode. In the case of the nitrite X–ligand, the Mes–NHC initiates at approximately half the rate constant of the nitrate

analogue, and this trend is seen in the homodimerization reactivity. However, the DIPP–

NHC catalyst **2.3** has an initiation rate constant an order of magnitude lower than its

nitrate analogue, which is apparent in the low conversions at early time points. It is not a

simple relationship between initiation rate and metathesis reactivity since catalyst **2.3** has

comparable conversions at later time points for allylbenzene and allyl acetate.
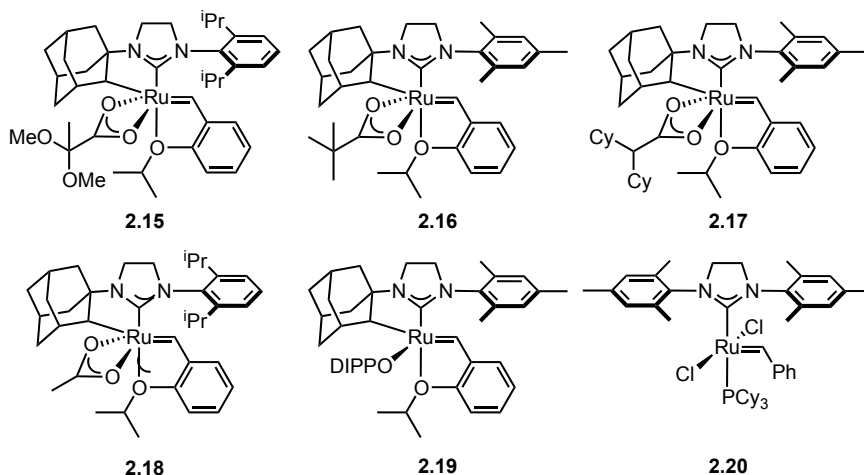
Figure 2.5. Previously reported NHC–Ru metathesis catalysts.

When applied to ring–opening metathesis polymerization, the slow initiation rate

of catalyst **2.3** is evident in the corresponding low yields, high PDI and, for **poly–2.21**,

high M_n (Table 2.2).[1e] High M_n can be attributed to a high rate of propagation (k_p) relative

to the rate of initiation (k_i) or incomplete catalyst initiation. This was observed for

catalyst **2.2**, which has a slow initiation rate compared to faster initiating catalysts (e.g.,

2.20). The nitrite X–ligand catalysts resulted in greater *cis* content compared to catalyst

2.2, although higher PDIs in the case of **poly–2.21**. In contrast to homodimerization

reactions where **2.4** outperformed **2.2** in terms of *Z*-selectivity, in ROMP reactions **2.4**

had comparable yields and higher *Z*-selectivity. ROMP of **2.22** also gave polymer with

higher *cis*-selectivities with **2.3** and **2.4** than with **2.2** (Table 2.3). In contrast to

homodimerization reactions where **2.4** outperformed **2.2** in terms of *Z*-selectivity, in

ROMP reactions, **2.4** had comparable yields and higher *Z*-selectivity.[1e] The generally poor initiation rates were evident in the resulting PDIs of the polymers. The tacticity and functional group tolerance of this catalyst will be investigated further, in addition to further testing of both **2.3** and **2.4** in homodimerizations and cross metathesis reactions.

Table 2.2. Ring–Opening Metathesis Polymerization of Monomer **2.21** with Catalysts **2.1–2.4**.

[Ru]	% cis	Yield (%)[a]	M_n (kDa)	PDI
2.2	88	94	347	1.87
2.3	>95	15	24.9	2.44
2.4	94	>95	17.5	2.24

Table 2.3. Ring–Opening Metathesis Polymerization of Monomer **2.22** with Catalysts **2.1–2.4**.

[Ru]	% cis	Yield (%)[a]	M_n (kDa)	PDI
2.2	86	91	_[a]	_[a]
2.3	90	10	278	1.42
2.4	94	>95	57.2	1.23

[a] M_n and PDI could not be determined due to insolubility in THF.

Conclusions

In summary, salt metathesis of I–ruthenium complexes **2.5** and **2.6** with AgNO$_2$ results in stable, chelated *Z*–selective ruthenium olefin metathesis catalysts **2.3** and **2.4**. The nitrite–containing catalysts are slower initiating and, therefore, have lower conversions at early time points in homodimerization and ring-opening metathesis polymerization. Both types of X-ligands result in exceptional *Z*-selectivity. This high *Z*-selectivity is retained at longer reaction times where, in many cases, catalysts

2.3 and **2.4** reach comparable conversions. Both **2.3** and **2.4** exhibit greater *cis*-selectivity in ring-opening metathesis polymerization than previously observed with **2.2**, and **2.4** gave higher yields.[1e] Given that **2.3** and **2.4** have much slower initiation rates, the retention of reactivity and selectivity merits further investigation of these catalysts as well as examination of other X-type ligands.

Experimental

General Information

Unless otherwise specified, all manipulations were carried out under air-free conditions in dry glassware in a Vacuum Atmospheres Glovebox filled with N_2. General solvents were purified by passing through solvent purification columns and sparged with Ar prior to use. Commercially available substrates were used as received. All substrates were sparged with Ar before bringing into the glovebox and filtered over basic alumina (Brockmann I) prior to use. **2.1**[9a], **2.2**[5a], and **2.6**[5a] were synthesized according to literature procedure.

Kinetic NMR experiments were performed on Varian 500 MHz and Varian 600 MHz spectrometer with an AutoX probe. Spectra were analyzed using MestReNova Ver. 8.1.2. ^{1}H NMR spectra for homodimerization reactions were taken on Varian Inova 300 MHz and automated Varian Inova 500 MHz instruments. [1]H and ^{13}C spectra for catalysts **2.3** and **2.4** were recorded on a Varian Inova 600 MHz instrument or an automated Varian Inova 500 MHz instrument (126 MHz for ^{13}C). Initiation rate experiments were monitored using Varian Inova 500 MHz and Varian Inova 600 MHz instruments.

Molecular weights and polydispersity indexes of polymer samples were determined using multi-angle light scattering gel permeation chromatography employing

an Agilent 1200 UV-Vis detector and a Wyatt Technology miniDAWN TREOS light scattering detector, Viscostar viscometer, and OptilabRex refactive index detector. dn/dc values were determined by assuming 100% mass recovery of the sample to calculate molecular weights.

High-resolution mass spectrometry (HRMS) was performed using FAB+ ionization on a JEOL MSRoute mass spectrometer.

Synthesis of Catalyst 2.3

In a N_2-filled glovebox, reaction of **2.5** (50 mg, 0.74 mmol) with 25 equivalents of $AgNO_2$ (285 mg, 1.8 mmol) in benzene yields **2.3** (33.6 mg, 0.5 mmol, 69% yield) within 1 h at room temperature. The reaction mixture was filtered to remove unreacted starting material and AgI, and the solvent was removed *in vacuo*. The solids were triturated with an Et_2O/pentane solution to give catalyst **2.3** in a 63% yield.

[1H] NMR (600 MHz, C_6D_6) (δ, ppm): 14.83 (s, 1H), 7.45 (d, 7.5 Hz 1H), 7.15 (m, 3H), 7.08 (dd, 7.5 Hz, 1H), 7.02 (dd, 7.5 Hz, 1H), 6.85 (t, 7.5 Hz, 3H), 6.47 (d, 8.5 Hz, 1H), 4.54 (hept, 6.0 Hz, 1H), 3.77 (m, 2H), 3.51 (m, 1H), 3.34 (m, 1H), 3.24 (m, 1H), 3.08 (heptet, 6.5 Hz, 1H), 2.27 (s, 1H), 2.06 (s, 1H), 1.94 (t, 9.5 Hz, 2H), 1.80 (m, 3H), 1.64 (d, 6.5 Hz, 4H), 1.41 (m, 3H), 1.35 (d, 6.5 Hz, 3H), 1.29 (d, 7.0 Hz, 3H), 1.18 (d, 7.0 Hz, 3H), 1.15 (d, 7.0 Hz, 1H), 1.10 (d, 6.0 Hz, 2H), 1.08 (m, 2H), 0.88 (d, 6.0 Hz, 3H), 0.58 (d, 7.5 Hz, 1H).

[13C] NMR (126 MHz, C_6D_6) (δ, ppm): 261.3, 212.1, 154.3, 147.4, 146.9, 142.8, 136.0, 128.5, 125.9, 124.0, 123.6, 123.0, 123.1, 122.9, 122.9, 112.5, 74.4, 72.8, 67.4, 62.8, 54.0, 42.6, 41.2, 39.9, 37.6, 37.5, 37.3, 32.9, 30.5, 29.4, 28.3, 28.1, 28.1, 27.2, 26.4, 25.4, 25.4, 23.3, 22.4, 20.8, 20.1.

HRMS (FAB+): [(M+H)−H$_2$]$^+$ C$_{35}$H$_{46}$O$_3$N$_3$Ru Calculated − 658.2583, Found − 658.2583.

Synthesis of Catalyst 2.4

In a N$_2$-filled glovebox, reaction of **2.6** (50 mg, 0.79 mmol) with 7 equivalents of AgNO$_2$ (85 mg, 0.55 mmol) in benzene cleanly forms **2.4** (30.7 mg, 0.50 mmol, 63% yield) over a reaction time of 2 h at room temperature. The reaction mixture was filtered to remove unreacted starting material and AgI, and the solvent was removed *in vacuo*. The solids were triturated with diethyl ether for a 69% yield of catalyst **2.4**.

^{1}H NMR (600 MHz, C$_6$D$_6$) (δ, ppm): 14.83 (s, 1H), 7.40 (d, 7.5 Hz 1H), 7.18 (t, 7.9 Hz, 1H), 6.84 (td, 7.4 Hz, 1H), 6.81 (s, 1H), 6.74 (s, 1H), 6.52 (d, 8.7 Hz, 1H), 4.59 (heptet, 6.45 Hz, 1H), 3.61 (s, 1H), 3.41 (heptet, 10.5 Hz, 1H), 3.23 (m, 3H), 2.45 (s, 3H), 2.32 (m, 1H), 2.23 (s, 3 H), 2.12 (t, 3.3 Hz, 3H), 2.09 (s, 3H), 2.00 (m, 2H), 1.91 (br d, 11.0 Hz, 1H), 1.79 (d, 12.0 Hz, 1H), 1.65 (m, 1), 1.48 (m, 2H), 1.39 (d, 6.4 Hz, 3H), 1.26 (m, 1H), 1.12 (m, 3H), 0.91 (d, 6.2 Hz, 7H), 0.61 (d, 12.2 Hz, 1H).

^{13}C NMR (126 MHz, C$_6$D$_6$) (δ, ppm): 259.5, 214.1, 154.3, 143.0, 137.4, 136.8, 136.3, 135.3, 129.4, 128.8, 125.8, 123.0, 122.9, 112.4, 74.3, 73.5, 67.4, 62.7, 51.3, 42.7, 41.3, 39.9, 37.6, 37.4, 37.1, 33.0, 30.6, 29.5, 25.4, 20.9, 20.6, 20.0, 18.3, 18.2.

HRMS (FAB+): [(M+H)−H$_2$]$^+$ C$_{35}$H$_{46}$O$_3$N$_3$Ru Calculated − 616.2114, Found − 616.2119.

General Procedure for Homodimerizations

To an open 4 mL vial charged with a stir bar in a N$_2$-filled glovebox, 1.23 mmol of the olefin substrate and the appropriate volume of THF were added such that the total volume of the resulting solution was 225 μL. A solution of 1.23 μmol catalyst in 200 μL THF

was added to the substrate and the reaction was stirred at 35 °C. At appropriate time points, 10 μL aliquots were taken and diluted with 0.70 mL chloroform–d_1 and analyzed using ^{1}H NMR spectroscopy.

General Procedure for ROMP

In an 8 mL vial charged with a stir bar, 1 mL of 0.32 M stock solution of monomer was added under an argon atmosphere. A solution of 3.2 μmol catalyst in 275 μL THF was added and the reaction was stirred at room temperature. After 1 hour, the reaction was quenched with 50 μL ethyl vinyl ether. The reaction mixture was then precipitated into methanol. The polymer samples were collected on a fine frit, washed with several portions of methanol, and dried under vacuum.

General Procedure for Initiation Rate Determination

In a N_2-filled glovebox, a 4-mL vial was charged with catalyst (0.012 mmol) and dissolved with 100 μL C_6D_6. A portion of the stock solution (0.2 mL, 0.003 mmol) was added to an NMR tube and diluted with C_6D_6 (0.4 mL). The NMR tube was sealed with a septa cap and placed in the NMR spectrometer at 30°C. Butyl vinyl ether (12 μL, 0.09 mmol) was added and the disappearance of the benzylidene proton resonance was monitored by arraying the 'pad' function in VNMRj. All reactions showed clean first–order kinetics over a period of at least three half–lives. Spectra were baseline corrected and integrated using MestReNova.

References

1. (a) Scholl, M.; Ding, S.; Lee, C. W.; Grubbs, R. H. *Org. Lett.* **1999** *1*, 953. (b) Grubbs, R. H.; Chang, S. *Tetrahedron* **1998** *54*, 4413. (c) Schwab, P.; Grubbs, R. H.; Ziller, J. W. *J. Am. Chem. Soc.* **1996** *118*, 100. (d) Grubbs, R.H.; Miller, S. J.; Fu, G.

C. *Acc. Chem. Res.* **1995** *28*, 446. (e) Keitz, B. K.; Federov, A.; Grubbs, R. H. *J. Am. Chem. Soc.* **2012** *134*, 2040. (f) Quigley; B. L.; Grubbs, R. H. *Chem. Sci.* **2014**, *5*, 501. (g) Cannon, J. S.; Grubbs, R. H. *Angew. Chem. Int. Ed.* **2013** *52*, 9001.

2. (a) Herbert, M. B.; Marx, V. M.; Pederson, R. L.; Grubbs, R. H. *Angew. Chem. Int. Ed.* **2013** *52*, 310. (b) Meek, S. J.; O'Brien, R. V.; Llaveria, J.; Schrock, R. R.; Hoveyda, A. H. *Nature* **2011** *471*, 461. (c) Yu, M.; Wang, C. B.; Kyle, A. F.; Jakubec, P.; Dixon, D. J.; Schrock, R. R.; Hoveyda, A. H. *Nature* **2011** *479*, 88. (d) Marx, V. M.; Herbert, M. B.; Keitz, B. K.; Grubbs, R. H. *J. Am. Chem. Soc.* **2013** *135*, 94.

3. (a) Ibrahem, I.; Yu, M.; Schrock, R. R.; Hoveyda, A. H. *J. Am. Chem. Soc.* **2009** *131*, 3844. (b) Flook, M. M.; Jiang, A. J.; Schrock, R. R.; Muller, P.; Hoveyda, A. H. *J. Am. Chem. Soc.* **2009** *131*, 7962. (c) Marinescu, S. C.; Schrock, R. R.; Muller, P.; Takase, M. K.; Hoveyda, A.H. *Organometallics* **2001** *30*, 1780. (d) Peryshkov, D. V.; Schrock, R. R.; Takase, M. K.; Muller, P.; Hoveyda, A. H. *J. Am. Chem. Soc.* **2011**, *133*, 20754. (e) Schrock, R. R. *Chem. Rev.* **2002** *102*, 145. (f) Schrock, R. R. Hoveyda, A. H. *Angew. Chem. Int. Ed.* **2003** *42*, 4592.

4. Endo, K.; Grubbs, R. H. *J. Am. Chem. Soc.* **2011** *133*, 8525.

5. (a) Keitz, B. K.; Endo, K.; Patel, P. R.; Herbert, M.B.; Grubbs, R.H. *J. Am. Chem. Soc.* **2012** *134*, 693. (b) Keitz, B. K.; Endo, K.; Herbert, M.B.; Grubbs, R.H. *J. Am. Chem. Soc.* **2011** *133*, 9686.

6. Liu, P.; Xu, X. F.; Dong, X. F.; Keitz, B. K.; Herbert, M. B.; Grubbs, R. H.; Houk, K. N. *J. Am. Chem. Soc.* **2012** *134*, 1464.

7. Jiang, A. J.; Zhao, Y.; Schrock, R. R.; Hoveyda, A. H. *J. Am. Chem. Soc.* **2009** *131*, 16630.

8. (a) Previously, nitrato ligands have been shown to decrease activity for other Ru-based metathesis catalysts: Jovic´, M.; Torker, S.; Chen, P. *Organometallics* **2011**, *30*, 3971; (b) Buchmeiser, M. R.; Ahmad, I.; Gurram, V.; Kumar, P. S. *Macromolecules* **2011**, *44*, 4098.

9. (a) Rosebrugh, L. E.; Herbert, M. B.; Marx, V. M.; Keitz, B. K.; Grubbs, R. H. *J. Am. Chem. Soc.* **2013** *135*, 1276. (b) Herbert, M. B.; Lan, Y.; Keitz, B. K.; Liu, P.; Endo, K.; Day, M. W.; Houk, K. N., Grubbs, R. H. *J. Am. Chem. Soc.* **2012** *134*, 7861. (c) Torker, S.; Khan, R. K. M.; Hoveyda, A. H. *J. Am. Chem. Soc.*, **2014**, *136*, 3439.

10. Occhipinti, G.; Hansen, F. R.; Törnroos, K. W.; Jensen, V.R. *J. Am. Chem. Soc.* **2013**, *135*, 3331.

11. Khan, R. K. M.; Torker, S.; Hoveyda, A. H. *J. Am. Chem. Soc.* **2013**, *135*, 10258.

12. (a) Other nitrite-containing Ruthenium complexes: (a) Michrowska, A.; Bujok, R.; Harutyunyan, S.; Sashuk, V.; Dolgonos, G.; Grela, K. *J. Am. Chem. Soc.*, **2004**, *126*, 9318. (b) Gordon, C. M.; Feltham, R. D.; Turner, J. J. *J. Phys. Chem.*, **1991**, *95*, 2889. (c) Ohtsu, H.; Oka, N.; Yamaguchi, T. *Inorg. Chim. Acta* **2012**, *383*, 1.

13. (a) Thiel, V.; Hendann, M.; Wannowius, K.–J.; Plenio, H. *J. Am. Chem. Soc.*, **2012**, *134*, 1104. (b) Torker, S.; Merki, D.; Chen, P. *J. Am. Chem. Soc.* **2008**, *130*, 4808. (c) Monsaert, S.; Vila, A. L.; Drozdzak, R.; Van Der Voort, P.; Verpoort, F. *Chem. Soc. Rev.* **2009**, *38*, 3360.

14. Dang, Y.; Wang, Z. X.; Wang, X. *Organometallics* **2012**, *31*, 7222.

15. Dang, Y.; Wang, Z. X.; Wang, X. *Organometallics* **2012**, *31*, 8654.

Chapter 3

Probing Stereoselectivity in Ring-Opening Metathesis

Polymerization Mediated by Cyclometalated Ruthenium-Based

Catalysts: A Combined Experimental and Computational Study

Abstract

The microstructures of polymers produced by ring-opening metathesis polymerization (ROMP) with cyclometalated Ru-carbene metathesis catalysts were investigated. A strong bias for a *cis*, syndiotactic microstructure with minimal head-to-tail bias was observed. In instances where *trans* errors were introduced, it was determined that these regions were also syndiotactic. Furthermore, hypothetical reaction intermediates and transition structures were analyzed computationally. Combined experimental and computational data support a reaction mechanism in which *cis*, syndio-selectivity is a result of stereogenic metal control, while microstructural errors are predominantly due to alkylidene isomerization via rotation about the Ru=C double bond.

Introduction

The physical and mechanical properties of polymers formed in ring-opening metathesis polymerization (ROMP) reactions of mono- and polycyclic olefins are intricately related to the degree of order in the polymer microstructures.[1] Norbornene- and norbornadiene-derived ROMP polymers in particular contain a number of primary structural elements that must be precisely controlled if polymers with well-defined properties are desired: namely, the newly-formed double bonds can be *cis* or *trans*; the polymers can be isotactic (*m*) or syndiotactic (*r*) depending on the relative stereochemistry of the allylic carbons along the chain; and, in the case of polymers derived from unsymmetrically substituted monomers, the substituents can be oriented either in the same direction to form head-tail (HT) dyads or in opposite directions to give head-head (HH) and tail-tail (TT) dyads (Figure 3.1).[2] Precise control of these primary structural elements is fundamental to preparing polymers with well-defined properties.
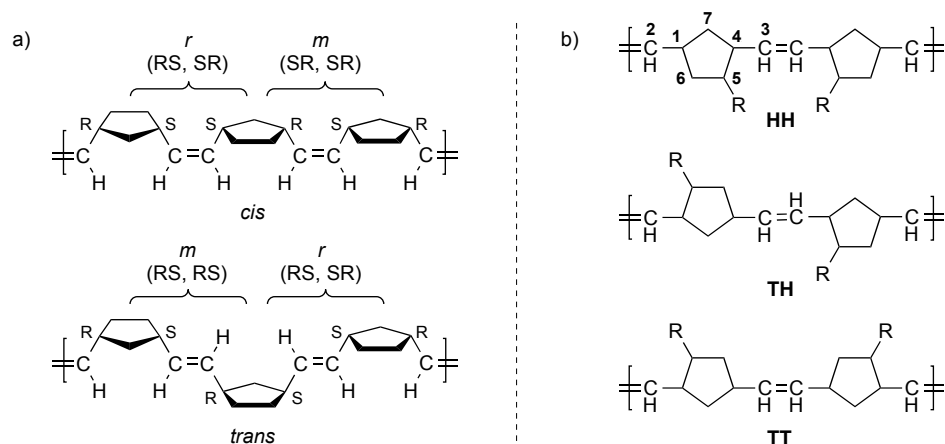
Figure 3.1. (a) Structural possibilities of polymers made from unsubstituted or symmetrically-substituted norbornenes (b) Head-head, head-tail, and tail-tail dyads resulting from polymerization of unsymmetrically-substituted norbornenes.

Significant microstructural control of norbornene- and norbornadiene-based polymers was first achieved using classical, metal-salt type initiators (e.g., $RuCl_3$, $ReCl_5$ and $OsCl_3$), in which selectivity is usually a result of chain-end control.[2] However, because this type of control results from an influence of the polymer chain on the propagation step, whether through steric crowding or the coordination of recently-formed double bonds to the metal center, the stereoselectivity of these systems can vary dramatically with the type of monomer and/or reaction conditions employed; as a result, examples of ROMP polymers composed predominantly of a single structure produced by these systems are rare.

More recently, the development of molybdenum- and tungsten-based initiators with discrete ligand environments and mechanisms of action has led to the preparation of an increasing number of ROMP polymers with singular microstructures.[3-6] Fully *cis, isotactic* polymers can be produced from a range of norbornene- and norbornadiene-based monomers using W and Mo biphenolate and binaphtholate initiators, which operate through enantiomorphic site control, a primarily steric directing effect derived from the

29

chirality of the biphenolate or binaptholate ligand.[4] Additionally, pure *cis,*syndiotactic microstructures are accessible through the use of MAP (MonoAryloxide Pyrrolide) alkylidene complexes as a result of stereogenic metal control, arising from the inversion of the absolute configuration of the metal center that occurs with each forward metathesis step.[6] Finally, a few examples of predominantly *trans*, syndiotactic and *trans,* isotactic polymers have been prepared with certain Mo initiators as a consequence of chain-end control and a "turnstile-like" non-metathesis-based polytopal rearrangement, respectively.[4b,5c,6]

In contrast, only limited control of *cis/trans* content and tacticity has been realized with discrete ruthenium alkylidenes; much like the classical initiators, this stereochemical control is generally dependent on the use of specialized monomers or reaction conditions.[7] A prevailing theory for the overall lack of stereoselectivity in these systems is that the low calculated barriers of rotation for Ru alkylidenes (on the order of 1−10 kcal/mol for a generic NHC Ru dichloride catalyst) preclude steric enforcement of polymer tacticities.[3a,5c,8] Despite this purported limitation, however, we recently reported the generation of highly *cis*, highly syndiotactic ROMP polymers by *N-*[t]Bu-cyclometalated catalyst **3.1**, marking the first time a norbornene-based polymer with a single structure had been produced by a ruthenium alkylidene complex (Figure 3.2).[9] Cyclometalated catalyst **3.2**, containing a chelated *N*-adamantyl-*N*-mesityl *N*-heterocyclic

3.1   **3.2**
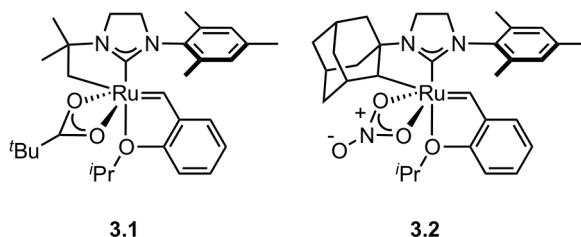
Figure 3.2. Cyclometalated catalysts **3.1** and **3.2** (Mes = 2,4,6-trimethylphenyl).

carbene (NHC) ligand, has also been shown to yield highly *cis* ROMP polymers, though these polymers were originally thought to be atactic.[10]

Because the stereochemical information contained in any given ROMP polymer represents a chronological "road map" of every catalytic cycle that took place over the course of the polymerization, careful microstructural analysis of the dyads and triads in a ROMP polymer can shed light on the exact nature of the propagation transition state(s). As a result, ROMP presents a powerful tool in which to gain additional insight into the mode of action of cyclometalated ruthenium catalysts in *cis*-selective metathesis transformations. To this end, we sought to conduct an experimental and computational study focused on elucidating the precise mechanisms responsible for *cis*-selectivity and tacticity in Ru-based catalysts such as **3.1** and **3.2** by determining how variation of the cyclometalated group, *N*-aryl substituent, and X-type ligand affects the resulting polymer microstructure. Herein, we report the results of these mechanistic studies and propose a general model for *cis*-selectivity and tacticity for cyclometalated Ru-based initiators. These results are envisioned to be fundamental to the mode-of-action of these catalysts and, as such, generally applicable to other transformations mediated by cyclometalated Ru-based catalysts. Thus, this work is also expected to aid in the future design of new *cis*-selective catalysts and to provide increased predictive power when employed in synthetic transformations.

Results and Discussion

General Reactivity, *Cis*-Selectivity, and Blockiness of ROMP Polymers Produced by Initiators 3.1−3.8

Reactions of a variety of cyclometalated catalysts (**3.1−3.8**, Figure 3.3) with norbornene (NBE, **3.9**) were screened to study general reactivity and *cis*-selectivity.[11] All

polymerizations were performed at room temperature in THF (0.25 M) at a ratio of [monomer]/[initiator] = 100 (1 mol %). In general, catalysts **3.1**−**3.8** were found to yield polymers with moderate to high *cis* contents ($\sigma_c > .95$ in many cases) (Table 3.1).[12]
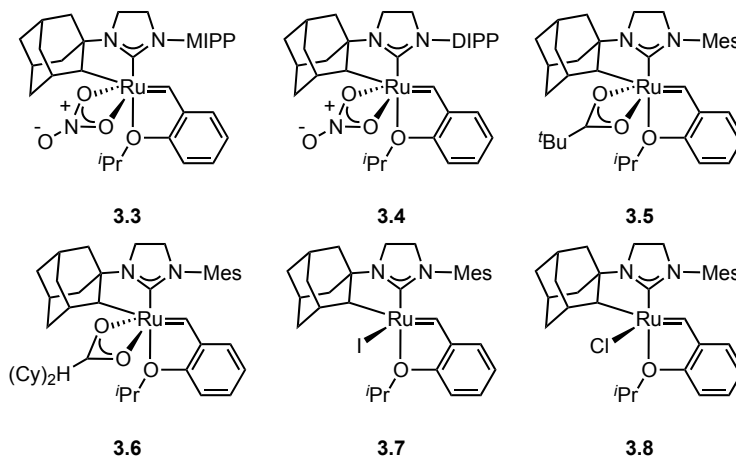
Figure 3.3. Catalysts **3.3**−**3.8**: MIPP = 2,6-methylisopropylphenyl (**3.3**); DIPP = 2,6-diisopropylphenyl (**3.4**); Mes =2,4,6-trimethylphenyl (**3.5**−**3.8**).

Table 3.1. Polymerization of Norbornene (**3.9**) with Catalysts **3.1**−**3.8**
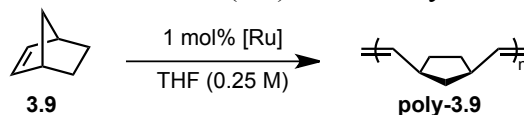
[Ru]	$\sigma_c{}^a$	$r_t{}^b$	$r_c{}^b$	$r_t r_c$
3.1	0.97	-	-	-
3.2	0.92	0.27	6.5	1.7
3.3	0.97	-	-	-
3.4	0.99	-	-	-
3.5	0.74	0.52	2.4	1.2
3.6	0.74	0.94	3.9	3.7
3.7	0.88	0.45	6.5	2.9
3.8	0.82	0.53	4.8	2.5

[a]Fraction of double bonds having *cis* configuration; average of four values derived from $C_{2,3}$, $C_{1,4}$, C_7, and $C_{5,6}$, resonances, with agreement generally within ±0.02. [b]Average of two values derived from $C_{1,4}$ and $C_{5,6}$ peaks.

In the case of poly(NBE) and related polymers, the distribution of *cis* and *trans* double bonds in a given chain can be readily determined from ^{13}C NMR, which provides information on the proportions of double-bond dyads in the polymer.[3b,13] This distribution, known as blockiness, is represented by the relationship $r_t r_c$, where r_t =

(tt)/(tc) and $r_c = (cc)/(ct)$. Understanding the nature of the double bond distribution in any ROMP polymer affords significant mechanistic insight: a random distribution, characterized by $r_t r_c = 1$, suggests that the formation of a *cis* double bond is independent of any previously-formed double bonds, whereas a blocky distribution ($r_t r_c > 1$) may indicate some influence of the polymer chain in the propagation step (i.e., chain-end control).

In general, predominantly *cis* (>50%) polymers of norbornene and related monomers formed by early generation ROMP catalysts are somewhat-to-highly blocky, with values of $r_t r_c$ ranging from 5 to 8 or more.[13a] Significantly, r_t is almost always greater than 1 (i.e., $tt > tc$), indicating a preference for *trans* double bonds to occur in pairs. One postulate for this observed behavior is the existence of multiple kinetically distinct propagating species each having a different selectivity for the formation of *cis* or *trans* double bonds. This is supported by careful examination of the proportions of double bond triads in the polymers (readily derived from the known proportions of dyads), from which it can be shown that in the classical systems, the probability of *cis* or *trans* double bond formation at any given propagation step varies greatly depending on the identity of the last- and/or second-to-last formed double bond, presumably due to some interaction of these recently-formed double bonds with the metal center or alkylidene.[14] Propagating species in which the most recently formed double bond is *cis* (P_c) are highly *cis*-directing, whereas the selectivity of species in which the last-formed double bond is *trans* depends on whether the configuration of the penultimate double bond is *cis* (P_{tc}, highly *trans*-directing) or *trans* (P_{tt}, essentially nonselective) (Scheme 3.1).[2b] These relative selectivities are ultimately responsible for the high incidence of *trans*−*trans* double bond

pairs observed in poly(NBE) samples produced by classical metathesis catalysts.

$$P_c \xrightarrow{\textbf{+M}} P_c \xrightarrow{\textbf{+M}} P_{tc} \xrightarrow{\textbf{+M}} P_{tt} \xrightarrow{\textbf{+M}} P_c$$

| Bond formed: | c | t | t | c |
| Probability: | 0.86 | 0.14 | 0.81 | 0.49 |
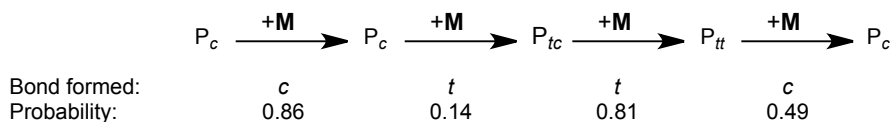
Scheme 3.1. Probabilities of forming *cis* or *trans* double bonds in W(CO)$_6$/*hv* catalyzed ROMP of norbornene (**3.9**). P_c refers to a propagating species that has just formed a cis double bond, while P_{tc} and P_{tt} describe species that have just formed a *trans* double bond but have different penultimate double bonds (*cis* and *trans*, respectively). Adapted with permission from ref 2b. Copyright 1997 Academic Press.

Values of $r_t r_c$ calculated for the poly(NBE)s produced by catalysts **3.1**−**3.8** ranged from 1.25 to 3.70 (Table 3.1), indicating only modest deviations from randomness in the *cis*/*trans* double bond distributions of the polymers. Moreover, all of the highly-*cis* polymers produced by catalysts **3.1**−**3.8** had r_t values that were less than unity; in conjunction with the overall low values of $r_t r_c$, these low r_t values suggest that *trans* double bonds occur as single, random errors throughout the polymers rather than in pairs as observed with the classical systems. Furthermore, calculation of the probabilities of forming a *cis* or *trans* double bond according to the identity of the last- or last-but-one double bond revealed no significant dependence of *cis*-selectivity on the configurations of these previously-formed double bonds in the polymerization of norbornene (Scheme 3.2). This suggests that chain-end control is most likely not the driving force behind the stereoselectivity in ROMP observed with initiators **3.1**−**3.8**.

$$P_c \xrightarrow{\textbf{+3.5}} P_c \xrightarrow{\textbf{+3.5}} P_{tc} \xrightarrow{\textbf{+3.5}} P_{tt} \xrightarrow{\textbf{+3.5}} P_{tt}$$

| Bond formed: | c | t | t | t |
| Probability: | 0.70 | 0.30 | 0.32 | 0.37 |
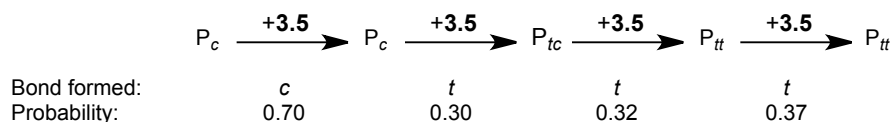
Scheme 3.2. Probabilities of forming *cis* or *trans* double bonds in the ROMP of norbornene (**3.9**) by catalyst **3.5**.

Tacticity and Head-Tail Bias of ROMP Polymers Yielded by Catalysts 3.1−3.8

To fully understand the origins of selectivity in cyclometalated catalysts **3.1**−**3.8**,

a complete microstructural picture, taking into account not only *cis/trans* content but also

tacticity and, in some cases, head-tail selectivity across dyads and triads, is essential. We

therefore first turned our attention towards more complex monomers that could be used

to quantify the extent of tacticity in polymers produced by these initiators. 2,3-

Dicarbomethoxynorbornadiene (DCMNBD, **3.10**) has been used extensively for this

purpose, as the *cis* $C_{1,4}$ peak displays *m/r* splitting that is sufficiently resolved for

quantitative analysis.[15] Accordingly, for polymerizations of **3.10** with catalysts **3.1−3.8**,

the fraction of *cis*, *r* dyads in each highly *cis* polymer was easily determined (Table 3.2).

Surprisingly, the *cis* portions of the polymers produced by catalysts **3.2−3.8** were found

to be highly syndiotactic and not atactic as previously thought (Figure 3.4). In fact,

monodentate catalysts **3.7** and **3.8** yielded polymers with almost exclusively a single

structure (*cis*, syndiotactic).

Table 3.2. Polymerization of Monomer **3.10** with Catalysts **3.1−3.8**.
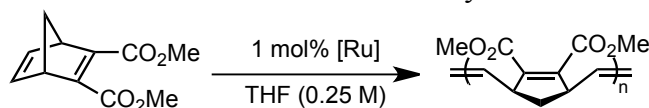
[Ru]	$\sigma_c{}^a$	% r (cis)^b
3.1	0.99	99
3.2	0.87	85
3.3	0.84	84
3.4	0.91	85
3.5	0.72	68
3.6	0.65	68
3.7	0.98	96
3.8	0.94	96

[a]Fraction of double bonds having *cis* configuration; average of two values derived from $C_{2,3}$ and $C_{1,4}$ resonances, with agreement generally within ±0.02. [b]Derived from *cis*, $C_{1,4}$ peaks.
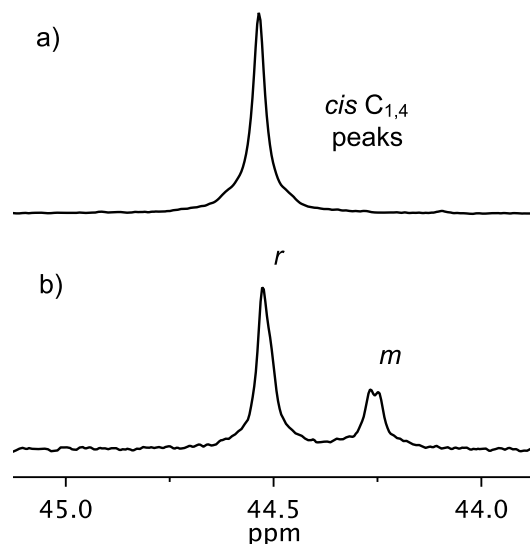
Figure 3.4. ^{13}C NMR spectra of (a) *cis,* syndiotactic **poly-3.10** produced by catalyst **3.1** and (b) 72% *cis*, 68% syndiotactic (*cis* regions) **poly-3.10** produced by catalyst **3.5**.

We next probed the effects of temperature and dilution on the polymerization of **3.10** by initiator **3.2**. If the propagation reaction is in competition with other processes occurring at the catalyst center, such as alkylidene isomerization, changes in *cis* content and/or tacticity can result from variations in temperature or monomer concentration.[3b] Decreasing monomer concentration in particular presents a simple method with which to slow propagation relative to these other processes. However, we found that the concentration of **3.10** had very little appreciable effect on the microstructures of the polymers produced by catalyst **3.2** (Table 3.3). Increasing the temperature from 25 to 40 °C, on the other hand, resulted in an approximately 5% decrease in both the *cis* content and tacticity of **poly-3.10/3.2**, while decreasing the temperature to 0 °C had the opposite effect. These results suggest that alkylidene isomerization might indeed be occurring at a rate comparable to (or faster than) propagation and could therefore feasibly be a major contributor in the resulting stereoselectivity of the polymerization.

Table 3.3. Temperature and Concentration Effects on the Polymerization of Monomer **3.10** with Catalyst **3.2**.

Temp (°C)	Conc (M)	$\sigma_c{}^a$	% r (cis)[b]
25	0.25	0.87	85
0	0.25	0.92	90
40	0.25	0.83	81
25	0.05	0.90	88
25	1.25	0.88	85

[a]Fraction of double bonds having *cis* configuration; average of two values derived from $C_{2,3}$ and $C_{1,4}$ resonances, with agreement generally within ±0.02. [b]Derived from *cis*, $C_{1,4}$ peaks.

As catalysts **3.1**, **3.2**, and **3.4** were found to cover the general range of microstructures produced by catalysts **3.1**−**3.8**, further polymerizations were performed using only these three systems. Results similar to monomer **3.10** were obtained when 2,3-bis(trifluoromethyl)norbornadiene (**3.11**) was polymerized using catalysts **3.1**, **3.2**, and **3.4** (Table 3.4);[16] the resulting polymers were also *cis*-biased with highly syndiotactic *cis* regions.

Table 3.4. Polymerization of Monomer **3.11** with Catalysts **3.1**, **3.2**, and **3.4**.
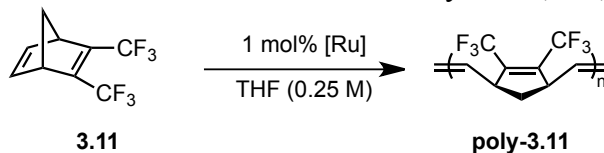
[Ru]	$\sigma_c{}^a$	% rr (cis)[b]
3.1	0.79	99
3.2	0.63	99
3.4	0.55	>99

[a]Fraction of double bonds having *cis* configuration; average of three values derived from $C_{2,3}$, $C_{1,4}$ and C_7 resonances, with agreement generally within ±0.02. [b]Derived from *cis* C_7 peaks.

To obtain a comprehensive understanding of the origins of *cis*-selectivity and tacticity in cyclometalated catalysts **3.1**−**3.8**, it is necessary to also determine the tacticity of the *trans* regions of polymers derived from these systems. However, the *trans* peaks in

polymers derived from monomers **3.10** and **3.11** are too small and not sufficiently resolved for meaningful analysis. Thus, we next turned our attention towards polymers with more easily analyzable *trans* regions, namely *exo, exo*-7-oxa-5-norbornene-2,3-dicarboxylic acid (**3.12**) and 7-methylnorbornene (7-MNBE, **3.13**).[15,17] Polymers produced from **3.12** had generally lower *cis* contents (σ_c = 0.73−0.94) (Table 3.5),

Table 3.5. Polymerization of Monomer **3.12** with Catalysts **3.1**, **3.2**, and **3.4**.
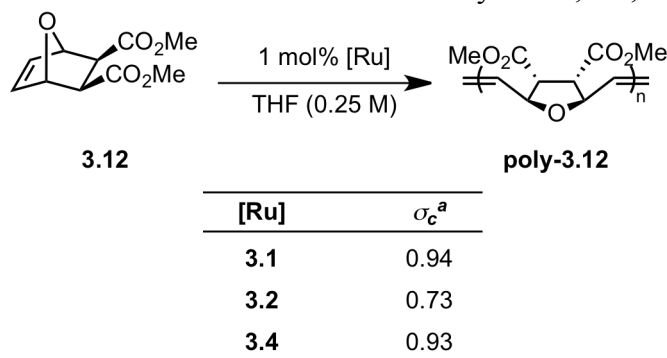
[Ru]	$\sigma_c{}^a$
3.1	0.94
3.2	0.73
3.4	0.93

[a]Fraction of double bonds having *cis* configuration; average of three values derived from CO_2Me, $C_{2,3}$ and $C_{1,4}$ resonances, with agreement generally within ±0.03. [b]Derived from *trans* $C_{1,4}$ peaks.

allowing for facile qualitative analysis of the *trans* portions via the *trans* $C_{1,4}$ peak, which displays *m/r* tacticity splitting. Although the *cis* peaks are not sensitive to tacticity splitting, a tacticity bias can be determined based on comparison with data from catalyst **3.1**, shown to consistently produce predominately syndiotactic polymers.[9] Catalysts **3.1** and **3.4** produced polymers with *trans* regions that were largely syndiotactic, while polymer produced by catalyst **3.2** appeared to have negligible bias for either *m* or *r* dyads in the *trans* regions (Figure 3.5).

Next, we exposed catalysts **3.1**, **3.2**, and **3.4** to a 1.2:1 *syn/anti* mixture of **3.13.** It is generally accepted that norbornene and related compounds react at the less-hindered *exo*-face in ROMP.[18] This was confirmed for catalysts **3.1** and **3.2** via the polymerization of **3.13**; both polymerized the *anti* monomer almost exclusively (<2% *syn*-derived
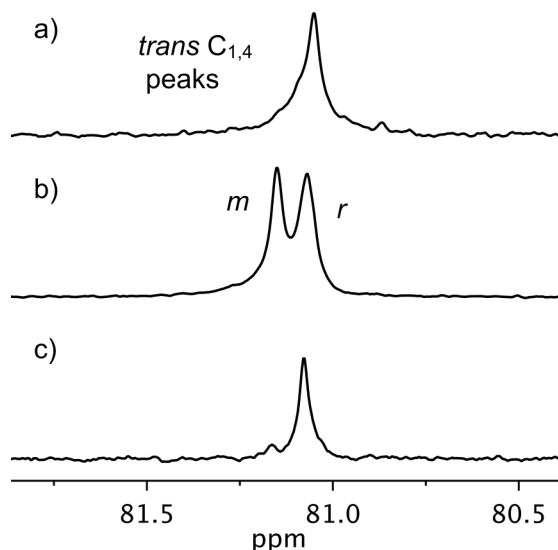
Figure 3.5. ^{13}C NMR spectra highlighting the *trans* $C_{1,4}$ regions of (a) 94% *cis* **poly-3.12** with 87% *r trans* regions produced by catalyst **3.1**, (b) 73% *cis* **poly-3.12** with 50% *r trans* regions produced by catalyst **3.2** and (c) 93% *cis* **poly-3.12** with 88% *r trans* regions produced by catalyst **3.4**.

polymer was observed by ^{13}C NMR). This occurs because the 7-methyl group in the *syn* monomer is positioned directly over the *exo*-face of the double bond, and as such polymerization via *exo* attack is prohibitively high in energy, whereas this is avoided in the *anti*-monomer. Gratifyingly, unambiguous determination of tacticity was achieved for both the *cis* and *trans* regions by analyzing polymers of *anti*-**3.13**, in which all of the carbons with the exception of C_7 are sensitive to tacticity. Samples of poly(*anti*-7-MNBE) produced by catalysts **3.1** and **3.2** were discovered to have highly syndiotactic *cis* regions (90-95% *r*) and highly syndiotactic *trans* regions (96-99% *r*) (Table 3.6). No appreciable amount of polymer was formed with initiator **3.4**; this is likely a result of the increased steric bulk associated with the *N*-2,6-diisopropylphenyl group of this particular catalyst.

Finally, we probed the extent of head-to-tail (HT) selectivity or bias exhibited by catalysts **3.1**, **3.2**, and **3.4** in the polymerization of unsymmetrically substituted

Table 3.6. Polymerization of a 1.2:1 *Syn*/*Anti* Mixture of 7-Methylnorbornene (**3.13**) with Catalysts **3.1**, **3.2**, and **3.4**.

1.2:1 *syn/anti* **3.13**　　　　　　　　　　　　　　**poly-3.13**

[Ru]	$\sigma_c{}^a$	Tacticity[b]
3.1	0.97	*cis* regions, 95% *r, trans,* >99% *r*
3.2	0.87	*cis*, 90% *r, trans,* >99% *r*
3.4[c]	-	-
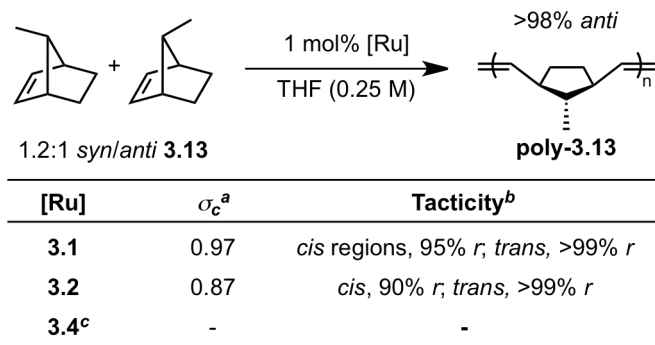
[a]Fraction of double bonds having *cis* configuration; derived from $C_{1,4}$ resonances. [b]Derived from *cis* and *trans,* $C_{1,4}$ peaks. [c]No reaction.

norbornenes. HT bias is measured by determining the ratios of head-head/head-tail (HH/HT) and tail-tail/tail-head (TT/TH) dyads in both the *cis* and *trans* regions of the polymer. The enantiomers are randomly distributed throughout the polymer when these values are equal to unity (i.e., no bias is present).

The degree of HT bias in polymers derived from substituted norbornenes is delicately related to electronic and steric effects associated with both the monomer substituent(s) and the catalyst. Additionally, any catalyst relaxation or isomerization processes occurring on the same timescale as propagation may also contribute to HT bias, as different propagating species can exhibit different levels of H/T discrimination. One way to probe the role of the catalyst in HT selectivity is via the polymerization of C_5- and C_6-substituted monomers. The substituents in these monomers are sufficiently remote from the double bond such that they generally do not exert any intrinsic head-to-tail bias resulting from steric effects; thus, any observed bias with these monomers is likely catalyst-dependent. An HT bias in the polymerization of C_5- and C_6-substituted monomers with a given catalyst, then, particularly one that increases with decreasing rate of polymerization (or increasing dilution), may point towards the existence of two or

more distinct propagating species with distinctive HT biases.[3b]

To test for HT-bias, catalysts **3.1**, **3.2**, and **3.4** were used to polymerize the unsymmetrically substituted racemic monomers 5-methylene-2-norbornene (**3.14**) and 5,5-dimethylnorbornene (DMNBE, **3.15**).[19,20] Although all of the catalysts were found to be essentially bias-free in the polymerization of monomer **3.14** (*cis* TT/TH ratios = 0.93−1.04), initiators **3.1** and **3.2** displayed more significant biases in the polymerization of **3.15** (*cis* TT/TH ratios = 1.11−1.51; *trans* TT/TH ratios = 0.20−1.00) (Table 3.7). Notably, the rate of polymerization of monomer **3.15** by initiators **3.1** and **3.2** was significantly lower than that of **3.14** (1−4 hours to full conversion vs. minutes), and as seen with monomer **3.13** no appreciable amount of **poly**-**3.15** was formed using catalyst **3.4** (likely as a consequence of the increased steric hindrance imparted by the *endo*-substitution in monomer **3.15**. The increase in HT bias with decreasing rate might be interpreted in terms of the existence of more than one propagating species (resulting from alkylidene isomerization or a similar process) each with a different inherent HT bias.

Table 3.7. Polymerization of Monomers **3.14** and **3.15** with Catalysts **3.1**, **3.2**, and **3.4**.

[Ru]	Monomer	$\sigma_c{}^a$	*cis* TT/TH[b]	*trans* TT/TH[c]
3.1	3.14	0.98	0.93	-[d]
3.2	3.14	0.87	0.95	-
3.4	3.14	0.94	1.0	-
3.1	3.15	0.78	1.1	0.20
3.2	3.15	0.77	1.5	0.50
3.4[e]	3.15	-	-	-

[a]Fraction of double bonds having *cis* configuration; derived from C_6 resonances (**3.14**) and C_2 resonances (**3.15**). [b]Derived from *cis* TT and TH $C_{2,3}$ peaks (**3.14**) and *cis* TT and TH C_2 peaks (**3.15**). [c]Derived from *trans* TT and TH C_2 peaks (**3.15**). [d]Here and below: overlap of *trans* TT and HH $C_{2,3}$ peaks in **poly**-**3.14** precluded *trans* TT/TH or HH/HT analysis. [e]No reaction.

Computational Investigations of Hypothetical Reaction Pathways and Proposed Model for *Cis*-Selectivity and Tacticity in Catalysts 3.1−3.8

The selectivity for *cis,* syndiotactic polymers exhibited by catalysts **3.1−3.8** is hypothesized to be a result of stereogenic metal control, as in the case of the Mo- and W-based MAP alkylidene complexes described earlier. Because initiators **3.1−3.8** are stereogenic-at-Ru, the absolute configuration of the metal center is inverted with each propagation step to generate enantiomeric (in the case of **3.1**) or diastereomeric (**3.2−3.8**) carbenes (Figure 3.6), resulting in the addition of incoming monomers to alternating sides of the Ru=C bond.

(R)-**3.1**   *(S)*-**3.1**   *(R,R)*-**3.2**   *(R,S)*-**3.2**

enantiomeric alkylidenes   *diastereomeric alkylidenes*
(3.1)   **(3.2)**
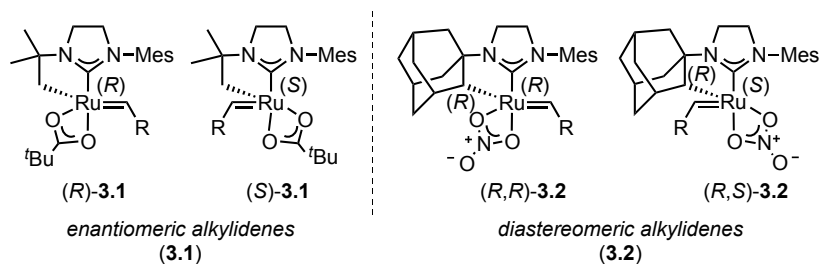
Figure 3.6. Enantiomeric (**3.1**) and diastereomeric (**3.2**) alkylidenes generated by the stereochemical inversion of the Ru metal center with each forward propagation step.

Previous computational and experimental work has shown that *cis*-selectivity in cross metathesis reactions using cyclometalated catalysts similar to **3.1** and **3.2** likely stems from the steric influence of the bulky *N*-aryl group positioned directly over the side-bound metallacycle, which results in the destabilization of the transition state leading to the formation of *trans* olefins.[21] It is hypothesized that monomer approach in ROMP is similarly influenced by the presence of the *N*-aryl group, in that one would expect norbornene and related derivatives to react at the less hindered *exo*-face with the methylene bridge pointed down, away from the *N*-aryl "cap."[22] In the terminology employed by Schrock and coworkers in regards to well-defined Mo and W initiators, this approach is designated *anti*, in that the bulk of the monomer points away from the *N*-aryl

group; the opposite approach is *syn*.[5c] Likewise, *syn* and *anti* Ru=CHR isomers are defined according to whether the R group of the alkylidene points towards or away from the *N*-aryl group. A consistently *anti* monomer approach leads to the formation of a *cis,* syndiotactic polymer (Scheme 3.3). However, if the incoming monomer were to occasionally adopt a *syn* approach to the *anti* alkylidene, a *trans,* isotactic dyad "error" would be produced (Scheme 3.4).
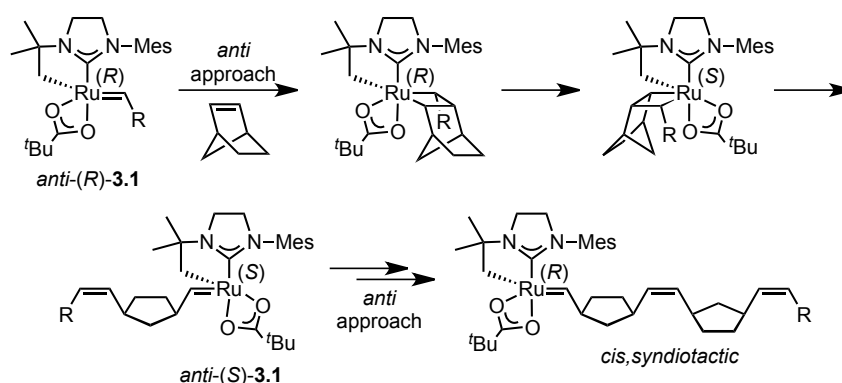
Scheme 3.3. Proposed mechanism for forming *cis,* syndiotactic polymers using cyclometalated catalyst **3.1** (Mes = 2,4,6-trimethylphenyl, R = *o*-isopropoxyphenyl); the *cis,* syndiotactic microstructure results from the monomer repeatedly approaching alternate sides of an *anti* alkylidene in an *anti* fashion.
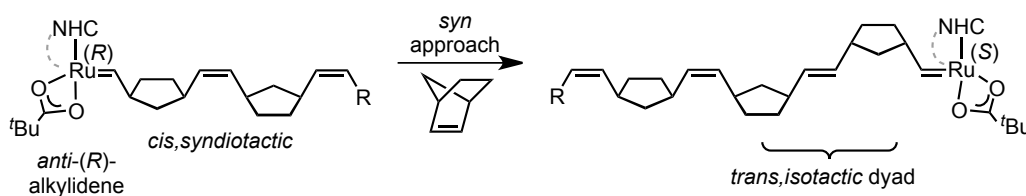
Scheme 3.4. Formation of a *trans*, isotactic dyad resulting from a *syn* approach of the monomer to an *anti* alkylidene (R = *o*-isopropoxyphenyl).

Mixed tacticities (i.e., *cis,* isotactic and *trans,* syndiotactic dyads) would result if isomerization of the *anti*-alkylidene were to occur between propagation steps, either through rotation about the M=C double bond to adopt a *syn* configuration or via a non-metathesis based polytopal rearrangement[23] between the stereoisomeric metal alkylidenes (i.e., *(R)*-**3.1** and *(S)*-**3.1**), were able to occur between propagation steps. Moreover, the degree to which these "errors" occur would be related to the barrier to these processes,

with an increase in regions of mixed tacticity being evidenced when the rate of alkylidene isomerization occurs on a comparable timescale to propagation. Competition between alkylidene isomerization and propagation would also provide a reasonable explanation for the HT bias detected in catalysts **3.1** and **3.2**, as well as the temperature effect observed in the polymerization of **3.10** with catalyst **3.2**, as outlined previously.

To explore these possible alkylidene isomerization processes, as well as to better understand how they may lead to a loss in *cis*-selectivity and tacticity in some of these cyclometalated ruthenium-based systems, DFT calculations on polymerization reactions involving catalysts **3.1** and **3.2** were performed.[24] All calculations were performed with Gaussian 09[25] at the M06/SDD-6-311+G(d,p)/SMD(THF)//B3LYP/SDD-6-31G(d) level of theory. See the Experimental for computational details.

We first investigated the likelihood of alkylidene isomerization through a non-metathesis-based polytopal rearrangement pathway. The computed energy profile of the polytopal rearrangement of the *N*-^{t}Bu-cyclometalated ruthenium alkylidene **3.16** to form its diastereomer **3.17** (using a 3-cyclopentenyl group as a model of the polymer chain) is shown in Figure 3.7. The multistep rearrangement process starts from alkylidene rotation (**3.18-TS**), which requires a relatively low barrier to form the *syn* alkylidene intermediate **3.19**. Isomerization of the alkylidene to the position *trans* to the NHC leads to highly unstable intermediate **3.21**. Complex **3.21** subsequently undergoes ring flip of the five-membered chelate (**3.22-TS**) and very unfavorable rearrangement of the pivalate ligand (**3.24-TS**) to form complex **3.25**, which then isomerizes to **3.17**. With the alkylidene *trans* to the NHC ligand, complexes **3.21**, **3.23**, and **3.25** are all highly unstable, and this process is highly disfavored.
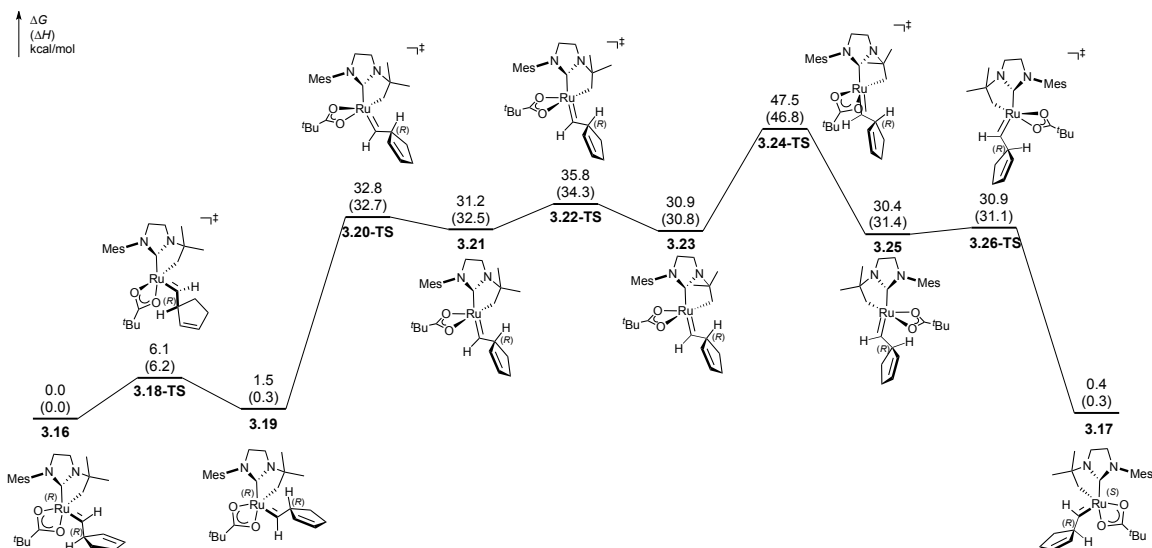
Figure 3.7. Polytopal rearrangement of ruthenium alkylidene **3.16** to its diastereomer **3.17**.

We next explored the probability of isomerization via rotation about the alkylidene Ru=C double bond. The computed rotational barriers for catalysts **3.1** and **3.2** are summarized in Table 3.8. Because of steric repulsions between the alkylidene R group and the *N*-aryl group, the *syn* alkylidene is less stable than the *anti* isomer. The

Table 3.8. Computed Alkylidene Rotation Barriers.

[Ru]	Alkylidene	$\Delta G^{\ddagger}_{rot}{}^{a}$ (kcal/mol)	$\Delta G^{\ddagger}_{(syn\text{-}anti)}{}^{b}$ (kcal/mol)
3.1		6.1	1.5
3.2		9.0	5.0
(*R,R*)-**3.2**		9.9	3.9
(*R,S*)-**3.2**		6.3	4.0

[a] Alkylidene rotational barrier with respect to the *anti* alkylidene. [b] Energy difference between *syn* and *anti* alkylidene isomers. All energies are in kcal/mol.

alkylidene rotation barrier is only slightly affected by the steric bulk of the substituent on the alkylidene and the cyclometalated group on the catalyst. In general, the barrier to alkylidene rotation is comparable to the barrier for monomer addition (see below).

Given the high barrier and the unstable intermediates in the polytopal rearrangement process, we conclude that a non-metathesis isomerization of the ruthenium alkylidene is highly unlikely to occur under the reaction conditions, and a pathway involving bond rotation about the Ru=C alkylidene is much more likely to be responsible for alkylidene isomerization. With this in mind, we can now complete our model for *cis*-selectivity and tacticity in catalysts **3.1**−**3.8** by factoring in the effects of alkylidene rotation on the final polymer microstructure. Namely, in a predominately *cis*, syndiotactic polymer resulting from stereogenic metal control, rotation of the alkylidene from *anti* to *syn* followed by monomer approach in either a *syn* or *anti* fashion would result in the formation of a *cis,* isotactic or *trans,* syndiotactic dyad, respectively (Scheme 3.5).
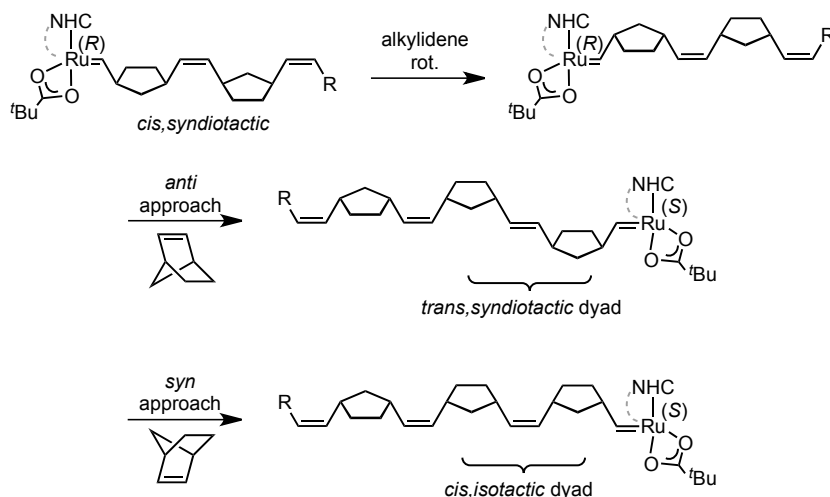
Scheme 3.5. Formation of a *trans,* syndiotactic or *cis,* isotactic dyad resulting from an *anti* or *syn* monomer approach, respectively, to a *syn* alkylidene following alkylidene rotation (*anti* to *syn*) in a predominately *cis,* syndiotactic polymer (R = *o*-isopropoxyphenyl).

We next set out to explore the possible pathways leading to the formation of each

46

type of dyad in more depth. We focused on the [2+2] cycloaddition step, as in reactions with norbornene and norbornadiene derivatives, the [2+2] cycloaddition step requires a significantly higher barrier than the [2+2] cycloelimination, and thus the [2+2] cycloaddition is effectively irreversible.[24b,26] Importantly, *cis/trans*-selectivity and tacticity are both determined in the [2+2] cycloaddition step. The four possible transition states derived for the [2+2] cycloaddition of monomer **3.10** at the *exo* face to ruthenium alkylidene **3.27**, a model of the propagating species of the *N*-^{t}Bu-cyclometalated catalyst **3.1**, are shown in Figure 3.8. Because isomerization between the *anti* and *syn* alkylidenes via rotation of the Ru=C bond occurs with a comparable barrier as propagation, monomer addition to both *anti* and *syn* alkylidenes were computed (**3.28-TS-A/B** and **3.28-TS-C/D**, respectively). In these transition states, the olefin approaches the catalyst from the side, i.e., *cis* to the NHC ligand, in line with our previous computational study of olefin cross-metathesis with cyclometalated *cis*-selective ruthenium catalysts.[21] The bottom-bound pathway, that is, olefin approaching *trans* to the NHC, and the addition to the *endo* face of the norbornadiene both require much higher activation energies (15−21 kcal/mol, see Experimental for details).

The most favorable [2+2] cycloaddition transition state is the one leading to the formation of a *cis,* syndiotactic dyad, **3.28-TS-A**, in which the *anti* alkylidene reacts with a monomer approaching in an *anti* fashion. The ligand-substrate steric repulsions in this *anti/anti* approach are minimized due to the bulk of the monomer and the alkylidene both being directed away from the *N*-aryl group. The next lowest energy transition state leads to the formation of a *trans,* syndiotactic double bond (**3.28-TS-C**), in which the *syn* alkylidene reacts with a monomer approaching in an *anti* fashion. This *anti/syn* approach

(**3.28-TS-C**) is 2.1 kcal/mol higher in energy than the *anti/anti* approach (**3.28-TS-A**), which is consistent with the high *cis*-selectivity observed experimentally. Both *trans,* isotactic and *cis,* isotactic dyads result from the monomer approaching in a *syn* fashion (**3.28-TS-B** and **3.28-TS-D**, respectively), which requires much higher activation energies due to the repulsion of the methylene bridge with the *N*-aryl group. This is in agreement with the high syndiotacticity of both the *cis* and *trans* regions observed experimentally, in the polymerizations of monomers **3.12** and **3.13** (Tables 3.4 and 3.5).
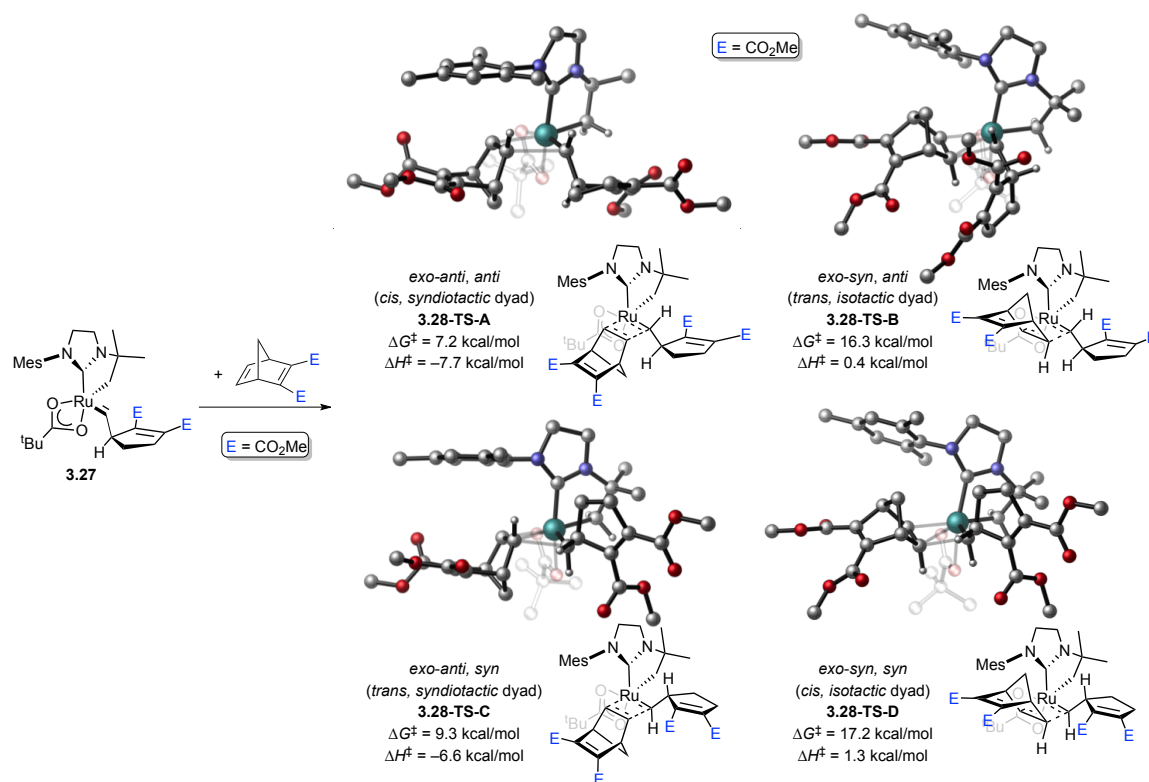
Figure 3.8. [2+2] cycloaddition transition states for the polymerization of monomer **3.10** with catalyst **3.27**. Energies are with respect to the separated ruthenium alkylidene and monomer **3.10**.

Experimentally, the polymerization of monomer **3.10** with *N*-adamantyl cyclometalated ruthenium catalysts (**3.2−3.8**) is both less *cis*-selective and less syndioselective than with catalyst **3.1** (Table 3.2). Interestingly, when the total content of

cis double bonds in **poly-3.10** is plotted against the percentage of *cis* double bonds composed as *cis, r* dyads for catalysts **3.1−3.8**, a linear dependence is observed (Figure 3.9). Because the barriers to alkylidene rotation in catalysts **3.1** and **3.2** with monomer **3.10** are comparable (*cf.* Table 3.8), this relationship is likely a result of the relative differences in the energetics of the propagation transition states for each catalyst (which also determine both *cis*- and syndioselectivity). Thus, the [2+2] cycloaddition transition states with monomer **3.10** and alkylidene **3.29**, a model of the propagating species of **3.2**, were calculated to further investigate the connection between *cis*-selectivity and tacticity in these systems.
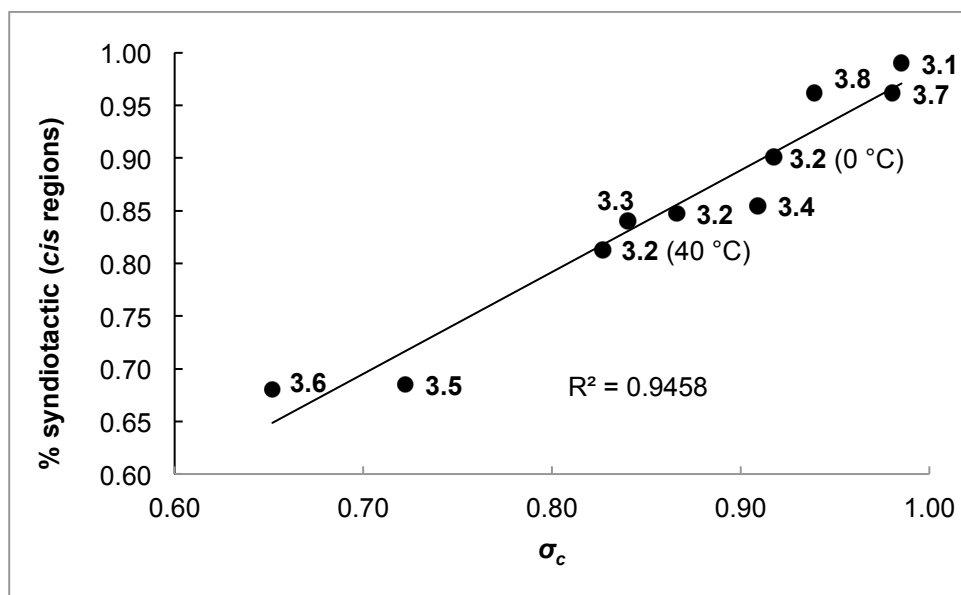
Figure 3.9. Linear relationship between *cis* content and tacticity of the *cis* regions in poly(DCMNBD) (**poly-3.10**) for catalysts **3.1−3.8** (data obtained from Table 3.2).

With the asymmetric *N*-adamantyl-cyclometalated group on catalyst **3.2**, an additional set of alkylidene diastereoisomers are possible, resulting in eight possible propagation transition states (Figure 3.10). In the most stable alkylidene isomer (*R,R*)-**3.29**, the Ru=C bond is *anti* to the *alpha* C−H bond on the cyclometalated carbon atom. In (*R,S*)-**3.29**, the Ru=C bond is *syn* to the *alpha* C−H bond. As discussed above, direct

Figure 3.10. [2+2] cycloaddition transition states for the polymerization of **3.10** with catalyst **3.2**. Energies are with respect to the separated ruthenium alkylidene and **3.10**.
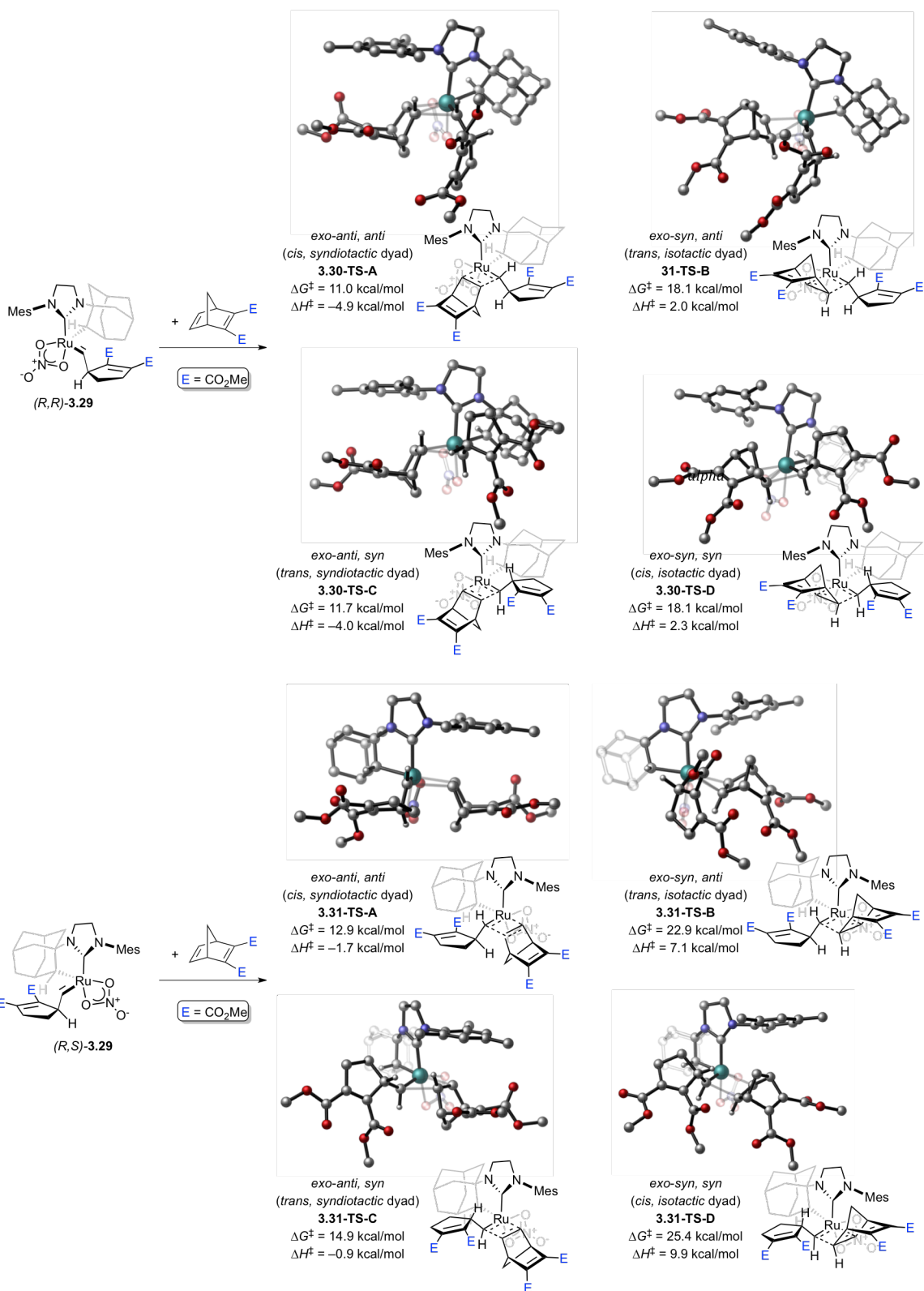
isomerization between (*R*,*R*)-**3.29** and (*R*,*S*)-**3.29** via polytopal rearrangement is not

possible. Instead, the configuration of ruthenium switches between (*R,R*)-**3.29** and (*R,S*)-**3.29** after each monomer addition.

Similar to the reaction with catalyst **3.1**, the *cis,* syndio-selective *anti/anti* approach is the most favorable with catalyst **3.2** (**3.30-TS-A** and **3.31-TS-A** for the addition to alkylidene (*R,R*)-**3.29** and (*R,S*)-**3.29**, respectively). However, the corresponding *trans,* syndio-selective transition states **3.30-TS-C** and **3.31-TS-C** are only 0.7 kcal/mol and 2.0 kcal/mol less stable, respectively. Similarly, the transition states leading to the formation of *trans,* isotactic and *cis,* isotactic dyads (**3.30-TS-B/D and 3.31-TS-B/D**, respectively), while still highly unfavorable, are also less destabilized relative to *cis,* syndio-selective **3.30-TS-A** and **3.31-TS-A**. The lower selectivity for *cis,* syndiotactic dyads is attributed to the increased steric repulsion between the alkylidene R group and the bulkier cyclometalated *N*-adamantyl group in the *cis,* syndio-selective transition states, in particular in **3.30-TS-A** where the steric bulk of the adamantyl chelate is closer to the R group than in **3.31-TS-A**. This conclusion likely extends to the other cyclometalated-*N*-adamantyl initiators **3.3−3.8**.

Conclusions

A series of cyclometalated Ru-based metathesis initiators were evaluated in the ring-opening metathesis polymerization (ROMP) of a variety of norbornene- and norbornadiene-derived monomers. Highly *cis*, syndiotactic polymers were generated in most cases. In polymers with an imperfect microstructure, the major errors were in the form of *trans,* syndiotactic regions. Using experimental and computational insights, a model was developed to explain the pattern of stereoselectivity exhibited by this family of catalysts in ROMP. The near-perfect *cis*, syndio-selectivity of these systems is

postulated to arise from the inversion of configuration at the metal center that occurs with each propagation step (i.e., stereogenic metal control), in conjunction with an almost exclusive approach of the monomer in an *anti* fashion to the energetically preferred *anti* alkylidene. The majority of microstructural errors are likely a result of interconversion between *syn* and *anti* alkylidene isomers in the propagating catalytic species. Addition of the monomer in an *anti* or *syn* fashion to the higher energy *syn* alkylidene leads to the formation of a *trans*, syndiotactic or *cis*, isotactic dyad, respectively. Finally, the highest *cis*, syndio-selectivity was exhibited by a catalyst containing a cyclometalated *N*-*t*Bu group. This was determined to originate from the decreased steric environment in this catalyst relative to the *N*-adamantyl-cyclometalated catalysts, as increased substitution close to the metal center is shown to minimize the differences in energy between transition states. The mechanistic insights gained in this study will not only aid in the development of new and improved *cis*-selective Ru-based catalysts, but also provide increased predictive power in synthetic transformations mediated by these systems.

Experimental

General Information

All reactions were carried out in dry glassware under an argon atmosphere using standard Schlenk techniques or in a Vacuum Atmospheres Glovebox under a nitrogen atmosphere, unless otherwise specified. All solvents were purified by passage through solvent purification columns and further degassed by bubbling argon. $CDCl_3$, CD_2Cl_2, and $(CD_3)_2CO$ were used as received. Monomers **3.10**,[27] **3.11**,[28] **3.12**,[29] **3.13**,[11a] and **3.15**[30] were synthesized according to literature procedure, while monomers **3.9** and **3.14** were purchased from Sigma Aldrich and used as received or distilled over CaH_2 prior to use,

respectively. Catalysts **3.2** and **3.4**, as well as RuCl$_2$(PCy$_3$)(=CH-o-O^{i}PrC$_6$H$_4$) (**S3.2**), were obtained from Materia, Inc. **3.1**,[9] **3.5**, **3.6**, **3.7**,[31] **3.8**[32] and *N*-heterocyclic carbene (NHC) **S3.1**[31] were synthesized according to literature procedures. Other commercially available reagents were used as received.

^{1}H NMR spectra were acquired at 500 MHz and ^{13}C spectra at 100 or 126 MHz as CDCl$_3$ solutions unless otherwise noted. Chemical shifts are reported in ppm downfield from Me$_4$Si by using the residual solvent peak as an internal standard. Spectra were processed and analyzed using MestReNova Ver. 9.0.

High-resolution mass spectra (HRMS) were provided by the California Institute of Technology Mass Spectrometry Facility using an IEOL JMS-600H High Resolution Mass Spectrometer. All HRMS were by FAB+ ionization.

Computational Details

Geometries were optimized with B3LYP and a mixed basis set of LANL2DZ for ruthenium and 6-31G(d) for other atoms. Single point calculations were performed with M06 and a mixed basis set of SDD for ruthenium and 6-311+G(d,p) for other atoms. The SMD solvation model with THF as solvent was used in the single point energy calculations. This is the same level of theory used in our previous calculations on ruthenium metathesis catalysts.

Preparation of Catalyst S3.3

53
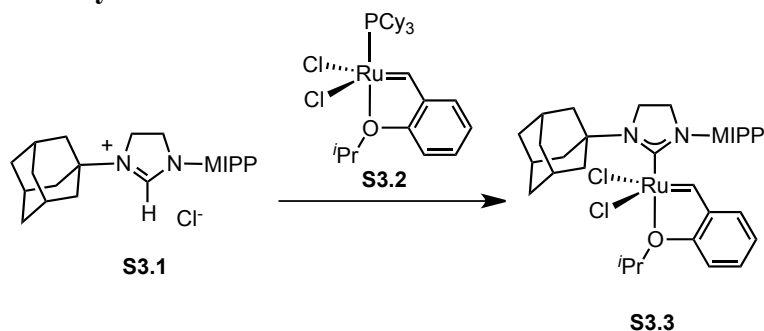
In a glovebox, a suspension of potassium *tert*-amylate (0.075 g, 0.57 mmol) in hexanes (6 mL) was added to NHC **S3.1** (0.19 g, 0.52 mmol), and the resulting solution was stirred in the glovebox box at 30 °C for 30 minutes. Then, **S3.2** (0.31 g, 0.52 mmol) was added, and the vessel was sealed, taken out of the glovebox and stirred for 2 h at 65 °C. The mixture was then cooled to RT, and the resulting solids were collected via filtration. The solids were washed thoroughly with hexanes, yielding **S3.3** (0.22 g, 65%) as a green powder.

^{1}H NMR (CDCl$_3$) δ 16.89 (1H, s), 7.54 (1H, m), 7.50 (1H, m), 7.41 (1H, m), 7.23 (1H, m), 6.93 (1H, m), 6.85 (1H, m), 5.07 (1H, m), 4.05 (2H, m), 3.88 (2H, m), 3.15 (1H, m), 2.97 (4H, m), 2.42 (3H, m), 2.33 (3H, s), 1.95 (3H, m), 1.84 (3H, m), 1.69 (3H, d, J = 6.1 Hz), 1.60 (3H, d, J = 6.1 Hz), 1.19 (3H, d, J = 6.7 Hz), 0.89 (3H, d, J = 6.7 Hz)

^{13}C NMR (CDCl$_3$) δ 208.6, 152.9, 149.0, 145.6, 141.0, 138.3, 131.0, 129.5, 129.3, 125.2, 124.2, 122.9, 113.6, 74.6, 57.6, 53.1, 44.9, 42.6 (2C), 36.5 (3C), 30.4 (3C), 28.0, 25.9, 24.2, 23.1, 22.6, 19.3

HRMS (FAB+): [M]$^{+}$ C$_{33}$H$_{44}$RuON$_2$Cl$_2$ Calculated – 656.1875, Found – 656.1894

Preparation of Catalyst S3.4
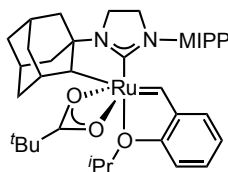
S3.4

In a glovebox, sodium pivalate (0.19 g, 1.5 mmol) in MeOH (1.5 mL) was added to complex **S3.3** (0.10 g, 0.15 mmol) in THF (1.5 mL). The solution was heated at 40 °C for ten hours in the glovebox, then concentrated. The residue was dissolved in dichloromethane, filtered over celite, and then concentrated. Purification via a short plug

of silica gel (eluant 4:1 pentane:diethyl ether) provided **S3.4** (0.052 g, 52%) as a purple solid

¹H NMR (CD$_2$Cl$_2$) δ 14.66 (1H, s), 7.38 (2H, m), 7.11 (2H, m), 6.98 (1H, m), 6.94 (1H, m), 6.92 (1H, m), 5.00 (1H, m), 3.88 (3H, m), 3.76 (3H, m), 2.20 (2H, m), 2.16 (3H, s), 2.15 (1H, m), 1.97 (2H, m), 1.71 (1H, m), 1.54 (3H, d, J = 6.1 Hz), 1.52 (3H, m), 1.40 (3H, d, J = 6.1 Hz), 1.25 (3H, d, J = 6.7 Hz), 1.21 (3H, d, J = 6.7 Hz), 1.00 (9H, s), 0.98 (1H, m), 0.23 (1H, m)

¹³C NMR (CD$_2$Cl$_2$) δ 215.8, 154.2, 147.7, 143.4, 138.7, 138.1, 128.8, 128.1, 125.8, 124.3, 123.2, 123.0, 114.1, 74.9, 69.3, 63.0, 53.1, 43.5, 41.9, 40.6, 39.4, 38.2, 37.9, 37.1, 33.7, 31.2, 30.1, 28.5, 28.3 (3C), 26.3, 24.0, 21.9, 21.8, 19.5

HRMS (FAB+): [M]$^+$ C$_{38}$H$_{52}$RuO$_3$N$_2$ Calculated – 686.3022, Found – 686.3039

Preparation of 3.3
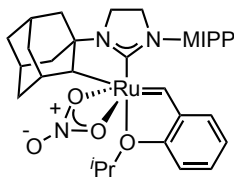
3.3

In a glovebox, complex **S3.4** (0.11 g, 0.15 mmol) and NH$_4$NO$_3$ (0.12 g, 1.5 mmol) were dissolved in THF (8 mL), stirred for 3 h at room temperature, then concentrated. The resulting solids were washed with Et$_2$O, then THF, to provide **3.3** (0.070 g, 72%) as a bright purple powder.

¹H NMR (CD$_2$Cl$_2$) δ 14.98 (1H, s), 7.48 (1H, m), 7.43 (1H, m), 7.13 (1H, m), 7.09 (1H, m), 6.98 (3H, m), 5.10 (1H, m), 3.90 (4H, m), 3.70 (2H, m), 2.23 (1H, m), 2.18 (3H, s), 2.07 (1H, m), 1.99 (1H, m), 1.93 (1H, m), 1.72 (1H, m), 1.65 (1H, m), 1.59 (1H, m), 1.55 (2H, m), 1.49 (3H, d, J = 6.1 Hz), 1.24 (3H, d, J = 6.1 Hz), 1.18 (3H, d, J = 6.7 Hz), 1.13

(3H, d, $J = 6.7$ Hz), 0.99 (2H, m), 0.25 (1H, m).

^{13}C NMR (CD$_2$Cl$_2$) δ 213.2, 154.9, 147.8, 143.2, 138.1, 137.5, 128.8, 128.4, 127.3, 124.2, 123.6 (2C), 113.1, 74.6, 67.8, 63.6, 52.8, 43.4, 42.4, 40.5, 38.0, 37.9, 37.8, 33.4, 31.1, 29.9, 28.5, 26.4, 23.7, 21.5, 20.8, 17.7.

HRMS (FAB+): [M+H]$^+$ C$_{33}$H$_{44}$RuO$_4$N$_3$ Calculated – 645.7706, Found – 646.2040

General Polymerization Procedure

In a glovebox, a solution of catalyst was prepared from **3.1** (5.8 mg, 9.8 μmol) and THF (0.84 mL) and added to an 8 mL vial with a septum cap. On a vacuum manifold, a Schlenk flask was flame-dried and charged with monomer (7.8 mmol) and THF (24 mL) to make a stock solution (0.32 M). The monomer solution was degassed via freeze-pump-thaw (3×). An aliquot (2.0 mL, 0.64 mmol) of monomer stock solution was added via gas-tight syringe to an air-tight vial with a septum cap under an argon balloon. An aliquot (0.55 mL, 6.4 μmol) of catalyst solution was then injected via gas-tight syringe. After stirring for 1 h at room temperature, the polymerization was quenched with ethyl vinyl ether (0.1 mL) and precipitated into vigorously stirred MeOH. The precipitate was collected by vacuum filtration using either a medium or fine porosity frit and dried under vacuum.

Preparation of Poly-3.9 Using Catalysts 3.1−3.8:

Poly-3.9 was prepared according to the general procedure using catalysts **3.1−3.8**. NMR samples were prepared by stirring **poly-3.9** in CDCl$_3$. ^{13}C NMR spectral assignments were consistent with the literature.[33]

Preparation of Poly-3.10 Using Catalysts 3.1−3.8:

Poly-3.10 was prepared according to the general procedure using catalysts **3.1−3.8**. NMR

samples were prepared by stirring **poly-3.10** in CDCl$_3$. ^{13}C NMR spectral assignments were consistent with the literature.[15]

Preparation of Poly-3.11 Using Catalysts 3.1, **3.2**, **and 3.4:**

Poly-3.11 was prepared according to the general procedure using catalysts **3.1**, **3.2**, and **3.4**. NMR samples were prepared by stirring **poly-3.11** in (CD$_3$)$_2$CO. ^{13}C NMR spectral assignments were consistent with the literature.[16]

Preparation of Poly-3.12 Using Catalysts 3.1, **3.2**, **and 3.4:**

Poly-3.12 was prepared according to the general procedure using catalysts **3.1**, **3.2**, and **3.4**. NMR samples were prepared by stirring **poly-3.12** in CD$_2$Cl$_2$. ^{13}C NMR spectral assignments were consistent with the literature.[15]

Preparation of Poly-3.13 Using Catalysts 3.1 and 3.2:

Poly-3.13 was prepared according to the general procedure using catalysts **3.1** and **3.2**. NMR samples were prepared by stirring **poly-3.13** in CDCl$_3$. ^{13}C NMR spectral assignments were consistent with the literature.[17]

Preparation of Poly-3.14 Using Catalysts 3.1, **3.2**, **and 3.4:**

Poly-3.14 was prepared according to the general procedure using catalysts **3.1**, **3.2**, and **3.4**. NMR samples were prepared by stirring **poly-3.14** in CDCl$_3$. ^{13}C NMR spectral assignments were consistent with the literature.[19]

Preparation of Poly-3.15 Using Catalysts 3.1 and 3.2:

Poly-3.15 was prepared according to the general procedure using catalysts **3.1** and **3.2**. NMR samples were prepared by stirring **poly-3.15** in CDCl$_3$. ^{13}C NMR spectral assignments were consistent with the literature.[20]

References

1. (a) Haas, F.; Theisen, D. Kautsch. *Gummi Kunstst.* **1970**, *23*, 502. (b) Edwards, J. H.; Feast, W. J.; Bott, D. C. *Polymer* **1984**, *25*, 395. (c) Ofstead, E. A. In *Encyclopedia of Polymer Science and Engineering*, 2nd ed.; Wiley: New York, 1988; Vol. *11*. (d) Park, L. Y.; Schrock, R. R.; Stieglitz, S. G.; Crowe, W. E. *Macromolecules* **1991**, *24*, 3489. (e) Dounis, P.; Feast, W. J.; Kenwright, A. M. *Polymer* **1995**, *36*, 2787. (f) Lee, C.; Wong, K.; Lam, W.; Tang, B. *Chem. Phys. Lett.* **1999**, *307*, 67. (g) Wong, K. S.; Lee, C. W.; Zang, B. Z. *Synth. Met.* **1999**, *101*, 505.

2. (a) Grubbs, R. H. In *Handbook of Metathesis*; Wiley-VCH: Weinheim, Germany, 2003. (b) Ivin, K. J.; Mol, J. C. *Olefin Metathesis and Metathesis Polymerization*; Academic Press: San Diego, 1997.

3. (a) Schrock, R. R. *Dalton Trans.* **2011**, *40*, 7484. (b) Schrock, R. R. *Acc. Chem. Res.* **2014**, *47*, 2457.

4. (a) McConville, D. H.; Wolf, J. R.; Schrock, R. R. *J. Am. Chem. Soc.* **1993**, *115*, 4413. (b) O'Dell, R.; McConville, D. H.; Hofmeister, G. E.; Schrock, R. R. *J. Am. Chem. Soc.* **1994**, *116*, 3414. (c) Schrock, R. R.; Lee, J. K.; O'Dell, R.; Oskam, J. H. *Macromolecules* **1995**, *28*, 5933. (d) Totland, K. M.; Boyd, T. J.; Lavoie, G. G.; Davis, W. M.; Schrock, R. R. *Macromolecules* **1996**, *29*, 6114.

5. (a) Flook, M. M.; Jiang, A. J.; Schrock, R. R.; Müller, P.; Hoveyda, A. H. *J. Am. Chem. Soc.* **2009**, *131*, 7962. (b) Flook, M. M.; Ng, V. W. L.; Schrock, R. R. *J. Am. Chem. Soc.* **2011**, *133*, 1784. (c) Flook, M. M.; Ng, V. W. L.; Schrock, R. R. *J. Am. Chem. Soc.* **2011**, *133*, 1784. (b) Schrock, R. R. *Dalton Trans.* **2011**, *40*, 7484. (d) Flook, M. M.; Börner, J. Kilyanek, S. M.; Gerber, L. C. H.; Schrock, R. R.

Organometallics **2012**, *31*, 6231. (e) Jeong, H.; Kozera, D. J.; Schrock, R. R.; Smith, S. J.; Zhang, J.; Ren, N.; Hillmyer, M. A. *Organometallics* **2012**, *31*, 6231. (f) Forrest, W. P.; Axtell, J. C.; Schrock, R. R. *Organometallics* **2014**, *33*, 2313. (g) Forrest, W. P.; Weis, J. G.; John, J. M.; Axtell, J. C.; Simpson, J. H.; Swager, T. M.; Schrock, R. R. *J. Am. Chem. Soc.* **2014**, *136*, 10910.

6. (a) Bazan, G. C.; Khosravi, E.; Schrock, R. R.; Feast, W. J.; Gibson, V. C.; O'Regan, M. B.; Thomas, J. K.; Davis, W. M. *J. Am. Chem. Soc.* **1990**, *112*, 8378.

7. (a) Delaude, L.; Demonceau, A.; Noels, A. F. *Macromolecules* **1999**, *32*, 2091. (b) Delaude, L.; Demonceau, A.; Noels, A. F. *Macromolecules* **2003**, *36*, 1446. (c) Lee, J. C.; Parker, K. A.; Sampson, N. S. *J. Am. Chem. Soc.* **2006**, *128*, 4578. (d) Lin, W.-Y.; Wang, H.-W.; Liu, Z.-C.; Xu, J.; Chen, C.-W.; Yang, Y.-C.; Huang, S.-L.; Yang, H.-C.; Luh, T.-Y. *Chem.—Asian J.* **2007**, *2*, 764. (e) Song, A. R.; Lee, J. C.; Parker, K. A.; Sampson, N. S. *J. Am. Chem. Soc.* **2010**, *132*, 10513. (f) Leitgeb, A.; Wappel, J.; Slugovc, C. *Polymer* **2010**, *51*, 2927. (g) Kobayashi, S.; Pitet, L. M.; Hillmyer, M. A. *J. Am. Chem. Soc.* **2011**, *133*, 5794. (h) Zhang, J.; Matta, M. E.; Martinez, H.; Hillmyer, M. A. *Macromolecules* **2013**, *46*, 2535.

8. Straub, B. F. *Adv. Synth. Catal.* **2007**, *349*, 204.

9. Rosebrugh, L. R.; Marx, V. M.; Keitz, B. K.; Grubbs, R. H. *J. Am. Chem. Soc.* **2013**, *135*, 10032.

10. Keitz, B. K.; Fedorov, A.; Grubbs, R. H. *J. Am. Chem. Soc.* **2012**, *134*, 2040.

11. (a) Grutzner, J. B.; Jautelat, M.; Dence, J. B.; Smith, R. A.; Roberts, J. D. *J. Am. Chem. Soc.* **1970**, *92*, 7107. (b) Ivin, K. J.; Laverty, D. T.; Rooney, J. J. *Makromol. Chem.* **1977**, *178*, 1545.

12. In general, quantitative conversion of monomer to polymer was observed when using catalysts **1**-**7**. Monodentate catalysts **8** and **9** were less active that their bidentate counterparts, however, giving 20-50% yield.

13. (a) Ivin, K. J.; Laverty, D. T.; Rooney, J. J. *Makromol. Chem.* **1978**, *179*, 253. (a) Ivin, K. J.; Laverty, D. T.; O'Donnell, J. H.; Rooney, J. J.; Stewart, C. D. *Makromol. Chem.* **1979**, *180*, 1989. (b) Gillan, E. M. D.; Hamilton, J. G.; Mackey, N. D.; Rooney, J. J. *J. Mol. Catal.* **1988**, *46*, 359.

14. Greene, R. M. E.; Hamilton, J. G.; Ivin, K. J.; Rooney, J. J. *Makromol. Chem.* **1986**, *187*, 619.

15. Amir-Ebrahimi, V.; Corry, D. A. K.; Hamilton, J. G.; Rooney, J. J. *J. Mol. Catal. A-Chem.* **1998**, *133*, 115.

16. (a) Davies, G. R.; Feast, W. J.; Gibson, V. C.; Hubbard, H. V. S. A.; Ivin, K. J.; Kenwright, A. M.; Khosravi, E.; Marshall, E. L.; Mitchell, J. P.; Ward, I. M.; Wilson, B. *Makromol. Chem., Macromol. Symp.* **1993**, *66*, 289. (b) McConville, D. H.; Wolf, J. R.; Schrock, R. R. *J. Am. Chem. Soc.* **1993**, *115*, 4413.

17. (a) Hamilton, J. G.; Ivin, K. J.; Rooney, J. J. *J. Mol Catal.* **1985**, *28*, 255. (b) Feast, W. J.; Gibson, V. C.; Ivin, K. J.; Khosravi, E.; Kenwright, A. M.; Marshall, E. L.; Mitchell, J. P. *Makromol. Chem.* **1992**, *193*, 2103.

18. (a) Arnold, D. R.; Trecker, D. J. Whipple, E. B. *J. Am. Chem. Soc.* **1965**, *87*, 2596. (b) Gilliom, L. R.; Grubbs, R. H. *J. Am. Chem. Soc.* **1986**, *108*, 733.

19. (a) Ivin, K. J.; Lapienis, G.; Rooney, J. J.; Stewart, C. D. *J. Mol. Catal.* **1980**, *8*, 203. (b) Ivin, K. J.; Laverty, D. T.; Reddy, B. S. R.; Rooney, J. J. *Makromol. Chem., Rapid Commun.,* **1980**, *1*, 467.

20. Ho, H. T.; Ivin, K. J.; Rooney, J. J. *Makromol. Chem.* **1982**, *183*, 1629.

21. Liu, P.; Xu, X.; Dong, X.; Keitz, B. K.; Herbert, M. H.; Grubbs, R. H.; Houk, K. N. *J. Am. Chem. Soc.* **2012**, *134*, 1464.

22. Hartung, J.; Grubbs, R. H. *J. Am. Chem. Soc.* **2013**, *135*, 10183.

23. (a) Khan, R. K. M.; Zhugralin, A. R.; Torker, S.; O'Brien, R. V.; Lombardi, P.J.; Hoveyda, A. H. *J. Am. Chem. Soc.* **2012**, *134*, 12438. (b) Torker, S.; Khan, R. K. M.; Hoveyda, A. H. *J. Am. Chem. Soc.* **2014**, *136*, 3439.

24. For computational studies on ROMP with noncyclometalated ruthenium catalysts: (a) Song, A.; Chul-Lee, J.; Parker, K. A.; Sampson, N. S. *J. Am. Chem. Soc.* **2010**, *132*, 10513. (b) Martinez, H.; Miro, P.; Charbonneau, P.; Hillmyer, M. A.; Cramer, C. *J. ACS Catal.* **2012**, *2*, 2547.

25. Frisch, M. J.; Trucks, G. W.; Schlegel, H. B.; Scuseria, G. E.; Robb, M. A.; Cheeseman, J. R.; Scalmani, G.; Barone, V.; Mennucci, B.; Petersson, G. A.; Nakatsuji, H.; Caricato, M.; Li, X.; Hratchian, H. P.; Izmaylov, A. F.; Bloino, J.; Zheng, G.; Sonnenberg, J. L.; Hada, M.; Ehara, M.; Toyota, K.; Fukuda, R.; Hasegawa, J.; Ishida, M.; Nakajima, T.; Honda, Y.; Kitao, O.; Nakai, H.; Vreven, T.; Montgomery, J. A., Jr.; Peralta, J. E.; Ogliaro, F.; Bearpark, M.; Heyd, J. J.; Brothers, E.; Kudin, K. N.; Staroverov, V. N.; Kobayashi, R.; Normand, J.; Raghavachari, K.; Rendell, A.; Burant, J. C.; Iyengar, S. S.; Tomasi, J.; Cossi, M.; Rega, N.; Millam, M. J.; Klene, M.; Knox, J. E.; Cross, J. B.; Bakken, V.; Adamo, C.; Jaramillo, J.; Gomperts, R.; Stratmann, R. E.; Yazyev, O.; Austin, A. J.; Cammi, R.; Pomelli, C.; Ochterski, J. W.; Martin, R. L.; Morokuma, K.; Zakrzewski, V. G.; Voth, G. A.; Salvador, P.; Dannenberg, J. J.; Dapprich, S.; Daniels, A. D.; Farkas, Ö.; Foresman, J.

B.; Ortiz, J. V.; Cioslowski, J.; Fox, D. J. Gaussian 09, revision D.01; Gaussian, Inc.: Wallingford, CT, 2009.

26. (a) Chen, P.; Adlhart, C. *J. Am. Chem. Soc.* **2004**, *126*, 3496. (b) Naumov, S.; Buchmeiser, M. R. *J. Phys. Org. Chem.* **2008**, *21*, 963.

27. Tabor, D.C.; White, F.H.; Collier, L.W.; Evans, S.A. *J. Org. Chem.* **1983**, *48*, 1638.

28. Alimuniar, A. B.; Blackmore, P. M.; Edwards, J. H.; Feast, W. J.; Wilson, B. *Polymer* **1986**, *27*, 1281.

29. Mühlebach, A.; Bernhard, P.; Bühler, N.; Karlen, T.; Ludi, A. *J. Mol. Catal.* **1994**, *90*, 143.

30. (a) Ishihara, K.; Hanaki, N.; Funahashi, M.; Miyata, M.; Yamamoto, H. *Bull. Chem. Soc. Jpn.* **1995**, *68*, 1721. (b) Evans, D. A.; Barnes, D. M.; Johnson, J. S.; Lectka, T.; von Matt, P.; Miller, S. J.; Murry, J. A.; Norcross, R. D.; Shaughnessy, E. A.; Campos, K. R. *J. Am. Chem. Soc.* **1999**, *121*, 7582. (c) Berson, J. A.; Walia, J. S.; Remanick, A.; Suzuki, S.; Reynolds-Warnhoff, P.; Willner, D. *J. Am. Chem. Soc.* **1961**, *83*, 3986.

31. Keitz, B. K.; Endo, K.; Patel, P. R.; Herbert, M. B.; Grubbs, R. H. *J. Am. Chem. Soc.* **2012**, *134*, 693.

32. Van Wingerden, M. M. PhD Dissertation, California Institute of Technology, 2012. It is worthy to note that although this procedure employs both NBu_4Cl and NH_4Cl, NBu_4Cl could be omitted, promoting ease of purification.

33. Ivin, K. J.; Laverty, D. T.; Rooney, J. J. *Makromol. Chem.* **1977**, *178*, 1545.

Chapter 4

Metathesis and Decomposition of Fischer Carbenes of Cyclometalated

Z-Selective Ruthenium Metathesis Catalysts

Abstract

The addition of vinyl ethers to *Z*-selective, cyclometalated ruthenium metathesis catalysts generates Fischer carbene complexes. Although Fischer carbenes are usually thought to be metathesis-inactive, we show that Fischer carbenes are metathesis-active under certain circumstances. These species were found to decompose facilely to Ru-hydride complexes identified by both experiment and computation. Since vinyl ethers are often used to quench metathesis reactions with Ru-based metathesis catalysts, their decomposition to hydrides can have a deleterious effect on the desired stereochemistry of the olefin product.

Introduction

Olefin metathesis has become a favored method for the generation of carbon-carbon double bonds and has been implemented in countless fields including green chemistry,[1] organic synthesis,[2] materials science,[3] and pharmaceuticals.[4] Ruthenium-based catalysts used for this transformation exhibit excellent stability, functional group tolerance, and general ease of use.[5] Reactions utilizing these catalysts are often quenched by the addition of an excess of a vinyl ether.[6] As an example, ethyl vinyl ether reacts with catalyst **4.1** to form Fischer carbene ruthenium complex **4.2** (Scheme 4.1).[7-9]
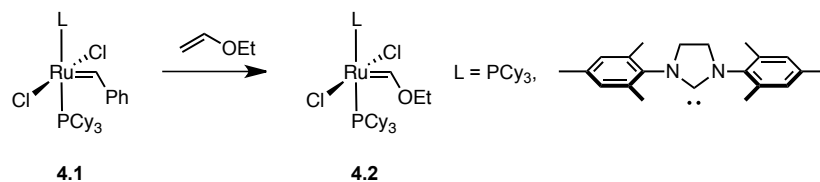
Scheme 4.1. Formation of Fischer carbene complexes by reaction of ethyl vinyl ether with olefin metathesis catalysts.

Due to their stabilities, Fischer carbenes are considered metathesis inactive under standard conditions. However, Fischer carbenes have been found to be active at elevated

temperatures and with specific substrates.[9,10] Takahira and Morizawa demonstrated the ability of **2**, bearing the 1,3-dimesityl-4,5-dihydroimidazol-2-ylidene (SIMes) ligand, to catalyze productive metathesis using heavily fluorinated olefins, albeit with very low catalyst turnover.[10] The unexpected activity of these ruthenium complexes is due to the relative thermodynamic stability of the fluoro-Fischer carbene formed by metathesis, or Fischer carbene exchange, with **4.2**.
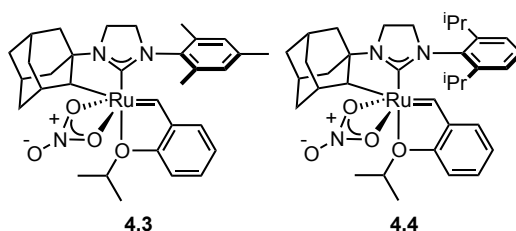
Figure 4.1. Prominent *Z*-selective catalysts.

In 2011, kinetically *Z*-selective ruthenium-based catalysts were reported bearing an adamantyl-chelated NHC ligand and pivalate X-type ligand.[11] Many analogs have now been synthesized, including the nitrate-substituted, highly active and *Z*-selective catalysts **4.3**[12] and **4.4** (Figure 4.1).[13] Mechanistic and decomposition studies of these types of cyclometalated complexes have been carried out with both experiment and theory.[14,15] Decomposition proceeds via irreversible insertion of the alkylidene into the chelating ruthenium-carbon bond to produce a ruthenium alkyl intermediate (**4.6**, Scheme 4.2). Subsequent α-hydride elimination gives **4.7** while β-hydride elimination provides **4.8**. Both experimental and theory show that β-hydride elimination from **4.6** to form **4.8** is the preferred mechanistic pathway for the catalyst diastereomeric form of **4.3**, **4.4**, and **4.5**.[15]

Because other Ru-based Fischer carbenes have exhibited impressive stability, reactions using these cyclometalated metathesis catalysts are also often quenched by vinyl ethers.[16] Herein we report reactions of **4.3** and **4.4** with vinyl ethers and identify a
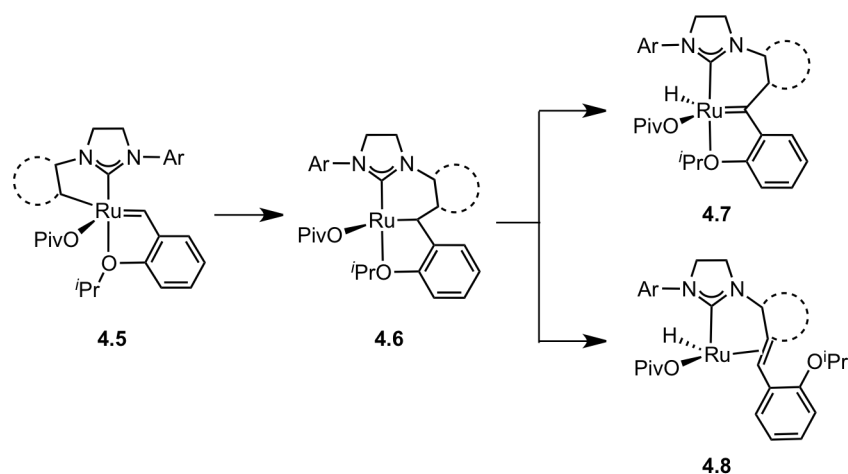
Scheme 4.2. Decomposition pathway of cyclometalated ruthenium catalyst **4.5**. (Dashed circle = adamantyl, *o*-tolyl; Ar = DIPP or Mes)

ruthenium hydride decomposition product potentially capable of causing olefin isomerization.[17] Computations were used to explore the decomposition and we have found that a metathesis reaction of the Fischer carbene is an integral part of the decomposition pathway.

Results and Discussion

The reactions of phenyl vinyl ether with chelated catalysts **4.3** and **4.4** were performed in THF-d_8 and monitored using ^{1}H NMR spectroscopy. For each of these catalysts, generation of a species posited to be a Fischer carbene was observed by the appearance of a peak shifted upfield (~14 ppm) with respect to the original alkylidene signal.[18] Subsequent formation of a Ru-hydride species from each of these complexes was observed by the appearance of ^{1}H NMR signals at −12.16 ppm and −11.97 ppm, respectively (Scheme 4.3).[19] Identification of these complexes by NMR spectroscopy was challenging due to significant overlap of aromatic ^{1}H and ^{13}C signals derived from phenyl vinyl ether, 2-isopropoxystyrene eliminated by reaction, and the *N*-mesityl group of the NHC ligand of the catalyst.[20] Consequently, the reaction of butyl vinyl ether with 1 equivalent of **4.3** in THF-d_8 was studied in order facilitate analysis of the complex by

NMR spectroscopy. The results of this reaction mirrored the observations of the reactions with phenyl vinyl ether. The disappearance of the ^{1}H signal corresponding to the benzylidene proton of **4.3** and the appearance of a broad peak of the proposed Fischer carbene at 13.83 ppm was observed.[21] The subsequent disappearance of this signal and concurrent appearance of a new signal at −12.62 ppm indicated the formation of the hydride species in quantitative yield.

4.9: Ar = Mes, R = Ph
4.10: Ar = DIPP, R = Ph
4.11: Ar = Mes, R = [n]Bu

decompose to Ru-H species
under reaction conditions

R = Ph, [n]Bu
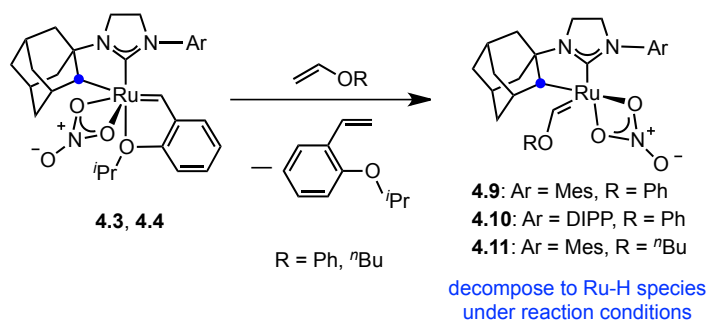
Scheme 4.3. Reactions of *Z*-selective catalysts **4.3** and **4.4** with vinyl ethers generate Fischer carbenes that decompose to Ru-hydride complexes as observed by ^{1}H NMR spectroscopy in THF-d_8.

Analogous to previously reported decomposition routes of cyclometalated Ru-based *Z*-selective catalysts, pathways from the Fischer carbene complex to two possible ruthenium hydride complexes were conceivable (Scheme 4.4). After initial insertion of

α-hydride elimination

4.13

4.12

β-hydride elimination

4.14
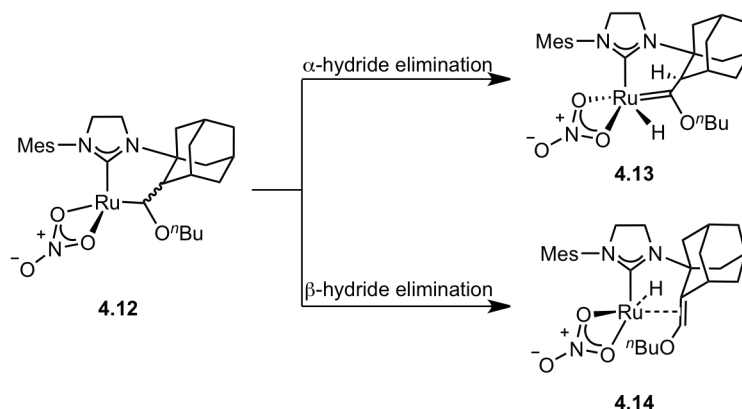
Scheme 4.4. Possible pathways of decomposition of the Fischer carbene complexes under reaction conditions to form Ru-hydride complexes **4.13** or **4.14** from insertion intermediate **4.12**.

the alkylidene into the Ru-adamantyl bond to form a ruthenium alkyl species **4.12**, α-hydride elimination would generate **4.13** while a β-hydride elimination pathway would give product **4.14**.

In the ^{1}H NMR spectrum of this reaction mixture, a singlet corresponding to a single proton appears at 5.12 ppm, consistent with that of the alkene proton of known β-hydride decomposition products of *Z*-selective catalysts.[15] Furthermore, a signal characteristic of the carbon of a Ru=C bond around 300 ppm was not observed in the ^{13}C NMR spectrum.[22,23] These data are consistent with the structure of the β-hydride elimination product **4.14** rather than **4.13**.

To confirm the connectivity and structure of the decomposition product, ^{1}H-^{13}C HMBC studies were performed and correlations between the methylenes of the butyl group to the aforementioned alkenyl singlet were observed at 5.12 ppm, which furthermore shows correlations with the protons of the adamantyl group. Further supporting this proposed structure, the hydride showed correlations with the alkenyl carbons, the carbene carbon of the NHC, and a methylene carbon of the butyl group in the ^{1}H-^{13}C HMBC. These correlations are consistent with the structure of **4.14**. ^{13}C-DEPT experiments showed the existence of 4 methyl groups, 10 methylene groups, 6 methine groups, 7 quarternary carbons in the structure of this complex, which agrees with the proposed structure.

Density functional calculations were performed to determine the decomposition pathways available to Fisher carbenes derived from complex **4.3**. Reaction of **4.3** with phenyl vinyl ether leads to formation of Fischer carbene complex **4.9** (Scheme 4.5). However, **4.9** cannot lead to the observed product **4.15** via migratory insertion and β-
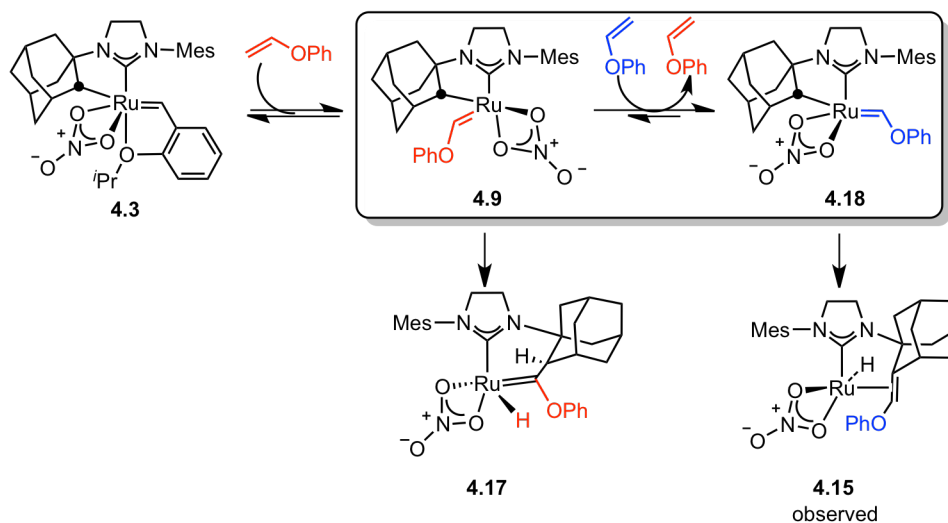
Scheme 4.5. Fischer carbene exchange pathway to reach the observed β-hydride elimination product **4.15**.

hydride elimination.[15] Figure 4.2 is a top view of **4.9** and the subsequent migratory insertion intermediate, **4.16**. The hydrogen on the chelated carbon of **4.9**, highlighted in green in the 3D images of Figure 4.2, is on the same side as the Fischer carbene and far from the ruthenium center. After migratory insertion to **4.16**, this green β-hydrogen is pushed even further from the ruthenium center, to a distance of 3.84 Å. The highlighted β-hydrogen is not available for elimination due to this distance and thus prevented from direct degradation to the observed product **4.15**. DFT results (Figure S4.18) indicate that
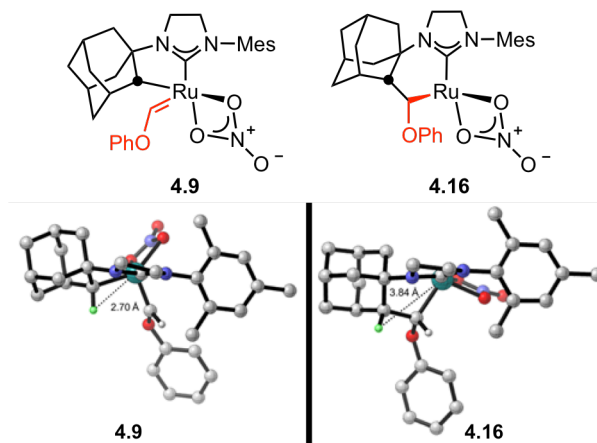
Figure 4.2. View of **4.9** and **4.16**, looking down on the NHC. β-hydrogen highlighted in green.

migratory insertion followed by rearrangement and α-hydride elimination could occur to produce **4.17** with a rate-determining barrier of 25.5 kcal/mol. However, this product has not been observed experimentally.

Since the calculations showed that **4.9** could not lead directly to the observed product **4.15**, there must be an alternative, lower energy path to decomposition of **4.9**. Based on recent precedent for Fischer carbene exchange,[10] we propose epimerization of Fischer carbene **4.9** to **4.18** via metathesis with excess vinyl ether.[24] Complex **4.18** could then decompose to experimentally observed hydride **4.15** via the previously reported pathway shown in Scheme 4.2.

The free energy surface for Fischer carbene exchange is shown in Figure 4.3. The [2+2] cycloaddition of **4.9** with phenyl vinyl ether has a barrier of only 14.2 kcal/mol to form metallacycle **4.20**. Isomerization of **4.20** to **4.21** followed by retro-[2+2] via **4.22-TS** leads to diastereomeric Fischer carbene **4.18**. Carbene rotation leads to the more stable conformer **4.18'**. Calculated barriers for the homodimerization of olefins with
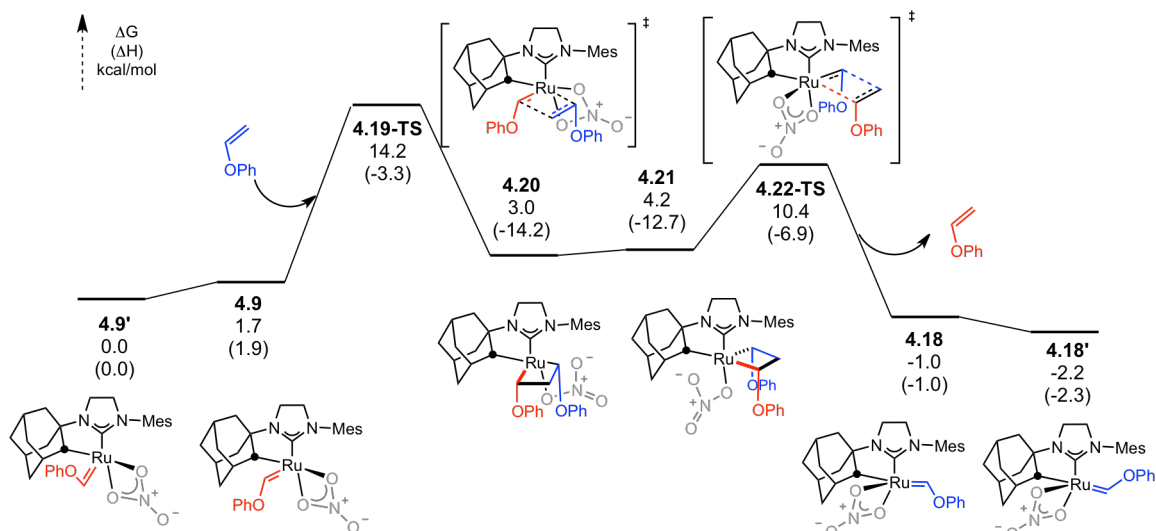
Figure 4.3. Metathesis of Fischer carbene **4.9** with phenyl vinyl ether to form the thermodynamically more stable diastereomer **4.18'**.

catalyst **4.3** and analogues range from ~11−15 kcal/mol and are comparable to the barrier for Fischer carbene exchange.[14,25] Metathesis of **4.9** with vinyl ethers is therefore both kinetically and thermodynamically feasible.

The decomposition pathways of complexes **4.18** and **4.18'** were also calculated. Decomposition of **4.18** leads to the more thermodynamically stable hydride and is shown in Figure 4.4.[26] Carbene insertion via **4.23-TS** has a barrier of 25 kcal/mol from **4.18**. This barrier is slightly lower than that reported for the carbene insertion of catalyst **4.5**.[15] β-hydride elimination from **4.24** is essentially barrierless and leads directly to hydride **4.15**, with the vinyl ether acting as a chelating π-ligand.

Reaction of catalyst **4.3** with 0.1 equivalents of butyl vinyl ether in THF-d_8 leads to quantitative conversion of the butyl vinyl ether to **4.15**, indicating that an excess of vinyl ether is not necessary for decomposition. This result is consistent with our predicted metathesis-dependent decomposition pathway as long as catalyst initiation to **4.9** is slower than Fischer carbene exchange from **4.9** to **4.18**. Wang et al. previously computed initiation of **4.3** with styrene. The rate-limiting step of the initiation is retro-[2+2] to form the free 2-isopropoxystyrene.[25] The computed barrier for this step in the reaction of **4.3** with phenyl vinyl ether is 23.4 kcal/mol.[27] Therefore, initiation is significantly slower than carbene exchange. During the decomposition process, only a small portion of the catalyst will be initiated to **4.9** then the remaining vinyl ether will react rapidly with **4.9**, epimerizing the complex to **4.18** (leading to hydride **4.15**). This final step regenerates an equivalent of vinyl ether, leading to net consumption of one equivalent of vinyl ether per equivalent of catalyst in the decomposition process.
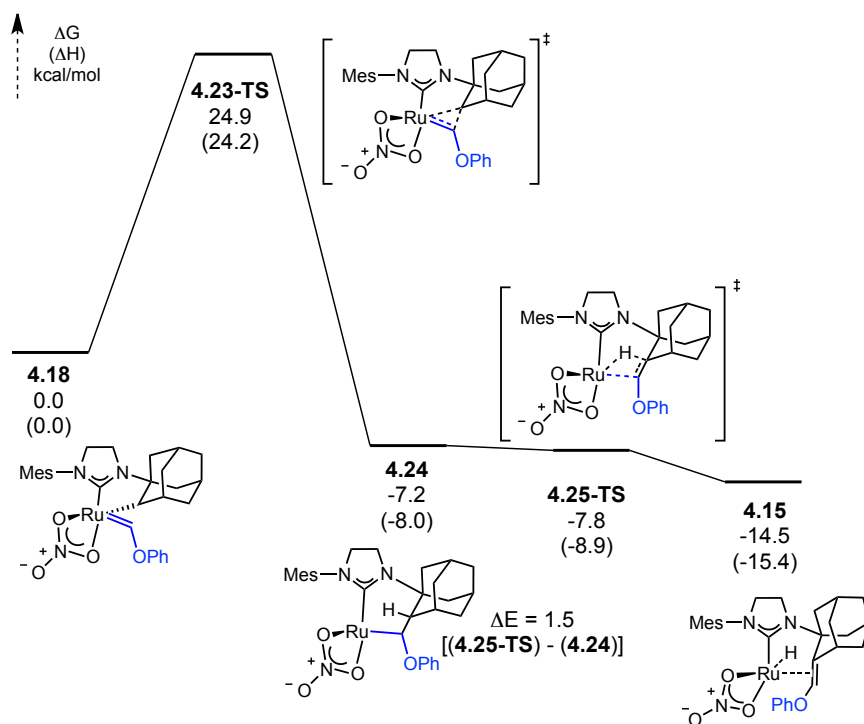
Figure 4.4. Decomposition of Fischer carbene **4.18** to hydride **4.15**.

Conclusions

It has been demonstrated that Fischer carbenes are formed from reactions of vinyl ethers with cyclometalated *Z*-selective ruthenium metathesis catalysts. These Fischer carbenes degrade to ruthenium hydrides rapidly under the reaction conditions, as identified by ^{1}H NMR experiments. Using DFT, we have also shown that Fischer carbenes such as **4.9** and **4.18** are not metathesis inactive if carbenes of similar stability result. These results have an important impact for future use of vinyl ethers to quench reactions involving cyclometalated *Z*-selective catalysts. When vinyl ethers are used to quench a metathesis reaction, ruthenium hydrides can form rapidly in the reaction mixture if the Fischer carbene is not separated promptly. The presence of hydrides can potentially lead to degradation of the *Z*-olefin content or olefin walking. Experiments to determine how these hydrides affect internal olefins are currently underway.

Experimental

General Information

Unless otherwise specified, all reactions were carried out under a nitrogen atmosphere in a Vacuum Atmospheres Glovebox in dry glassware. Solvents were purified by passage through solvent purification columns and sparged with argon. THF-d_8 was dried over Na/benzophenone, vacuum transferred into a dried Schlenk flask, and subsequently degassed by methods of freeze-pump-thaw. Phenyl vinyl ether was prepared by literature procedure.[28] Phenyl vinyl ether and butyl vinyl ether (Sigma-Aldrich) were sparged with argon and filtered over neutral alumina (Brockmann I) prior to use. Catalysts **4.3** and **4.4** were provided by Materia, Inc.

Standard NMR experiments were conducted using a Bruker 400 MHz instrument and a Varian Inova 400 MHz instrument unless otherwise specified. Variable temp NMR experiments were conducted on a Varian Inova 600 MHz instrument. Chemical shifts are reported in ppm downfield using the residual solvent peak as a reference. NMR spectra were analyzed and processed using MestReNova version 8.1.2-11880.

A JEOL MSRoute mass spectrometer was used to obtain high-resolution mass-spectrometry data using FAB+ ionization.

Synthesis of 2-isopropoxybenzaldehyde
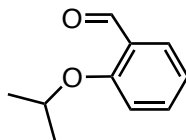
To a Schlenk flask charged with a stir bar was added potassium carbonate (4.54 g, 32.8 mmol). After evacuating and refilling the flask with argon three times, 15 mL dry DMF, salicaldehyde (1.00 mL, 9.38 mmol), and 2-iodopropane (1.12 mL,11.2 mmol) was

added. After stirring at 45 °C overnight, the reaction was quenched with water. The aqueous phase was extracted with ether (3×150 mL). The organic layer was then washed with water (3×100 mL) and dried over anhydrous $MgSO_4$, filtered, and solvents were removed *in vacuo* (1.12 g, 72%). Spectroscopic data was in accordance with those provided previously in the literature.[29]

^{1}H NMR (400 MHz, Chloroform-*d*) δ 10.49 (d, *J* = 0.8 Hz, 1H), 7.82 (dd, *J* = 7.9, 1.9 Hz, 1H), 7.51 (ddd, *J* = 8.4, 7.3, 1.9 Hz, 1H), 7.04 – 6.91 (m, 2H), 4.68 (pd, *J* = 6.0, 0.6 Hz, 1H), 1.40 (d, *J* = 6.1 Hz, 7H).

^{13}C NMR (101 MHz, CDCl3) δ 190.38, 160.74, 135.90, 128.42, 125.80, 120.51, 114.09, 71.20, 22.12.

Synthesis of 2-isopropoxystyrene
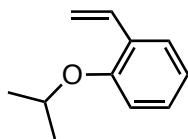
To a Schlenk flask charged with a stir bar was added methyltriphenylphosphonium bromide (652.6 mg, 1.827 mmol) and potassium *tert*-butoxide (205.0 mg, 1.827 mmol). After evacuating and refilling the flask with argon three times, 25 mL of dry diethyl ether was added, and the reaction mixture was stirred for 1 hour at 0 °C. 2-isopropoxybenzaldehyde (100.0 mg, 0.6096 mmol) was then added, and the reaction mixture was stirred for an additional hour at 0°C. Saturated aqueous NH_4Cl solution was then added to the mixture, and the aqueous phase was extracted with Et_2O (3×10 mL). The organic layer was dried over anhydrous $MgSO_4$, filtered, and solvents were removed *in vacuo*. The crude product was purified by column chromatography on silica using pentane as the eluent, giving the pure product (79.0 mg, 80%) as a colorless oil. Spectroscopic data was in accordance those provided previously in the literature.[30]

^{1}H NMR (400 MHz, THF-d_8) δ, 7.45 (dd, J = 7.7, 1.7 Hz, 1H), 7.14 (ddd, J = 8.7, 7.4,

1.7 Hz, 1H), 7.04 (dd, J = 17.8, 11.2 Hz, 1H), 6.91 (dd, J = 8.3, 1.1 Hz, 1H), 6.83 (td, J =

7.4, 1.1 Hz, 1H), 5.69 (dd, J = 17.9, 1.7 Hz, 1H), 5.13 (dd, J = 11.2, 1.7 Hz, 1H), 4.57

(hept, J = 6.1 Hz, 1H), 1.30 (d, J = 6.0 Hz, 6H).

^{13}C NMR (101 MHz, THF) δ, 155.94, 132.82, 129.23, 128.32, 126.84, 120.93, 114.47,

113.23, 70.90, 22.22.

Synthesis of Ru-Hydride Species From Reaction of 4.3 with Phenyl Vinyl Ether (Reaction 1)

4.3
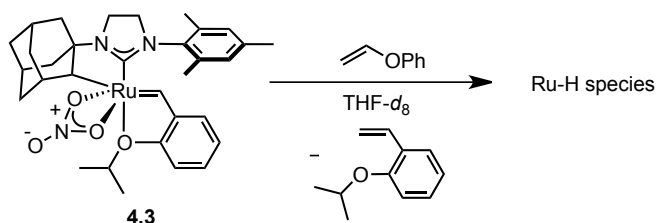
To a 4 mL vial charged with a stir bar was added catalyst **4.3** (2.2 mg, 0.0035 mmol),

0.65 mL THF-d_8, and phenyl vinyl ether (7.4 μL, 0.070 mmol). After 5 hours, a

ruthenium-hydride species could be seen by the appearance of a singlet in the ^{1}H NMR

(400 MHz) at −12.16 ppm.

Synthesis of Ru-Hydride Species From Reaction of 4.4 with Phenyl Vinyl Ether (Reaction 2)

4.4
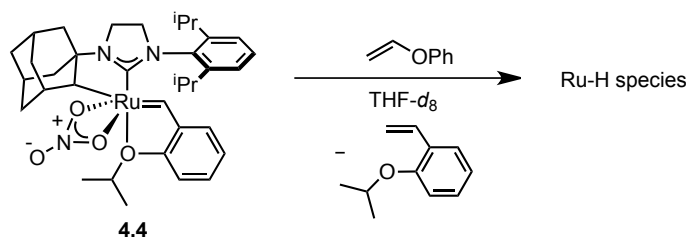
To a 4 mL vial charged with a stir bar was added catalyst **4.4** (2.4 mg, 0.0035 mmol),

0.25 mL of THF, and phenyl vinyl ether (7.4 μL, 0.070 mmol). After 4 hours, a 100.0 μL

aliquot of the reaction mixture was added to 0.6 mL THF-d_8 in an NMR tube. The

formation of the ruthenium-hydride species was seen by the appearance of a singlet in the ^{1}H NMR (400 MHz) at −11.97 ppm.

Synthesis of Ru-Hydride Species From Reaction of 4.3 with Butyl Vinyl Ether (Reaction 3)
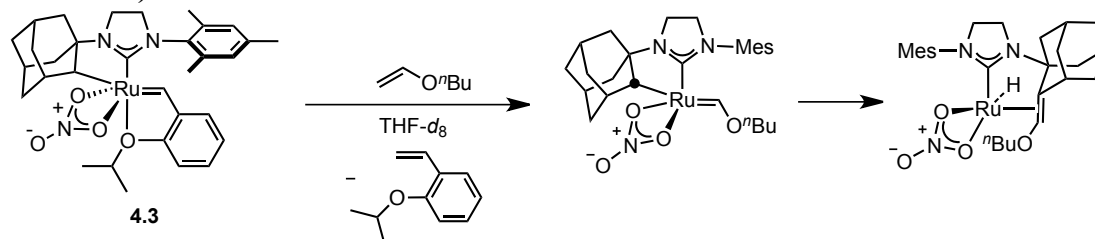
To a J. Young tube was added catalyst **4.3** (60.0 mg, 0.0711 mmol), 0.65 mL of THF-d_8, and butyl vinyl ether (9.2 μL, 0.0711 mmol). After taking a ^{1}H NMR spectrum after 10 minutes to see the initial formation of the Fischer carbene, the reaction to form the Ru-H complex was completed overnight at room temperature. Analysis by ^{1}H, ^{13}C, ^{1}H-^{1}H COSY, ^{1}H-^{13}C HSQC, and ^{1}H-^{13}C HSQC NMR spectroscopy was conducted using a Bruker 400 MHz instrument. ^{13}C-DEPT NMR studies were performed using a Varian Inova 400 MHz instrument.

^{1}H NMR (400 MHz, THF-d_8) δ, 6.81 (d, 2H), 5.11 (s, 1H), 3.94 (dt, J = 9.8, 6.2 Hz, 1H), 3.72-3.62 (m, 1H), 3.52 (t, 1H), 3.41 (td, J = 10.0, 4.2 Hz, 1H), 3.30-3.15 (m, 2H), 2.58 (dt, J = 11.9, 3.0 Hz, 1H), 2.32-2.17 (m, 6H, overlapping), 2.22 (s, 3H), 2.17 (s, 3H), 2.10 (s, 3H), 1.94-1.75 (m, 6H), 1.62-1.49 (m, 2H), 1.45-1.35 (m, 2H), 0.93 (t, J = 7.3 Hz, 3H), -12.63 (s, 1H).

^{13}C NMR (101 MHz, THF) δ 218.56, 137.64, 137.40, 136.89, 136.52, 129.57, 129.02, 93.09, 71.16, 65.38, 60.43, 51.93, 44.88, 41.52, 38.67, 38.33, 38.29, 35.16, 33.14, 32.92, 31.61, 30.85, 21.01, 20.14, 18.13, 17.75, 14.20.

HRMS (FAB+): [M]$^+$ RuC$_{27}$H$_{39}$N$_3$O$_4$ Calculated – 570.1906, Found – 570.1896.

Examination of Reaction 4.3 at 0 °C

To a J. Young tube was added catalyst **4.3** (26.1 mg, 0.0309 mmol), 0.65 mL of THF-d_8, butyl vinyl ether (4.0 μL, 0.0309 mmol). A ^{1}H NMR spectrum was taken after 10 minutes at 0 °C to see the initial formation of the Fischer carbene.

Examination of Conversions of Reaction 4.3 Using Internal Standards

Reaction with 1 equiv. butyl vinyl ether:

To a J. Young tube was added catalyst **4.3** (26.1 mg, 0.0309 mmol), 0.65 mL of THF-d_8, butyl vinyl ether (4.0 μL, 0.0309 mmol), and HMDSO (6.6 μL, 0.0309 mmol). The reaction to form the Ru-H complex was completed overnight at room temperature, and the conversion was determined by integration against HMDSO.

Reaction with 0.1 equiv. butyl vinyl ether:

To a J. Young tube was added catalyst **4.3** (52.2 mg, 0.0618 mmol), 0.65 mL of THF-d_8, butyl vinyl ether (0.8 μL, 0.00618 mmol), and HMDSO (1.3 μL, 0.00618 mmol). The reaction to form the Ru-H complex was completed overnight at room temperature, and the conversion was determined by integration against HMDSO.

Synthesis of Ru-Hydride Species From Reaction of 4.4 with Butyl Vinyl Ether (Reaction 4)
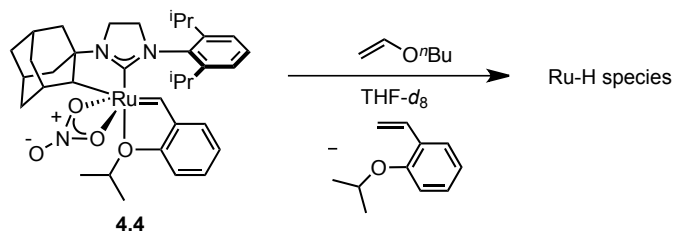
To a J. Young tube was added catalyst **4.4** (5.3 mg, 0.0079 mmol), 0.65 mL of THF-d_8, and phenyl vinyl ether (20.4 μL, 0.158 mmol). Decomposition to the ruthenium-hydride

species was completed overnight at room temperature as seen by the appearance of a singlet in the ^{1}H NMR (400 MHz) at -12.50 ppm.

Computational Details

Geometry optimizations on all intermediates and transition states were performed using the B3LYP[31] method of density functional theory (DFT) in the gas phase with a mixed basis set using LANL2DZ for ruthenium and 6-31G(d) for all other atoms. Frequency calculations were performed on all optimizations to confirm the location of relative minima (zero negative frequencies) and transition states (one negative frequency). Thermal corrections were computed from frequency calculations at the standard state of 1 atm and 298 K. All frequencies below 100 cm^{-1} were manually adjusted to 100 cm^{-1} to account for the breakdown of the harmonic oscillator approximation, as discussed by Truhlar and coworkers.[32] Intrinsic reaction coordinate (IRC) calculations were performed at the same level of theory on most transition states to confirm the connection of the transition states to the calculated intermediates. Single point energy calculations were performed on all optimized structures using the M06[33] functional and a mixed basis set using SDD for ruthenium and 6-311+G(d,p) for all other atoms. The SMD[34] solvation model for tetrahydrofuran was employed for all single point calculations. Electrostatic potential maps were generated from the respective optimizations of the 2 structures. All calculations were performed using the Gaussian 09 software.[35] All 3D structures were rendered using CYLView.[36]
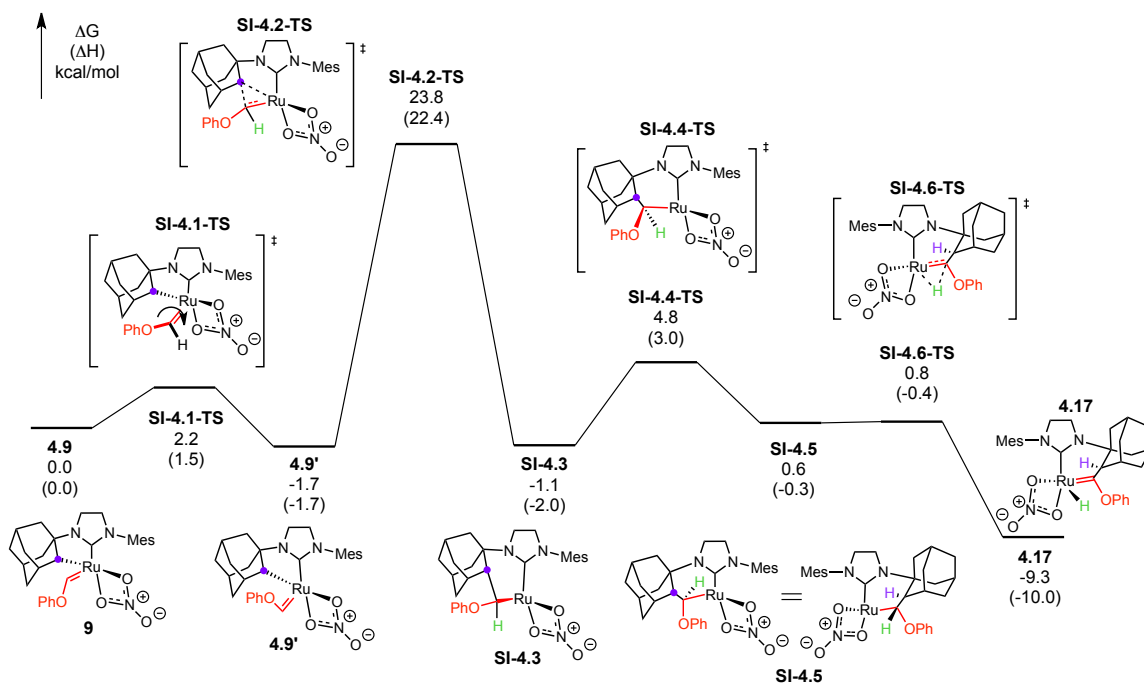
Figure S4.1. Decomposition pathway of **4.9** leading to hydride **4.17**.
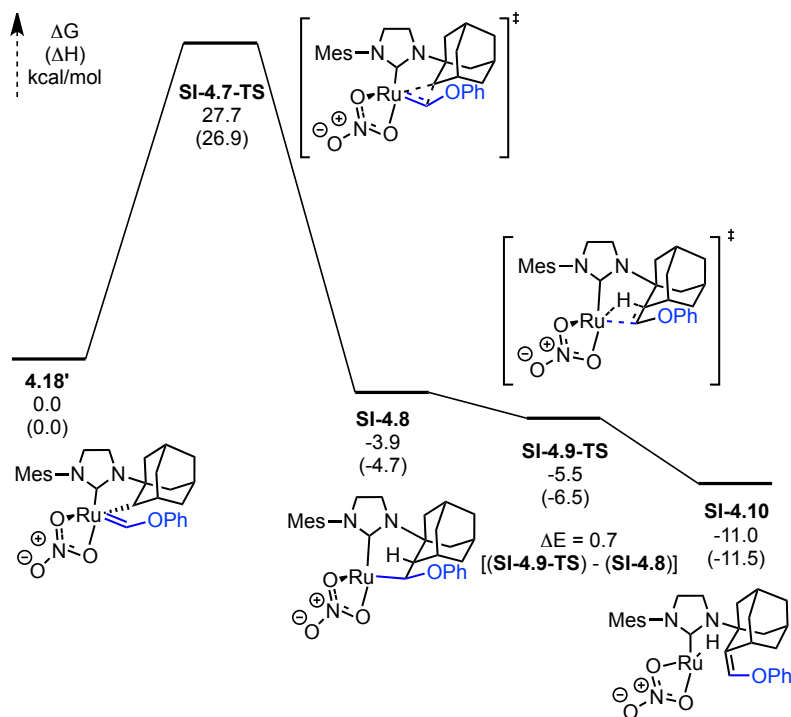
Figure S4.2. Decomposition pathway of **4.18'** to hydride **SI-4.10**.
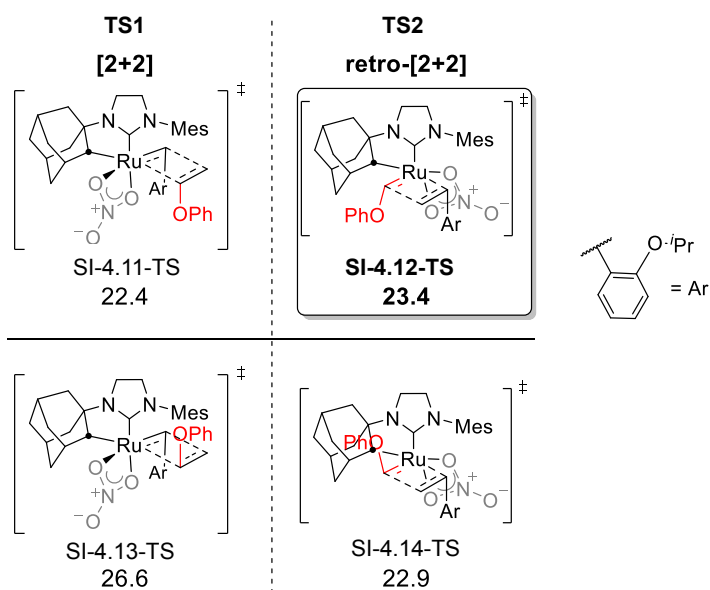
Figure S4.3. Transition states for initiation of **4.3** with phenyl vinyl ether.
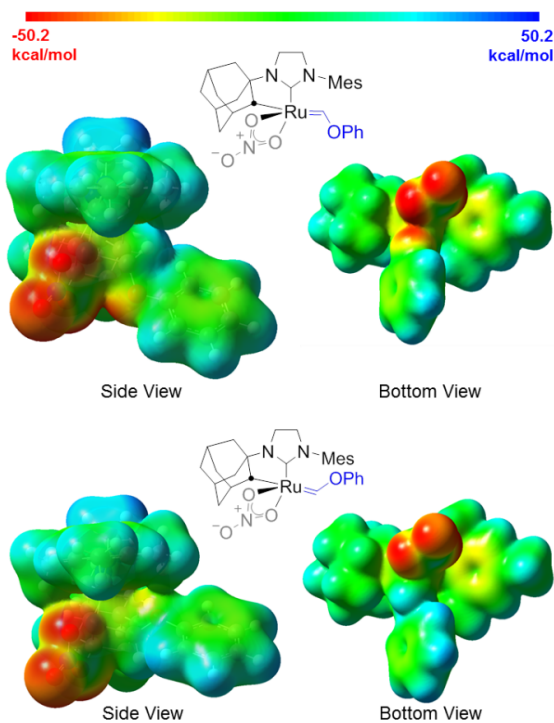
Figure S4.4. Electrostatic potential maps of **4.18** (top) and **4.18'** (bottom).

References

1.   Schrodi, Y.; Ung, T.; Vargas, A.; Mkrtumyan, G.; Lee, C. W.; Champagne, T. M.; Pederson, R. L.; Hong, S. H. *Clean: Soil, Air, Water*. **2008**, *36*, 669.

2. Grubbs, R. H., O'Leary, D. J.; *Handbook of Metathesis, Vol. 2*: *Applications in Organic Synthesis*, 2nd ed.; Wiley- VCH: Weinheim, Germany, 2015.

3. (a) Slugovc C. *Macromol. Rapid Commun*. **2004**, *25*, 1283. (b) Miyake, G. M.; Piunova, V. A.; Weitekamp, R. A.; Grubbs, R. H. *Angew. Chem. Int. Ed*. **2012**, *51*, 11246.

4. Cossy, J.; Arseniyadis, S.; Meyer, C.; *Metathesis in Natural Product Synthesis: Strategies, Substrates and Catalysts*.; Wiley-VCH: Weinheim, Germany, 2011.

5. Trnka, T. M.; Grubbs, R. H. *Acc. Chem. Res.* **2001**, *34*, 18.

6. For examples see: (a) Maynard, H. D.; Grubbs, R. H. *Macromolecules* **1999**, *32*, 6917. (b) Quigley, B. L; Grubbs, R. H. *Chem. Sci.*, **2014**, *5*, 501. (c) Ahmed, T. S.; Grubbs, R. H. *J. Am. Chem. Soc.*, **2017**, *139*, 1532. (d) Ahmed, T. S.; Grubbs, R. H. *Angew. Chem. Int. Ed.* **2017**, *56*, 11213.

7. Sanford, M. S.; Love, J. A.; Grubbs, R. H. *J. Am. Chem. Soc.* **2001**, *123*, 6543.

8. Vorfalt, T.; Wannowius, K.-J.; Plenio, H. *Angew. Chem. Int. Ed.* **2010**, *49*, 5533.

9. Louie, J.; Grubbs, R. H. *Organometallics,* **2002,** *21,* 2153.

10. Takahira, Y.; Morizawa, Y. *J. Am. Chem. Soc.* **2015**, *137*, 7031.

11. Endo, K.; Grubbs, R. H. *J. Am. Chem. Soc.* **2011**, *133*, 8525.

12. Keitz, B. K.; Endo, K.; Patel, P. R.; Herbert, M. B.; Grubbs, R. H. *J. Am. Chem. Soc.* **2012**, 134, 693.

13. Rosenbrugh, L. E.; Herbert, M. B.; Marx, V. M.; Keitz, B. K.; Grubbs, R. H. *J. Am. Chem. Soc.* **2013**, *135*, 1276.

14. Liu, P.; Xu, X.; Dong, X.; Keitz, B. K.; Herbert, M. B.; Grubbs, R. H.; Houk, K. N. *J. Am. Chem. Soc.* **2012**, *134*, 1464.

15. Herbert, M. B.; Lan, Y., Keitz, B. K.; Liu, P.; Endo, K.; Day, M. W.; Houk, K. N.; Grubbs, R. H. *J. Am. Chem. Soc*. **2012**, *134*, 7861.

16. See the Supporting Information of this reference for a recent example: Hartung, J.; Dornan, P. K.; Grubbs, R. H. *J. Am. Chem. Soc.* **2014**, *136*, 13029.

17. (a) Courchay, F. C., Sworen, J. C., Ghiviriga, I., Abboud, K. A., and Wagener, K. B. *Organometallics*, **2006**, 25, 6074. (b) Rowley, C. N.; Foucault, H. M.; Woo, T. K.; Fogg, D. E. *Organometallics*, **2008**, *27*, 1661. (c) Ashworth, I. W.; Hillier, I. H.; Nelso, D. J.; Percy, J. M.; Vincent, M. A. *Eur. J. Org. Chem.* **2012**, 5673. (d) Clark, J. R.; Griffiths, J. R.; Diver, S. T. *J. Am. Chem. Soc.* **2013**, *135*, 3327.

18. This observation is consistent with studies of previously reported Fischer carbenes: See ref. 9.

19. Shifts are consistent with other Ru-H complexes. See ref. 15.

20. Attempts at isolation of these complexes resulted in decomposition of the observed species.

21. Conducting this reaction at 0 °C allows for the observation of a very minor signal at 13.57 ppm (2% with respect to the signal at 13.83 ppm) in the ^{1}H NMR spectrum, which could possibly belong to another isomer of the Fischer carbene.

22. To further confirm this absence, no correlations to this region were observed in the ^{1}H-^{13}C HMBC spectrum.

23. For typical Ru=C ^{13}C NMR shifts, see ref. 15.

24. Ref. 14 discusses the direct epimerization of the ruthenium center via reorientation of the alkylidene in the supporting information. Intermediates along this pathway were substantially higher in energy than metathesis via our computed pathway.

25. Dang, Y.; Wang, Z.-X.; Wang, X. *Organometallics*, **2012**, *31*, 8654.

26. Decomposition of **4.18'** is shown in the supporting information as Figure S4.2.

27. See Figure S4.3 for diagram.

28. Okimoto, Y.; Sakaguchi, S.; Ishil, Y. *J. Am. Chem. Soc.* **2002**, *124*, 1590.

29. Hamlin, T. A.; Kelly, C. B.; Leadbeater, N. E. *Eur. J. Org. Chem.* **2013**, *18*, 3658.

30. Krause, J. O.; Nuyken, O.; Wurst, K.; Buchmeiser, M. R. *Chem. Eur. J.* **2004**, *10*, 777.

31. (a) Becke, A. D. *Phys. Rev. A* **1988**, *38*, 3098. (b) Becke, A. D. *J. Chem. Phys.* **1993**, *98*, 5648. (c) Lee, C.; Yang, W.; Parr, R. G. *Phys. Rev. B* **1988**, *37*, 785.

32. (a) Zhao, Y.; Truhlar, D. G. *Phys. Chem. Chem. Phys.* **2008**, *10*, 2813. (b) Ribeiro, R. F.; Marenich, A. V.; Cramer, C. J.; Truhlar, D. G. *J. Phys. Chem. B.* **2011**, *115*, 14556.

33. (a) Zhao,Y.; Truhlar, D. G. *Theor. Chem. Acc.* **2008**, *120*, 215. (b) Zhao, Y.; Truhlar, D. G. *Acc. Chem. Res.* **2008**, *41*, 157.

34. Marenich, A. V.; Cramer, C. J.; Truhlar, D. G. *J. Phys. Chem. B* **2009**, *113*, 6378.

35. Gaussian 09, Revision D.01, M. J. Frisch, G. W. Trucks, H. B. Schlegel, G. E. Scuseria, M. A. Robb, J. R. Cheeseman, G. Scalmani, V. Barone, B. Mennucci, G. A. Petersson, H. Nakatsuji, M. Caricato, X. Li, H. P. Hratchian, A. F. Izmaylov, J. Bloino, G. Zheng, J. L. Sonnenberg, M. Hada, M. Ehara, K. Toyota, R. Fukuda, J. Hasegawa, M. Ishida, T. Nakajima, Y. Honda, O. Kitao, H. Nakai, T. Vreven, J. A. Montgomery, Jr., J. E. Peralta, F. Ogliaro, M. Bearpark, J. J. Heyd, E. Brothers, K. N. Kudin, V. N. Staroverov, T. Keith, R. Kobayashi, J. Normand, K. Raghavachari, A. Rendell, J. C. Burant, S. S. Iyengar, J. Tomasi, M. Cossi, N. Rega, J. M. Millam,

M. Klene, J. E. Knox, J. B. Cross, V. Bakken, C. Adamo, J. Jaramillo, R. Gomperts, R. E. Stratmann, O. Yazyev, A. J. Austin, R. Cammi, C. Pomelli, J. W. Ochterski, R. L. Martin, K. Morokuma, V. G. Zakrzewski, G. A. Voth, P. Salvador, J. J. Dannenberg, S. Dapprich, A. D. Daniels, O. Farkas, J. B. Foresman, J. V. Ortiz, J. Cioslowski, and D. J. Fox, Gaussian, Inc., Wallingford CT, 2013.

36. CYLview, 1.0b; Legault, C. Y., Université de Sherbrooke, 2009 (http://www.cylview.org).

Chapter 5

High *Trans* Kinetic Selectivity in Ruthenium-Based Olefin Cross-Metathesis through Stereoretention

Abstract

The first kinetically controlled, highly *trans*-selective (>98%) olefin cross metathesis reaction is demonstrated using Ru-based catalysts. Reactions with either *trans* or *cis* olefins afford products with highly *trans* or *cis* stereochemistry, respectively. This *E*-selective olefin cross metathesis is shown to occur between two *trans* olefins and between a *trans* olefin and a terminal olefin. Additionally, new stereoretentive catalysts have been synthesized for improved reactivity.

Introduction

Transition metal-catalyzed olefin metathesis is widely accepted as a powerful synthetic methodology for the construction of carbon-carbon double bonds.[1] Broad functional group tolerance and straightforward implementation have allowed for the application of this technology to a variety of fields.[1a] In recent years, syntheses of well-defined catalysts and detailed mechanistic studies have resulted in Ru-,[2] W- and Mo-based[3] complexes capable of *Z*-selective olefin metathesis. Mechanistically similar, each complex is posited to afford *cis*-olefins by sterically controlling the geometry of substituents decorating the key metallacyclobutane intermediate (Figure 5.1).[4]
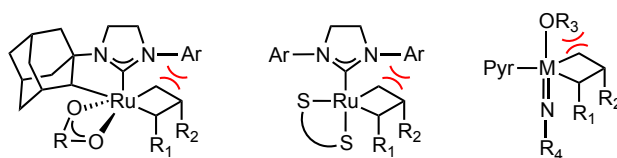
Figure 5.1. Key steric interactions in theorized metallocyclobutane intermediates resulting in *Z*-selectivity.

Though *trans*-olefins are usually thermodynamically preferred to *cis*-olefins, kinetically *E*-selective olefin metathesis remains challenging.[5] Allowing metathesis reactions to achieve equilibrium affords *trans*-enriched olefins that can subsequently be "purified" by *Z*-selective ethenolysis/alkenolysis to afford *trans*-olefins in high

stereopurity (Figure 5.2).[6] While products are accessible in high purity, utilizing an

equilibrium mixture of olefin as starting material limits the overall yield of the

transformation. Furthermore, alkenolysis/ethenolysis introduces an additional purification

step.

| 80:20 *E:Z* | | | >95:5 *E:Z* | ~20% |
| | | | ~80% | |

Z-Selective catalyst
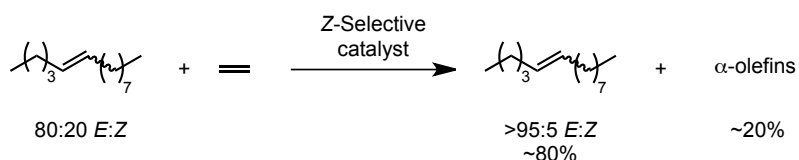
+ α-olefins

Figure 5.2. Stereoselective ethenolysis affording *E*-olefins.

Alternate methods for the stereoselective preparation of *trans*-olefins include

well-established organic transformations (e.g., Birch-type reductions[7] and Wittig

olefinations with stabilized ylides[8]) but most suffer from limited substrate compatibility,

the need for specialized substrates, or the generation of stoichiometric amounts of waste.

An important advance was the discovery of an efficient two-step transformation

comprising of catalytic *trans*-hydrosilylation of an alkyne followed by mild

protodesilylation.[9] Subsequent improvements have afforded the direct semi-

hydrogenation of alkynes to *E*-alkenes catalyzed by a frustrated Lewis pair,[10] an acridine-

based PNP iron complex,[11] or an *in situ* mixture of Cp*Ru(COD)Cl/AgOTf.[12] Though

each of these systems requires an appropriate alkyne, Cp*Ru(COD)Cl/AgOTf has been

demonstrated to tolerate a variety of reducible functionalities.

During the course of internal investigations with dithiolate-ligated ruthenium

complexes (Figure 5.3), we observed that they were competent for transformations with

E-olefins in contrast to other *Z*-selective catalysts. In fact, reactions of *E*-olefins afforded

E-products in high stereopurity. Herein we report the first kinetically controlled, highly

trans selective olefin cross metathesis.

Results and Discussion
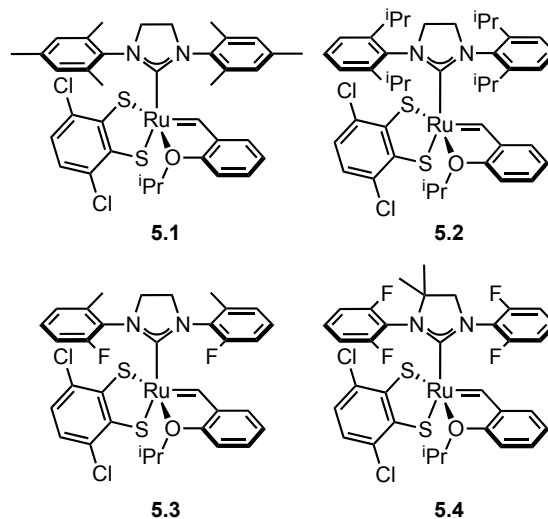
Figure 5.3. Ruthenium-based metathesis catalysts in this study.

Catalyst **5.1** was reacted with *cis* and *trans* isomers of 5-tetradecene (5C14)
independently (Table 5.1). Unexpectedly, after 2 hours at 40 °C, reactions of each
starting material (>98% stereoisomerically pure) catalyzed by 1 mol % **5.1** reached a near
equilibrium distribution of products while retaining the stereochemistry of the starting
material in high fidelity.

Table 5.1. Self-Metathesis of 5-Tetradecene[a]
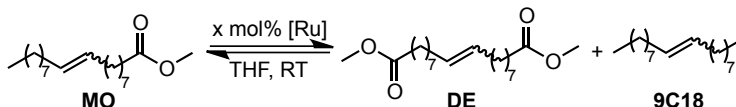
5C14	%5C14 (*Z/E*)	%5C10 (*Z/E*)	%9C18
>98% *cis*	50 (97/3)	25 (97/3)	25
>98% *trans*	54 (4/96)	23 (5/95)	23

[a]General conditions: 5-tetradecene (0.150 mL, 0.588 mmol), **5.1** (4.5 mg, 0.0059 mmol),
1 mL THF, 40 °C, 2 h. Yields and stereoselectivies were determined by gas
chromatography.

Due to interest in expanding the substrate scope and improving catalyst
activity, the self-metathesis of methyl-9-octadecenoate (MO) catalyzed by **5.1** and **5.2**
(the sIPr analogue of **5.1**) was subsequently examined (Table 5.2). Catalyst **5.2** was

remarkably efficient at catalyzing the self-metathesis of *cis*-methyl-9-octadecenoate as a

0.01 mol % (100 ppm) loading affording an equilibrium distribution of product within 2

hours with excellent stereoretention (>99% *Z*) (entry 1). Under these same conditions, no

reaction was observed with *trans*-methyl-9-octadecenoate (entry 2). Catalyst **5.1** (0.5 mol

%) only afforded 20% conversion of *cis*-methyl-9-octadecenoate and failed to afford any

reaction with *trans*-methyl-9-octadecenoate after 2 hours (entries 3 and 4). Fortunately,

increasing the catalyst loading restored reactivity with *trans*-methyl-9-octadecenoate

(entries 5−7) and after 20 hours, **5.1** (7.5 mol %) afforded a near equilibrium distribution

of products with good stereoretention (96% *E*).[13] The small amount of erosion in *E*-

selectivity after prolonged reaction times may be attributed to catalyst decomposition.

Table 5.2. Self-Metathesis of Methyl Oleate[a]

entry	[Ru] (mol%)	MO[b]	time (h)	%MO[b] (Z/E)	%DE[c] (Z/E)	%9C18[d] (Z/E)
1	**5.2** (0.01)	>99% Z	0.5	64 (>99/1)	18 (>99/1)	18 (>99/1)
			1.5	53 (>99/1)	23 (>99/1)	24 (>99/1)
			2	52 (>99/1)	24 (>99/1)	24 (>99/1)
2	**5.2** (0.01)	>97% E	0.5	100 (<1/99)	ND[e]	ND[e]
			1.5	100 (<1/99)	ND[e]	ND[e]
			2	100 (<1/99)	ND[e]	ND[e]
3	**5.1** (0.5)	>99% Z	0.5	90 (>99/1)	5 (>99/1)	5 (>99/1)
			1.5	84 (>99/1)	8 (>99/1)	8 (>99/1)
			2	80 (>99/1)	10 (>99/1)	10 (>99/1)
4	**5.1** (0.5)	>97% E	2	100 (<1/99)	ND[b]	ND[e]
5	**5.1** (2.5)	>97% E	4	98 (<1/99)	1 (<1/99)	1 (<1/99)
			20	92 (<1/99)	4 (<1/99)	4 (<1/99)
6	**5.1** (5.0)	>97% E	4	93 (<1/99)	3 (<1/99)	3 (<1/99)
			20	72 (1/99)	14 (3/97)	14 (3/97)
7	**5.1** (7.5)	>97% E	4	80 (<1/99)	10 (<1/99)	10 (<1/99)
			20	52 (4/96)	24 (4/96)	24 (4/96)

[a]General conditions: methyl-9-octadecenoate (0.150 mL, 0.442 mmol), 1 mL THF, RT. Yields and stereoselectivities were determined by GC. [b]MO = methyl-9-octadecenoate [c]DE = "diester" = dimethyl 9-octadecenedioate [d]9C18 = 9-octadecene [e]not detected

The disparity in the reactivity between the *cis* and *trans* isomers was also

observed during investigations into the cross metathesis of matched stereoisomers of 4-

octene and 1,4-diacetoxy-2-butene (Table 5.3). Contacting a mixture of *cis*-1,4-diacetoxy-2-butene and *cis*-4-octene (4:1) with **5.1** (3.0 mol %) afforded *cis*-2-hexenyl acetate in 91% yield (>99% *Z*) (entry 1). Reactions between *trans*-1,4-diacetoxy-2-butene and *trans*-4-octene were considerably slower (entries 2 and 3) but after 72 hours, a mixture of *trans*-1,4-diacetoxy-2-butene and *trans*-4-octene (4:1) with **5.1** (7.5 mol %) afforded *trans*-2-hexenyl acetate in 47% yield (>99% *E*).

Table 5.3. Cross Metathesis of 4-Octene and 1,4-Diacetoxy-2-Butene[a]
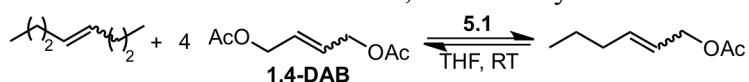
entry	5.1 (mol%)	4C8[b]/1,4-DAB[c]	time (h)	% conv	% yield	*Z/E*
1	3.0	*cis/cis*	0.25	54	49	>99/1
			1.5	94	91	>99/1
			2.5	95	91	>99/1
			5	95	91	>99/1
2	5.0	*trans/trans*	1	9	6	<1/99
			2	15	11	<1/99
			4	19	17	<1/99
			5	22	20	<1/99
			72	33	31	<1/99
3	7.5	*trans/trans*	1	15	11	<1/99
			2	21	19	<1/99
			4	30	27	<1/99
			5	33	31	<1/99
			72	50	47	<1/99

[a]General conditions: 4-octene (0.100 mL. 0.32 mmol), 1,4-diacetoxy-2-butene (0.406 mL. 2.55 mmol), 0.5 mL THF, RT. Yields and stereoselectivies were determined by gas chromatography. [b]4C8 = 4-octene [c]1,4-DAB = 1,4-diacetoxy-2-butene

Though transformations possessed high levels of stereoretention, the prolonged reaction times and elevated catalyst loadings required for substrates with *trans* stereochemistry warranted an improved catalyst. Inspired by the lack of reactivity between **5.2** and *trans* substrates,[14] and in accord with the proposed model (*vide infra*), we sought to examine the effect of reducing the steric bulk of the NHC ligand. Catalysts **5.3** and **5.4** were prepared providing examples where *ortho*-methyl groups on the mesityl ring of the NHC ligand in **5.1** have been replaced with smaller fluorine atoms.

To evaluate these new catalysts, a mixture of *trans*-1,4-diacetoxy-2-butene and *trans*-4-octene (4:1) were combined with ruthenium catalyst (3.0 mol %) yielding *trans*-2-hexenyl acetate (Table 5.4). After 72 hours, **5.1** afforded 13% yield of *trans*-2-hexenyl acetate (entry 1) whereas **5.3** and **5.4** afforded improved yields of 24 and 28%, respectively (entries 2−4).

Table 5.4. Cross Metathesis of *trans*-4-Octene and *trans*-1,4-Diacetoxy-2-Butene[a]
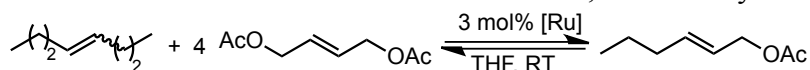
entry	[Ru]	time (h)	% yield	Z/E
1	5.1	1	0	ND[b]
		2	2	<1/99
		4	4	<1/99
		72	13	<1/99
2	5.3	1	2	<1/99
		2	5	<1/99
		4	11	<1/99
		72	24	<1/99
3	5.4	1	4	<1/99
		2	7	<1/99
		4	14	<1/99
		72	28	<1/99

[a]General conditions: *trans*-4-octene (0.050 mL. 0.32 mmol), *trans*-1,4-diacetoxy-2-butene (0.203 mL, 1.27 mmol), [Ru] (0.0096 mmol), 1 mL THF, RT. Yields and stereoselectivies were determined by gas chromatography. [b]Not determined

Additionally, this family of catalysts was evaluated for the more demanding cross metathesis of 1-decene and 4-octene. Mitigating catalyst decomposition in the presence of terminal olefin in addition to outpacing the self-metathesis of the desired product was challenging. Reactions were conducted by combining a mixture of 1-decene and *cis*-4-octene (1:3) with **5.1**−**5.4** (3.0 mol %) in tetrahydrofuran (2.0 mL) (Table 5.5). After 1 hour, **5.2** afforded a 75% yield of *cis*-4-tridecene with >98% *Z* (entry 1). Prolonged exposure to reaction conditions eroded the observed selectivity. Catalysts **5.1**, **5.3**, and **5.4** were less active but afforded 54−58% yield of *cis*-4-tridecene with exceptional stereoretention (>99% *Z*) (entries 3, 5, and 7). Self-metathesis of *cis*-4-tridecene to afford 9-octadecene and 4-octene was the major contributor to the fact that

91

conversions were on average 25−30% higher than observed yields. As previously observed, reactions with *trans*-4-octene were less productive. Unlike reactions of *cis*-4-octene, the disparity between conversion and yield is largely attributed to isomerization of 1-decene. After 4 hours catalyst **5.2** afforded 4% yield but managed to convert 92% of the starting 1-decene (entry 2). Stereoretention is likely poor due to the significant amount of isomerization observed. Catalyst **5.1** afforded a marginally better 7% yield with significantly less isomerization though stereoretention was excellent (>99% *E*) (entry 4). Yields were noticeably better in reactions conducted with catalysts **5.3** and **5.4**, affording 29 and 31% yield of *cis*-4-tridecene, respectively, with excellent stereoretention (>99% *E*) (entries 6 and 8).

Table 5.5. Cross Metathesis of 1-Decene and 4-Octene[a]

entry	[Ru]	4C8[b]	time (h)	%conv	% yield	Z/E
1	**5.2**	*cis*	1	90	75	98/2
			2	90	75	97/3
			4	89	74	96/4
2		*trans*	1	90	3	12/88
			2	91	4	12/88
			4	92	4	13/88
3	**5.1**	*cis*	1	84	55	>99/1
			2	85	55	>99/1
			4	84	58	>99/1
4		*trans*	1	36	7	<1/99
			2	36	7	<1/99
			4	36	7	<1/99
5	**5.3**	*cis*	1	82	58	>99/1
			2	87	59	97/3
			4	88	57	97/3
6		*trans*	1	50	21	<1/99
			2	54	26	<1/99
			4	53	29	<1/99
7	**5.4**	*cis*	1	66	42	>99/1
			2	74	49	>99/1
			4	79	54	>99/1
8		*trans*	1	43	19	<1/99
			2	51	25	<1/99
			4	53	31	<1/99

[a]General conditions: 1-decene (0.050 mL, 0.26 mmol), 4-octene (0.125 mL. 0.79 mmol), Ru (0.0078 mmol), 2 mL THF, RT. Yields and stereoselectivies were determined by GC. [b]4C8 = 4-octene. [c]Not detected.

92
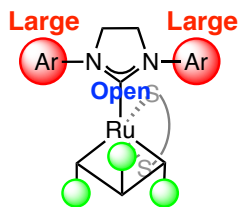
Figure 5.3. Proposed metallacyclic intermediate in *trans*-selective cross metathesis.

Maintaining the side-bound geometry of the metallocyclobutane requisite for these catalysts to facilitate *Z*-selective transformations, the observed *E*-selectivity is proposed to arise from the ability of the substituent at the beta position of the metallacycle to point "up" into the "open" space located in front of the plane containing the N-C-N bonds of the NHC and between the two *N*-aryl groups. Due to steric repulsion, substituents at the alpha positions are forced down, away from the NHC. Provided the disubstituted olefin used for cross metathesis initially has *trans* stereochemistry, the kinetic product should also have *trans* stereochemistry. Comparing the reactivities of catalysts **5.1−5.4** supports this model. As the size of the *ortho* substituents of the *N*-aryl groups decreases (F < Me < ^{i}Pr), conversions tend to increase, presumably due an increase in "open" space.

Conclusions

We have demonstrated the first kinetically controlled, highly *trans* selective system for olefin cross metathesis. Catalysts **5.1**, **5.3**, and **5.4** react with either *E* or *Z* olefins stereoretentively to yield *E* and *Z* products, respectively, with high stereopurity. Reactions of *E*-olefinic hydrocarbons proceeded more rapidly than reactions of *E*-olefins bearing ester functionalities, however both substrate classes afforded high stereoselectivities. The reaction of *E*-olefins with terminal olefins was also demonstrated to occur with high *E*-selectivity. For each reaction examined, *cis* olefins reacted more quickly than their *trans* analogues. Catalysts **5.3** and **5.4,** bearing smaller *ortho*

substituents on the *N*-aryl group of the NHC, were prepared and catalytic reactions resulted in improved yields while retaining high *E*-stereoselectivity. These findings support the proposed model whereby *trans*-olefinic substrates are increasingly compatible with catalysts as steric encumbrance is reduced.

Experimental

All manipulations were carried out under an inert atmosphere using an argon-filled glovebox or standard Schlenk techniques. All glassware was oven dried prior to use. All solvents were anhydrous grade. All reagents, unless specified, were obtained from commercial sources and used without further purification. ^{1}H, ^{13}C{^{1}H}, ^{31}P{^{1}H}, and ^{19}F{^{13}C} NMR spectra were obtained at 400, 101, 162 and 376 MHz respectively. 1H NMR spectra were recorded relative to residual protio-solvent. ^{13}C{^{1}H} NMR spectra were recorded relative to the solvent resonance. ^{31}P{^{1}H} and ^{19}F{^{13}C} NMR spectra were recorded relative to external standards (85% phosphoric acid and trifluoroacetic acid). **1**[2g] and *trans*-1,4-diacetoxy-2-butene[15] were prepared as previously published. Preparations of *N,N'*-bis(2,6-difluorophenyl)formimidamide[16] and 1,3-bis(2,6-difluorophenyl)-4,4-dimethyl-4,5-dihydro-1H-imidazol-3-ium tetrafluoroborate[17] have been detailed in the literature but are included for completeness.

Synthesis of 5.2
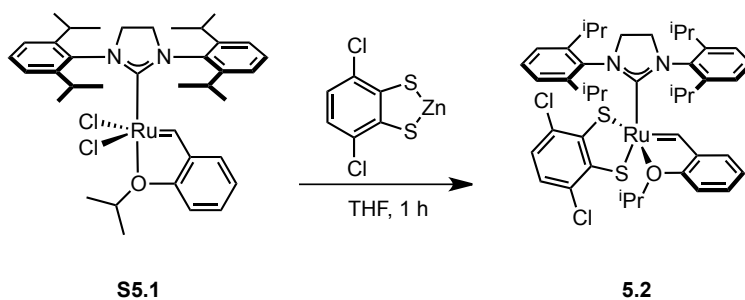
In an argon filled glovebox, a 40 mL scintillation vial equipped with a magnetic stirbar was charged with **S5.1** (0.500 g, 0.703 mmol), (3,6-dichlorobenzene-1,2-dithiolato)

(ethylenediamine)zinc(II) (0.259 g, 0.774 mmol), and 15 mL THF. The resulting suspension was stirred for 6 hours at room temperature then devolatilized. The resulting residue was redissolved in a minimal amount of dichloromethane, filtered through a pad of celite, devolatilized and recrystallized from dichloromethane/diethyl ether at -35 ºC. The red/brown crystals were isolated by filtration then dried in vacuo to afford **5.2** (0.462 g, 77.4% yield).

^{1}H NMR (400 MHz, CD$_2$Cl$_2$) δ 14.52 (s, 1H), 7.52-7.34 (m, 4H), 7.31 (d, J = 6.8 Hz, 1H), 7.20 (d, J = 6.4 Hz, 1H), 6.97-6.86 (m, 2H), 6.82 (t, J = 7.3 Hz, 2H), 6.74 (d, J = 7.0 Hz, 1H), 6.55 (d, J = 6.3 Hz, 1H), 4.97 (hept, J = 5.6 Hz, 1H), 4.36 (dd, J = 20.2, 10.5 Hz, 1H), 4.18 (dd, J = 19.1, 9.4 Hz, 1H), 4.02 (dd, J = 17.6, 9.5 Hz, 1H), 3.96-3.80 (m, 3H), 3.21 – 2.99 (m, 1H), 2.54-2.34 (m, 1H), 1.91 (d, J = 5.5 Hz, 3H), 1.43 (d, J = 5.8 Hz, 3H), 1.38 (d, J = 5.9 Hz, 3H), 1.20-1.35 (m, 6H), 1.00-1.10 (m, 6H), 0.94 (d, J = 5.9 Hz, 3H), 0.54 (d, J = 5.6 Hz, 3H), 0.04 (d, J = 5.4 Hz, 3H).

^{13}C NMR (101 MHz, CD$_2$Cl$_2$) δ 260.6 (d, J = 9.5 Hz), 220.3, 156.0, 153.8, 149.6, 148.9, 147.3, 145.7, 143.1, 141.9, 138.8, 136.1, 131.4, 130.6, 130.1, 129.2, 129.1, 126.0, 126.0, 125.6, 125.4, 124.5, 123.5, 122.9, 121.9, 115.0, 76.5, 54.4, 54.4, 30.1, 29.5, 29.1, 28.8, 27.5, 27.3, 26.7, 26.1, 26.1, 24.2, 23.4, 21.9, 21.2, 20.4.

HRMS (FAB+): [M]$^+$ C$_{43}$H$_{52}$Cl$_2$N$_2$ORuS$_2$ Calculated – 848.1942, Found – 848.1960.

Synthesis of N_1,N_2 -bis(2-fluoro-6-methylphenyl)oxalamide

To a 500 mL round bottom flask equipped with a magnetic stirbar was added 2-methyl-6-fluoroaniline (15.0 mL, 130 mmol), tetrahydrofuran/water (1:1, 200 mL), sodium hydroxide (5.19 g, 130 mmol), and triethylamine (0.90 mL, 6.5 mmol). The suspension was stirred vigorously at 0 ºC and oxalyl chloride (6.58 mL, 77.8 mmol) was added

dropwise. After complete addition the reaction was stirred for 1 hour while warming to ambient temperature. The resulting solid was isolated by filtration, washed with 1M HCl (50 mL), water (3 x 50 mL), and diethyl ether (2 x 50 mL) then dried in vacuo to afford N_1, N_2 -bis(2-fluoro-6-methylphenyl)oxalamide (7.05 g, 35.7% yield).

^{1}H NMR (400 MHz, DMSO-d_6) δ 10.52 (s, 2H), 7.32-7.24 (m, 2H), 7.19-7.11 (m, 4H), 2.24 (s, 6H).

^{13}C NMR (101 MHz, DMSO-d_6) (peak list) δ 158.8, 158.7, 156.4, 137.8, 137.8, 128.4, 128.3, 125.9, 125.8, 123.1, 123.0, 113.4, 113.2, 17.6, 17.6.

^{19}F NMR (376 MHz, DMSO-d_6) (peak list) δ -120.22, -120.23, -120.24, -120.26.

HRMS (FAB+): [M+H]$^+$ $C_{16}H_{15}F_2N_2O_2$ Calculated – 305.1102, Found – 305.1090.

Synthesis of 1,3-bis(2-fluoro-6-methylphenyl)-4,5-dihydro-1H-imidazol-3-ium chloride

In an argon filled glovebox, lithium aluminum hydride (3.74 g, 98.6 mmol) and tetrahydrofuran /toluene (1:1, 100 mL) were combined in a 500 mL round bottom flask equipped with a magnetic stirbar. N_1, N_2 -bis(2-fluoro-6-methylphenyl)oxalamide (6.00 g, 19.7 mmol) was subsequently added to the suspension in small portions with stirring. The reaction was sealed, removed from the glovebox, fitted with a reflux condenser and heated to 50 ºC under argon for 12 h. After cooling to ambient temperature the reaction was quenched by slowly adding water (3.8 mL), followed by aqueous sodium hydroxide (15 wt%, 3.8 mL), then an additional portion of water (11.4 mL). The reaction was stirred rapidly for 2 hours then decanted away from solid residues and dried over magnesium sulfate. Filtration through a pad of celite afforded a clear solution, which was combined with hydrochloric acid (2.0 M in ether, 30 mL, 60 mmol). The resulting precipitate was isolated by filtration then combined with triethyl orthoformate (30 mL) and heated to 130

ºC for 1 hour. After cooling the reaction to ambient temperature, the precipitate was isolated by filtration, washed with diethyl ether (2 x 25 mL), hexanes (2 x 50 mL), then dried *in vacuo* to afford 1,3-bis(2-fluoro-6-methylphenyl)-4,5-dihydro-1H-imidazol-3-ium chloride (4.56 g, 71.7% yield)

^{1}H NMR (400 MHz, DMSO-d_6) δ 9.63 (s, 1H), 7.55-7.47 (m, 2H), 7.38 (t, J = 9.2 Hz, 2H), 7.31 (d, J = 7.8 Hz, 2H), 4.57 (s, 4H), 2.48 (s, 6H).

^{13}C NMR (101 MHz, DMSO-d_6) (peak list) δ 161.6, 158.7, 156.2, 137.9, 131.5, 131.4, 127.2, 127.1, 122.5, 122.3, 114.4, 114.2, 51.8, 51.8, 17.1, 17.1.

^{19}F NMR (376 MHz, DMSO-d_6) (peak list) δ -122.06, -122.08, -122.09, -122.10.

HRMS (FAB+): [M]$^+$ $C_{17}H_{17}F_2N_2$ Calculated – 287.1360, Found – 287.1367

Synthesis of S5.2
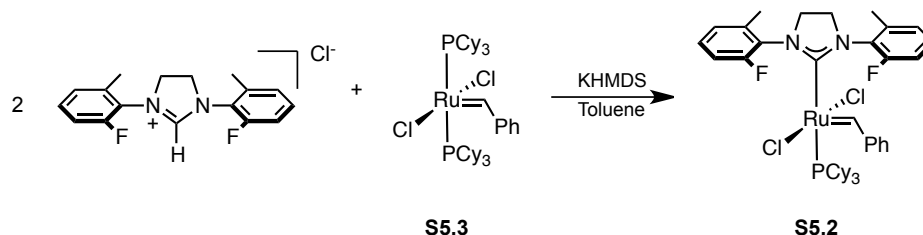
In an argon filled glovebox, **S5.3** (0.676 g, 0.822 mmol), 1,3-bis(2-fluoro-6-methylphenyl)-4,5-dihydro-1H-imidazol-3-ium chloride (0.500 g, 1.64 mmol) and toluene (50 mL) were combined in a 250 mL round bottom flask equipped with a magnetic stirbar. A solution of potassium bis(trimethylsilyl)amide (0.328 g, 1.64 mmol) in toluene (20 mL) was subsequently added and the solution stirred at ambient temperature for 2 hours. All volatiles were subsequently removed *in vacuo*. The resulting residue was redissolved in dichloromethane (10 mL), filtered through a pad of Celite, and devolatilized. The crude product was triturated with hexanes (2 x 20 mL) then recrystallized from toluene/hexanes at ambient temperature. The red/brown crystalline

complex was isolated by filtration and dried *in vacuo* to afford C829 (0.454 g, 66.7% yield).

^{1}H NMR (400 MHz, CD$_2$Cl$_2$) δ 19.28 (s, 1H), 9.4-8.0 (br s 1H), 7.41-7.30 (m, 2 H). 7.20 (d, J = 7.6 Hz, 1H), 7.16-7.04 (m, 3H), 6.90-5.80 (br s, 3H), 6.72-6.62 (m, 1H), 4.22-3.75 (m, 4H), 2.75 (pseudo d, J = 16.5 Hz, 3H), 2.55-2.05 (br s, 3H), 2.11 (pseudo dd, J = 22.7, 11.9 Hz, 3H), 1.65- 1.23 (m, 15H), 1.10-0.72 (m, 15H).

^{31}P NMR (162 MHz, CD$_2$Cl$_2$) δ 28.5 (s).

^{19}F NMR (376 MHz, CD$_2$Cl$_2$) (peak list) δ -110.7 (br s), -111.7 (br s), -119.7 (br s), -120.4.

HRMS (FAB+): [M]$^+$ C$_{42}$H$_{55}$Cl$_2$F$_2$N$_2$PRu Calculated – 828.2492, Found – 828.2493.

Synthesis of 5.3

In an argon filled glovebox, **S5.2** (0.300 g, 0.362 mmol), 1-isopropoxy-2-(prop-1-en-1-yl)benzene (0.638 g, 3.62 mmol) and toluene (10 mL) were combined in a 40 mL scintillation vial equipped with a magnetic stirbar. The reaction was stirred at ambient temperature for 14 hours then directly adsorbed onto silica gel. Purification by column chromatography (silica gel, 2 to 6 % gradient of ethyl acetate / hexanes) afforded 0.190 g (90% pure by NMR spectroscopy) of crude intermediate. The impure intermediate was subsequently combined with (3,6-dichlorobenzene-1,2-dithiolato)(ethylenediamine)zinc(II) (0.115 g, 0.345 mmol) and tetrahydrofuran (5 mL) in a 20 mL scintillation vial equipped with a magnetic stirbar. After 4 hours of stirring at ambient temperature, all volatiles were removed, the residue redissolved in dichloromethane, filtered through celite, devolatilized and recrystallized from dichloromethane/diethyl ether at -35 ºC. The resulting yellow/brown crystals were

isolated by filtration, washed with cold diethyl ether (2 x 5 mL) then dried in vacuo to afford 3 (0.116 g, 35.7% yield)

^{1}H NMR (400 MHz, CD$_2$Cl$_2$) [three conformers in solution, 8:25:67] δ 14.42 (s, 0.08H), 14.39 (s, 0.25H), 14.36 (s, 0.67H), 7.37-7.27 (m, 1H), 7.26-7.02 (m, 2.7H), 7.02-6.62 (m, 7.3H), 6.41 (s, 0.4H), 6.10 (t, J = 9.0 Hz, 0.6H), 5.47-5.38 (m, 1H), 4.13-3.86 (m, 4H), 2.61-2.40 (m, 5H), 1.85-1.65 (m, 7H).

^{19}F NMR (376 MHz, CD2Cl2) (peak list) -118.7 (br s), -119.6 (br s), -120.4 (br s), -123.8 -123.9 (m).

HRMS (FAB+): [M]$^+$ C$_{33}$H$_{30}$Cl$_{37}$ClF$_2$N$_2$ORuS$_2$ Calculated – 746.0159, Found – 746.0132

Synthesis of *N,N′*-bis(2,6-difluorophenyl)formimidamide

To a 100 mL round bottom flask equipped with a magnetic stirbar was added 2,6-difluoroaniline (10.0 mL, 95.9 mmol) and triethyl orthoformate (8.11 mL, 48.8 mmol). To the stirring solution was added hydrochloric acid (0.040 mL, 12 M, 0.48 mmol) and the reaction was stirred at ambient temperature for 10 minutes. The reaction solidified and was subsequently sonicated for an additional 10 minutes. The resulting precipitate was isolated by filtration, washed with hexanes (2 x 30 mL) then dried *in vacuo* to afford *N,N′*-bis(2,6-difluorophenyl)formimidamide (8.47 g, 67.9% yield).

^{1}H NMR (400 MHz, DMSO-*d$_6$*) δ 9.47 (br s, 1H), 8.03 (s, 1H), 7.10 (br s, 6H).

^{19}F NMR (376 MHz, DMSO-*d$_6$*) δ -117.1 (br s, 1F), -125.3 (br s, 3F).

Synthesis of 1,3-bis(2,6-difluorophenyl)-4,4-dimethyl-4,5-dihydro-1H-imidazol-3-ium tetrafluoroborate

To a 250 mL round bottom flask equipped with a magnetic stirbar was added *N,N′*-bis(2,6-difluorophenyl)formimidamide (4.00 g, 14.9 mmol), 3-bromo-2-methylpropene

(1.65 mL, 16.4 mmol), and chlorobenzene (120 mL). The reaction was heated to 125 ºC for 24 h. After cooling the resulting precipitate was isolated by filtration and washed with diethyl ether (2 x 20 mL). The crude product was then partitioned between dichloromethane and an aqueous sodium tetrafluoroborate solution (100 mL, 1:1, 2.0 g NaBF4/50 mL). The organic layer was separated, dried over magnesium sulfate, filtered through celite and all volatiles were removed by rotary evaporation. The resulting residue was recrystallized from dichloromethane/diethyl ether to afford 1,3-bis(2,6-difluorophenyl)-4,4-dimethyl-4,5-dihydro-1H-imidazol-3-ium tetrafluoroborate (3.25 g, 53.1% yield).

^{1}H NMR (400 MHz, DMSO-d_6) δ 9.59 (s, 1H), 7.79 (m, 1H), 7.70-7.60 (m, 1H), 7.55-7.42 (m, 4H), 4.55 (s, 2H), 1.54 (s, 6H).

^{13}C NMR (101 MHz, DMSO-d_6) (peak list) δ 161.6, 159.9, 159.8, 157.7, 157.7, 157.3, 157.3, 155.2, 155.2, 133.9, 133.8, 133.7, 131.7, 131.6, 131.5, 113.3, 113.3, 113.2, 113.2, 113.2, 113.2, 113.1, 113.1, 113.0, 113.0, 113.0, 109.4, 109.3, 109.1, 71.5, 62.5, 62.5, 62.5, 40.2, 39.9, 39.7, 39.5, 39.3, 39.1, 38.9, 24.5.

^{19}F NMR (376 MHz, DMSO-d_6) (peak list) -116.4 (pseudo triplet, J = 7.9 Hz, 2F), -119.8 (pseudo triplet, J = 8.3 Hz, 2F), -148.3 (s, 4F)

Preparation of S5.4

S5.4
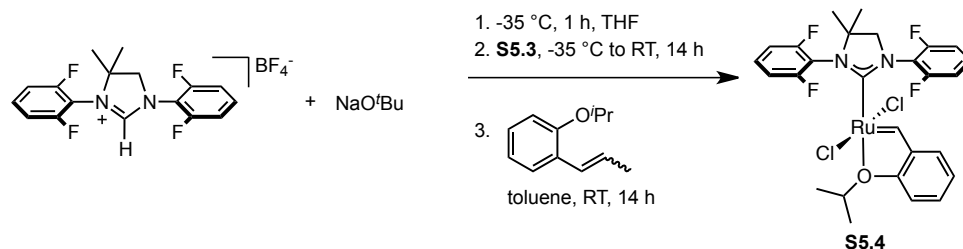
In an argon filled glovebox, 1,3-bis(2,6-difluorophenyl)-4,4-dimethyl-4,5-dihydro-1H-imidazol3-ium tetrafluoroborate (0.500 g, 1.22 mmol), sodium *tert*-butoxide (0.117 g,

1.22 mmol), and **S5.3** (0.502 g, 0.610 mmol) were weighed into separate 40 mL scintillation vials equipped with magnetic stirbars and each dissolved/suspended in tetrahydrofuran (10 mL). The solutions/suspensions were cooled to −35 ºC then the solution of sodium *tert*-butoxide was added to the solution of 1,3-bis(2,6-difluorophenyl)-4,4-dimethyl-4,5-dihydro-1H-imidazol-3-ium tetrafluoroborate over 2 minutes. The reaction was stirred at −35 ºC for 1h then combined with the chilled suspension of **S5.3** and stirred for an additional hour at −35 ºC before allowing the reaction to slowly warm to ambient temperature overnight. The reaction was subsequently devolatilized, triturated with hexanes (2 x 40 mL), redissolved in toluene (10 mL), and filtered through celite. The crude solution was combined with a solution of 1-isopropoxy-2-(prop-1-en-1-yl)benzene (0.400 g, 2.27 mmol) in toluene (2 mL) and stirred overnight at ambient temperature. The resulting green precipitate was isolated by filtration, washed with toluene/hexanes (1:3, 2 x 10 mL) then dried *in vacuo* to afford **S5.4** (0.221 g, 56.4% yield).

1H NMR (400 MHz, CD$_2$Cl$_2$) δ 16.76 (s, 1H), 7.59-7.54 (m, 1H), 7.53-7.41 (m, 2H), 7.17-7.07 (m, 5H), 6.98-6.90 (m, 2H), 5.07-4.96 (sept, J = 6.2 Hz, 1H), 4.06 (s, 2H), 1.49 (s, 3H), 1.48 (s, 3H), 1.42 (d, J = 6.1 Hz, 6H).

19F NMR (376 MHz, CD2Cl2) -107.7 (s, 2F), -114.4 (pseudo triplet, J = 6.0 Hz, 2F).

HRMS (FAB+): [M]$^+$ C$_{27}$H$_{26}$Cl$_2$F$_4$N$_2$ORu Calculated – 642.0402, Found – 642.0421

Synthesis of 5.4

In an argon filled glovebox, **S5.4** (0.150 g, 0.234 mmol) and (3,6-dichlorobenzene-1,2-dithiolato)(ethylenediamine)zinc(II) (0.086 g, 0.26 mmol) were combined in a 20 mL scintillation vial equipped with a magnetic stirbar and dissolved in tetrahydrofuran (10

mL). The reaction was stirred for 60 minutes then devolatilized, redissolved in dichloromethane, filtered, and recrystallized from dichloromethane/diethyl ether at −35 ºC. The resulting yellow/brown crystals were washed with cold diethyl ether (2 x 3 mL) then dried *in vacuo* to afford **5.4** (0.128 g, 70.2% yield).

¹H NMR (400 MHz, CD$_2$Cl$_2$) [two conformers in solution, 40:60] δ 14.52 br s (0.4H), 14.43 (br s, 0.6H), 7.33 (t, J = 7.4 Hz, 1H), 7.08 (d, J = 8.4 Hz, 1H), 7.05-6.67 (m, 9H), 6.13 (br s, 1H), 5.42 (br s, 1H), 3.94 (br q, J = 8.0 Hz, 1.2H), 3.78 (br s, 0.8H), 1.88-1.74 (m, 6H), 1.50-1.28 (m, 6H).

¹⁹F NMR (376 MHz, CD$_2$Cl$_2$) (peak list) δ -100.7, -108.5 (broad), -111.9, -113.1, -115.2 (broad), -116.7, -117.9, -121.8.

HRMS (FAB+): [M]$^+$ C$_{33}$H$_{28}$Cl$_{37}$ClF$_4$N$_2$ORuS$_2$ Calculated – 781.9971, Found – 781.9982

Table 5.1: Self-Metathesis of 5-Tetradecene

In an Ar-filled glovebox, a 20 mL scintillation vial equipped with a magnetic stirbar was charged with **5.1** (4.5 mg, 0.0059 mmol) and tetrahydrofuran (1 mL). 5-tetradecene (*cis* or *trans*) (0.150 mL, 0.588 mmol) was subsequently added, the vial sealed and heated to 40 ºC for 2 hours. Yields and stereoselectivies were determined by gas chromatography (Method 1).

Table 5.2: Self-Metathesis of Methyl Oleate

In an Ar-filled glovebox, a 20 mL scintillation vial equipped with a magnetic stirbar was charged with either **5.1** (0.5-7.5 mol %) or **5.2** (0.01 mol %) and tetrahydrofuran (1 mL). Methyl-9-octadecenoate (*cis* or *trans*) (0.150 mL, 0.442 mmol) was subsequently added, the vial sealed and stirred at ambient temperature. Reactions were sampled at appropriate

time intervals and yields/stereoselectivies were determined by gas chromatography (Method 2).

Table 5.2, Entry 1 [isolated yield]

In an Ar-filled glovebox, a 20 mL scintillation vial equipped with a magnetic stirbar was charged with **5.2** (0.8 mg, 0.09 μmol, 0.01 mol %) and tetrahydrofuran (2 mL). Methyl *cis*-9-octadecenoate (0.300 mL, 0.88 mmol) was subsequently added, the vial sealed and stirred at ambient temperature for 2 hours. The reaction was directly adsorbed onto silica gel and purified by column chromatography, eluting with a gradient of 0 to 5% ethyl acetate in hexanes. All three reaction products were isolated as colorless oils.

Table 5.3: Cross Metathesis of 4-Octene and 1,4-Diacetoxy-2-Butene

In an Ar-filled glovebox, a 20 mL scintillation vial equipped with a magnetic stirbar was charged with catalyst and tetrahydrofuran (0.50 mL). 4-Octene (0.100 mL, 0.64 mmol) and 1,4-diacetoxy-2-butene (0.406 mL, 2.55 mmol) were subsequently added, the vial sealed and stirred at ambient temperature. Reactions were sampled at appropriate time intervals and yields/stereoselectivies were determined by gas chromatography (Method 2).

Table 5.3, Entry 1 [isolated yield]:

In an Ar-filled glovebox, a 20 mL scintillation vial equipped with a magnetic stirbar was charged with **5.1** (14.6 mg, 0.0191 mmol, 3 mol %) and tetrahydrofuran (0.5 mL). *Cis*-4-octene (0.100 mL, 0.636 mmol) and *cis*-1,4-diacetoxy-2-butene (0.406 mL, 2.55 mmol) were subsequently added, the vial sealed and stirred at ambient temperature for 5 hours. The reaction was directly adsorbed onto silica gel and purified by column

chromatography, eluting with a gradient of 0 to 5% ethyl acetate in hexanes to afford (*Z*)-hex-2-en-1-yl acetate (74.6 mg, 0.525 mmol, 82.5% yield) as a colorless oil.

Table 5.4: Cross Metathesis of *trans*-4-Octene and *trans*-1,4-Diacetoxy-2-Butene

In an Ar-filled glovebox, a 4 mL scintillation vial equipped with a magnetic stirbar was charged with catalyst and tetrahydrofuran (1 mL). *Trans*-4-octene (0.050 mL, 0.32 mmol) and *trans*-1,4-diacetoxy-2-butene (0.203 mL, 1.27 mmol) were subsequently added, the vial sealed and stirred at ambient temperature. Reactions were sampled at appropriate time intervals and yields/stereoselectivies were determined by gas chromatography (Method 2).

Table 5.5: Cross Metathesis of 1-Decene and 4-Octene

In Ar-filled glovebox, a 4 mL scintillation vial equipped with a magnetic stirbar was charged with catalyst and tetrahydrofuran (2 mL). 4-Octene (*cis* or *trans*) (0.125 mL, 0.79 mmol) and 1-decene (0.050 mL, 0.26 mmol) were subsequently added, the vial sealed and stirred at ambient temperature. Reactions were sampled at appropriate time intervals and yields/stereoselectivies were determined by gas chromatography (Method 1).

GC Methods

Volatile products were analyzed using an Agilent 6850 gas chromatography (GC) instrument with a flame ionization detector (FID). The following conditions and equipment were used:

Method 1

Column: DB-225, 30m x 0.25mm (ID) x 0.25μm film thickness. Manufacturer: Agilent GC and column conditions: Injector temperature: 220 ºC, Detector temperature: 220 ºC

Oven temperature: Starting temperature: 35 ºC, hold time: 0.5 minutes. Ramp rate 10 ºC/min to 130 ºC, hold time: 0 minutes. Ramp rate 20 ºC/min to 220 ºC, hold time: 5 minutes. Carrier gas: Helium Mean gas velocity: 25 cm/sec Split ratio: 20:1

Method 2

Column: HP-5, 30m x 0.25mm (ID) x 0.25μm film thickness. Manufacturer: Agilent GC and column conditions: Injector temperature: 250 ºC, Detector temperature: 280 ºC Oven temperature: Starting temperature: 100 ºC, hold time: 1 minute Ramp rate 10 ºC/min to 270 ºC, hold time: 12 minutes. Carrier gas: Helium Average velocity: 30 cm/sec Split ratio: 40.8:1

References

1. Grubbs, R. H.; Wenzel, A. G.; O'Leary, D. J.; Khosravi, E., Eds.; *Handbook of Metathesis*; Wiley-VCH Verlag GmbH & Co. KGaA: Weinheim, Germany, 2015. (b) Ivan, K. J. ; Mol, J. C. *Olefin Metathesis and Metathesis Polymerization*, Academic Press, San Diego, CA; 1997.

2. Endo, K.; Grubbs, R. H. *J. Am. Chem. Soc.* **2011**, *133*, 8525. (b) Keitz, B. K.; Endo, K.; Herbert, M. B.; Grubbs, R. H. *J. Am. Chem. Soc.* **2011**, *133*, 9686. (c) Keitz, B. K.; Endo, K.; Patel, P. R.; Herbert, M. B.; Grubbs, R. H. *J. Am. Chem. Soc.* **2011**, *134*, 693. (d) Occhipinti, G.; Hansen, F. R.; Törnroos, K. W.; Jensen, V. R. *J. Am. Chem. Soc.* **2013**, *135*, 3331. (e) Khan, R. K. M.; Torker, S.; Hoveyda, A. H. *J. Am. Chem. Soc.* **2013**, *135*, 10258. (f) Koh, M. J.; Khan, R. K. M.; Torker, S.; Hoveyda, A. H. *Angew. Chem. Int. Ed.* **2014**, 53, 1968. (g) Koh, M. J.; Khan, R. K. M.; Torker, S.; Yu, M.; Mikus, M. S.; Hoveyda, A. H. *Nature* **2015**, *517*, 181.

3. Flook, M. M.; Jiang, A. J.; Schrock, R. R.; Müller, P.; Hoveyda, A. H. *J. Am. Chem. Soc.* **2009**, *131*, 7962. (b) Jiang, A. J.; Zhao, Y.; Schrock, R. R.; Hoveyda, A. H. *J. Am. Chem. Soc.* **2009**, *131*, 16630. (c) Meek, S. J.; O'Brien, R. V.; Llaveria, J.; Schrock, R. R.; Hoveyda, A. H. *Nature* **2011**, *471*, 461. (d) Yu, M.; Wang, C.; Kyle, A. F.; Jakubec, P.; Dixon, D. J.; Schrock, R. R.; Hoveyda, A. H. *Nature* **2011**, *479*, 88.

4. Liu, P.; Xu, X.; Dong, X.; Keitz, B. K.; Herbert, M. B.; Grubbs, R. H.; Houk, K. N. *J. Am. Chem. Soc.* **2012**, *134*, 1464. (b) Dang, Y.; Wang, Z. X.; Wang, X. *Organometallics* **2012**, *31*, 7222. (c) Dang, Y.; Wang, Z. X.; Wang, X. *Organometallics* **2012**, *31*, 8654. (d) Occhipinti, G.; Koudriavtsev, V.; Törnroos, K. W.; Jensen, V. R. *Dalton Trans.* **2014**, *43*, 11106. (e) Torker, S.; Khan, R. K. M.; Hoveyda, A. H. *J. Am. Chem. Soc.* **2014**, *136*, 3439.

5. Early reports with ill-defined W-, Mo- and Cr- based catalysts disclosed appreciable levels of stereoretention in cross-metatheses of olefinic hydrocarbons. (a) Bilhou, J. L.; Basset, J. M.; Mutin, R.; Graydon, W. F. *J. Am. Chem. Soc.* **1977**, *99*, 4083. (b) Leconte, M.; Basset, J. M. *J. Am. Chem. Soc.* **1979**, *101*, 7296. (c) Leconte, M.; Basset, J. M. *Ann. N. Y. Acad. Sci.* **1980**, *333*, 165.

6. Marinescu, S. C.; Levine, D. S.; Zhao, Y.; Schrock, R. R.; Hoveyda, A. H. *J. Am. Chem. Soc.* **2011**, *133*, 11512. (b) Miyazaki, H.; Herbert, M. B.; Liu, P.; Dong, X.; Xu, X.; Keitz, B. K.; Ung, T.; Mkrtumyan, G.; Houk, K. N.; Grubbs, R. H. *J. Am. Chem. Soc.* **2013**, *135*, 5848.

7. Pasto, D. J. in *Comprehensive Organic Synthesis*; Trost, B. M., Fleming, I., Ed.; Pergamon Press: Oxford, 1991; Vol. 8, Chapter 3.3.

8. Vedejs, E.; Peterson, M. J. *Top. Stereochem*. **1994**, *21*, 1.

9. Trost, B. M.; Ball, Z. T.; Jöge, T. *J. Am. Chem. Soc*. **2002**, *124*, 7922.

10. Liu, Y.; Hu, L.; Chen, H.; Du, H. *Chem. Eur. J*. **2015**, *124*, 3495.

11. Srimani, D.; Diskin-Posner, Y.; Ben-David, Y.; Milstein, D. *Angew. Chem Int. Ed*. **2013**, *52*, 14131.

12. Radkowski, K.; Sundararaju, B.; Fürstner, A. *Angew. Chem. Int. Ed.* **2013**, *52*, 355.

13. Results similar to Table 5.2, entry 7 were attainable by conducting the reaction with 1 mol % **1** at 45 °C for 5 hours.

14. The self-metathesis of *trans*-methyl-9-octadecenoate conducted in the presence of 7.5 mol % **2** did not afford any desired product.

15. Rodriguez, R. A.; Steed D. B.; Kawamata, Y.; Su, S.; Smith, P. A.; Steed, T. C.; Romesberg, F. E.; Baran, P. S. *J. Am. Chem. Soc.* **2014**, *136*, 15403.

16. Hobbs, M. G.; Knapp, C. J.; Welsh, P. T.; Borau-Garcia, J.; Ziegler, T.; Roesler, R. *Chem. Eur. J.* **2010**, *16*, 14520.

17. Jazzar, R.; Bourg, J. B.; Dewhurst, R. D.; Donnadieu, B.; Bertrand, G. *J. Org. Chem*. **2007**, *72*, 3492.

Chapter 6

Fast-Initiating, Ruthenium-based Catalysts for Improved Activity in

Highly *E*-Selective Cross Metathesis

Abstract

Ruthenium-based olefin metathesis catalysts bearing dithiolate ligands have been recently employed to generate olefins with high *E*-selectivity (>99% *E*) but have been limited by low to moderate yields. In this report, ^{1}H NMR studies reveal that a major contributing factor to this low activity is the extremely low initiation rates of these catalysts with *trans* olefins. Introducing a 2-isopropoxy-3-phenylbenzylidene ligand in place of the conventional 2-isopropoxybenzylidene ligand resulted in catalysts that initiate rapidly under reaction conditions. As a result, reactions were completed in significantly less time and delivered higher yields than in previous reports while maintaining high stereoselectivity (>99% *E*).

Introduction

Given its robustness and general ease of implementation, transition metal-catalyzed olefin metathesis has become an increasingly ubiquitous method for generating C–C double bonds in a wide variety of fields including organic synthesis, green chemistry, and biochemistry.[1] Over the last several years, olefin metathesis has been significantly advanced through the synthesis of well-defined catalysts, where methodical tuning of catalyst architecture has allowed for the development of different catalysts that can each achieve a specific purpose including enantioselectivity,[2] stereoselectivity,[3] or increased activity.[4]

Achieving high selectivity for 1,2-disubstituted olefinic products with a particular stereochemistry (*E* or *Z*) was a longstanding challenge in olefin metathesis until discrete Ru-,[3e-h] Mo-, and W-based[3b-d] catalysts were developed in recent years for the metathesis of terminal olefins to produce high levels of *cis* olefins. Each of these catalysts exploits

steric impedances within the catalyst structure to favor the *syn* over the *anti* metallacyclobutane pathway.[5]

Until very recently, methods of achieving high kinetic *trans* selectivity through olefin metathesis had remained elusive. *Trans* selectivity in olefin metathesis can often be achieved by allowing the reaction to reach equilibrium so that the thermodynamically favored product, often *trans*, is present in higher quantities.[6] However, the difference in energy between some *cis* and *trans* isomers may be insignificant, and, hence, this method is not reliable for obtaining all *trans* products in high selectivity. Other methods for preparing *trans* olefins with high stereoselectivity include *Z*-selective ethenolysis of *E/Z*-olefin mixtures,[7] Wittig reactions of stabilized ylides,[8] Julia olefinations,[9] and Peterson olefinations.[10] In addition, alkyne metathesis followed by Na/NH_3 reduction,[11] catalytic *trans*-hydrosilylation/protodesilylation,[12] or semihydrogenation[13] can also furnish *trans* olefins. These methods, however, are either harsh or require multiple steps to reach the desired *trans* product.

The first demonstration of highly kinetically *trans*-selective transition metal-catalyzed olefin cross metathesis was reported this year with the unexpected discovery that ruthenium-based catalysts bearing chelated dithiolate ligands are able to perform cross metathesis between two *trans* olefins or between a *trans* olefin and a terminal olefin to generate products with high *trans* selectivity (>98% *E*).[31] These catalysts had been previously demonstrated to react with *cis* starting materials to form highly *cis* products.[3k] Hence, these catalysts are stereoretentive, preserving the stereochemical purity of the starting olefins in the product olefins. The *E*-selectivity of the catalysts is proposed to arise from the two *N*-aryl groups of the NHC forcing the α substituents of a side-bound

metallacycle to point down while the β substituent can point into the open space in front of the plane containing the N-C-N bonds of the NHC and between the two *N*-aryl groups (Figure 6.1). This proposed model was supported by the observation that reducing the size of the *ortho* substituents of the *N*-aryl groups of the NHC led to increased catalyst activity in this transformation. A subsequent report from the Hoveyda and Schrock groups demonstrated a similar approach to achieving *trans*-selective cross metathesis using Mo-based catalysts.[3m] Steric interactions of the substituents of the metallacycle with surrounding ligands in combination with the minimization of unfavorable eclipsing interactions of these substituents was their proposed rationale for the favorable formation of *anti* metallacycles.
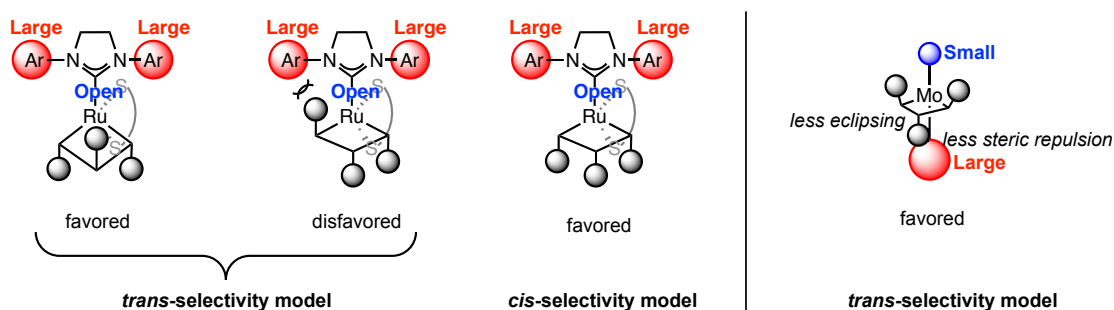
Figure 6.1. Proposed models for high kinetic *trans and cis* selectivity in cross metathesis with Ru catalysts[31] (left) and high *trans* selectivity with Mo catalysts[3m] (right).

In many instances, the *trans*-selective, Ru dithiolate catalysts generated low yields of products. Two possible reasons for the low activity can be envisioned: slow catalyst initiation and the inherently small "open space" in which the β substituent can place itself. Herein, we establish that poor initiation is indeed a significant factor in the low conversions observed with previous dithiolate catalysts. We address this through the development of new catalysts with improved initiation efficiency that demonstrate significantly improved conversions and reaction times in comparison to previous catalysts.

Results and Discussion

When examining the self-metathesis of *trans*-2-hexenyl acetate catalyzed by 1 mol % of **6.1**, uninitiated catalyst was evident in the ^{1}H NMR after 24 h at 45 °C, at which time only 85% of the catalyst had initiated (Figure 6.2). Based on this result, new
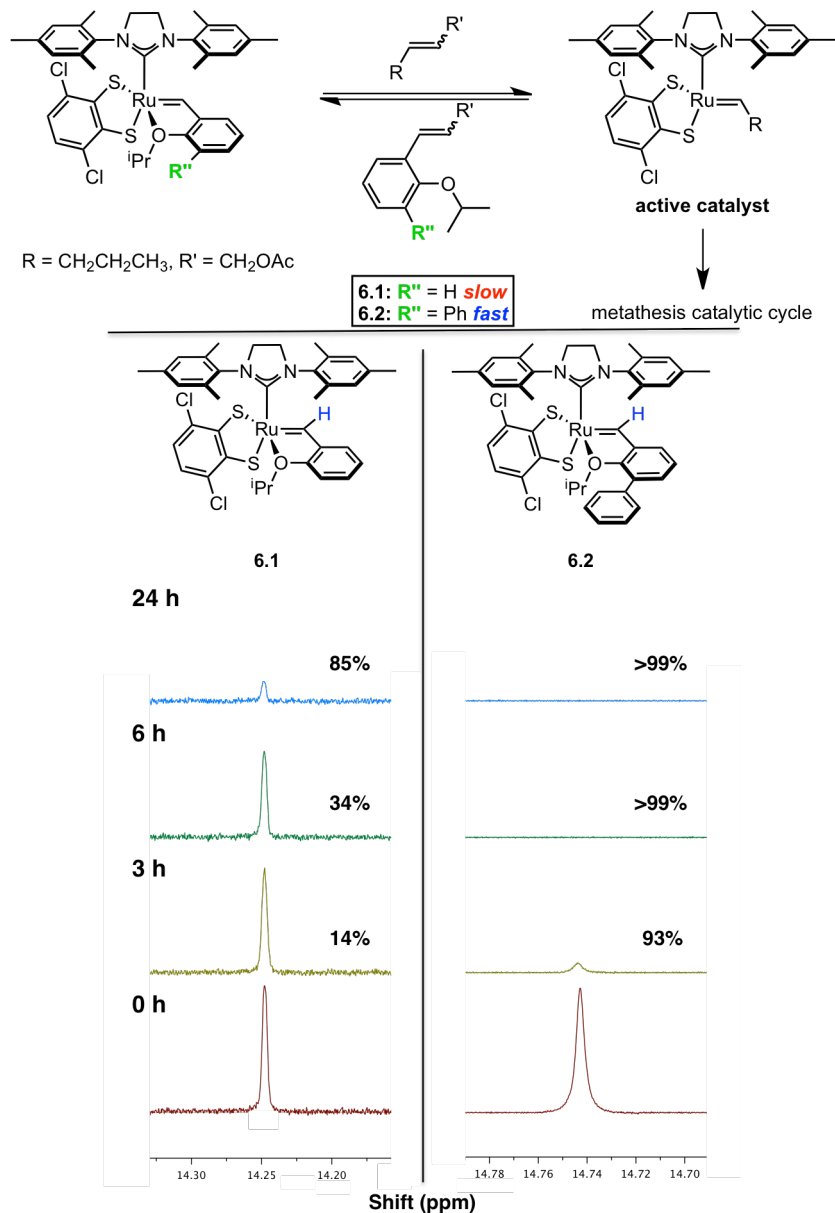
Figure 6.2. Signals corresponding to the benzylidene protons of **6.1** and **6.2** over the course of the reaction with *trans*-2-hexenyl acetate (0.5 M) in THF-d_8 at 45 °C. Percentages shown are percentages of catalyst initiated as determined by the decrease in the benzylidene signal over time upon reaction with substrate.

catalyst **6.2** bearing a chelating 2-isopropoxy-3-phenylbenzylidene ligand in place of the 2-isopropoxybenzylidene of catalyst **6.1**, was synthesized. This alteration has been shown to drastically increase rates of initiation in other ruthenium-based metathesis catalysts.[4c-f] Under the same aforementioned reaction conditions with *trans*-2-hexenyl acetate, 93% of **6.2** initiated after only 3 h and fully initiated within 6 h. For each catalyst, loss of the chelated benzylidene ligand is required prior to entrance into the catalytic cycle of olefin metathesis. Given the poor initiation of **6.1** even under relatively forcing conditions of elevated temperatures and high *trans*-substrate concentration, the concentration of active catalyst is significantly lower than that expected from the catalyst loading. As a result, the yields of products are diminished, limiting the use of this catalyst. This issue is resolved with catalyst **6.2**.

Initiation rate constants (k_{init}) were calculated for **6.1** and **6.2** under these reaction conditions and were determined to be 2.52×10^{-5} s^{-1} and 1.75×10^{-4} s^{-1}, respectively (Figure 6.3). The relative rate constant (k_{rel}) hence has a value of ~7. Thus, one-seventh of the catalyst loading of **6.1** can be used to achieve the same active catalyst concentration with catalyst **6.2**. Given the low activity seen in previous studies of **6.1** in cross metathesis
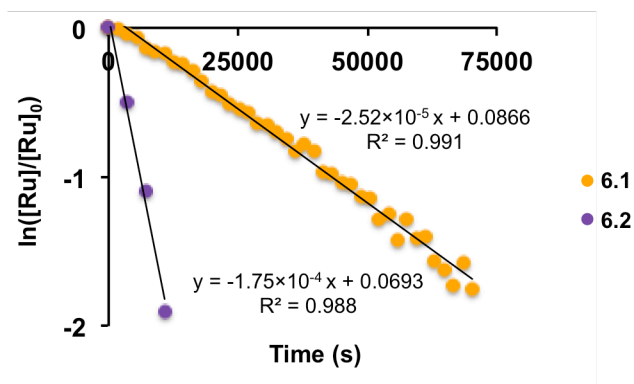
Figure 6.3. Plot of ln([Ru]/[Ru]$_0$) versus time. Plots remain approximately linear over the course of three-half lives of the reaction.

reactions involving *trans* olefins and the inability of this catalyst to initiate efficiently even under forcing conditions, the difference in the ability between **6.1** and **6.2** to initiate under normal reaction conditions can make a significant difference in the ability to provide meaningful yields of products.

Varying the size of the *ortho* substituents of the *N*-aryl groups of the NHC, a series of other fast-initiating catalysts, **6.3**, **6.4**, and **6.5**, were synthesized (Scheme 6.1). **6.2–6.5** were synthesized from phosphine-bound catalysts **6.2a–6.5a**. The chelating 2-isopropoxy-3-phenylbenzylidene ligand is installed by reaction of **6.2a–6.5a** with CuCl and (*E/Z*)-2-isopropoxy-3-(prop-1-en-1-yl)-1,1'-biphenyl to generate **6.2b–6.5b**. This is followed by the exchange of the two chloride X-ligands with a dithiolate ligand using a zinc transmetallating agent to produce **6.2–6.5** (Figure 6.4).

6.2a: Ar = 2,4,6-trimethylphenyl, R= H
6.3a: Ar = 2,6-diisopropylphenyl, R = H
6.4a: Ar = 2-fluoro-6-methylphenyl, R = H
6.5a: Ar = 2,6-difluorophenyl, R = Me

6.2b: Ar = 2,4,6-trimethylphenyl, R= H
6.3b: Ar = 2,6-diisopropylphenyl, R = H
6.4b: Ar = 2-fluoro-6-methylphenyl, R = H
6.5b: Ar = 2,6-difluorophenyl, R = Me
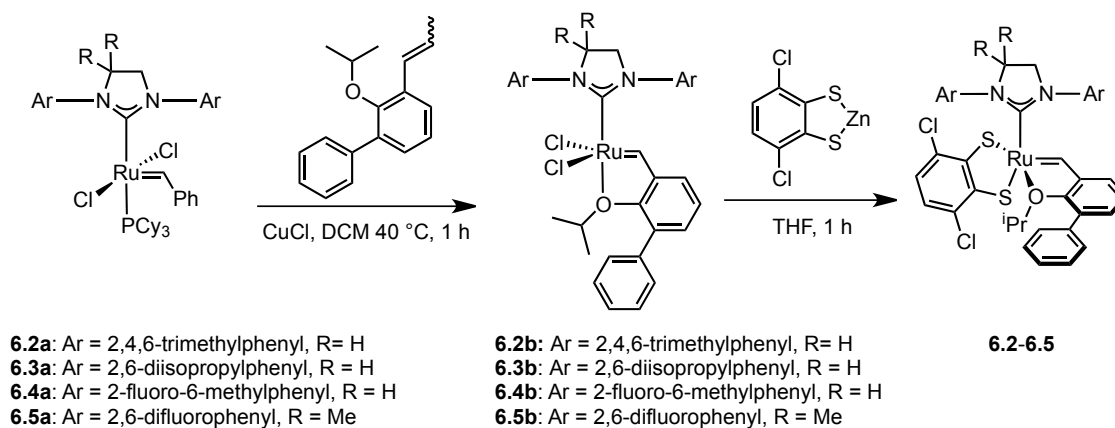
6.2-6.5

Scheme 6.1. Synthetic routes to catalysts **6.2–6.5**.

To observe differences in reactivity of catalysts **6.1–6.5**, the self-metathesis of the *trans* isomer of the substrate methyl 9-octadecenoate (MO) to produce dimethyl 9-octadecenedioate (DE) and 9-octadecene (9C18) was examined (Table 6.1, entries 1–7). With 1 mol% of **6.1**, this reaction requires 15 h to reach equilibrium whereas the same reaction with **6.2** reaches equilibrium in 3 h while maintaining the same high stereoselectivity (>99% *E*). To examine the relationship between the size of the *ortho*

substituents of the *N*-aryl group of the NHC and catalyst activity, **6.3**, **6.4**, and **6.5** were then studied in this reaction. **6.3** reaches equilibrium in 2.5 hours, whereas it only takes **6.4** 30 min and **6.5** 20 min to achieve the same distribution while high *trans* selectivity is conserved (>99% *E*). The catalyst loading of **6.4** and **6.5** can be dropped to 0.5 mol %, and the reaction still reaches equilibrium within 1 h and 40 min, respectively.
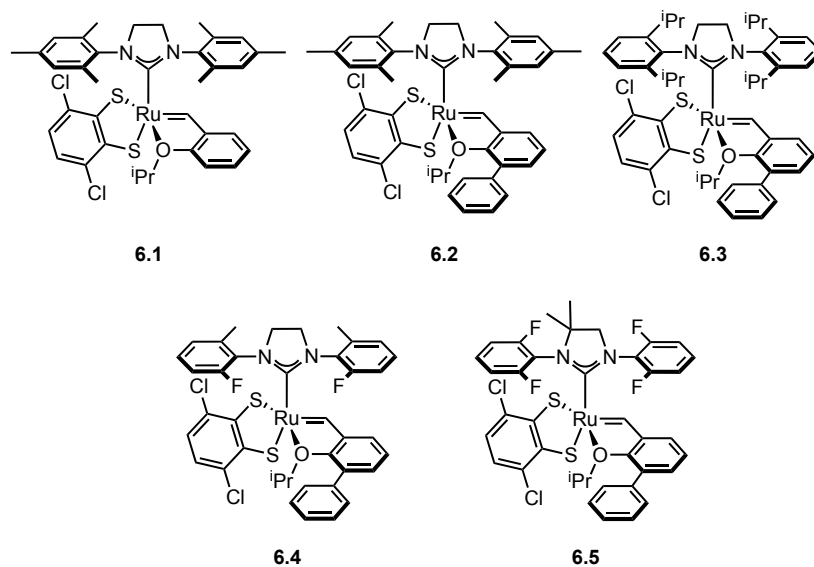
[Ru]	k_Z/k_E
6.2	60
6.3	200
6.4	7.5
2.4	4

Figure 6.4. Catalysts examined in this study.

The self-metathesis of the *cis* analogue of this substrate, *Z*-methyl 9-octadecenoate, was also analyzed (Table 6.1, entries 8–13). These catalysts were markedly more active in this reaction than that of the *E*-isomer. Catalyst **6.3** (0.5 mol %) is strikingly fast and reaches equilibrium in 90 seconds while the products retain the stereochemistry of the starting material (>99% *Z*). The catalyst loading can be reduced ten-fold to 0.05 mol %, and the reaction reaches equilibrium in 15 min. With 0.1 mol %

Table 6.1. Self-Metathesis of Methyl 9-octadeceonate[a]
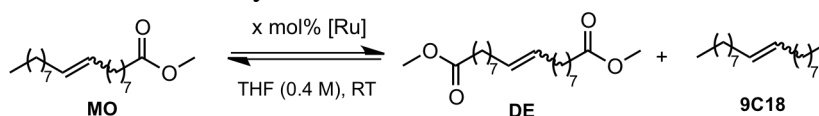
entry	Starting Material	Ru (mol%)	Time	% MO (E/Z)	% DE (E/Z)	% 9C18 (E/Z)
1	E	6.1 (1.0)	1 h	99 (>99/1)	0.5 (>99/1)	0.5 (>99/1)
			3 h	92 (>99/1)	4 (>99/1)	4 (>99/1)
			11 h	54 (>99/1)	23 (>99/1)	23 (>99/1)
			15 h	50 (>99/1)	25 (>99/1)	25 (>99/1)
2	E	6.2 (1.0)	1 h	80 (>99/1)	10 (>99/1)	10 (>99/1)
			3 h	50 (>99/1)	25 (>99/1)	25 (>99/1)
3	E	6.3 (1.0)	30 min	88 (>99/1)	6 (>99/1)	6 (>99/1)
			2.5 h	50 (>99/1)	25 (>99/1)	25 (>99/1)
4	E	6.4 (1.0)	10 min	84 (>99/1)	8 (>99/1)	8 (>99/1)
			20 min	60 (>99/1)	20 (>99/1)	20 (>99/1)
			30 min	50 (>99/1)	25 (>99/1)	25 (>99/1)
5	E	6.4 (0.5)	1 h	50 (>99/1)	25 (>99/1)	25 (>99/1)
6	E	6.5 (1.0)	10 min	62 (>99/1)	19 (>99/1)	19 (>99/1)
			20 min	50 (>99/1)	25 (>99/1)	25 (>99/1)
7	E	6.5 (0.5)	40 min	50 (>99/1)	25 (>99/1)	25 (>99/1)
8	Z	6.1 (0.1)	30 min	98 (<1/99)	1 (<1/99)	1 (<1/99)
			1 h	92 (<1/99)	4 (<1/99)	4 (<1/99)
			3 h	54 (<1/99)	23 (<1/99)	23 (<1/99)
			5 h	50 (<1/99)	25 (<1/99)	25 (<1/99)
9	Z	6.2 (0.1)	15 min	80 (<1/99)	10 (<1/99)	10 (<1/99)
			30 min	50 (<1/99)	25 (<1/99)	25 (<1/99)
10	Z	6.3 (0.5)	30 s	70 (<1/99)	15 (<1/99)	15 (<1/99)
			60 s	60 (<1/99)	20 (<1/99)	20 (<1/99)
			90 s	50 (<1/99)	25 (<1/99)	25 (<1/99)
11	Z	6.3 (0.05)	15 min	50 (<1/99)	25 (<1/99)	25 (<1/99)
12	Z	6.4 (0.1)	15 min	76 (<1/99)	12 (<1/99)	12 (<1/99)
			40 min	50 (<1/99)	25 (<1/99)	25 (<1/99)
13	Z	6.5 (0.1)	25 min	62 (<1/99)	19 (<1/99)	19 (<1/99)
			50 min	50 (<1/99)	25 (<1/99)	25 (<1/99)

[a]Product distribution and selectivity analyzed by GC using tridecane as an internal standard.

catalyst, the reaction reaches equilibrium in 30 min with **6.2,** 40 min with **6.4**, and 50 min with **6.5**. Catalyst **6.1**, however, requires 5 h at the same loading to achieve equilibrium.

To examine the disparity of the rates of reaction of each of these catalysts with the *E*- and *Z*-isomers of methyl 9-octadecenoate, a relative rate constant (k_Z/k_E) was calculated using the times needed for the reactions to reach equilibrium (t_E and t_Z) and

assuming first-order kinetics with respect to initial catalyst concentration ($[Ru]_E$ and $[Ru]_Z$).[14]

$$k_Z/k_E = [Ru]_E t_E/([Ru]_Z t_Z) \tag{1}$$

For catalysts **6.3**, **6.2**, **6.4**, and **6.5**, k_Z/k_E values were determined to be 200, 60, 7.5, and 4 (Figure 6.4). This is in accordance with our proposed model for selectivity, where *E*-olefin formation proceeds through a metallacycle in which the *β*-substituent points into the "open space" between the two *N*-aryl groups. Thus, reducing the size of the *ortho* substituents of the *N*-aryl groups increases the ability of the *E*-olefin to react with the catalysts.

In order to examine the reactivity of these catalysts with substrates bearing functional groups closer to the double bond, cross metathesis between *trans*-4-octene and *trans*-1,4-diacetoxy-2-butene (4:1 mole ratio) was examined (Figure 6.5). Using **6.1** (7.5 mol %), this reaction reaches a conversion of only 4% in 1 h to *trans*-2-hexenyl acetate (>99% *E*). Under identical conditions, **6.2** achieves 24% conversion in 1 h. After 7 h, the reaction reaches 80% conversion with **6.2** while parent catalyst **6.1** requires 3 days to reach 65% conversion. Consistent with the proposed model for selectivity, **6.3**, with bulky *N*-diisopropylphenyl groups of the NHC, has lower activity for these *trans* substrates in comparison to **6.2**, but is more active than **6.1** in this transformation. Catalyst **6.4** is remarkably fast in this reaction, achieving 80% conversion to the product (>99% *E*) in only 25 min. Also in agreement with the proposed model that suggests increased activity with decreasing *ortho* substituent size of the *N*-aryl groups, **6.5** demonstrated high initial conversion early in the reaction, but was found to decompose under reaction conditions, only reaching 36% overall conversion.
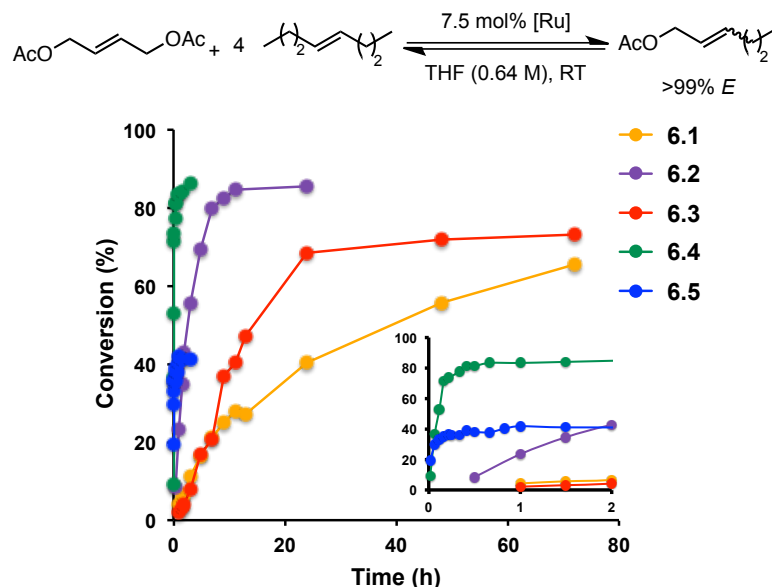
Figure 6.5. Cross Metathesis of *trans*-1,4-Diacetoxy-2-butene with *trans*-4-Octene Conversions determined using ^{1}H NMR. Stereoselectivity determined by GC. Inset shows early timepoints.
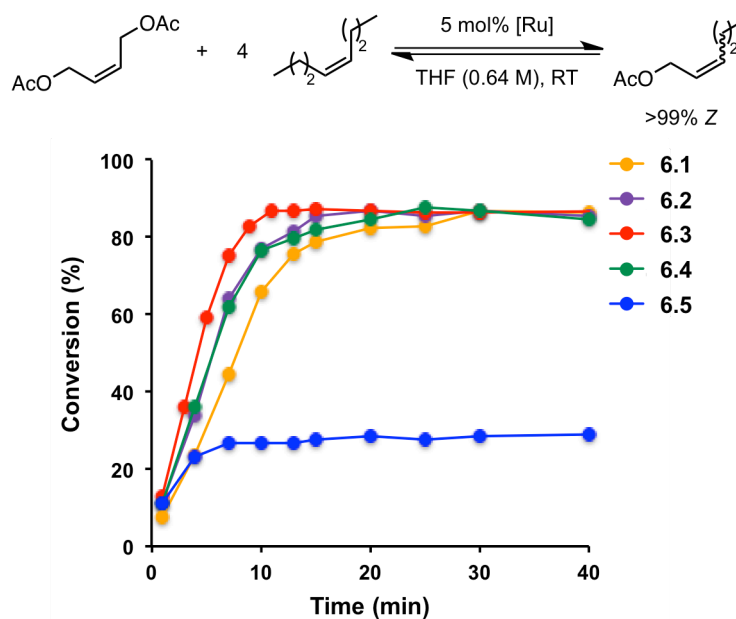
Figure 6.6. Cross Metathesis of *cis*-1,4-Diacetoxy-2-butene with *cis*-4-Octene Conversions determined using ^{1}H NMR. Stereoselectivity determined by GC.

As seen in the reaction with methyl 9-octadecenoate, the reaction of the *cis* isomers of these substrates, *cis*-4-octene and *cis*-1,4-diacetoxy-2-butene (4:1 molar ratio), was significantly more facile than the corresponding *trans* isomers with the catalysts

118

(Figure 6.6). **6.3** was the most active catalyst in this reaction, reaching 86% conversion in 11 min. **6.2** and **6.4** performed similarly, both reaching 81% conversion in 15 min. **6.1** reached 80% conversion in this reaction in 20 min. Catalyst **6.5** again decomposed under reaction conditions, reaching an overall yield of 28%. At the start of the reaction, however, it displayed reactivity less than that of catalysts **6.2**–**6.4** but greater than that of parent catalyst **6.1**. In this set of reactions, the opposite trend is seen with respect to changing the identity of the *ortho* substituents: as the NHC substituents get smaller, the reactivity with this substrate decreases. Because degradation is seen in both the reaction with the *cis* and *trans* isomers, the decomposition of **6.5** is likely due to a side reaction with 1,4-diacetoxy-2-butene.

The more challenging reaction of the cross metathesis of a disubstituted olefin, *trans*-4-octene, and a terminal olefin, 1-decene, to generate 4-tridecene was then

Table 6.2. Cross Metathesis of 1-Decene and *trans*-4-Octene[a]
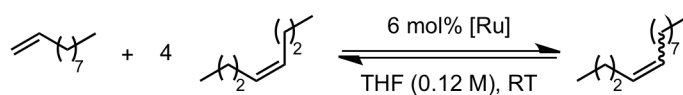
entry	[Ru]	Time (h)	Yield	E/Z
1	**6.1**	0.25	17	>99/1
		1	20	>99/1
		2	20	>99/1
		4	21	>99/1
2	**6.2**	0.25	24	>99/1
		1	25	>99/1
		2	26	>99/1
		4	27	>99/1
3	**6.3**	0.25	16	90/10
		1	17	90/10
		2	17	90/10
		4	19	90/10
4	**6.4**	0.25	47	>99/1
		1	49	>99/1
		2	50	>99/1
		4	49	>99/1
5	**6.5**	0.25	51	>99/1
		1	52	>99/1
		2	52	>99/1
		4	52	>99/1

[a]Yield and selectivity analyzed by GC using tetradecane as an internal standard.

attempted (Table 6.2). This reaction proved difficult for all catalysts due to rapid decomposition of these catalysts, likely due to the formation of the unstable ruthenium methylidenes under these conditions. As a result, yields of the product in this reaction for each of these catalysts did not change significantly after 15 min. Catalyst **6.3** (6 mol %) was the least active, reaching a maximum of 19% yield (90% *E*).[15] **6.2** generated the product in 27% yield, slightly higher than that of **6.1**, 21% yield. **6.4** and **6.5**, however, were efficient at reaching moderate yields of products with 50% and 52% yields, respectively, again in agreement with the proposed model by which reducing *ortho* substituent size of *N*-aryl groups is proposed to increase catalytic activity.[16] Catalysts **6.1**, **6.2**, **6.4**, and **6.5** all delivered high selectivity of the *trans* product (>99% *E*).

In the cross metathesis of *cis*-4-octene and 1-decene, yields were consistent across

Table 6.3. Cross Metathesis of 1-Decene and *cis*-4-Octene[a]

entry	[Ru]	Time (h)	Yield	E/Z
1	**6.1**	0.25	73	<1/99
		1	74	<1/99
		2	74	<1/99
		4	75	<1/99
2	**6.2**	0.25	75	<1/99
		1	75	<1/99
		2	76	<1/99
		4	77	<1/99
3	**6.3**	0.25	77	<1/99
		1	77	2/98
		2	77	2/98
		4	78	5/95
4	**6.4**	0.25	75	<1/99
		1	75	<1/99
		2	75	<1/99
		4	74	<1/99
5	**6.5**	0.25	65	<1/99
		1	70	<1/99
		2	70	<1/99
		4	70	<1/99

[a]Yield and selectivity analyzed by GC using tetradecane as an internal standard.

catalysts **6.1**–**6.4**, ranging from 75–78% with high stereoretention (>95% *Z*) throughout the reaction (Table 6.3).[17] Catalyst **5** generated the product in a slightly lower 70% yield.

Conclusions

^{1}H NMR studies were used to determine that recently reported highly stereoretentive ruthenium-based catalysts bearing dithiolate ligands suffer from poor catalyst initiation in reactions with *trans* olefins. In order to improve initiation characteristics, a series of fast-initiating catalysts **6.2**–**6.5** possessing a 2-isopropoxy-3-phenylbenzylidene ligand in place of the 2-isopropoxybenzylidene ligand were synthesized. These catalysts demonstrate significantly improved initiation compared to **6.1**, resulting in considerably increased activity of these catalysts in reactions of *trans* olefins, demonstrating higher yields at shorter reaction times, while maintaining high stereoselectivity of products (>99% *E*). Some improvement was also observed in reactions with *cis* olefins compared to previously reported catalysts, although the difference was more marginal as the previous catalysts were efficient at catalyzing reactions involving *cis* olefins with high stereoselectivity (>99% *Z*).

Experimental

General Information

Unless otherwise specified, all manipulations were carried out under air-free conditions in dry glassware in a Vacuum Atmospheres Glovebox filled with N_2. General solvents were purified by passing through solvent purification columns. Commercially available substrates were used as received. All solvents and substrates were sparged with Ar before being brought into the glovebox and filtered over basic alumina (Brockmann I) prior to use. THF-d_8 was dried over Na/benzophenone and vacuum transferred to another

Schlenk flask followed by degassing via methods of freeze, pump, thaw (×3). **6.1**,[3k] **6.2b**,[4f] **6.3b**,[4e] **6.4a**,[3l] (3,6-dichlorobenzene-1,2-dithiolato)zinc(II),[3k] and (*E/Z*)-2-isopropoxy-3-(prop-1-en-1-yl)-1,1'-biphenyl[4d] (**A**) were synthesized according to literature procedure.

Kinetic NMR experiments were performed on a Varian 500 MHz spectrometer with an AutoX probe. Spectra were analyzed using MestReNova Ver. 8.1.2. ^{1}H and ^{13}C NMR characterization data were obtained on a Bruker 400 with Prodigy broadband cryoprobe and referenced to residual protio-solvent. ^{19}F and ^{31}P NMR data were acquired on Varian 400 MHz and 300 MHz spectrometers. ^{1}H NMR spectra for determining conversions the cross metathesis of 4-octene and 1,4-diacetoxy-2-butene were obtained using the Bruker 400 with Prodigy broadband cryoprobe.

GC conversion data was obtained using an HP-5 capillary column with an Agilent 6850 FID gas chromatograph. GC selectivity data for the self-metathesis of methyl 9-octadeconate was also obtained on this HP-5 capillary column. GC selectivity data for the reactions of 4-octene with 1,4-diacetoxy-2-butene and with 1-decene were obtained using a DB-1 column with an Agilent 6890 FID gas chromatograph. Accurate conversion and yield data was produced by determining response factors by making solutions of varying concentrations of internal standard and the desired compound to be analyzed as described by Grubbs et. al.[6d] 4-tridecene was synthesized as previously described for this purpose.[19]

High-resolution mass spectrometry (HRMS) was performed using FAB+ ionization on a JEOL MSRoute mass spectrometer.

Synthesis of Catalyst 6.2

To a vial charged with a stir bar was added **6.2b** (40.0 mg, 0.057 mmol), (3,6-dichlorobenzene-1,2-dithiolato)zinc(II) (31.2 mg, 0.114 mmol) and 0.2 mL THF. After the reaction mixture was stirred at room temperature for 1 h, the solvent was removed *in vacuo* followed by co-evaporation with pentane. Dichloromethane was then added, and the mixture was filtered over a pad of Celite. Solvents were removed *in vacuo* followed by co-evaporation with pentane to yield the product as a brown solid (45.5 mg, 95% yield).

^{1}H NMR (400 MHz, Methylene Chloride-d_2) δ 14.82 (s, 1H), 7.59 - 7.44 (m, 5H), 7.38 (d, J = 1.7 Hz, 1H), 7.12 (d, J = 2.0 Hz, 1H), 7.04 (t, J = 7.5 Hz, 1H), 6.99 (d, J = 2.0 Hz, 1H), 6.96 (d, J = 8.1 Hz, 1H), 6.89 (d, J = 8.1 Hz, 1H), 6.81 (d, J = 2.0 Hz, 1H), 6.68 (dd, J = 7.5, 1.7 Hz, 1H), 6.30 (d, J = 2.1 Hz, 1H), 4.50 (hept, J = 6.5 Hz, 1H), 4.20 - 4.02 (m, 2H), 3.94 - 3.80 (m, 2H), 2.76 (s, 3H), 2.61 (s, 3H), 2.32 (s, 3H), 2.31 (s, 3H), 2.17 (s, 3H), 1.60 (s, 3H), 1.12 - 1.05 (d, 3H), 0.83 (d, J = 6.4 Hz, 3H).

^{13}C NMR (101 MHz, CD$_2$Cl$_2$) δ 255.91, 255.66, 216.74, 153.54, 152.58, 144.53, 143.09, 140.49, 140.45, 139.80, 138.03, 137.41, 137.34, 136.91, 136.04, 134.50, 132.22, 132.09, 131.92, 131.59, 130.53, 130.43, 130.38, 130.30, 130.24, 130.17, 129.73, 129.45, 129.24, 128.47, 128.36, 126.90, 125.08, 124.79, 123.53, 122.33, 79.96, 52.16, 52.05, 23.01, 21.33, 21.24, 20.08, 19.84, 19.49, 18.35.

HRMS (FAB+): [(M+H)−H$_2$] C$_{43}$H$_{43}$N$_2$ORuS$_2$Cl$_2$ Calculated - 839.1238, Found – 839.1278

Synthesis of Catalyst 6.3

To a vial charged with a stir bar was added **6.3b** (35.0 mg, 0.044 mmol), (3,6-dichlorobenzene-1,2-dithiolato)zinc(II) (24.4 mg, 0.088 mmol) and 0.150 mL THF. After the reaction mixture was stirred at room temperature for 1 h, the solvent was removed *in vacuo* followed by co-evaporation with pentane. Dichloromethane was then added, and the mixture was filtered over a pad of Celite. Solvents were removed *in vacuo* followed by co-evaporation with pentane to yield the product as a brown solid (37.8 mg, 93% yield).

^{1}H NMR (400 MHz, Methylene Chloride-d_2) δ 14.61 (s, 1H), 7.53 - 7.25 (m, 10H), 7.16 (dd, J = 7.5, 1.8 Hz, 2H), 6.89 (t, J = 7.5 Hz, 2H), 6.79 (d, J = 8.1 Hz, 1H), 6.60 (dd, J = 7.4, 1.8 Hz, 1H), 4.41 (hept, J = 6.4 Hz, 1H), 4.13 (s, 4H), 2.05 - 1.44 (m, 10H), 1.34 (dd, J = 9.4, 6.1 Hz, 6H), 1.03 (t, J = 6.3 Hz, 6H), 1.02 - 0.93 (m, 3H), 0.81 (d, J = 6.3 Hz, 3H), 0.41 (d, J = 6.9 Hz, 6H).

^{13}C NMR (101 MHz, CD$_2$Cl$_2$) δ 261.78, 261.52, 219.77, 152.92, 152.64, 148.20, 143.84, 143.15, 141.31, 134.09, 131.95, 131.32, 129.88, 129.77, 129.73, 129.64, 129.51, 128.62, 128.62, 128.15, 126.00, 125.79, 125.53, 125.45, 125.30, 125.11, 125.01, 124.21, 123.62, 123.49, 123.47, 122.03, 78.43, 78.32, 54.46, 54.40, 32.49, 30.27, 30.24, 30.07, 29.93, 29.86, 29.66, 29.58, 29.37, 26.77, 25.72, 23.93, 23.54, 23.26, 22.25, 21.76, 20.93, 14.45.

HRMS (FAB+): [M]$^+$ C$_{49}$H$_{56}$N$_2$ORuS$_2$Cl$_2$ Calculated – 924.2255, Found – 924.2210

Synthesis of Catalyst 6.4b/6.4

To a vial charged with a stir bar was added **6.4a** (0.100 g, 0.120 mmol), CuCl (11.9 mg, 0.120 mmol), **A** (30.4 mg, 0.120 mmol), and 1 mL dichloromethane. This mixture was stirred at 40°C for 1 hr. Pentane was added, and the reaction mixture was filtered over

Celite. The filtrate was added directly to a silica gel column. Organic byproducts were eluted with 4:1 pentane:diethyl ether followed by elution of crude **6.4b** (24.6 mg, green solid, NMR spectrum included below) with 1:1 pentane:diethyl ether. Solvents were removed *in vacuo*. To crude **6.4b** was added (3,6-dichlorobenzene-1,2-dithiolato)zinc(II) (19.8 mg, 0.072 mmol) and 0.150 mL THF. After the reaction mixture was stirred at room temperature for 1 h, the solvent was removed *in vacuo* followed by co-evaporation with pentane. Dichloromethane was then added, and the mixture was filtered over a pad of Celite. Solvents were removed *in vacuo* followed by co-evaporation with pentane. The pure product was obtained upon precipitation of the compound by adding cold pentane to a concentrated solution of the crude product in diethyl ether as a brown solid (20.0 mg, 20% overall yield).

6.4b: ^{1}**H NMR** (400 MHz, Methylene Chloride-d_2) δ 16.40 (s, 1H), 7.51 - 7.28 (m, 8H), 7.25 - 7.19 (m, 2H), 7.13 (q, J = 8.6 Hz, 2H), 6.99 (t, J = 7.4 Hz, 1H), 6.94 (dd, J = 7.5, 1.8 Hz, 1H), 4.45 - 4.34 (m, 1H), 4.33 - 4.23 (m, 2H), 4.17 (ddd, J = 13.3, 6.6, 4.2 Hz, 2H), 2.58 (s, 3H), 2.54 (s, 2H), 0.87 - 0.77 (m, 6H).

6.4b: ^{13}**C NMR** (101 MHz, CD$_2$Cl$_2$) δ 293.88, 215.19, 214.26, 191.20, 162.66, 162.55, 160.16, 160.04, 150.51, 149.75, 149.72, 148.31, 148.29, 142.34, 142.30, 139.63, 137.78, 133.94, 133.91, 133.10, 132.08, 131.13, 130.87, 130.82, 130.78, 130.73, 129.78, 129.71, 129.48, 129.39, 129.25, 129.04, 128.95, 128.61, 128.47, 128.31, 128.12, 127.48, 127.26, 126.87, 126.84, 125.43, 124.49, 124.19, 124.08, 121.80, 114.77, 114.68, 114.57, 114.48, 78.23, 78.20, 53.07, 52.88, 30.23, 27.48, 27.37, 26.83, 26.70, 22.24, 22.01, 20.61, 20.57, 19.15, 18.99.

6.4b: **HRMS** (FAB+): [(M+H)−H$_2$] C$_{33}$H$_{31}$F$_2$N$_2$ORuCl$_2$ Calculated − 681.0826, Found − 681.0831

6.4: **^{1}H NMR** (400 MHz, Methylene Chloride-d_2) (three conformers in solution) δ 14.99 (s, 0.31H), 14.92 (s, 0.17H), 14.86 (s, 0.53H), 7.75 - 7.65 (m, 1H), 7.61 - 7.48 (m, 2H), 7.44 (t, J = 6.9 Hz, 1H), 7.37 (d, J = 7.5 Hz, 1H), 7.28 - 7.20 (m, 3H), 7.12 (d, J = 7.6 Hz, 1H), 7.01 (d, J = 7.8 Hz, 1H), 6.94 (d, J = 7.5 Hz, 1H), 6.87 (q, J = 7.4 Hz, 3H), 6.57 (t, J = 7.6 Hz, 1H), 6.20 (t, J = 9.0 Hz, 1H), 4.69 - 4.47 (m, 1H), 4.00 (ddd, J = 19.3, 15.1, 9.2 Hz, 4H), 2.77 - 2.62 (m, 3H), 2.23 (d, J = 24.1 Hz, 3H), 1.58 (s, 1H), 1.26 (s, 1H), 1.23 - 1.02 (m, 2H), 0.77 (dd, J = 9.2, 6.0 Hz, 2H).

6.4: **^{13}C NMR** (101 MHz, CD$_2$Cl$_2$) δ 254.03, 253.83, 220.96, 220.45, 220.04, 161.69, 160.33, 159.22, 157.86, 154.90, 152.58, 144.51, 141.30, 139.91, 139.73, 139.38, 131.66, 131.45, 130.82, 130.73, 130.11, 130.03, 129.81, 129.54, 129.37, 128.87, 128.30, 127.12, 126.68, 125.48, 123.59, 123.32, 122.37, 122.19, 115.17, 114.97, 114.73, 114.64, 114.53, 114.45, 114.28, 114.08, 113.83, 81.40, 76.51, 74.85, 68.29, 53.33, 52.91, 52.33, 30.24, 26.12, 23.17, 22.49, 21.59, 20.12, 19.39, 19.06, 18.63, 16.74.

6.4: **^{19}F NMR** (376 MHz, CD$_2$Cl$_2$) δ -113.32, -116.93, -118.23, -119.84, -121.75, -123.33.

6.4: **HRMS** (FAB+): [M]$^+$ C$_{39}$H$_{34}$F$_2$N$_2$ORuS$_2$Cl$_2$ Calculated − 820.0502, Found − 820.0493

Synthesis of Catalyst 6.5a

The synthesis of this catalyst was performed just as previously described in the literature.[4] However, the product was isolated as a pure product. The crude solution was filtered over Celite, and solvents were removed *in vacuo*. 10 mL of pentane were added,

and the product was sonicated for 10 minutes. Solids were collected on a medium frit and washed with methanol (3 × 5 mL) to generate the pure product as a maroon solid (236.2 mg, 45% yield)

¹H NMR (400 MHz, Methylene Chloride-d_2) (two conformers in solution) δ 19.53 (d, J = 29.2 Hz, 0.5H), 19.45 (m, 0.5H), 7.57 - 7.33 (m, 4H), 7.33 - 7.10 (m, 4H), 6.95 - 6.67 (m, 1H), 6.44 (s, 2H), 3.96 (s, 1H), 3.82 (s, 1H), 2.22 - 2.00 (m, 3H), 1.75 (d, J = 12.9 Hz, 3H), 1.56 - 1.19 (m, 18H), 1.03 (dq, J = 21.2, 11.4 Hz, 15H).

Due to multiple conformers being present in solution and extensive fluorine coupling, fluorine splitting resonances are reported as peaks: **¹³C NMR** (101 MHz, CD$_2$Cl$_2$) δ 296.81, 296.68, 296.60, 296.54, 296.45, 224.29, 224.16, 223.51, 223.37, 162.63, 162.60, 161.99, 161.95, 161.38, 161.35, 160.72, 160.69, 160.08, 160.05, 159.44, 159.40, 158.87, 158.83, 158.20, 158.16, 157.72, 155.76, 152.64, 151.76, 151.59, 148.52, 137.27, 134.37, 133.87, 133.77, 133.67, 132.13, 132.03, 131.94, 131.57, 131.47, 131.37, 131.16, 131.06, 130.97, 130.91, 130.81, 130.76, 130.71, 130.57, 130.23, 130.13, 130.03, 129.88, 129.78, 129.68, 129.54, 129.08, 128.98, 128.83, 128.67, 128.65, 128.62, 128.49, 128.13, 127.61, 126.41, 120.79, 119.38, 119.04, 118.88, 118.72, 117.97, 117.82, 117.66, 115.63, 115.47, 115.31, 114.43, 114.27, 114.11, 113.83, 113.63, 113.20, 113.16, 113.12, 112.99, 112.96, 112.92, 112.68, 112.64, 112.57, 112.54, 112.47, 112.43, 112.37, 112.34, 112.22, 112.15, 112.12, 111.99, 111.82, 111.79, 111.76, 111.69, 111.65, 111.61, 111.58, 111.55, 111.50, 111.47, 111.38, 111.30, 111.25, 111.20, 111.12, 71.91, 67.94, 67.91, 67.73, 67.71, 66.94, 66.15, 66.13, 66.01, 65.77, 64.10, 35.46, 35.40, 35.21, 34.85, 33.26, 33.10, 32.13, 32.05, 31.97, 31.86, 31.81, 29.69, 29.57, 29.13, 28.85, 28.76, 28.73, 27.85, 27.80, 27.75, 27.69, 27.59, 27.46, 27.41, 27.32, 27.17, 27.07, 26.99, 26.96, 26.84, 26.72, 26.60, 26.53, 26.42,

26.31, 26.28, 26.18, 26.16, 25.89, 25.78, 25.74, 25.69, 25.59, 25.53, 25.37, 24.83, 24.77, 24.29.

31P NMR (121 MHz, CD$_2$Cl$_2$) δ 26.22, 26.11.

HRMS (FAB+): [M]$^+$ C$_{42}$H$_{53}$Cl$_2$F$_4$N$_2$PRu Calculated – 864.2304, Found – 864.2311.

Synthesis of Catalyst 6.5b

To a vial charged with a stir bar was added **6.5a** (0.100 g, 0.120 mmol), CuCl (11.9 mg, 0.120 mmol), **A** (30.4 mg, 0.120 mmol), and 1 mL dichloromethane. This mixture was stirred at 40 °C for 1 hr. Pentane was added, and the reaction mixture was filtered over Celite. The filtrate was added directly to a silica gel column. Organic byproducts were eluted with 4:1 pentane:diethyl ether followed by elution of the product with 1:1 pentane:diethyl ether. Solvents were removed *in vacuo* to yield the product as a green solid (20.3 mg, 24% yield).

1H NMR (400 MHz, Methylene Chloride-d_2) δ 16.80 (s, 1H), 7.66 - 7.21 (m, 9H), 7.16 - 7.06 (m, 3H), 7.08 - 6.97 (m, 2H), 4.46 (hept, J = 6.3 Hz, 1H), 4.08 (s, 2H), 1.49 (d, J = 2.9 Hz, 6H), 0.92 (d, J = 6.2 Hz, 6H).

13C NMR (101 MHz, CD$_2$Cl$_2$) δ 292.04, 291.83, 215.42, 163.33, 163.30, 161.97, 161.93, 160.81, 160.78, 159.46, 159.42, 150.33, 148.26, 139.58, 137.78, 133.94, 132.35, 131.69, 131.66, 131.59, 131.50, 131.49, 130.49, 130.39, 130.29, 129.78, 129.48, 129.34, 129.26, 129.12, 128.96, 128.53, 128.35, 128.13, 127.26, 125.51, 124.49, 124.24, 121.20, 120.22, 120.07, 119.92, 116.66, 116.50, 116.34, 113.03, 113.00, 112.98, 112.94, 112.92, 112.89, 112.83, 112.81, 112.78, 112.75, 112.73, 112.71, 108.16, 78.36, 77.38, 68.21, 66.05, 26.51, 26.49, 26.46, 20.69.

19F NMR (376 MHz, CD$_2$Cl$_2$) δ -108.17, -115.14.

HRMS (FAB+): [M]$^+$ C$_{33}$H$_{30}$Cl$_2$F$_4$N$_2$ORu Calculated – 718.0715, Found – 718.0718

Synthesis of Catalyst 6.5

To a vial charged with a stir bar was added **6.5b** (20.3 mg, 0.0283 mmol), (3,6-dichlorobenzene-1,2-dithiolato)zinc(II) (15.5 mg, 0.0566 mmol) and 0.1 mL THF. After the reaction mixture was stirred at room temperature for 1 hour, the solvent was removed *in vacuo* followed by co-evaporation with pentane. Dichloromethane was then added, and the mixture was filtered over a pad of Celite. Solvents were removed *in vacuo* followed by co-evaporation with pentane to yield the product as a brown solid (23.0 mg, 95% yield).

^{1}H NMR (400 MHz, Methylene Chloride-d_2) δ 14.93 (s, 0.56H), 14.62 (s, 0.44H), 7.66 (d, J = 7.5 Hz, 1H), 7.62 (d, J = 7.5 Hz, 1H), 7.52 (td, J = 7.7, 3.3 Hz, 2H), 7.47 - 7.39 (m, 2H), 7.33 - 7.29 (m, 1H), 7.25 (dt, J = 6.3, 2.1 Hz, 1H), 7.19 - 7.06 (m, 3H), 6.99 (dq, J = 8.7, 4.4, 4.0 Hz, 1H), 6.94 (t, J = 8.0 Hz, 1H), 6.85 - 6.76 (m, 2H), 6.71 (d, J = 8.2 Hz, 0.47H), 6.65 (dd, J = 7.6, 1.7 Hz, 0.61H), 6.57 (dd, J = 7.4, 1.7 Hz, 1H), 6.40 (dd, J = 14.5, 8.9 Hz, 1H), 4.73 (p, J = 6.4 Hz, 0.47H), 4.61 (p, J = 6.6 Hz, 0.53H), 3.95 - 3.74 (m, 2H), 3.28 (dt, J = 12.3, 6.1 Hz, 0.33H), 3.01 (s, 0.76H), 2.48 (q, J = 7.1 Hz, 0.43H), 2.29 (t, J = 7.6 Hz, 0H), 1.43 - 1.33 (m, 3H), 1.38 - 1.28 (m, 3H), 0.93 (d, J = 6.2 Hz, 2H), 0.83 (d, J = 6.3 Hz, 2H), 0.72 (d, J = 6.1 Hz, 1H), 0.48 (t, J = 6.5 Hz, 1H).

Due to multiple conformers being present in solution because of extensive fluorine coupling, fluorine splitting resonances are reported as peaks: **^{13}C NMR** (101 MHz, CD$_2$Cl$_2$) δ 252.42, 252.14, 222.64, 221.58, 173.61, 161.94, 161.53, 160.61, 159.39, 158.99, 158.11, 158.03, 156.03, 154.77, 154.46, 153.99, 153.80, 151.14, 144.56, 143.74, 142.85, 142.77, 140.20, 139.69, 139.54, 136.93, 135.39, 134.54, 134.14, 132.29, 132.23,

132.19, 132.09, 131.61, 131.55, 131.52, 131.41, 131.36, 131.28, 131.18, 131.14, 131.08, 130.71, 130.69, 130.59, 130.49, 130.40, 130.10, 129.78, 129.74, 129.71, 129.49, 129.34, 129.30, 129.22, 128.98, 128.96, 128.91, 128.63, 128.61, 128.54, 128.36, 128.30, 128.22, 127.16, 125.74, 125.67, 125.56, 125.44, 125.35, 124.61, 124.20, 124.16, 123.65, 123.59, 122.96, 122.67, 122.55, 122.38, 122.34, 121.94, 120.97, 119.50, 117.16, 116.52, 114.58, 113.10, 113.07, 112.95, 112.92, 112.89, 112.85, 112.81, 112.76, 112.72, 112.64, 112.61, 112.57, 112.02, 108.16, 82.19, 80.80, 77.65, 76.20, 75.01, 69.62, 69.27, 68.50, 66.78, 66.40, 65.72, 62.56, 60.00, 48.96, 48.76, 38.65, 34.66, 34.48, 32.69, 32.48, 31.96, 31.65, 30.24, 29.92, 29.77, 29.66, 29.61, 29.30, 28.44, 28.41, 27.63, 26.97, 26.66, 26.62, 26.51, 26.48, 26.32, 25.93, 25.88, 25.38, 23.73, 23.25, 22.99, 22.49, 22.43, 22.39, 22.35, 22.31, 22.29, 22.24, 21.65, 21.55, 20.83, 20.22, 14.44, 14.35, 10.13.

^{19}F NMR (376 MHz, CD$_2$Cl$_2$) δ -102.19, -107.21, -109.43, -110.03, -110.92, -113.88, -114.12, -114.92, -115.37, -115.39, -116.50, -119.15, -119.17, -119.19.

HRMS (FAB+): [M]$^+$ C$_{39}$H$_{32}$Cl$_2$F$_4$N$_2$ORu Calculated – 856.03134, Found – 856.03090

Synthesis of *trans*-1,4-diacetoxy-2-butene

To a vial charged with a stir bar under argon atmosphere was added *trans*-2-butene-1,4-diol (5.00 g, 56.7 mmol), 4.9 mL dichloromethane, and Ac$_2$O (18.2 mL, 0.192 mol) at 0 °C. Pyridine (14.0 mL, 0.174 mol) was then added dropwise to the reaction mixture. After 30 minutes, the reaction mixture was allowed to rise to room temperature and was stirred for an additional 18 h. Extraction of the product with DCM was followed by washing of the organic layer with 2M HCl, saturated aq. NaCl, and 2M aq. Na$_2$CO$_3$. The organic layer was dried over anhydrous MgSO$_4$, filtered, and solvents were removed *in*

vacuo. The product was distilled at 120 mtorr at 110 °C (7.45 g, 76% yield). Spectroscopic data matched those previously reported in the literature.[20]

General Procedure for NMR Initiation Experiments.

To a vial containing catalyst (0.00275 mmol) was added THF-d_8 (506.5 µL) and *trans*-2-hexenyl acetate (43.5 µL, 0.275 mmol). This solution was transferred to a J. Young Tube and monitored by observing the disappearance of the benzylidene signal by ^{1}H NMR using an array at 45 °C.

General Procedure for Cross Metathesis of Methyl 9-octadecenoate Experiments.

To a vial charged with a stir bar, the appropriate amount of catalyst was added and dissolved in 383.1 µL THF. Tridecane (48.8 µL, 0.2 mmol) and methyl 9-octadecenoate (68.1 µL, 0.2 mmol) were then added and the vial was capped. At the specified time points, 5 µL aliquots were taken and quenched with butyl vinyl ether, and the product distribution was analyzed by GC.

General Procedure for Cross Metathesis of *Trans*-4-octene and *Trans*-1,4-diacetoxy-2-butene Experiments.

To a vial charged with a stir bar, catalyst (0.0192 mmol) was added and dissolved in 294.8 µL THF. 147.4 µL THF of this catalyst stock solution was added to a vial containing *trans*-1,4-diacetoxy-2-butene (30.6 µL, 0.128 mmol), *trans*-4-octene (120.4 µL, 0.512 mmol), and a stir bar. The vial was capped, and the reaction mixture was stirred. At the specified time points, 3 µL aliquots were added to a septum-capped NMR tube to which was added $CDCl_3$, and the product distribution was analyzed by ^{1}H NMR. Stereoselectivity of the product was determined by GC.

General Procedure for Cross Metathesis of *Cis*-4-octene and *Cis*-1,4-diacetoxy-2-butene Experiments.

To a vial was added catalyst (0.0128 mmol) that was dissolved in 294.8 μL THF. 147.4 μL of this catalyst stock solution was added to a vial containing *cis*-1,4-diacetoxy-2-butene (30.6 μL, 0.128 mmol), *cis*-4-octene (120.4 μL, 0.512 mmol), and stir bar. The vial was capped, and the reaction mixture was stirred. At the specified time points, 3 μL aliquots were added to a septum-capped NMR tube to which was added CDCl$_3$, and the product distribution was analyzed by ^{1}H NMR. Stereoselectivity of the product was determined by GC.

General Procedure for Cross Metathesis of *Cis*/*Trans*-4-octene and 1-decene.

To a vial was added catalyst (0.0072 mmol) that was dissolved in 870.8 μL THF. 435.4 μL of the catalyst stock solution was added to a vial containing tetradecane (15.6 μL, 0.06 mmol), 4-octene (37.6 μL, 0.24 mmol), 1-decene (11.4 μL, 0.06 mmol), and a stir bar. The vial was capped, and the reaction mixture was stirred. At the specified time points, 20 μL aliquots were quenched with butyl vinyl ether, and the product distribution was analyzed by GC.

GC Methods

Self-Metathesis of MO (Conversion and Selectivity) and Cross Metathesis of 4-Octene and 1-Decene (Conversion)

HP-5 Agilent Column 30m × 0.25mm (ID) × 0.25μm film thickness; Injector temperature: 250 °C; Detector temperature: 350 °C; Oven temperature: Starting temperature: 50 °C, hold time: 2 min.; Ramp rate: 11 °C/min to 300 °C, hold time: 3 min. Carrier gas: He; Average velocity: 31 cm/s; Split ratio: 48.9:1.

Cross Metathesis of 4-Octene and 1,4-Diacetoxy-2-butene (Selectivity) and Cross Metathesis of 4-Octene and 1-Decene (Selectivity)

DB-1 Agilent Column 10 m × 0.100mm (ID) × 0.40μm film thickness; Injector temperature: 250 °C; Detector temperature: 350 °C; Oven temperature: Starting temperature: 35 °C, hold time: 0.5 min.; Ramp rate: 10 °C/min to 135 °C, hold time: 0 min., 20 °C/min to 290 °C; Carrier gas: He; Average velocity: 20 cm/s; Split ratio: 103:1

References

1. Grubbs, R. H.; Wenzel, A. G.; O'Leary, D. J.; Khosravi, E., Eds. Handbook of Metathesis; Wiley−VCH: Weinheim, 2015.

2. (a) Hoveyda, A. H; Schrock, R. R. *Chem. Eur. J*, 2001, *7*, 945. (b) Van Veldhuizen, J. J.; Campbell, J. E.; Guidici, R. E.; Hoveyda, A. H. *J. Am. Chem. Soc*. **2005**, *127*, 6877. (c) Funk, T. W.; Berlin, J. M.; Grubbs, R. H. *J. Am. Chem. Soc.* **2006**, *128*, 1840. (d) Berlin, J. M.; Goldberg, S. D.; Grubbs, R. H *Angew. Chem. Int. Ed*. **2006**, *45*, 7591. (e) Tiede, S.; Berger, A.; Schlesiger, D.; Rost, D.; Lühl, A.; Blechert, S. *Angew. Chem. Int. Ed.* **2010**, *49*, 3972. (f) Fürstner, A.; Ackermann, L.; Gabor, B.; Goddard, R.; Lehmann, C. W.; Mynott, R.; Stelzer, F.; Thiel, O. R. *Chem. Eur. J.* **2001**, *7*, 3236.

3. (a) Flook, M. M.; Jiang, A. J.; Schrock, R. R.; Müller, P.; Hoveyda, A. H. *J. Am. Chem. Soc.* **2009**, *131*, 7962. (b) Jiang, A. J.; Zhao, Y.; Schrock, R. R.; Hoveyda, A. H. *J. Am. Chem. Soc.* **2009**, *131*, 16630. (c) Meek, S. J.; O'Brien, R. V.; Llaveria, J.; Schrock, R. R.; Hoveyda, A. H. *Nature* **2011**, *471*, 461. (d) Yu, M.; Wang, C.; Kyle, A. F.; Jakubec, P.; Dixon, D. J.; Schrock, R. R.; Hoveyda, A. H. *Nature* **2011**, *479*, 88. (e) Endo, K.; Grubbs, R. H. *J. Am. Chem. Soc.* **2011**, *133*, 8525. (f) Keitz, B. K.; Endo, K.; Herbert, M. B.; Grubbs, R. H. *J. Am. Chem. Soc.* **2011**, *133*, 9686. (g) Keitz, B. K.; Endo, K.; Patel, P. R.; Herbert, M. B.; Grubbs, R. H. *J. Am. Chem. Soc*.

2011, *134*, 693. (h) Occhipinti, G.; Hansen, F. R.; Törnroos, K. W.; Jensen, V. R. *J. Am. Chem. Soc.* **2013**, *135*, 3331. (i) Khan, R. K. M.; Torker, S.; Hoveyda, A. H. *J. Am. Chem. Soc.* **2013**, *135*, 10258. (j) Koh, M. J.; Khan, R. K. M.; Torker, S.; Hoveyda, A. H. *Angew. Chem. Int. Ed.* **2014**, 53, 1968. (k) Koh, M. J.; Khan, R. K. M.; Torker, S.; Yu, M.; Mikus, M. S.; Hoveyda, A. H. *Nature* **2015**, *517*, 181. (l) Johns, A. M.; Ahmed, T. S.; Jackson, B. W.; Grubbs, R. H.; Pederson, R. L. *Org. Lett.* **2016**, *18*, 772. (m) Nguyen, T. T.; Koh, M. J.; Shen, X.; Romiti, F.; Schrock, R. R.; Hoveyda, A. H. *Science* **2016**, *352*, 6285.

4. (a) Scholl, M.; Ding, S.; Lee, C. W.; Grubbs, R. H. *Org. Lett.* **1999**, *1*, 953. (b) Fürstner, A.; Ackermann, L.; Gabor, B.; Goddard, R.; Lehmann, C. W.; Mynott, R.; Stelzer, F.; Thiel, O. R. *Chem. Eur. J.* **2001**, *7*, 3236-3253. (c) Wakamatsu, H.; Blechert, S. *Angew. Chem. Int. Ed.* **2002**, *41, 2403.* (d) Bujok, R.; Bieniek, M.; Masnyk, M.; Michrowska, A.; Sarosiek, A.; Stępowska, H.; Arlt, D.; Grela, K. *J. Org. Chem.* **2004**, *69*, 6894. (e) Nelson, D. J.; Queval, P.; Rouen, M.; Magrez, M.; Toupet, L.; Caijo, F.; Borre, E.; Laurent, I.; Crévisy, C.; Baslé, O.; Mauduit, M.; Percy, J. M. *ACS Catal.* **2013**, *3*, 259. (f) Engle, K. M.; Lu, G.; Luo, S.; Henling, L. M.; Takase, M. K.; Liu, P.; Houk, K. N.; Grubbs, R. H. *J. Am. Chem. Soc.* **2015**, *137*, 5782.

5. (a) Liu, P.; Xu, X.; Dong, X.; Keitz, B. K.; Herbert, M. B.; Grubbs, R. H.; Houk, K. N. *J. Am. Chem. Soc.* **2012**, *134*, 1464. (b) Dang, Y.; Wang, Z. X.; Wang, X. *Organometallics* **2012**, *31*, 7222. (c) Dang, Y.; Wang, Z. X.; Wang, X. *Organometallics* **2012**, *31*, 8654. (d) Occhipinti, G.; Koudriavtsev, V.; Törnroos, K.

W.; Jensen, V. R. *Dalton Trans.* **2014**, *43*, 11106. (e) Torker, S.; Khan, R. K. M.; Hoveyda, A. H. *J. Am. Chem. Soc.* **2014**, *136*, 3439.

6. (a) Bilhou, J. L.; Basset, J. M.; Mutin, R.; Graydon, W. F. *J. Am. Chem. Soc.* **1977**, *99*, 4083. (b) Leconte, M.; Basset, J. M. *J. Am. Chem. Soc.* **1979**, *101*, 7296. (c) Leconte, M.; Basset, J. M. *Ann. N. Y. Acad. Sci.* **1980**, *333*, 165. (d) Ritter, T.; Hejl, A.; Wenzel, A. J.; Funk, T. W.; Grubbs, R. H. *Organometallics* **2006**, *25* (24), 5740.

7. (a) Marinescu, S. C.; Levine, D. S.; Zhao, Y.; Schrock, R. R.; Hoveyda, A. H. *J. Am. Chem. Soc.* **2011**, *133*, 11512. (b) Miyazaki, H.; Herbert, M. B.; Liu, P.; Dong, X.; Xu, X.; Keitz, B. K.; Ung, T.; Mkrtumyan, G.; Houk, K. N.; Grubbs, R. H. *J. Am. Chem. Soc.* **2013**, *135*, 5848.

8. Vedejs, E.; Peterson, M. J. *Top. Stereochem.* **1994**, *21*, 1.

9. Blakemore, P.R. *J. Chem. Soc., Perkin Trans. 1*, **2002**, 2563.

10. van Staden, L. F.; Gravstock, D.; Ager, D. J. *J. Chem. Soc. Rev.*, **2002**, *31*, 195.

11. Pasto, D. J. in *Comprehensive Organic Synthesis*; Trost, B. M., Fleming, I., Ed.; Pergamon Press: Oxford, 1991; Vol. 8, Chapter 3.3.

12. Trost, B. M.; Ball, Z. T.; Jöge, T. *J. Am. Chem. Soc.* **2002**, *124*, 7922.

13. (a) Srimani, D.; Diskin-Posner, Y.; Ben-David, Y.; Milstein, D. *Angew. Chem Int. Ed.* **2013**, *52*, 14131. (b) Radkowski, K.; Sundararaju, B.; Fürstner, A. *Angew. Chem. Int. Ed.* **2013**, *52*, 355. (c) Liu, Y.; Hu, L.; Chen, H.; Du, H. *Chem. Eur. J.* **2015**, *124*, 3495.

14. By increasing catalyst concentration by a certain factor, reaction rate was increased by the same factor. See SI for data (Table S6.1).

15. In this case, conversion of 1-decene to a variety of isomers was also seen, and this isomerization process might be responsible for the degraded level of *E*-selectivity.

16. Previous studies have shown that Ru---F interactions sometimes occur in particular olefin metathesis systems (see ref. 18). Although there is no evidence of this in this system, this type of interaction might play a role in this reaction.

17. Lower yields than expected in this reaction could be attributed to the self-metathesis of the product, 4-tridecene, to form 4-octene and 9-octadecene as detected by GC. Degradation of Z-content with 3 is likely due to secondary metathesis processes promoted by this very active catalyst.

18. Ritter, T.; Grubbs, R. H. *J. Am. Chem. Soc.* **2006**, *128*, 11768.

19. Zhu, J.; Unelius, R. C.; Park, K. C.; Ochieng, S. A.; Obrycki, J. J.; Baker, T. C. *J. Chem. Ecol.* **2000**, *26*, 2421.

20. Stehouwer, J. S.; Daniel, L. M.; Chen, P.; Voll, R. J.; Williams, L., Plott, S. J.; Votaw, J. R.; Owens, M. J.; Howell, L. Goodman, M. M. *J. Med. Chem.* **2010**, *53*, 5549.

Chapter 7

A Highly Efficient Synthesis of *Z*-Macrocycles using Stereoretentive,

**Ruthenium-Based Metathesis Catalysts**

Abstract

A highly efficient, *Z*-selective ring-closing metathesis system for the formation of macrocycles using a stereoretentive, ruthenium-based catalyst supported by a dithiolate ligand is reported. This catalyst is demonstrated to be remarkably active as observed in initiation experiments showing complete catalyst initiation at –20 °C within 10 min. Macrocyclization reactions generated *Z*-products from easily accessible diene starting materials bearing a *Z*-olefin moiety. This stereoretentive approach provides a more efficient and selective route to *Z*-macrocycles than in previously reported systems. Reactions were completed in appreciably shorter reaction times, and turnover numbers of up to 100 could be achieved. Macrocyclic lactones ranging in size from twelve-membered to seventeen-membered rings are synthesized in moderate to high yields (68 – 79% yield) with excellent *Z*-selectivity (95% – 99% *Z*).

Introduction

Transition metal-catalyzed ring-closing metathesis (RCM) has become a powerful method for generating cyclic molecules.[1] It is widely used in the synthesis of pharmaceuticals as well as in the production of pheromones and musks as replacements for toxic, synthetic polycyclic and nitroarene musks.[2] The stereochemistry of the alkene, *E* or *Z*, in these cyclic structures is often crucial to the biological activity of a molecule or its olfactory characteristics, and small amounts of impurity of the other stereoisomer in chemical mixtures can drastically decrease their potency. It is often particularly difficult to separate *E*- and *Z*-isomers as techniques for their separation are not general. As such, methods for producing stereochemically pure cyclic compounds are of paramount importance.

Controlling olefin stereochemistry in RCM reactions can be difficult. When using common non-selective metathesis catalysts, selectivity is controlled by the thermodynamic stability of the olefin products and can vary depending on ring size and double bond position.[3] Because of the dilute conditions required to prevent oligomerization, high catalyst loadings are often needed for macrocyclization reactions using RCM, but removing residual metals can be challenging. For some applications, this requires further purification with lead or phosphine additives or with multiple chromatographic columns followed by treatment with charcoal.[4] Reducing catalyst loadings required for these reactions is thus an important goal.

One established method for stereoselectively generating *Z*-macrocycles is ring-closing alkyne metathesis followed by Lindlar hydrogenation.[5] *Z*-macrocycles have also been synthesized by reaction of terminal olefins with internal vinyl silanes followed by protodesilylation.[6] However, these approaches require multiple steps to synthesize the desired product, and thus more direct methods using olefin metathesis are desirable. In 2011, the first report of *Z*-selective RCM was disclosed. Mo- and W-based catalysts **7.1−7.3** were used to synthesize a 16-membered macrocyclic lactone (91 – 95% *Z*), nakadomarin A (90 – 97% *Z*), and epothilone C (69 – 97% *Z*) (Figure 7.1).[3e] While these catalysts afforded exceptional selectivity, they required catalyst loadings of 5 to 6 mol %. One year later, *Z*-selective cyclometallated ruthenium-based catalyst **7.4** (7.5 mol %) was reported to generate macrocyclic lactones, lactams, and ketones (75 – 94% *Z*) with the purpose of synthesizing pheromones and fragrances.[2f] This method was limited by long reaction times, required the use of high boiling solvents and elevated temperatures, and delivered most products with ca. 85% *Z*-selectivity.

7.1　　　　　　**7.2**　　　　　　**7.3**　　　　　　**7.4**
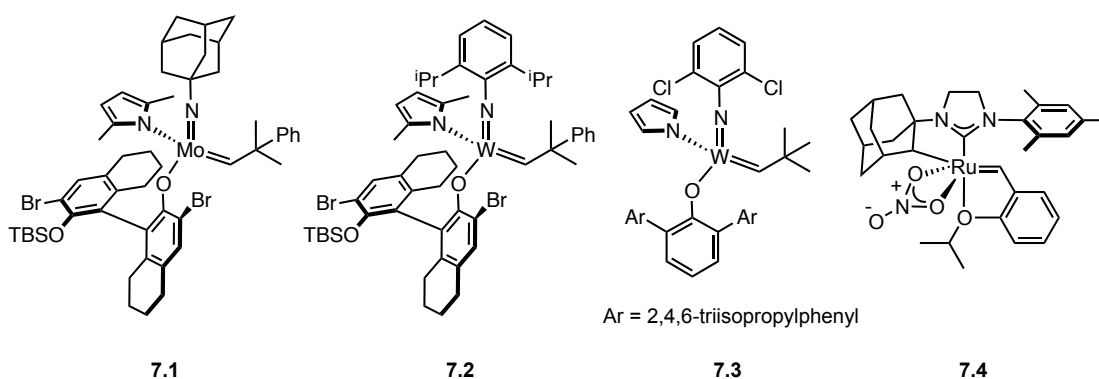
Figure 7.1. Catalysts used previously to selectively generate highly *Z*-macrocycles.

In 2015, Hoveyda reported cross metathesis of *Z*-olefins and terminal olefins to generate highly *Z*-products (>96% *Z*) using Ru-based complexes supported by dithiolate ligands.[7] Additional studies of these catalysts in 2016 demonstrated that they were highly stereoretentive, also capable of cross metathesis between two *E*-olefins or between an *E*-olefin and a terminal olefin to deliver products with kinetic *E*-selectivity (>98% *E*).[8] The proposed model for *Z*-selectivity using these catalysts is based on a proposed side-bound metallacyclobutane intermediate in which stereoselectivity arises from the α-substituents of the metallacyclobutane favorably positioned away from the large *N*-aryl groups of the *N*-heterocyclic carbene (NHC) ligand (Figure 7.2). Given that the reacting olefin has *Z*-stereochemistry, the β-substituent points down in the favored proposed intermediate.
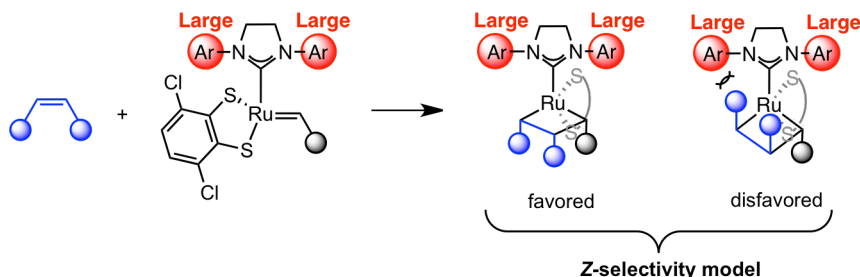

Figure 7.2. Model for *Z*-selectivity using stereoretentive metathesis catalysts in cross metathesis.

Subsequent cycloreversion of this metallocyclobutane intermediate leads to the formation of the *Z*-product.

Results and Discussion

Based on this model for selectivity, it was expected that highly *Z*-selective RCM to generate *Z*-macrocycles could be possible from diene substrates containing a *Z*-olefin and a terminal olefin using these catalysts (Figure 7.3a). These substrates are easily synthesized in high yield by reaction of commercially available *Z*-hydroxy olefins with alkenoyl chlorides (Figure 7.3b). Substrates were designed such that RCM of these substrates would give the desired product as well as a gaseous byproduct, propylene or 1-butene, which could be readily removed from the reaction mixture under static vacuum.
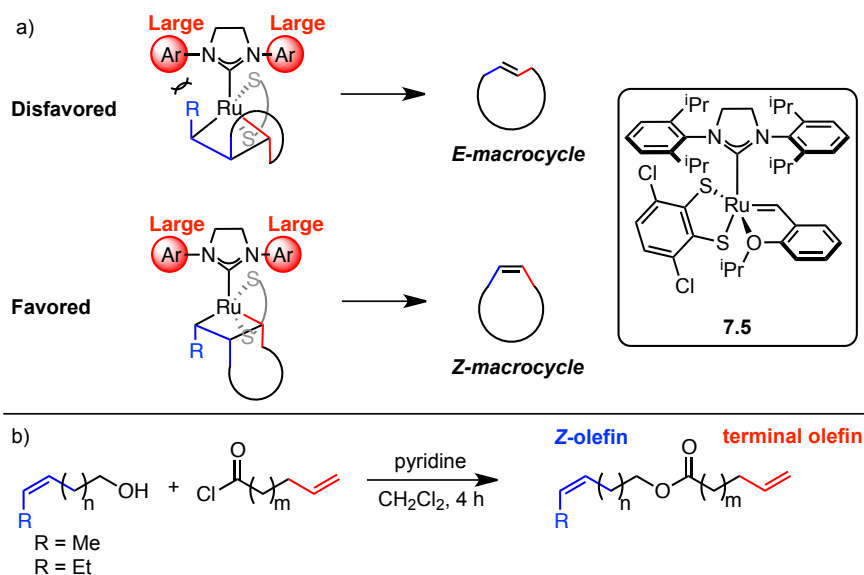
Figure 7.3. (a) Proposed disfavored and favored metallacyclobutane intermediates in macrocylization reactions implementing stereoretentive catalyst **7.5**. (b) Synthesis of diene substrates from acyl chlorides and *Z*-hydroxy olefins.

For these reactions, catalyst **7.5**, bearing an NHC with *N*-2,6-diisopropylphenyl groups, was chosen due to its remarkable activity in cross metathesis reactions of *Z*-olefins.[7] To compare the initiation rates of **7.4** and **7.5**, the reactions of butyl vinyl ether with each catalyst were monitored by ^{1}H NMR (Figure 7.4). Under standard conditions at

30 °C,[9] catalyst **7.5** had already fully initiated within the 15 s required to acquire the first spectrum, and thus a rate constant could not be determined. The reaction was then monitored at 0 °C and was completed within 2 min with **7.5** while **7.4** required 1.5 h. Values of k_{init} for **7.4** and **7.5** at this temperature were determined to be 1.00×10^{-3} s^{-1} and 2.42×10^{-2} s^{-1}, respectively. Thus, there is an order of magnitude of difference in the initiation rates of these catalysts, $k_{rel} = k_{init7.5}/k_{init7.4} = 24.2$. Furthermore, full initiation of **7.5** was remarkably complete at –20 °C within 10 min with $k_{init} = 6.14 \times 10^{-3}$ s^{-1}.[10] Negligible Fischer carbene formation could be observed using **7.4** at –20 °C. This stark difference in initiation rate is a direct reflection of the significantly greater activity of **7.5** compared to **7.4**.
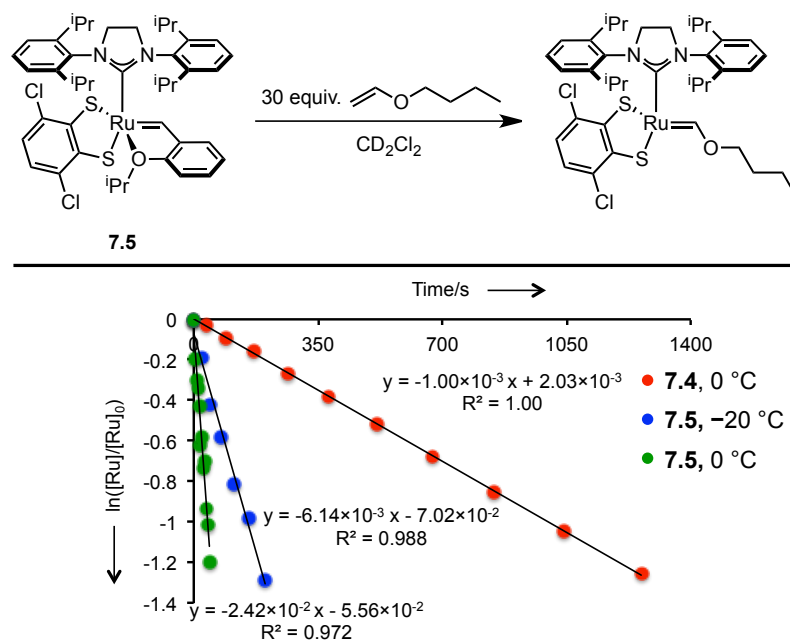
Figure 7.4. Plot of ln([Ru]/[Ru]$_0$) versus time for initiation experiments conducted with catalysts **7.4** and **7.5** at 0 °C and –20 °C monitored by disappearance of the benzylidene signal by ^{1}H NMR. Plots remain approximately linear for three half-lives of the reaction.

RCM was then attempted using **7.5** and was shown to be possible using a variety of substrates, **7.6**–**7.12** (Table 7.1). Using a standard catalyst loading of 6 mol % often

used in macrocylization reactions, reactions were completed within 1 h in

Table 7.1. Synthesis of Macrocycles Using **7.5**.

Entry	Substrate	Product	Yield[a]	Z/E[b]
1	**7.6**	12 **7.13**	70% yield	>99/1
2	**7.7**	13 **7.14**	68% yield	95/5
3	**7.8**	14 **7.15**	67% yield (60% yield)[c]	95/5 (98/2)
4	**7.9**	14 **7.16**	72% yield	98/2
5	**7.10**	15 **7.17**	74% yield	99/1
6	**7.11**	16 **7.18**	79% yield	95/5
7	**7.12**	17 **7.19**	75% yield	95/5

[a]Yields shown are isolated yields. [b]Selectivity determined by gas chromatography. Selectivity of **7.13** and **7.14** can be determined by ^{1}H NMR. [c]Reaction was run on a preparative scale.

143

dichloromethane under static vacuum at 40 °C. Twelve- to seventeen-membered rings were all synthesized with high *Z*-selectivity (95 – 99% *Z*) in moderate to high yields (68 – 79% isolated yield). Yuzu lactone, **7.14**, is in high demand by the perfume industry and can be synthesized more rapidly and selectively using **7.5** than in previous reports.[2f,11] Larger macrocyclic lactones, fifteen-membered to seventeen-membered rings, were synthesized in slightly higher yields than with smaller twelve- to fourteen-membered rings.

Given the exceptional activity exhibited by **7.5** in initiation experiments and its high activity in macrocyclic RCM (turnover numbers, TON, of 11−13 were achieved using 6 mol % catalyst loading), the limit for the catalyst loading required for reaction was examined. Using 0.5 mol % **7.5**, 50% conversion (TON of 100) was attained in the macrocyclization of **7.8** within 1 h as determined by observation of aliquots of the reaction by ^{1}H NMR. With 1 mol % **7.5**, complete conversion of the starting material to the macrocyclic product and a small amount of unidentified byproduct, possibly an oligomer of the starting material, was observed. This is significantly lower than reported catalyst loadings used for achieving high conversion in previously reported *Z*-selective macrocyclizations.

Conclusions

Highly active, stereoretentive Ru-based catalyst **7.5** was used for generating highly *Z*-macrocycles (95 – 99% *Z*) from easily available diene substrates with a *Z*-olefin moiety. The exceptional activity exhibited by this catalyst was determined through initiation studies and showed that full catalyst initiation could be achieved at –20 °C within minutes. Twelve- to seventeen-membered macrocycles, including yuzu lactone,

were synthesized using this method in moderate to high yields (67 – 79% yield). These reactions were completed in significantly shorter times, and the use of lower catalyst loadings than in previously reported *Z*-selective systems was shown to be possible with TON of up to 100. Further studies using stereoretention for *E*-selective macrocyclization are underway.

Experimental

General Information

Unless otherwise specified, all manipulations were carried out under air-free conditions in dry glassware in a Vacuum Atmospheres Glovebox filled with N_2. General solvents were purified by passing through solvent purification columns. Commercially available substrates were used as received. All solvents and substrates were sparged with Ar before bringing into the glovebox and filtered over neutral alumina (Brockmann I) prior to use. **7.5**[8a] was synthesized according to literature procedure. **7.5** was provided by Materia, Inc.

Kinetic NMR experiments were performed on a Varian 600 MHz spectrometer with an AutoX probe. Spectra were analyzed using MestReNova Ver. 8.1.2. 1 H and 13C NMR characterization data were obtained on a Bruker 400 with Prodigy broadband cryoprobe and referenced to residual protio-solvent.

Synthesis of (*Z*)-hex-4-en-1-yl oct-7-enoate (7.6)

To a 100 mL round-bottom flask charged with a stir bar was added 50 mL dichloromethane, 7-octenoic acid (1.54 mL, 10.0 mmol) and pyridine (80.7 uL, 1.00 mmol). Oxalyl chloride (1.00 mL, 11.8 mmol) was added dropwise, and the reaction was stirred for overnight. Solvents were then removed *in vacuo*. 20 mL dichloromethane and

pyridine (0.81 mL, 10.0 mmol) were added, and *cis*-4-hexenol (1.09 mL, 9.3 mmol) was subsequently added dropwise at 0 °C. After bringing the reaction to room temperature, it was stirred for an additional 4 h. The reaction mixture was extracted with 1M aq. HCl (200 mL), sat. aq. NaHCO₃ (200 mL). The organic layer was dried over anhydrous MgSO₄, filtered, and solvents were removed *in vacuo*. The product was purified by column chromatography on silica gel (5:95 Et₂O: pentane) to yield a colorless oil (1.58 g, 76% yield).

¹H NMR (400 MHz, Chloroform-d_1) δ 5.79 (ddt, J = 16.9, 10.2, 6.7 Hz, 1H), 5.49 (dddd, J = 10.7, 8.2, 6.7, 5.2 Hz, 1H), 5.42 - 5.29 (m, 1H), 4.99 (dq, J = 17.1, 1.7 Hz, 1H), 4.93 (ddt, J = 10.2, 2.3, 1.2 Hz, 1H), 4.06 (t, J = 6.6 Hz, 2H), 2.30 (t, J = 7.5 Hz, 2H), 2.16 - 1.98 (m, 4H), 1.73 - 1.55 (m, 7H), 1.46 - 1.28 (m, 4H).

¹³C NMR (101 MHz, CDCl₃) δ 174.00, 138.94, 129.24, 125.03, 114.53, 63.89, 34.45, 33.70, 28.74, 28.66, 28.56, 24.98, 23.31, 12.85.

HRMS (FAB+): [M]⁺ C₁₄H₂₄O₂ Calculated – 224.1776, Found – 224.1745.

Synthesis of (*Z*)-hex-3-en-1-yl dec-9-enoate (7.7)

To a 100 mL round-bottom flask charged with a stir bar was added 50 mL dichloromethane, 9-decenoic acid (1.85 mL, 10.0 mmol) and pyridine (80.7 uL, 1.00 mmol). Oxalyl chloride (1.00 mL, 11.8 mmol) was added dropwise, and the reaction was stirred for overnight. Solvents were then removed *in vacuo*. 20 mL dichloromethane and pyridine (0.81 mL, 10.0 mmol) were added, and *cis*-3-hexenol (1.10 mL, 9.3 mmol) was subsequently added dropwise at 0 °C. After bringing the reaction to room temperature, it was stirred for an additional 4 h. The reaction mixture was extracted with 1M aq. HCl (200 mL), sat. aq. NaHCO₃ (200 mL). The organic layer was dried over anhydrous

MgSO$_4$, filtered, and solvents were removed *in vacuo*. The product was purified by column chromatography on silica gel (5:95 Et$_2$O: pentane) to yield a colorless oil (2.02 g, 86% yield).

^{1}H NMR (400 MHz, Chloroform-d_1) δ 5.79 (ddt, J = 16.9, 10.2, 6.7 Hz, 1H), 5.64 – 5.37 (m, 1H), 5.37 – 5.14 (m, 1H), 5.02 – 4.94 (m, 1H), 4.92 (ddt, J = 10.2, 2.3, 1.2 Hz, 1H), 4.05 (t, J = 6.9 Hz, 2H), 2.43 – 2.32 (m, 2H), 2.28 (t, J = 7.5 Hz, 2H), 2.12 – 1.89 (m, 4H), 1.67 – 1.50 (m, 2H), 1.42 – 1.19 (m, 8H), 0.96 (t, J = 7.5 Hz, 3H).

^{13}C NMR (101 MHz, CDCl$_3$) δ 174.01, 139.22, 134.61, 123.90, 114.31, 63.88, 34.46, 33.89, 29.23, 29.21, 29.04, 28.97, 26.89, 25.07, 20.73, 14.37.

HRMS (FAB+): [M]$^+$ C$_{17}$H$_{30}$O$_2$ Calculated – 266.2246, Found – 266.2216.

Synthesis of (*Z*)-hex-3-en-1-yl undec-10-enoate (7.8)

To a 100 mL round-bottom flask charged with a stir bar was added 20 mL dichloromethane, undecenoyl chloride (2.37 mL, 11.0 mmol), and pyridine (0.89 mL, 11.0 mmol). *Cis*-3-hexenol (1.18 mL, 10.0 mmol) was then added dropwise at 0 °C. The reaction mixture was brought to room temperature and stirred for 4 h. The reaction mixture was extracted with 1M aq. HCl (200 mL), sat. aq. NaHCO$_3$ (200 mL). The organic layer was dried over anhydrous MgSO$_4$, filtered, and solvents were removed *in vacuo*. The product was purified by column chromatography on silica gel (5:95 Et$_2$O: pentane) to yield a colorless oil (2.53 g, 95% yield).

^{1}H NMR (400 MHz, Chloroform-d_1) δ 5.80 (ddt, J = 16.9, 10.2, 6.7 Hz, 1H), 5.55 – 5.45 (m, 1H), 5.36 – 5.26 (m, 1H), 4.99 (dq, J = 17.1, 1.7 Hz, 1H), 4.92 (ddt, J = 10.2, 2.3, 1.2 Hz, 1H), 4.06 (t, J = 6.9 Hz, 2H), 2.43 – 2.31 (m, 2H), 2.32 – 2.24 (m, 2H), 2.04 (dddd, J

= 14.8, 7.9, 5.0, 1.5 Hz, 4H), 1.67 – 1.54 (m, 2H), 1.42 – 1.33 (m, 2H), 1.33 – 1.24 (m, 8H), 0.97 (t, J = 7.5 Hz, 3H).

^{13}**C NMR** (101 MHz, CDCl$_3$) δ 174.06, 139.32, 134.63, 123.92, 114.28, 63.89, 34.49, 33.94, 29.43, 29.35, 29.26, 29.20, 29.04, 26.90, 25.11, 20.75, 14.39.

HRMS (FAB+): [M]$^+$ C$_{17}$H$_{30}$O$_2$ Calculated – 266.2246, Found – 266.2216.

Synthesis of (*Z*)-hex-4-en-1-yl dec-9-enoate (7.9)

To a 100 mL round-bottom flask charged with a stir bar was added 50 mL dichloromethane, 9-decenoic acid (1.85 mL, 10.0 mmol) and pyridine (80.7 uL, 1.00 mmol). Oxalyl chloride (1.00 mL, 11.8 mmol) was added dropwise, and the reaction was stirred for overnight. Solvents were then removed *in vacuo*. 20 mL dichloromethane and pyridine (0.81 mL, 10.0 mmol) were added, and *cis*-4-hexenol (1.09 mL, 9.3 mmol) was subsequently added dropwise at 0 °C. After bringing the reaction to room temperature, it was stirred for an additional 4 h. The reaction mixture was extracted with 1M aq. HCl (200 mL), sat. aq. NaHCO$_3$ (200 mL). The organic layer was dried over anhydrous MgSO$_4$, filtered, and solvents were removed *in vacuo*. The product was purified by column chromatography on silica gel (5:95 Et$_2$O: pentane) to yield a colorless oil (2.05 g, 87% yield).

^{1}**H NMR** (400 MHz, Chloroform-d_1) δ 5.80 (ddt, J = 13.2, 10.0, 7.2 Hz, 1H), 5.60 - 5.44 (m, 1H), 5.44 - 5.32 (m, 1H), 5.12 - 4.96 (m, 1H), 4.93 (ddd, J = 10.2, 2.3, 1.2 Hz, 1H), 4.07 (t, J = 6.5 Hz, 2H), 2.30 (t, J = 8.0 Hz, 2H), 2.20 - 1.96 (m, 4H), 1.81 - 1.58 (m, 7H), 1.49 - 1.24 (m, 8H).

^{13}**C NMR** (101 MHz, CDCl$_3$) δ 174.12, 139.29, 129.27, 125.05, 114.34, 63.89, 34.53, 33.92, 29.26, 29.07, 29.00, 28.59, 25.14, 23.34, 12.88.

HRMS (FAB+): [M+H] $C_{16}H_{29}O_2$ Calculated – 253.2158, Found – 253.2168.

Synthesis of (*Z*)-hex-4-en-1-yl undec-10-enoate (7.10)

To a 100 mL round-bottom flask charged with a stir bar was added 20 mL dichloromethane, undecenoyl chloride (2.37 mL, 11.0 mmol), and pyridine (0.89 mL, 11.0 mmol). *Cis*-4-hexenol (1.17 mL, 10.0 mmol) was then added dropwise at 0 °C. The reaction mixture was brought to room temperature and stirred for 4 h. The reaction mixture was extracted with 1M aq. HCl (200 mL), sat. aq. NaHCO$_3$ (200 mL). The organic layer was dried over anhydrous MgSO$_4$, filtered, and solvents were removed *in vacuo*. The product was purified by column chromatography on silica gel (5:95 Et$_2$O: pentane) to yield a colorless oil (2.45 g, 92% yield).

¹H NMR (400 MHz, Chloroform-d_1) δ 5.80 (ddt, *J* = 16.9, 10.2, 6.7 Hz, 1H), 5.49 (dddd, *J* = 10.7, 8.2, 6.7, 5.2 Hz, 1H), 5.36 (dtq, *J* = 10.7, 7.3, 1.7 Hz, 1H), 4.99 (dq, *J* = 17.2, 1.8 Hz, 1H), 4.92 (ddt, *J* = 10.2, 2.3, 1.2 Hz, 1H), 4.06 (t, *J* = 6.6 Hz, 2H), 2.29 (t, *J* = 7.5 Hz, 2H), 2.11 (qt, *J* = 7.2, 1.2 Hz, 2H), 2.07 – 1.99 (m, 2H), 1.73 – 1.64 (m, 2H), 1.60 (ddt, *J* = 6.7, 1.8, 0.9 Hz, 6H), 1.36 (dt, *J* = 8.3, 4.8 Hz, 2H), 1.28 (q, *J* = 4.1, 3.3 Hz, 7H).

¹³C NMR (101 MHz, CDCl$_3$) δ 174.12, 139.33, 129.26, 125.04, 114.28, 63.89, 34.54, 33.94, 29.44, 29.36, 29.28, 29.21, 29.04, 28.58, 25.15, 23.33, 12.86.

HRMS (FAB+): [M+H] $C_{17}H_{31}O_2$ Calculated – 267.2324, Found – 267.2335.

Synthesis of (*Z*)-oct-5-en-1-yl undec-10-enoate (7.11)

To a 100 mL round-bottom flask charged with a stir bar was added 20 mL dichloromethane, undecenoyl chloride (2.37 mL, 11.0 mmol), and pyridine (0.89 mL, 11.0 mmol). *Cis*-5-octenol (1.51 mL, 10.0 mmol) was then added dropwise at 0 °C. The reaction mixture was brought to room temperature and stirred for 4 h. The reaction

mixture was extracted with 1M aq. HCl (200 mL), sat. aq. NaHCO₃ (200 mL). The organic layer was dried over anhydrous MgSO₄, filtered, and solvents were removed *in vacuo*. The product was purified by column chromatography on silica gel (5:95 Et₂O: pentane) to yield a colorless oil (2.82 g, 96% yield).

¹H NMR (400 MHz, Chloroform-d_1) δ 5.82 (ddt, J = 16.9, 10.1, 6.7 Hz, 1H), 5.46 - 5.37 (m, 1H), 5.36 - 5.25 (m, 1H), 5.01 (dq, J = 17.1, 1.8 Hz, 1H), 4.94 (ddt, J = 10.2, 2.4, 1.2 Hz, 1H), 4.08 (t, J = 6.7 Hz, 2H), 2.31 (t, J = 7.6 Hz, 2H), 2.06 (dddd, J = 10.9, 9.5, 5.3, 1.6 Hz, 6H), 1.72 - 1.61 (m, 4H), 1.47 - 1.27 (m, 12H), 0.97 (t, J = 7.5 Hz, 3H).

¹³C NMR (101 MHz, CDCl₃) δ 173.99, 139.17, 132.16, 128.49, 114.14, 64.22, 34.39, 33.80, 29.31, 29.22, 29.14, 29.07, 28.90, 28.23, 26.63, 26.05, 25.02, 20.54, 14.36.

HRMS (FAB+): [M+H] $C_{19}H_{35}O_2$ Calculated – 295.2637, Found – 295.2639.

Synthesis (*Z*)-non-6-en-1-yl undec-10-enoate (7.12)

To a 100 mL round-bottom flask charged with a stir bar was added 20 mL dichloromethane, undecenoyl chloride (2.37 mL, 11.0 mmol), and pyridine (0.89 mL, 11.0 mmol). *Cis*-6-nonenol (1.67 mL, 10.0 mmol) was then added dropwise at 0 °C. The reaction mixture was brought to room temperature and stirred for 4 h. The reaction mixture was extracted with 1M aq. HCl (200 mL), sat. aq. NaHCO₃ (200 mL). The organic layer was dried over anhydrous MgSO₄, filtered, and solvents were removed *in vacuo*. The product was purified by column chromatography on silica gel (5:95 Et₂O: pentane) to yield a colorless oil (2.74 g, 89% yield).

¹H NMR (400 MHz, Chloroform-d_1) δ 5.80 (ddt, J = 16.9, 10.2, 6.7 Hz, 1H), 5.50 – 5.16 (m, 2H), 5.04 – 4.94 (m, 1H), 4.94 – 4.88 (m, 1H), 4.05 (t, J = 6.7 Hz, 2H), 2.35 – 2.22

(m, 2H), 2.13 – 1.96 (m, 6H), 1.61 (dt, J = 11.8, 4.1 Hz, 4H), 1.36 (dt, J = 6.5, 2.2 Hz, 6H), 1.32 – 1.25 (m, 8H), 0.95 (t, J = 7.5 Hz, 3H).

^{13}**C NMR** (101 MHz, CDCl$_3$) δ 174.14, 139.32, 131.99, 128.96, 114.28, 64.47, 34.54, 33.94, 29.48, 29.44, 29.36, 29.28, 29.21, 29.03, 28.70, 27.07, 25.70, 25.15, 20.66, 14.52.

HRMS (FAB+): [M]$^+$ C$_{20}$H$_{37}$O$_2$ Calculated – 309.2794, Found – 309.2779.

General Procedure for Catalyst Initiation Experiments

To an NMR tube was added a solution of catalyst (0.003 mmol) in 0.6 mL CD$_2$Cl$_2$. The tube was then was sealed with a rubber septum, taken out of the glovebox, and placed in a dry ice/acetone bath. Butyl vinyl ether (12 μL, 0.090 mmol) was injected into the tube, and the reaction was monitored by observing the disappearance of the benzylidene signal by ^{1}H NMR using an array at the appropriate temperature.

Synthesis of (*Z*)-oxacyclododec-8-en-2-one (7.13)

To a 150 mL Schlenk tube equipped with a stir bar was added **7.6** (21.0 mg, 0.0938 mmol) in 30.3 mL DCM and a solution of **7.5** (4.8 mg, 0.00563 mmol) in 1 mL DCM. The tube was sealed and taken out of the glovebox. After one freeze-pump-thaw cycle, the reaction flask was heated at 40 °C for 1 h and then quenched with 1 mL butyl vinyl ether. Solvents were removed *in vacuo*, and the product was purified by column chromatography on silica gel (1:49 Et$_2$O: pentane) to yield a colorless oil (12.0 mg, 70% yield).

^{1}**H NMR** (400 MHz, Chloroform-d_1) δ 5.45 - 5.21 (m, 2H), 4.10 - 3.96 (m, 2H), 2.49 - 2.28 (m, 4H), 2.18 (q, J = 6.3 Hz, 2H), 1.89 - 1.81 (m, 2H), 1.68 (ddq, J = 8.2, 4.0, 2.0 Hz, 2H), 1.47 - 1.40 (m, 2H), 1.26 - 1.18 (m, 2H).

¹³C NMR (101 MHz, CDCl$_3$) δ 174.18, 131.37, 128.57, 62.31, 35.73, 26.80, 26.30, 25.14, 24.18, 23.08, 22.42.

HRMS (FAB+): [M]$^+$ C$_{11}$H$_{18}$O$_2$ Calculated – 182.1307, Found – 182.1303.

Synthesis of (*Z*)-oxacyclotridec-10-en-2-one (7.14)

To a 150 mL Schlenk tube equipped with a stir bar was added **7.7** (23.7 mg, 0.0938 mmol) in 30.3 mL DCM and a solution of **7.5** (4.8 mg, 0.00563 mmol) in 1 mL DCM. The tube was sealed and taken out of the glovebox. After one freeze-pump-thaw cycle, the reaction flask was heated at 40 °C for 1 h and then quenched with 1 mL butyl vinyl ether. Solvents were removed *in vacuo*, and the product was purified by column chromatography on silica gel (1:49 Et$_2$O: pentane) to yield a colorless oil (12.5 mg, 68% yield).

¹H NMR (400 MHz, Chloroform-*d*$_1$) δ 5.50 - 5.32 (m, 2H), 4.30 - 4.15 (m, 2H), 2.43 (q, *J* = 5.0 Hz, 2H), 2.35 - 2.25 (m, 2H), 2.15 - 2.04 (m, 2H), 1.73 - 1.64 (m, 2H), 1.49 (q, *J* = 6.3 Hz, 2H), 1.41 - 1.33 (m, 2H), 1.22 - 1.15 (m, 2H).

¹³C NMR (101 MHz, CDCl$_3$) δ 174.89, 132.41, 127.26, 64.34, 35.54, 29.86, 27.66, 27.41, 26.15, 26.02, 24.73, 23.67.

HRMS (EI): C$_{12}$H$_{21}$O$_2$ Calculated – 197.1542, Found – 197.1536.

Synthesis of (*Z*)-oxacyclotetradec-11-en-2-one (7.15)

To a 150 mL Schlenk tube equipped with a stir bar was added **7.8** (25.0 mg, 0.0938 mmol) in 30.3 mL DCM and a solution of **7.5** (4.8 mg, 0.00563 mmol) in 1 mL DCM. The tube was sealed and taken out of the glovebox. After one freeze-pump-thaw cycle, the reaction flask was heated at 40 °C for 1 h and then quenched with 1 mL butyl vinyl ether. Solvents were removed *in vacuo*, and the product was purified by column

chromatography on silica gel (1:49 Et$_2$O: pentane) to yield a colorless oil (13.2 mg, 67% yield).

Large Scale Preparation:

To a 500 mL Schlenk tube equipped with a stir bar was added **7.8** (200.0 mg, 0.750 mmol) in 246.4 mL DCM and a solution of **7.5** (38.4 mg, 0.0450 mmol) in 4 mL DCM. The tube was sealed and taken out of the glovebox. After one freeze-pump-thaw cycle, the reaction flask was heated at 40 °C for 1 h and then quenched with 8 mL butyl vinyl ether. Solvents were removed *in vacuo*, and the product was purified by column chromatography on silica gel (1:49 Et$_2$O: pentane) to yield a colorless oil (94.9 mg, 60% yield).

^{1}H NMR (400 MHz, Chloroform-d_1) δ 5.55 (dtt, J = 11.1, 7.7, 1.7 Hz, 1H), 5.45 – 5.33 (m, 1H), 4.28 – 4.11 (m, 2H), 2.50 – 2.40 (m, 2H), 2.40 – 2.29 (m, 2H), 2.10 – 1.99 (m, 2H), 1.66 (ddt, J = 6.3, 4.5, 2.5 Hz, 2H), 1.43 – 1.30 (m, 10H).

^{13}C NMR (101 MHz, CDCl$_3$) δ 174.13, 132.47, 127.22, 63.89, 33.46, 27.85, 27.65, 26.25, 26.14, 25.67, 25.56, 25.34, 23.65.

HRMS (FAB+): [M+H] C$_{13}$H$_{23}$O$_2$ Calculated – 211.1698, Found – 211.1706.

Synthesis of (*Z*)-oxacyclotetradec-10-en-2-one (7.16)

To a 150 mL Schlenk tube equipped with a stir bar was added a solution of **7.9** (23.7 mg, 0.0938 mmol) in 30.3 mL DCM and a solution of **7.5** (4.8 mg, 0.00563 mmol) in 1 mL DCM. The tube was sealed and taken out of the glovebox. After one freeze-pump-thaw cycle, the reaction flask was heated at 40 °C for 1 h and then quenched with 1 mL butyl vinyl ether. Solvents were removed *in vacuo*, and the product was purified by column

chromatography on silica gel (1:49 Et$_2$O: pentane) to yield a colorless oil (14.2 mg, 72% yield).

^{1}H NMR (400 MHz, Chloroform-d_1) δ 5.48 (dtt, J = 10.5, 7.6, 1.5 Hz, 1H), 5.33 (dtt, J = 10.5, 7.6, 1.3 Hz, 1H), 4.22 – 4.02 (m, 2H), 2.51 – 2.37 (m, 2H), 2.25 (qd, J = 7.5, 1.4 Hz, 2H), 2.14 – 1.95 (m, 2H), 1.79 – 1.65 (m, 4H), 1.49 – 1.28 (m, 8H).

^{13}C NMR (101 MHz, CDCl$_3$) δ 173.98, 131.23, 128.50, 62.84, 33.57, 29.11, 27.00, 26.77, 26.03, 25.23, 25.04, 24.63, 23.73.

HRMS (FAB+): [M+H] C$_{13}$H$_{23}$O$_2$ Calculated – 211.1698, Found – 211.1690.

Synthesis of (*Z*)-oxacyclopentadec-11-en-2-one (7.17)

To a 150 mL Schlenk tube equipped with a stir bar was added a solution of **7.10** (25.0 mg, 0.0938 mmol) in 30.3 mL DCM and a solution of **7.5** (4.8 mg, 0.00563 mmol) in 1 mL DCM. The tube was sealed and taken out of the glovebox. After one freeze-pump-thaw cycle, the reaction flask was heated at 40 °C for 1 h and then quenched with 1 mL butyl vinyl ether. Solvents were removed *in vacuo*, and the product was purified by column chromatography on silica gel (1:49 Et$_2$O: pentane) to yield a colorless oil (15.6 mg, 70% yield).

^{1}H NMR (400 MHz, Chloroform-d_1) δ 5.57 - 5.38 (m, 1H), 5.30 (dt, J = 10.9, 6.9 Hz, 1H), 4.18 - 3.95 (m, 2H), 2.46 - 2.32 (m, 2H), 2.23 (qd, J = 7.1, 1.7 Hz, 2H), 2.02 (q, J = 7.1 Hz, 2H), 1.72 (dtd, J = 8.9, 6.9, 4.3 Hz, 4H), 1.36 (dt, J = 8.7, 5.9 Hz, 10H).

^{13}C NMR (101 MHz, CDCl$_3$) ? 174.45, 131.47, 128.85, 63.36, 34.51, 28.81, 28.24, 27.96, 27.12, 27.05, 27.01, 26.35, 24.63, 23.75.

HRMS (FAB+): [M]$^+$ C$_{14}$H$_{24}$O$_2$ Calculated – 224.1776, Found – 224.1774.

Synthesis of (*Z*)-oxacyclohexadec-11-en-2-one (7.18)

To a 150 mL Schlenk tube equipped with a stir bar was added a solution of **7.11** (27.6 mg, 0.0938 mmol) in 30.3 mL DCM and a solution of **7.5** (4.8 mg, 0.00563 mmol) in 1 mL DCM. The tube was sealed and taken out of the glovebox. After one freeze-pump-thaw cycle, the reaction flask was heated at 40 °C for 1 h and then quenched with 1 mL butyl vinyl ether. Solvents were removed *in vacuo*, and the product was purified by column chromatography on silica gel (1:49 Et$_2$O: pentane) to yield a colorless oil (17.7 mg, 79% yield).

^{1}H NMR (400 MHz, Chloroform-*d*) δ 5.53 - 5.20 (m, 2H), 4.14 (t, *J* = 6.3 Hz, 2H), 2.43 - 2.27 (m, 2H), 2.03 (qd, *J* = 7.0, 3.1 Hz, 4H), 1.63 (dq, *J* = 9.2, 6.3 Hz, 4H), 1.45 - 1.37 (m, 2H), 1.30 (q, *J* = 5.5, 4.6 Hz, 10H).

^{13}C NMR (101 MHz, CDCl$_3$) δ 174.09, 130.24, 129.71, 64.24, 34.01, 29.28, 28.54, 28.31, 28.07, 27.76, 27.32, 27.25, 26.73, 26.61, 25.38.

HRMS (FAB+): [M+H] C$_{15}$H$_{27}$O$_2$ Calculated – 239.2011, Found – 239.2017.

Synthesis of (*Z*)-oxacycloheptadec-11-en-2-one (7.19)

To a 150 mL Schlenk tube equipped with a stir bar was added a solution of **7.12** (28.9 mg, 0.0938 mmol) in 30.3 mL DCM and a solution of **7.5** (4.8 mg, 0.00563 mmol) in 1 mL DCM. The tube was sealed and taken out of the glovebox. After one freeze-pump-thaw cycle, the reaction flask was heated at 40 °C for 1 h and then quenched with 1 mL butyl vinyl ether. Solvents were removed *in vacuo*, and the product was purified by column chromatography on silica gel (1:49 Et$_2$O: pentane) to yield a colorless oil (17.8 mg, 75% yield).

¹H NMR (400 MHz, Chloroform-d_1) δ 5.39 - 5.22 (m, 2H), 4.19 - 4.01 (m, 2H), 2.38 - 2.22 (m, 2H), 2.06 (dq, J = 18.6, 6.1 Hz, 4H), 1.71 - 1.52 (m, 4H), 1.47 - 1.17 (m, 14H).

¹³C NMR (101 MHz, CDCl₃) δ 174.57, 130.37, 130.29, 64.75, 34.43, 29.45, 28.88, 28.84, 28.79, 28.76, 28.19, 27.73, 27.32, 26.57, 26.22, 25.57.

HRMS (FAB+): [M+H] $C_{16}H_{28}O_2$ Calculated – 252.2087, Found – 252.2089.

For determining selectivity, *E/Z* mixtures of lactones were synthesized using (PCy₃)₂Ru=CHPh as references for GC and ¹³C NMR studies for comparison.

Synthesis of (*E/Z*)-oxacyclotetradec-10-en-2-one (*E/Z*-7.16)

To a 150 mL Schlenk tube equipped with a stir bar was added a solution of **7.9** (23.7 mg, 0.0938 mmol) in 30.3 mL DCM and a solution of (PCy₃)₂Ru=CHPh (4.6 mg, 0.00563 mmol) in 1 mL DCM. The tube was sealed and taken out of the glovebox. After one freeze, pump, thaw cycle, the reaction flask was heated at 40 °C for 4 h and then quenched with 1 mL butyl vinyl ether. Solvents were removed *in vacuo*, and the product was purified by column chromatography on silica gel (1:49 Et₂O: pentane) to yield a colorless oil (13.0 mg, 67% yield).

¹H NMR (400 MHz, Chloroform-d_1) δ 5.68 - 5.42 (m, 1H), 5.42 - 5.24 (m, 1H), 4.29 - 3.98 (m, 2H), 2.53 - 2.18 (m, 4H), 2.14 - 2.05 (m, 2H), 1.79 - 1.64 (m, 4H), 1.49 - 1.20 (m, 12H).

¹³C NMR (101 MHz, CDCl₃) δ 174.28, 173.86, 131.11, 130.62, 130.40, 128.38, 64.81, 62.72, 33.45, 33.01, 31.42, 30.91, 28.98, 28.18, 27.06, 26.88, 26.65, 26.53, 25.91, 25.11, 24.98, 24.92, 24.51, 24.08, 23.61.

HRMS (FAB+): [M]⁺ $C_{13}H_{22}O_2$ Calculated – 210.1620, Found – 210.1633.

Synthesis of (*E*/*Z*)-oxacyclopentadec-11-en-2-one (*E*/*Z* -7.17)

To a 150 mL Schlenk tube equipped with a stir bar was added a solution of **7.10** (25.0 mg, 0.0938 mmol) in 30.3 mL DCM and a solution of $(PCy_3)_2Ru=CHPh$ (4.6 mg, 0.00563 mmol) in 1 mL DCM. The tube was sealed and taken out of the glovebox. After one freeze, pump, thaw cycle, the reaction flask was heated at 40 °C for 4 h and then quenched with 1 mL butyl vinyl ether. Solvents were removed *in vacuo*, and the product was purified by column chromatography on silica gel (1:49 Et_2O: pentane) to yield a colorless oil (11.7 mg, 52% yield).

^{1}H NMR (400 MHz, Chloroform-d_1) δ 5.50 - 5.20 (m, 2H), 4.19 - 4.04 (m, 2H), 2.40 - 2.29 (m, 2H), 2.20 (qd, *J* = 7.4, 6.3, 1.6 Hz, 2H), 2.09 - 1.96 (m, 2H), 1.85 - 1.54 (m, 5H), 1.45 - 1.22 (m, 11H).

^{13}C NMR (101 MHz, CDCl$_3$) δ 174.48, 174.45, 131.97, 131.48, 129.87, 128.85, 64.30, 63.36, 35.01, 34.51, 31.02, 30.32, 28.81, 28.24, 27.96, 27.85, 27.56, 27.13, 27.05, 27.03, 27.01, 26.82, 26.63, 26.35, 25.03, 24.63, 24.57, 23.75.

HRMS (FAB+): $[M]^+$ $C_{14}H_{24}O_2$ Calculated – 224.1776, Found – 224.1767.

Synthesis of (*E*/*Z*)-oxacyclohexadec-11-en-2-one (*E*/*Z*-7.18)

To a 150 mL Schlenk tube equipped with a stir bar was added a solution of **7.11** (27.6 mg, 0.0938 mmol) in 30.3 mL DCM and a solution of $(PCy_3)_2Ru=CHPh$ (4.6 mg, 0.00563 mmol) in 1 mL DCM. The tube was sealed and taken out of the glovebox. After one freeze-pump-thaw cycle, the reaction flask was heated at 40 °C for 4 h and then quenched with 1 mL butyl vinyl ether. Solvents were removed *in vacuo*, and the product was purified by column chromatography on silica gel (1:49 Et_2O: pentane) to yield a colorless oil (16.8 mg, 75% yield).

¹H NMR (400 MHz, Chloroform-d_1) δ 5.52 - 5.15 (m, 2H), 4.22 - 4.01 (m, 2H), 2.45 - 2.22 (m, 2H), 2.03 (ddt, J = 9.1, 6.8, 3.8 Hz, 4H), 1.61 (dtd, J = 15.7, 7.1, 4.0 Hz, 4H), 1.42 - 1.11 (m, 12H).

¹³C NMR (101 MHz, CDCl₃) δ 174.09, 174.07, 131.95, 130.46, 130.24, 129.71, 64.24, 64.08, 34.89, 34.01, 32.16, 32.12, 29.28, 28.54, 28.47, 28.41, 28.34, 28.31, 28.14, 28.07, 27.76, 27.34, 27.32, 27.25, 26.73, 26.68, 26.61, 25.60, 25.38, 25.30.

HRMS (FAB+): [M]⁺ $C_{15}H_{26}O_2$ Calculated – 238.1933, Found – 238.1926.

Synthesis of (*E*/*Z*)-oxacycloheptadec-11-en-2-one (*E*/*Z* -7.19)

To a 150 mL Schlenk tube equipped with a stir bar was added a solution of **7.12** (28.9 mg, 0.0938 mmol) in 30.3 mL DCM and a solution of (PCy₃)₂Ru=CHPh (4.6 mg, 0.00563 mmol) in 1 mL DCM. The tube was sealed and taken out of the glovebox. After one freeze-pump-thaw cycle, the reaction flask was heated at 40 °C for 4 h and then quenched with 1 mL butyl vinyl ether. Solvents were removed *in vacuo*, and the product was purified by column chromatography on silica gel (1:49 Et₂O: pentane) to yield a colorless oil (16.4 mg. 69% yield).

¹H NMR (400 MHz, Chloroform-d_1) δ 5.39 - 5.22 (m, 2H), 4.19 - 4.02 (m, 2H), 2.40 - 2.25 (m, 2H), 2.04 (ddt, J = 14.3, 11.9, 4.8 Hz, 4H), 1.68 - 1.56 (m, 4H), 1.48 - 1.22 (m, 14H).

¹³C NMR (101 MHz, CDCl₃) δ 173.38, 129.79, 129.71, 129.18, 129.10, 63.87, 63.56, 33.64, 33.24, 31.57, 30.70, 28.66, 28.26, 28.19, 28.14, 27.71, 27.68, 27.65, 27.60, 27.57, 27.38, 27.14, 27.00, 26.94, 26.91, 26.54, 26.13, 25.93, 25.38, 25.02, 24.96, 24.38, 24.30, 24.28.

HRMS (FAB+): [M]⁺ $C_{16}H_{28}O_2$ Calculated – 252.2079, Found – 252.2089.

References

1. Grubbs, R. H., Wenzel, A. G., O'Leary, D. J., Khosravi, E., Eds. *Handbook of Metathesis*; Wiley–VCH: Weinheim, 2015.

2. (a) Michrowska, A.; Wawrzyniak, P.; Grela, K. *Eur. J. Org. Chem.* **2004**, 2053. (b) Rimkus, G. G. The Handbook of Environmental Chemistry; Springer: Berlin, 2004; Vol. 3X. (c) Rowe, D. J. Chemistry and Technology of Flavors and Fragrances; Blackwell: Oxford, U.K., 2005. (d) Gradillas, A.; Perez-Castells, J. *Angew. Chem., Int. Ed.* **2006**, *45*, 6086. (e) Ohloff, G.; Pickenhagen, W.; Kraft, P. Scent and Chemistry: The Molecular World of Odors; Verlag Helvetica Acta: Zürich, 2011. (f) Marx, V. M.; Herbert, M. B.; Keitz, B. K.; Grubbs, R. H. *J. Am. Chem. Soc.* **2013**, 135, 94. (g) Higman, C. S.; Lummiss, J. A. M.; Fogg, D. E. *Angew. Chem.*, *Int. Ed.* **2016**, *55*, 3552.

3. (a) Fürstner, A.; Langemann, K. *J. Org. Chem.* **1996**, *61*, 3942. (b) Fürstner, A.; Langemann, K. *Synthesis* **1997**, 792. (c) Goldberg, W. P. D.; Hobber, A .S.; Weiler, L. *Tetrahedron Lett*. **1998**, *39*, 4955. (d) Lee, C. W.; Grubbs, R. H. *Org. Lett.*, **2000**, *2* (14), 2145. (e) Yu, M.; Wang, C.; Kyle, A. F.; Jakubec, P.; Dixon, D. J.; Schrock, R. R.; Hoveyda, A. H. *Nature* **2011**, 479, 88.

4. (a) Paquette, L. A.; Schloss, J. D.; Efremov, I.; Fabris, F.; Gallou, F.; Mendez-Andino, J.; Yang, J. Org. Lett. **2000**, *2*, 1259. (b) Maynard, H.; Grubbs, R. H. *Tetrahedron Lett.* **1999**, *40*, 4137.

5. (a) Fürstner, A.; Mathes, C.; Lehmann, C. W. *Chem. Eur. J.* **2001**, 7, 5299. (b) Nilson, M. G. & Funk, R. L. *Org. Lett.* **2010**, *12*, 4912. (c) Fürstner, A. *Angew. Chem. Int. Ed.* **2013**, *52*, 2794. (d) Fürstner, A. *Science* **2013**, *341*, 1229713.

6. Wang, Y.; Jimenez, M.; Hansen, A. S.; Raiber, E.-A.; Schreiber, S. L.; Young, D. W. *J. Am. Chem. Soc*. **2011**, *133*, 9196.

7. Koh, M. J.; Khan, R. K. M.; Torker, S.; Yu, M.; Mikus, M. S.; Hoveyda, A. H. *Nature*, **2015**, *517*, 181.

8. (a) Johns, A. M.; Ahmed, T. S.; Jackson, B. W.; Grubbs, R. H.; Pederson, R. L. *Org. Lett.* **2016**, *18* (4), 772. (b) Ahmed, T. S.; Grubbs, R. H. *J. Am. Chem. Soc.* **2017**, *139* (4), 1532. Stereoretention has been seen in metathesis previously: Bilhou, J. L.; Basset, J. M.; Graydon, W. F. *J. Am. Chem. Soc.* **1977**, *99* (12), 4083.

9. Keitz, B. K.; Endo, K.; Patel, P. R. Herbert, M. B.; Grubbs, R. H. *J. Am. Chem. Soc.*, **2012**, *134* (1), 693.

10. Substantial initiation of catalysts at low temperatures is often difficult using common metathesis catalysts: Romero, P. E.; Piers, W. E.; Mcdonald, R. *Angew. Chem., Int. Ed.* **2004**, *43* (41), 6161.

11. Alternative synthesis of yuzu lactone using alkyne metathesis: Fürstner, A.; Guth, O.; Rumbo, A.; Seidel, G. *J. Am. Chem. Soc.* **1999**, *121* (48), 11108.

Chapter 8

Using Stereoretention for the Synthesis of *E*-Macrocycles with
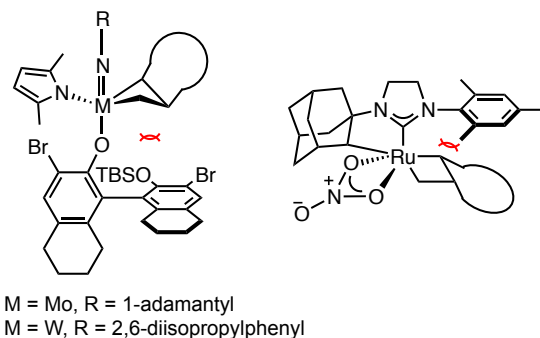
Ruthenium-based Olefin Metathesis Catalysts

Abstract

The synthesis of *E*-macrocycles is achieved using stereoretentive, Ru-based olefin metathesis catalysts supported by dithiolate ligands. Kinetic studies elucidate marked differences in activity among the catalysts tested, with catalyst **8.4** providing meaningful yields of products in much shorter reaction times than stereoretentive catalysts **8.2** and **8.3**. Macrocycles were generated with excellent selectivity (>99% *E*) and in moderate to high yields (47% − 80% yield) from diene starting materials bearing two *E*-configured olefins. A variety of rings were constructed, ranging from 12- to 18-membered macrocycles, including the antibiotic recifeiolide.

Introduction

Ring-closing metathesis (RCM) has gained widespread use in organic synthesis for the production of macrocyclic frameworks.[1] This transition metal-catalyzed reaction is commonly used in the synthesis of many biologically active and olfactory compounds.[2] The stereochemistry of the olefin often governs the properties of these cyclic molecules. Consequently, the stereochemical purity of olefin mixtures is important. The separation of *E*- and *Z*-isomers can be challenging, and thus methods for stereoselectively generating macrocycles are desirable.

The synthesis of *Z*-macrocycles has been reported using an array of Ru-,[3] W-, and Mo-based[4] olefin metathesis catalysts. The steric environment of each of these catalysts is tuned such that the *syn* metallacyclobutane pathway is favored over the *anti* metallacyclobutane pathway (Figure 8.1). Cycloreversion of this *syn* intermediate gives the macrocycle with *Z*-configuration.

M = Mo, R = 1-adamantyl
M = W, R = 2,6-diisopropylphenyl

Figure 8.1. Key metallacyclobutane intermediates for making *Z*-macrocycles using Mo-, W-, and Ru-based olefin metathesis catalysts.

In 2013, Hoveyda and co-workers reported Ru-based catalysts bearing dithiolate ligands that were able to perform highly *Z*-selective cross metathesis from *Z*-olefin starting materials.[5] In 2015, we demonstrated that these catalysts were further capable of cross metathesis between two *E*-olefins or between an *E*-olefin and a terminal olefin to generate *E*-products with high selectivity (>98% *E*).[6] This was the first reported example of highly *E*-selective cross metathesis through kinetic control.

The stereoretention exhibited by these complexes is proposed to arise from the *α* substituents of the metallacyclobutane pointing away from the large *N*-aryl groups of the N-heterocyclic carbene (NHC) ligand (Figure 8.2a). Depending on the stereochemistry of the starting olefin, the *β* substituent can either point down or up into the open space between the two *N*-aryl groups and in front of the imidazol-2-ylidene ring. Given that the olefin starting material stereochemistry is *Z*, the *β* substituent in the favored intermediate will point down, and the product formed after cycloreversion will be *Z*. Conversely, if the starting olefin has *E* stereochemistry, the *β* substituent will point up, and the product from the favored intermediate will be *E*. Soon after this report, Schrock and Hoveyda described Mo-based catalysts capable of a similar transformation, by which *E*-selectivity in cross metathesis is achieved from *E*-alkenyl halide starting materials (Figure 8.2b).[7]
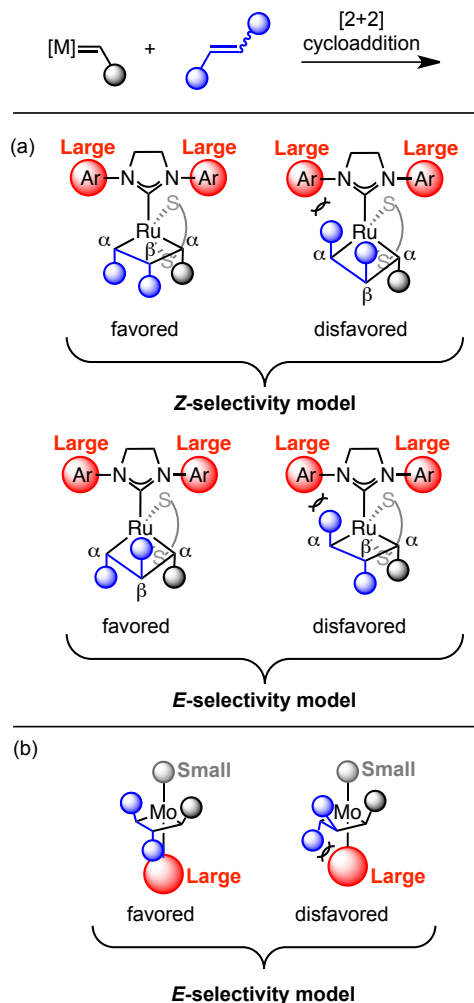
Figure 8.2. Models for selectivity in cross metathesis using stereoretentive olefin metathesis catalysts for a) Ru catalysts and b) Mo catalysts.

E-selective cross metathesis using stereoretentive Ru-based catalysts was often marred by low yields in reactions involving functionalized substrates or terminal olefins. Although the low yields observed in reactions with terminal olefins were attributed to decomposition of Ru methylidenes,[6] studies performed in our group showed that a large contributing factor to low activity with functionalized substrates is slow catalyst initiation in reactions of these catalysts with *E*-olefins.[8] A series of fast-initiating catalysts **8.1−8.4** was reported to significantly improve activity of stereoretentive catalysts in highly *E*-selective reactions (Figure 8.3).
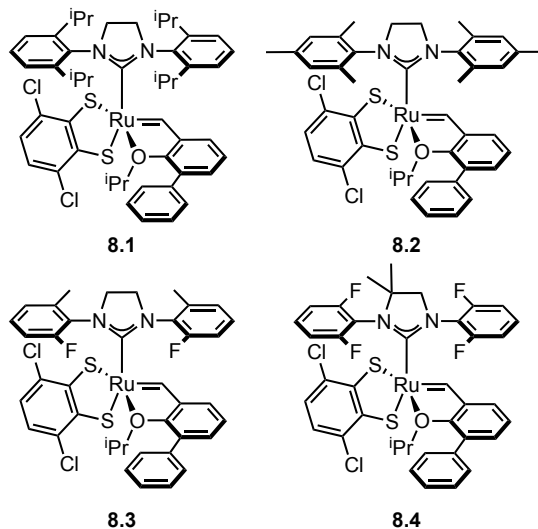
Figure 8.3. Series of fast-initiating, Ru-based catalysts used in achieving efficient synthesis of *E*-products in cross metathesis.

The first example of the stereoselective synthesis of macrocycles using stereoretention was reported using Mo-based catalysts to generate *E*-macrocycles (91 – >98% *E*) from diene substrates containing an *E*-alkenyl-B(pinacolato) moiety and a terminal olefin.[9] We recently reported a highly efficient synthesis of *Z*-macrocycles (95 – 99% *Z*) using stereoretention with Ru-based catalysts and substrates bearing a *Z*-olefin and a terminal olefin.[10] Hoveyda and co-workers then provided further examples of *Z*-macrocyclizations using other stereoretentive Ru catalysts and one example of *E*-macrocycle synthesis using **8.3**.[11] Additional methods of obtaining *E*-macrocycles include *Z*-selective ethenolysis of stereochemical mixtures of macrocycles[3] and alkyne metathesis followed by *E*-selective semihydrogenation catalyzed by Cp*Ru(COD)Cl/AgOTf.[12]

Results and Discussion

We anticipated that *E*-macrocycles could be generated from diene starting materials containing an *E*-olefin using stereoretentive Ru catalysts. The proposed favored metallacyclobutane intermediate avoids steric clashing of the α substituent with the *N*-

ary group as proposed in the disfavored intermediate (Figure 8.4). Catalysts **8.2−8.4**
were chosen for studying RCM with these substrates as they had previously exhibited
remarkable activity and selectivity in cross metathesis of *E*-olefins.[8] Based on the
aforementioned proposed model for stereoretention, we expected that reducing the *ortho*
substituent size of the *N*-aryl groups would allow for better accommodation of the *β*
substituent in *E*-selective RCM. Therefore the reactivity of **8.4** with *E*-olefins would be
greater than **8.3**, which would furthermore be greater than that of **8.2**.
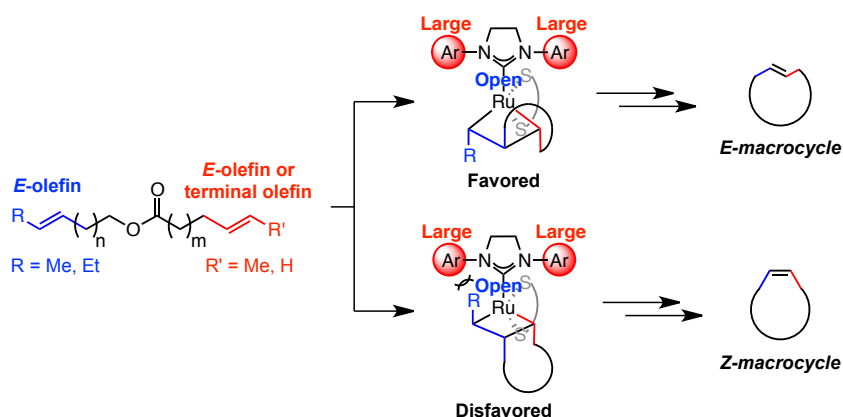
Figure 8.4. Proposed favored and disfavored intermediates in the formation of
macrocycles from dienes containing an *E*-olefin.

Using the approach we established in the synthesis of *Z*-macrocycles, we
attempted to make *E*-macrocycle **8.6** from diene starting material **8.5** bearing an *E*-olefin
and a terminal olefin (Scheme 8.1). Using a standard 7.5 mol % catalyst loading typical
of macrocyclization reactions,[13] catalysts **8.2**, **8.3**, and **8.4** reached a maximum of 4%,
30%, and 39% conversion, respectively, to the desired product **8.6** with high *E*-selectivity
(>99% *E*) at 35 °C. This low conversion is presumably a result of the instability and
decomposition of unstable Ru methylidenes formed in this reaction.[14] Previous studies
have shown that reaction of these catalysts with *E*-olefins is considerably slower than
with *Z*-olefins.[8] Therefore it is proposed that Ru methylidenes persist longer in solution in

reactions with *E*-olefins and are accordingly more prone to decomposition in reactions with *E*-olefins than in those with *Z*-olefins.
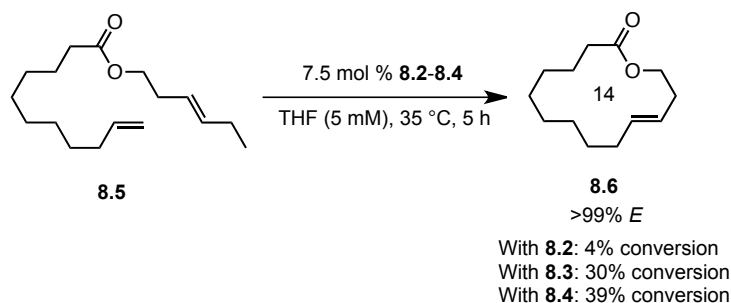

Scheme 8.1. Synthesis of *E*-macrocycle **8.6** from **8.5** using **8.2**−**8.4**. Conversion determined by ^{1}H NMR. Selectivity determined using gas chromatography.

To avoid the formation of Ru methylidenes, diene substrates containing two *E*-olefins were synthesized. Using substrate **8.7**, the formation of 12-membered macrocycle **8.8** was monitored using catalysts **8.2**−**8.4** at 35 °C (Figure 8.5a). Catalyst **8.4** displayed remarkable activity in this reaction. After 30 minutes, the reaction reached 30% conversion to **8.8** with **8.4**, while **8.3** provided just 5% conversion and **8.2** reached 2% conversion. After just 1 h, **8.4** achieves 57% conversion. To reach the same conversion, **8.3** requires 9 h, while **8.2** never attains this level of conversion. A maximum of 70% conversion to **8.8** is achieved using **8.4**, while **8.3** reaches a maximum of 62% conversion and **8.2** gives 51% conversion. With each of these catalysts, high *E*-selectivity (>99% *E*) was maintained throughout the course of the reaction.

Assuming first-order kinetics with respect to diene **8.7**, rate constants were measured for catalysts **8.2**, **8.3**, and **8.4** under these reaction conditions and were determined to be 3.92×10^{-2} s^{-1}, 3.27×10^{-1} s^{-1}, and 8.64×10^{-1} s^{-1}, respectively (Figure 8.5b). The relative rate constants hence have values of $k_{\text{rel}8.4} = k_{\text{obs}8.4}/k_{\text{obs}8.2} = 22.0$ and $k_{\text{rel}8.3} = k_{\text{obs}8.3}/k_{\text{obs}8.2} = 8.46$. Given the previously observed low reactivity of *E*-olefins

167

with these catalysts,[6,8] these large disparities in activity highlight the difference in the ability of each of these catalysts to provide significant yields of products.
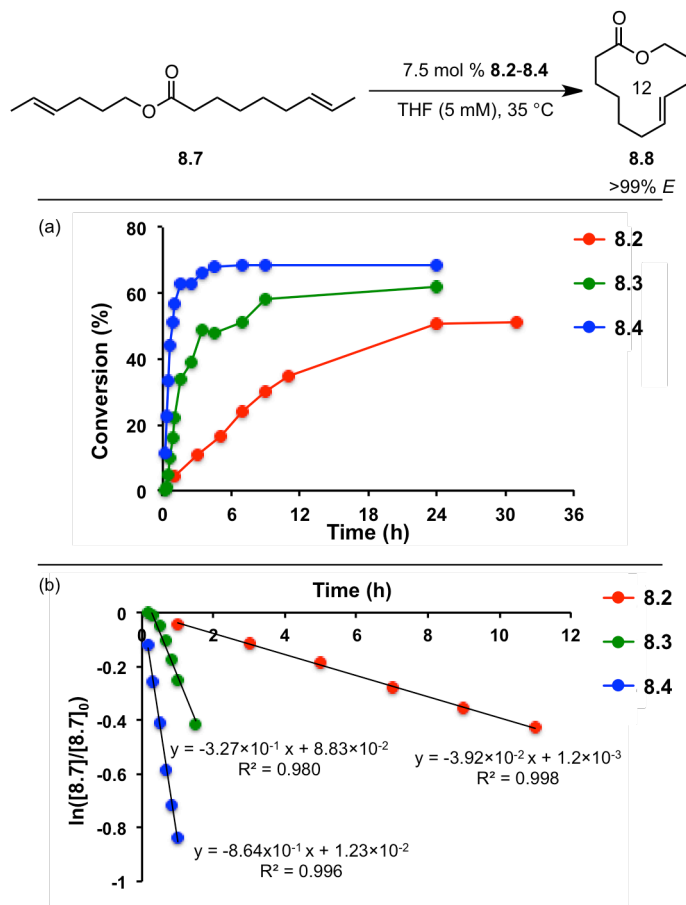
Figure 8.5. (a) Plot of conversion vs. time for RCM of **8.7** to **8.8** using catalysts **8.2−8.4**. (b) Plot of $\ln([\mathbf{8.7}]/[\mathbf{8.7}]_0)$ vs. time for this reaction. Conversion determined by ^{1}H NMR. Selectivity determined using gas chromatography.

An array of diene substrates bearing two *E*-olefins were synthesized from internal alkyne starting materials which could be reduced by Li/NH$_3$ or LiAlH$_4$ (Scheme 8.2). Subsequent Jones oxidation was used to generate the carboxylate moiety of the desired ester product. EDC coupling of this carboxylic acid with the corresponding alcohol gives the substrate in a scalable synthesis.

168
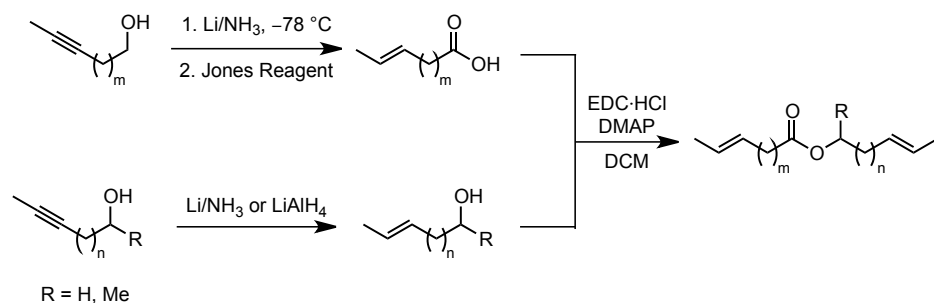
Scheme 8.2. Synthesis of diene substrates bearing two *E*-olefins.

Using these substrates, a variety of macrocyclic lactones were synthesized, ranging in size from 12- to 18-membered rings (Table 8.1). Each of these macrocycles

Table 8.1. Synthesis of macrocyclic lactones using catalysts **8.2** and **8.4**.
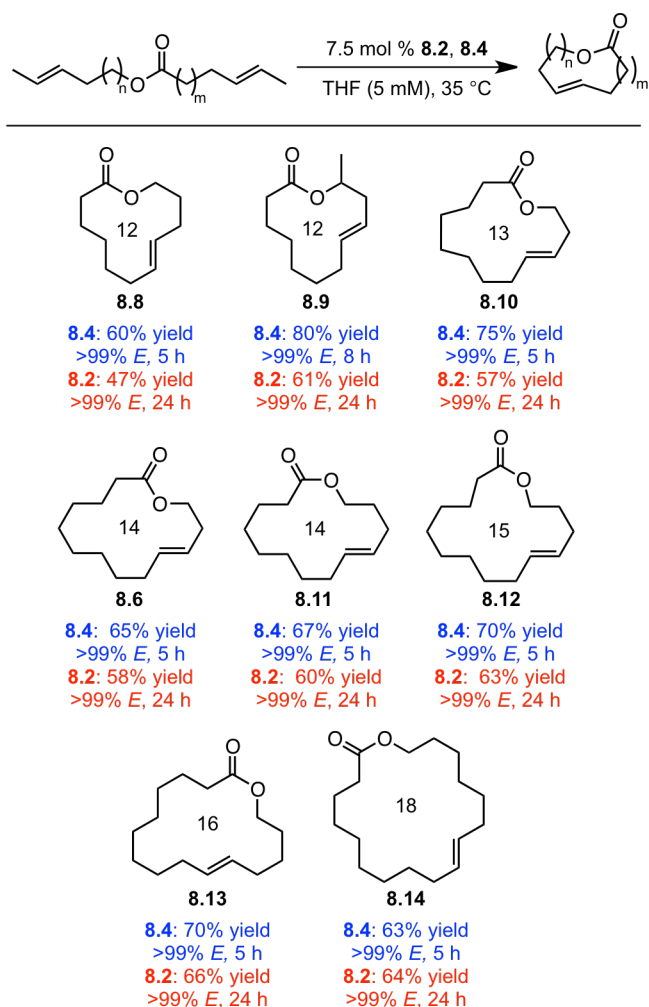
Yields shown are isolated yields. Stereoselectivity determined by gas chromatography.

169

was generated with the concomitant loss of gaseous *trans*-2-butene, which could be easily removed from the reaction mixture. Using catalyst **8.2**, products were obtained in moderate to good yields (47% − 66%) and with high *E*-selectivity (>99% *E*) in 24 h at 35 °C. Much shorter reaction times could be achieved using **8.4**, which provided these macrocycle products in 5 h in good to high yields (60% − 80%) while high *E*-selectivity was maintained (>99% *E*). Using **8.4**, the antibiotic recifeiolide **8.9** was synthesized in 80% yield with >99% *E*-selectivity in 8 h. Longer reaction times were likely required for this reaction due to steric encumbrance of the methyl group in the starting material.

Conclusions

We have demonstrated that stereoretentive Ru catalysts supported by dithiolate ligands can be used in the synthesis of *E*-macrocycles with exceptional selectivity (>99% *E*) from diene starting materials bearing two *E*-olefins. Catalyst **8.4** delivers meaningful yields of macrocyclic products in appreciably shorter reaction times than other stereoretentive Ru catalysts **8.2** and **8.3** as evidenced by kinetic studies. Using this method, 12- to 18-membered macrocycles including recifeiolide were synthesized in moderate to high yield (47% − 80% yield).

Experimental

General Information

Unless otherwise specified, all manipulations were carried out under air-free conditions in dry glassware in a Vacuum Atmospheres Glovebox filled with N_2. General solvents were purified by passing through solvent purification columns. Commercially available substrates were used as received. All solvents and substrates were sparged with Ar before bringing into the glovebox and filtered over basic alumina (Brockmann I) prior

to use. **8.2−8.4**,[8] *trans*-3-penten-1-ol,[15] *trans*-4-hexen-1-ol,[16] 5-heptyn-1-ol,[17] 6-octyn-1-ol,[18] 7-nonyn-1-ol,[19] 10-dodecyn-1-ol[20] were synthesized according to literature procedure.

Kinetic NMR experiments were performed on a Varian 600 MHz spectrometer with an AutoX probe. Spectra were analyzed using MestReNova Ver. 8.1.2. ^{1}H and ^{13}C NMR characterization data were obtained on a Bruker 400 with Prodigy broadband cryoprobe and referenced to residual protio-solvent.

GC conversion data was obtained using an HP-5 capillary column with an Agilent 6850 FID gas chromatograph. High-resolution mass spectrometry (HRMS) was performed using FAB+ ionization on a JEOL MSRoute mass spectrometer. Some accurate masses were determined by electrospray ionization, in the positive ion mode, using a Waters LCT Premier XE time-of-flight mass spectrometer.

Synthesis of (*E*)-hex-3-en-1-yl undec-10-enoate (8.5)

To a round-bottom flask charged with a stir bar were added 20 mL dichloromethane, undecenoyl chloride (2.37 mL, 11.0 mmol), and pyridine (0.89 mL, 11.0 mmol). *Trans*-3-hexenol (1.22 mL, 10.0 mmol) was then added dropwise at 0 °C. The reaction mixture was brought to room temperature and stirred for 4 h. The reaction mixture was extracted with 1M aq. HCl (200 mL) and saturated aq. $NaHCO_3$ (200 mL). The organic layer was dried over anhydrous $MgSO_4$, filtered, and solvents were removed *in vacuo*. The product was purified by column chromatography on silica gel (5:95 Et_2O: pentane) to yield a colorless oil (2.53 g, 95% yield).

^{1}H NMR (400 MHz, Chloroform-d_1) δ 5.81 (ddt, *J* = 16.9, 10.1, 6.7 Hz, 1H), 5.55 (dtt, *J* = 15.3, 6.3, 1.3 Hz, 1H), 5.36 (dtt, *J* = 15.2, 6.8, 1.5 Hz, 1H), 4.99 (dq, *J* = 17.1, 1.7 Hz,

1H), 4.93 (ddt, *J* = 10.2, 2.2, 1.2 Hz, 1H), 4.07 (t, *J* = 6.9 Hz, 2H), 2.36 – 2.24 (m, 4H), 2.12 – 1.95 (m, 4H), 1.68 – 1.59 (m, 2H), 1.41 – 1.33 (m, 2H), 1.32 – 1.22 (m, 8H), 0.96 (t, *J* = 7.4 Hz, 3H).

^{13}C NMR (101 MHz, CDCl$_3$) δ 174.04, 139.33, 135.14, 124.24, 114.28, 64.04, 34.52, 33.94, 32.13, 29.44, 29.36, 29.27, 29.21, 29.04, 25.77, 25.15, 13.89.

HRMS (EI+): [M]$^+$ C$_{17}$H$_{30}$O$_2$ Calculated – 266.2246, Found – 266.2239.

Synthesis of *trans*-4-hexen-2-ol

To an oven-dried, round-bottomed flask equipped with a magnetic stir bar was added 4-pentyn-2-ol (500 mg, 5.94 mmol) and THF (8.87 mL) under an argon atmosphere. The flask was placed in a dry ice/acetone bath at −78 °C, and *n*-butyllithium (8.92 mL, 12.48 mmol) was added slowly. The reaction mixture was stirred at −78 °C for 1.5 h. Methyl iodide (1.11 mL, 17.82 mmol) was added to the reaction mixture. The reaction was warmed to ambient temperature and stirred for 8 h. The reaction was quenched with a saturated aq. NaHCO$_3$ solution and extracted with diethyl ether (3 x 20 mL). The organic extracts were combined and washed with a saturated aq. NH$_4$Cl solution. The organic phase was dried over anhydrous MgSO$_4$, filtered, and concentrated to give the methylated alkyne product as colorless oil.

Adapted from Sigman *et al. J. Am. Chem. Soc.* **2015**, *137*, 3462.

To an oven-dried round-bottomed flask equipped with a magnetic stir bar and charged with lithium aluminum hydride (557 mg, 14.7 mmol), toluene (6.5 mL), and THF (3.5 mL) was added the crude alcohol product (450 mg). The round-bottomed flask was equipped with a condenser and stirred at 90 °C for 24 h. The reaction was cooled to ambient temperature, diluted with diethyl ether, and quenched with water (**dropwise 1**

mL, as this results in vigorous release of hydrogen gas, *Extreme Caution* should be taken). A 20 wt% solution of potassium hydroxide in water was added followed by excess water. The aqueous phase was extracted with diethyl ether (2 x 30 mL). The combined organic extracts were washed with brine (2 x 20 mL), dried over anhydrous MgSO$_4$, filtered, and concentrated. The crude product was purified *via* flash column chromatography (diethyl ether:pentane, 1:7) to furnish the desired product as a colorless oil (120 mg, 20% yield). *Note*: The product is slightly volatile, so concentration to remove solvent should be slow.

^{1}H NMR (400 MHz, Chloroform-d_1) δ 5.61 – 5.50 (m, 1H), 5.43 (dddq, *J* = 15.6, 8.0, 6.4, 1.5 Hz, 1H), 3.86 – 3.71 (m, 1H), 2.27 – 2.13 (m, 1H), 2.07 (dtt, *J* = 13.8, 7.7, 1.0 Hz, 1H), 1.78 – 1.66 (m, 3H), 1.66 – 1.57 (m, 1H), 1.18 (dd, *J* = 6.2, 0.5 Hz, 3H).

^{13}C NMR (101 MHz, CDCl$_3$) δ 129.16, 127.25, 67.32, 42.69, 22.80, 18.23.

HRMS (EI+): [M]$^+$ C$_6$H$_{12}$O Calculated – 100.0888, Found – 100.0901.

Synthesis of *trans*-7-nonen-1-ol

To an oven-dried, three-necked flask equipped with a condenser and charged with glass-coated stir bar was added a solution of 7-nonyn-1-ol (500 mg, 3.56 mmol) in *t*BuOH/THF (10:16 mL, 26 mL) under argon atmosphere. The flask was placed in a dry ice/acetone bath at −78 °C, and ammonia (30 mL) was condensed into the flask. Lithium metal (259 mg) was added and the reaction was stirred for 1.5 h. The ammonia was allowed to evaporate while bringing to room temperature, and the reaction was quenched with saturated aq. NH$_4$Cl solution immediately upon disappearance of the blue color. The aqueous layer was extracted with pentane (4 × 100 mL) and washed with brine (2 × 50 mL). The organic phase was dried over anhydrous MgSO$_4$, filtered, and concentrated to

give the product as colorless oil (453 mg, 90% yield) *Note*: If reaction did not reach full

conversion to reduced product, the crude mixture was resubjected to reaction conditions.

^{1}H NMR (400 MHz, Chloroform-d_1) δ 5.64 – 5.23 (m, 2H), 3.65 (t, J = 6.6 Hz, 2H), 2.06

– 1.92 (m, 2H), 1.66 (dq, J = 4.0, 1.3 Hz, 3H), 1.58 (dq, J = 8.4, 6.3 Hz, 2H), 1.47 – 1.24

(m, 7H).

^{13}C NMR (101 MHz, CDCl$_3$) δ 131.61, 124.83, 63.18, 32.89, 32.64, 29.67, 29.07, 25.74,

18.07.

HRMS (EI+): [M]$^+$ C$_9$H$_{18}$O Calculated – 142.1358, Found – 142.1310.

Synthesis of *trans*-7-nonenoic acid

To a vial charged with a stir bar was added *trans*-7-nonen-1-ol (200.0 mg, 1.41 mmol)

and acetone (2.80 mL). Jones reagent (1.05 mL, 2.0 M, 2.11 mmol) was added dropwise

at 0 °C, and the reaction was stirred for 1.5 h. 5 mL Et$_2$O was added and the product was

extracted with saturated aq. NaHCO$_3$ solution (4 × 5 mL). The aqueous phase was then

acidified dropwise with concentrated H$_2$SO$_4$ at 0 °C. The product was extracted with

ethyl acetate (3 × 5 mL). The organic phase was dried over anhydrous MgSO$_4$, filtered,

and concentrated to give the product as a colorless oil (188 mg, 85% yield).

^{1}H NMR (400 MHz, Chloroform-d_1) δ 9.34 (s, 1H)’ 5.61 – 5.28 (m, 2H), 2.37 (t, J = 7.5

Hz, 2H), 1.99 (tddd, J = 6.1, 5.3, 3.7, 2.6, 1.4 Hz, 2H), 1.74 – 1.58 (m, 5H), 1.37 (pt, J =

4.0, 2.3 Hz, 4H).

^{13}C NMR (101 MHz, CDCl$_3$) δ 180.31, 131.33, 125.07, 34.18, 32.47, 29.29, 28.67,

24.68, 18.07.

HRMS (FAB+): [M+H]$^+$ C$_9$H$_{17}$O$_2$ Calculated – 157.1229, Found – 157.1234.

Synthesis of 8-decyn-1-ol

To a vial charged with a stir bar and KO^{t}Bu (1.5 g, 13.0 mmol) and sealed with a septum cap under argon atmosphere was added anhydrous DMSO (22 mL) and 9-decyn-1-ol (1.15 mL, 6.5 mmol). After stirring for 3 h, the reaction was quenched with 1M aq. HCl. After extraction with diethyl ether (3 × 100 mL) and washing with water (1 × 100 mL), the organic phase was dried over anhydrous MgSO$_4$ and filtered. Solvents were removed *in vacuo* to yield the product as a colorless oil (901 mg, 90% yield).

^{1}H NMR (400 MHz, Chloroform-d_1) δ 3.69 − 3.55 (m, 2H), 2.10 (ddt, J = 7.1, 4.7, 2.5 Hz, 2H), 1.77 (q, J = 2.5 Hz, 3H), 1.64 − 1.51 (m, 2H), 1.51 − 1.42 (m, 2H), 1.42 − 1.20 (m, 7H).

^{13}C NMR (101 MHz, CDCl$_3$) δ 79.43, 75.54, 63.12, 32.86, 29.11, 29.09, 28.95, 25.76, 18.82, 3.61.

HRMS (EI+): [M]$^+$ C$_{10}$H$_{17}$O Calculated − 153.1279, Found − 153.1320.

Synthesis of *trans*-8-decen-1-ol

To an oven-dried, three-necked flask equipped with a condenser and charged with glass-coated stir bar was added a solution of 8-decyn-1-ol (100 mg, 0.65 mmol) in *t*BuOH/THF (2 mL: 3 mL, 5 mL) under argon atmosphere. The flask was placed in a dry ice/acetone bath at −78 °C, and ammonia (10 mL) was condensed into the flask. Lithium metal (22 mg, 3.24 mmol) was added and the reaction was stirred for 1.5 h. The ammonia was allowed to evaporate while bringing to room temperature, and the reaction was quenched with saturated aq. NH$_4$Cl solution immediately upon disappearance of the blue color. The aqueous layer was extracted with pentane (4 × 25 mL) and washed with brine (2 × 10 mL). The organic phase was dried over anhydrous MgSO$_4$, filtered, and concentrated to

give the product as colorless oil (74 mg, 73% yield) *Note*: If reaction did not reach full conversion to reduced product, the crude mixture was resubject to reaction conditions.

^{1}H NMR (400 MHz, Chloroform-d_1) δ 5.49 – 5.30 (m, 2H), 3.63 (t, J = 6.7 Hz, 2H), 2.06 – 1.86 (m, 2H), 1.63 (dt, J = 4.7, 1.4 Hz, 3H), 1.61 – 1.51 (m, 2H), 1.37 – 1.28 (m, 9H).

^{13}C NMR (101 MHz, CDCl$_3$) δ 131.70, 124.77, 63.23, 32.93, 32.72, 29.67, 29.44, 29.26, 25.85, 18.09.

HRMS (EI+): [M]$^+$ C$_{10}$H$_{20}$O Calculated – 156.1514, Found – 156.1504.

Synthesis of *trans*-8-decenoic acid

To a vial equipped with a magnetic stir bar was added *trans*-8-decen-1-ol (74 mg, 0.47 mmol) and acetone (1 mL). The reaction mixture was cooled to 0 °C and Jones reagent (0.355 mL, 0.71 mmol) was added dropwise. The reaction was stirred at ambient temperature for 1.5 h. Diethyl ether (10 mL) was added and the mixture was extracted with saturated aq. Na HCO$_3$ solution (5 x 10 mL). The aqueous extracts were combined, acidified with H$_2$SO$_4$, and extracted with ethyl acetate (3 x 10 mL). The organic extracts were combined, dried with Na$_2$SO$_4$, and concentrated to deliver the desired product as a colorless oil (47 mg, 59% yield).

^{1}H NMR (400 MHz, Chloroform-d_1) δ 11.42 (s, 1H), 5.40 (dq, J = 4.6, 2.1 Hz, 2H), 2.34 (t, J = 7.5 Hz, 3H), 1.96 (ddd, J = 8.6, 5.2, 3.1 Hz, 2H), 1.64 (dt, J = 4.9, 1.4 Hz, 5H), 1.35 – 1.22 (m, 6H).

^{13}C NMR (101 MHz, CDCl$_3$) δ 180.24, 131.54, 124.90, 34.17, 32.63, 29.49, 29.05, 28.87, 24.78, 18.08.

HRMS (EI+): [M]$^+$ C$_{10}$H$_{18}$O$_2$ Calculated: 170.1307, Found: 170.1309.

Synthesis of 9-undecyn-1-ol

To a vial charged with a stir bar and KO^{t}Bu (0.63 g, 5.6 mmol) and sealed with a septum cap under argon atmosphere was added anhydrous DMSO (11 mL) and 10-undecyn-1-ol (0.53 mL, 2.8 mmol). After stirring for 3 h, the reaction was quenched with 1M aq. HCl. After extraction with diethyl ether (3 × 50 mL) and washing with water (1 × 100 mL), the organic phase was dried over anhydrous MgSO$_4$ and filtered. Solvents were removed *in vacuo* to yield the product as a colorless oil (450 mg, 96% yield).

^{1}H NMR (400 MHz, Chloroform-d_1) δ 3.63 (t, J = 6.6 Hz, 2H), 2.10 (ddq, J = 9.6, 7.3, 2.5 Hz, 2H), 1.77 (t, J = 2.6 Hz, 3H), 1.62 – 1.51 (m, 2H), 1.51 – 1.40 (m, 3H), 1.40 – 1.19 (m, 8H).

^{13}C NMR (101 MHz, CDCl$_3$) δ 79.49, 75.50, 63.17, 32.89, 29.44, 29.26, 29.17, 28.94, 25.82, 18.84, 3.61.

HRMS (FAB+): [M+H]$^+$ C$_{11}$H$_{21}$O Calculated – 169.1591, Found – 169.1592.

Synthesis of *trans*-9-undecen-1-ol

To an oven-dried, three-necked flask equipped with a condenser and charged with glass-coated stir bar was added a solution of 9-undecyn-1-ol (300 mg, 1.78 mmol) in *t*BuOH/THF (5 mL: 8 mL, 13 mL) under argon atmosphere. The flask was placed in a dry ice/acetone bath at −78 °C, and ammonia (15 mL) was condensed into the flask. Lithium metal (130 mg) was added and the reaction was stirred for 1.5 h. The ammonia was allowed to evaporate while bringing to room temperature, and the reaction was quenched with saturated aq. NH$_4$Cl solution immediately upon disappearance of the blue color. The aqueous layer was extracted with pentane (4 × 50 mL) and washed with brine (2 × 25 mL). The organic phase was dried over anhydrous MgSO$_4$, filtered, and

concentrated to give the product as colorless oil (268 mg, 89% yield) *Note*: If reaction did not reach full conversion to reduced product, the crude mixture was resubjected to reaction conditions.

^{1}H NMR (400 MHz, Chloroform-d_1) δ 5.50 – 5.32 (m, 2H), 3.63 (t, J = 6.6 Hz, 2H), 1.95 (dddd, J = 7.9, 5.0, 3.1, 1.6 Hz, 2H), 1.67 – 1.50 (m, 6H), 1.39 – 1.23 (m, 10H).

^{13}C NMR (101 MHz, CDCl$_3$) δ 131.76, 124.72, 63.24, 32.94, 32.74, 29.73, 29.62, 29.54, 29.25, 25.87, 18.09.

HRMS (EI+): [M]$^+$ C$_{11}$H$_{22}$O Calculated – 170.1671, Found – 170.1681.

Synthesis of *trans*-9-undecenoic acid

To a vial charged with a stir bar was added *trans*-9-undecen-1-ol (200.0 mg, 1.17 mmol) and acetone (2.16 mL). Jones reagent (0.88 mL, 2.0 M, 1.76 mmol) was added dropwise at 0 °C, and the reaction was brought to room temperature and stirred for 1.5 h. 5 mL Et$_2$O was added and the product was extracted with saturated aq. NaHCO$_3$ solution (4 × 5 mL). The aqueous phase was then acidified dropwise with concentrated H$_2$SO$_4$ at 0 °C. The product was extracted with ethyl acetate (3 × 5 mL). The organic phase was dried over anhydrous MgSO$_4$, filtered, and concentrated to give the product as a colorless solid (190 mg, 88% yield).

^{1}H NMR (400 MHz, Chloroform-d_1) δ 9.14 (s, 1H), 5.61 – 5.21 (m, 2H), 2.37 (t, J = 7.5 Hz, 2H), 1.98 (dddd, J = 7.3, 4.6, 2.8, 1.4 Hz, 2H), 1.74 – 1.59 (m, 5H), 1.38 – 1.28 (m, 8H).

^{13}C NMR (101 MHz, CDCl$_3$) δ 180.00, 131.68, 124.80, 34.13, 32.70, 29.66, 29.25, 29.16, 29.08, 24.80, 18.09.

HRMS (EI+): [M]$^+$ C$_{11}$H$_{20}$O$_2$ Calculated – 184.1463, Found – 184.1469.

Synthesis of *trans*-10-dodecen-1-ol

To an oven-dried, three-necked flask equipped with a condenser and charged with glass-coated stir bar was added a solution of 10-dodecyn-1-ol (500 mg, 2.75 mmol) in *t*BuOH/THF (7.5 mL: 12.5 mL, 20 mL) under argon atmosphere. The flask was placed in a dry ice/acetone bath at −78 °C, and ammonia (30 mL) was condensed into the flask. Lithium metal (200 mg) was added and the reaction was stirred for 1.5 h. The ammonia was allowed to evaporate while bringing to room temperature, and the reaction was quenched with saturated aq. NH_4Cl solution immediately upon disappearance of the blue color. The aqueous layer was extracted with pentane (4 × 100 mL) and washed with brine (2 × 50 mL). The organic phase was dried over anhydrous $MgSO_4$, filtered, and concentrated to give the product as colorless oil (417 mg, 83% yield) *Note*: If reaction did not reach full conversion to reduced product, the crude mixture was resubjected to reaction conditions.

^{1}H NMR (400 MHz, Chloroform-d_1) δ 5.55 − 5.25 (m, 2H), 3.63 (t, J = 6.6 Hz, 2H), 1.95 (dtd, J = 7.9, 5.1, 2.5 Hz, 2H), 1.69 − 1.61 (m, 3H), 1.56 (dq, J = 8.3, 6.8 Hz, 2H), 1.40 − 1.23 (m, 13H).

^{13}C NMR (101 MHz, $CDCl_3$) δ 131.79, 124.69, 63.23, 32.94, 32.75, 29.75, 29.71, 29.59, 29.56, 29.31, 25.87, 18.08.

HRMS (FAB+): $[M+H]^+$ $C_{12}H_{25}O$ Calculated − 185.1905, Found − 185.1912.

Synthesis of *trans*-10-dodecenoic acid

To a vial charged with a stir bar was added *trans*-10-dodecen-1-ol (200.0 mg, 1.08 mmol) and acetone (2.16 mL). Jones reagent (0.81 mL, 2.0 M, 1.62 mmol) was added dropwise at 0 °C, and the reaction was brought to room temperature and stirred for 1.5 h. 5 mL

Et$_2$O was added and the product was extracted with saturated aq. NaHCO$_3$ solution (4 × 5 mL). The aqueous phase was then acidified dropwise with concentrated H$_2$SO$_4$ at 0 °C. The product was extracted with ethyl acetate (3 × 5 mL). The organic phase was dried over anhydrous MgSO$_4$, filtered, and concentrated to give the product as a white solid (179 mg, 84% yield).

^{1}H NMR (400 MHz, Chloroform-d_1) δ 5.52 – 5.34 (m, 2H), 2.37 (t, J = 7.5 Hz, 3H), 1.97 (dqt, J = 7.7, 2.7, 1.5 Hz, 2H), 1.73 – 1.52 (m, 5H), 1.44 – 1.21 (m, 10H).

^{13}C NMR (101 MHz, CDCl$_3$) δ 179.57, 131.75, 124.74, 34.08, 32.73, 29.71, 29.43, 29.34, 29.24, 29.19, 24.82, 18.09.

HRMS (EI+): [M]$^+$ C$_{12}$H$_{22}$O$_2$ Calculated – 198.1620, Found – 198.1640.

Synthesis of *trans*-5-hepten-1-ol

To an oven-dried, three-necked flask equipped with a condenser and charged with glass-coated stir bar was added a solution of 5-heptyn-1-ol (125 mg, 1.14 mmol) in *t*BuOH/THF (3 mL: 5 mL, 8 mL) under argon atmosphere. The flask was placed in a dry ice/acetone bath at −78 °C, and ammonia (20 mL) was condensed into the flask. Lithium metal (83 mg, 11.4 mmol) was added and the reaction was stirred for 1.5 h. The ammonia was allowed to evaporate while bringing to room temperature, and the reaction was quenched with saturated aq. NH$_4$Cl solution immediately upon disappearance of the blue color. The aqueous layer was extracted with pentane (4 × 25 mL) and washed with brine (2 × 10 mL). The organic phase was dried over anhydrous MgSO$_4$, filtered, and concentrated to give the product as colorless oil (97 mg, 76% yield) *Note*: If reaction did not reach full conversion to reduced product, the crude mixture was resubjected to reaction conditions.

¹H NMR (400 MHz, Chloroform-d_1) δ 5.52 – 5.34 (m, 2H), 3.64 (t, J = 6.6 Hz, 2H), 2.00 (dddd, J = 7.2, 6.1, 4.0, 1.2 Hz, 2H), 1.64 (dt, J = 5.0, 1.3 Hz, 3H), 1.62 – 1.50 (m, 2H), 1.46 – 1.35 (m, 2H), 1.34 – 1.27 (m, 1H).

¹³C NMR (101 MHz, CDCl₃) δ 131.22, 125.27, 63.07, 32.41, 32.37, 25.78, 18.07.

HRMS (EI+): [M+H]⁺ $C_7H_{13}O$ Calculated – 113.0966, Found – 113.0987.

Synthesis of (*E*)-(*E*)-hex-4-en-1-yl non-7-enoate (8.7)

To a vial charged with a stir bar was added *trans*-7-nonenoic acid (143.7 mg, 0.9198 mmol), DMAP (23.0 mg, 0.184 mmol), EDC hydrochloride (352.1 mg, 1.840 mmol), and 7.5 mL dry dichloromethane under argon atmosphere. *Trans*-4-hexen-1-ol (216 μL, 1.840 mmol) was added, and the reaction was stirred for 3 h. 1 M aq. HCl (15 mL) was added to quench the reaction, the product was extracted with DCM (4 x 15 mL). This organic phase was dried over MgSO₄, filtered, and concentrated *in vacuo*. The product was purified by column chromatography (5:95 Et₂O:pentane) to yield the product as a colorless oil (201.7 mg, 92% yield).

¹H NMR (400 MHz, Chloroform-d_1) δ 5.52 – 5.36 (m, 4H), 4.08 (t, J = 6.7 Hz, 2H), 2.31 (t, J = 7.5 Hz, 2H), 2.11 – 2.03 (m, 2H), 1.99 (dddd, J = 8.7, 6.5, 3.0, 1.3 Hz, 2H), 1.74 – 1.59 (m, 10H), 1.42 – 1.26 (m, 4H).

¹³C NMR (101 MHz, CDCl₃) δ 173.95, 131.28, 129.97, 125.81, 124.86, 63.78, 34.37, 32.39, 29.21, 28.88, 28.66, 28.47, 24.91, 17.94, 17.93.

HRMS (EI+): [M]⁺ $C_{15}H_{26}O_2$ Calculated – 238.1933, Found – 238.1935.

Synthesis of (*E*)-(*E*)-hex-4-en-2-yl dec-8-enoate

To a vial charged with a stir bar was added *trans*-8-decenoic acid (47.0 mg, 0.276 mmol), DMAP (6.74 mg, 0.0552 mmol), EDC hydrochloride (105.8 mg, 0.5520 mmol), and 2.3

mL dry dichloromethane under argon atmosphere. *Trans*-4-hexen-2-ol (55.3 mg, 0.552 mmol) was added, and the reaction was stirred for 3 h at ambient temperature. 1 M aq. HCl (10 mL) was added to quench the reaction, the product was extracted with DCM (4 x 10 mL). The organic extracts were combined, dried over $MgSO_4$, filtered, and concentrated *in vacuo*. The product was purified by column chromatography (5:95 Et_2O:pentane) to yield the product as a colorless oil (47 mg, 67% yield).

^{1}H NMR (400 MHz, Chloroform-d_1) δ 5.54 – 5.43 (m, 1H), 5.42 – 5.29 (m, 3H), 4.90 (h, J = 6.3 Hz, 1H), 2.30 – 2.22 (m, 3H), 2.22 – 2.12 (m, 1H), 2.00 – 1.90 (m, 2H), 1.69 – 1.55 (m, 8H), 1.39 – 1.24 (m, 6H), 1.18 (d, J = 6.3 Hz, 3H).

^{13}C NMR (101 MHz, $CDCl_3$) δ 173.54, 131.60, 128.33, 126.29, 124.83, 70.39, 39.26, 34.86, 32.65, 29.54, 29.14, 28.94, 25.20, 19.62, 18.15, 18.08.

HRMS (EI+): $[M]^+$ $C_{16}H_{28}O_2$ Calculated – 252.2089, Found – 252.2074.

Synthesis of (*E*)-(*E*)-pent-3-en-1-yl undec-9-enoate

To a vial charged with a stir bar was added *trans*-9-undecenoic acid (53.4 mg, 0.290 mmol), DMAP (7.1 mg, 0.0580 mmol), EDC hydrochloride (111.1 mg, 0.580 mmol), and 2.3 mL dry dichloromethane under argon atmosphere. *Trans*-3-penten-1-ol (59.3 µL, 0.580 mmol) was added, and the reaction was stirred for 3 h. 1M aq. HCl (5 mL) was added to quench the reaction, and the product was extracted with DCM (4 x 5 mL). This organic phase was dried over $MgSO_4$, filtered, and concentrated *in vacuo*. The product was purified by column chromatography (5:95 Et_2O:pentane) to yield the product as a colorless oil (65.7 mg, 90% yield).

^{1}H NMR (400 MHz, Chloroform-d_1) δ 5.60 – 5.31 (m, 1H), 4.06 (t, J = 6.9 Hz, 1H), 2.36 – 2.22 (m, 1H), 1.99 – 1.89 (m, 1H), 1.72 – 1.51 (m, 2H), 1.39 – 1.23 (m, 2H).

^{13}**C NMR** (101 MHz, CDCl$_3$) δ 174.04, 131.69, 127.97, 126.52, 124.76, 64.00, 34.51, 32.70, 32.15, 29.67, 29.28, 29.24, 29.11, 25.14, 18.14, 18.08.

HRMS (EI+): [M]$^+$ C$_{16}$H$_{28}$O$_2$ Calculated – 252.2089, Found – 252.2095.

Synthesis of (*E*)-(*E*)-hex-4-en-1-yl undec-9-enoate

To a vial charged with a stir bar was added *trans*-9-undecenoic acid (51.4 mg, 0.280 mmol), DMAP (6.8 mg, 0.0560 mmol), EDC hydrochloride (106.9 mg, 0.560 mmol), and 2.2 mL dry dichloromethane under argon atmosphere. *Trans*-4-hexen-1-ol (65.6 µL, 0.560 mmol) was added, and the reaction was stirred for 3 h. 1M aq. HCl (5 mL) was added to quench the reaction, and the product was extracted with DCM (4 x 5 mL). This organic phase was dried over MgSO$_4$, filtered, and concentrated *in vacuo*. The product was purified by column chromatography (5:95 Et$_2$O:pentane) to yield the product as a colorless oil (68.3 mg, 92% yield).

^{1}**H NMR** (400 MHz, Chloroform-*d$_1$*) δ 5.46 – 5.25 (m, 4H), 3.99 (t, *J* = 6.7 Hz, 2H), 2.27 – 2.15 (m, 2H), 1.97 (tdd, *J* = 7.6, 5.9, 1.5 Hz, 2H), 1.92 – 1.85 (m, 2H), 1.65 – 1.49 (m, 10H), 1.32 – 1.13 (m, 8H).

^{13}**C NMR** (101 MHz, CDCl$_3$) δ 174.12, 131.69, 130.10, 125.93, 124.76, 63.90, 34.53, 32.70, 29.66, 29.27, 29.26, 29.11, 29.02, 28.60, 25.15, 18.08, 18.06.

HRMS (EI+): [M]$^+$ C$_{17}$H$_{30}$O$_2$ Calculated – 266.2237, Found – 266.2246.

Synthesis of (*E*)-(*E*)-pent-3-en-1-yl dodec-10-enoate

To a vial charged with a stir bar was added *trans*-10-dodecenoic acid (45.8 mg, 0.231 mmol), DMAP (5.6 mg, 0.0462 mmol), EDC hydrochloride (88.6 mg, 0.462 mmol), and 1.8 mL dry dichloromethane under argon atmosphere. *Trans*-3-penten-1-ol (47.3 µL, 0.462 mmol) was added, and the reaction was stirred for 3 h. 1M aq. HCl (5 mL) was

added to quench the reaction, and the product was extracted with DCM (4 x 5 mL). This organic phase was dried over MgSO$_4$, filtered, and concentrated *in vacuo*. The product was purified by column chromatography (5:95 Et$_2$O:pentane) to yield the product as a colorless oil (51.4 mg, 84% yield).

^{1}H NMR (400 MHz, Chloroform-d_1) δ 5.60 – 5.29 (m, 4H), 4.06 (t, J = 6.9 Hz, 2H), 2.37 – 2.22 (m, 4H), 1.95 (dtt, J = 7.9, 5.1, 1.5 Hz, 2H), 1.72 – 1.56 (m, 8H), 1.40 – 1.24 (m, 10H).

^{13}C NMR (101 MHz, CDCl$_3$) δ 174.05, 131.76, 127.98, 126.53, 124.73, 64.01, 34.52, 32.74, 32.16, 29.73, 29.48, 29.39, 29.30, 29.28, 29.26, 25.16, 18.16, 18.10.

HRMS (EI+): [M]$^+$ C$_{17}$H$_{30}$O$_2$ Calculated – 266.2237, Found – 266.2261.

Synthesis of (*E*)-(*E*)-hex-4-en-1-yl dodec-10-enoate

To a vial charged with a stir bar was added *trans*-10-dodecenoic acid (45.6 mg, 0.230 mmol), DMAP (5.6 mg, 0.0460 mmol), EDC hydrochloride (88.2 mg, 0.460 mmol), and 1.4 mL dry dichloromethane under argon atmosphere. *Trans*-4-hexen-1-ol (41.3 mg, 0.460 mmol) was added, and the reaction was stirred for 3 h. 1M aq. HCl (5 mL) was added to quench the reaction, and the product was extracted with DCM (4 x 5 mL). This organic phase was dried over MgSO$_4$, filtered, and concentrated *in vacuo*. The product was purified by column chromatography (5:95 Et$_2$O:pentane) to yield the product as a colorless oil (47.2 mg, 73% yield).

^{1}H NMR (400 MHz, Chloroform-d_1) δ 5.53 – 5.32 (m, 4H), 4.05 (t, J = 6.7 Hz, 2H), 2.28 (t, J = 7.5 Hz, 2H), 2.04 (dtd, J = 7.9, 6.1, 1.5 Hz, 2H), 1.98 – 1.91 (m, 2H), 1.73 – 1.52 (m, 11H), 1.33 – 1.22 (m, 12H).

¹³C NMR (101 MHz, CDCl₃) δ 174.13, 131.76, 130.11, 125.93, 124.72, 63.90, 34.54, 32.73, 29.72, 29.47, 29.38, 29.29, 29.26, 29.02, 28.60, 25.16, 18.09, 18.06.

HRMS (EI+): [M]⁺ $C_{18}H_{32}O_2$ Calculated – 280.2402, Found – 280.2379.

Synthesis of (*E*)-(*E*)-hept-5-en-1-yl dodec-10-enoate

To a vial charged with a stir bar was added *trans*-10-dodecenoic acid (35.9 mg, 0.181 mmol), DMAP (4.4 mg, 0.0362 mmol), EDC hydrochloride (69.4 mg, 0.362 mmol), and 1.4 mL dry dichloromethane under argon atmosphere. *Trans*-5-hepten-1-ol (41.3 mg, 0.362 mmol) was added, and the reaction was stirred for 3 h. 1M aq. HCl (5 mL) was added to quench the reaction, and the product was extracted with DCM (4 x 5 mL). This organic phase was dried over MgSO₄, filtered, and concentrated *in vacuo*. The product was purified by column chromatography (5:95 Et₂O:pentane) to yield the product as a colorless oil (41.0 mg, 77% yield).

¹H NMR (400 MHz, Chloroform-*d*₁) δ 5.52 – 5.31 (m, 4H), 4.05 (t, *J* = 6.7 Hz, 2H), 2.28 (t, *J* = 7.5 Hz, 2H), 2.06 – 1.86 (m, 4H), 1.67 – 1.55 (m, 10H), 1.47 – 1.35 (m, 2H), 1.35 – 1.20 (m, 10H).

¹³C NMR (101 MHz, CDCl₃) δ 174.15, 131.74, 130.98, 125.41, 124.71, 64.38, 34.53, 32.73, 32.25, 29.72, 29.47, 29.37, 29.29, 29.25, 28.25, 25.99, 25.15, 18.08, 18.06.

HRMS (EI+): [M]⁺ $C_{19}H_{34}O_2$ Calculated – 294.2559, Found – 294.2578.

Synthesis of (*E*)-(*E*)-non-7-en-1-yl dodec-10-enoate

To a vial charged with a stir bar was added *trans*-10-dodecenoic acid (35.9 mg, 0.188 mmol), DMAP (4.6 mg, 0.0376 mmol), EDC hydrochloride (72.1 mg, 0.376 mmol), and 1.5 mL dry dichloromethane under argon atmosphere. *Trans*-7-nonen-1-ol (53.5 mg, 0.376 mmol) was added, and the reaction was stirred for 3 h. 1M aq. HCl (5 mL) was

added to quench the reaction, the product was extracted with DCM (4 x 5 mL). This organic phase was dried over MgSO$_4$, filtered, and concentrated *in vacuo*. The product was purified by column chromatography (5:95 Et$_2$O:pentane) to yield the product as a colorless oil (42.4 mg, 70% yield).

^{1}H NMR (400 MHz, Chloroform-d_1) δ 5.41 (ddt, J = 5.0, 3.7, 1.7 Hz, 4H), 4.05 (t, J = 6.7 Hz, 2H), 2.28 (t, J = 7.5 Hz, 2H), 2.03 – 1.88 (m, 4H), 1.69 – 1.54 (m, 10H), 1.34 – 1.23 (m, 16H).

^{13}C NMR (101 MHz, CDCl$_3$) δ 174.16, 131.76, 131.54, 124.89, 124.71, 64.51, 34.55, 32.74, 32.62, 29.72, 29.59, 29.48, 29.38, 29.30, 29.26, 28.90, 28.76, 25.96, 25.17, 18.09.

HRMS (EI+): [M]$^+$ C$_{21}$H$_{38}$O$_2$ Calculated – 322.2872, Found – 322.2896.

Procedure for Synthesis of 8.6 from 8.5

In an N$_2$-filled glovebox, **8.5** (5.0 mg, 18.8 μmol) and 2.8 mL THF were added to a vial charged with a stir bar. A solution of catalyst (1.4 μmol) in 1 mL of THF was then added to this mixture. The vial was loosely capped, and the reaction was stirred at 35 °C for the reported amount of time. 0.5 mL aliquots were taken out of the box at 2 and 5 h, and solvents were removed *in vacuo*. Conversions were determined by ^{1}H NMR of these aliquots, and stereoselectivity was determined by GC.

Procedure for Synthesis of 8.8 from 8.7

In an N$_2$-filled glovebox, **8.7** (10.0 mg, 42.0 μmol) and 7.4 mL THF were added to a vial charged with a stir bar. A solution of catalyst (3.1 μmol) in 1 mL of THF was then added to this mixture. The vial was loosely capped, and the reaction was stirred at 35 °C for the reported amount of time. 0.5 mL aliquots were taken out of the box, and solvents were

removed *in vacuo*. Conversions were determined by ^{1}H NMR of these aliquots, and stereoselectivity was determined by GC.

Synthesis of (*E*)-oxacyclododec-8-en-2-one (8.8)

In an N$_2$-filled glovebox, (*E*)-(*E*)-hex-4-en-1-yl non-7-enoate (20.0 mg, 83.9 μmol) and 15.8 mL THF were added to a vial charged with a stir bar. A solution of catalyst (6.3 μmol) in 1 mL of THF was then added to this mixture. The vial was loosely capped, and the reaction was stirred at 35 °C for the reported amount of time. The vial was taken out of the glovebox and quenched with 0.5 mL butyl vinyl ether. Solvents were removed *in vacuo*, and the product was purified with column chromatography on silica gel (1:49 Et$_2$O:pentane) to yield the product as a colorless oil (7.2 mg, 47% yield with **8.2**; 9.1 mg, 60 % yield with **8.4**).

^{1}**H NMR** (400 MHz, Chloroform-*d*$_1$) δ 5.50 (dtt, *J* = 15.3, 7.1, 1.3 Hz, 1H), 5.24 – 5.10 (m, 1H), 4.14 – 4.04 (m, 2H), 2.36 – 2.26 (m, 2H), 2.24 – 2.18 (m, 2H), 2.14 – 2.07 (m, 2H), 1.84 – 1.76 (m, 2H), 1.55 (tdd, *J* = 9.6, 8.5, 4.3, 2.4 Hz, 2H), 1.48 – 1.39 (m, 2H), 1.28 – 1.19 (m, 2H).

^{13}**C NMR** (101 MHz, CDCl$_3$) δ 173.92, 133.38, 127.22, 66.38, 35.35, 32.60, 29.67, 28.12, 25.16, 24.99, 21.10.

HRMS (EI+): [M]$^+$ C$_{11}$H$_{18}$O$_2$ Calculated – 182.1307, Found – 182.1308.

Synthesis of (*E*)-12-methyloxacyclododec-9-en-2-one (8.9)

In an N$_2$-filled glovebox, (*E*)-hex-4-en-2-yl (*E*)-dec-8-enoate (20.0 mg, 79.2 μmol) and 14.8 mL THF were added to a vial charged with a stir bar. A solution of catalyst (5.9 μmol) in 1 mL of THF was then added to this mixture. The vial was loosely capped, and the reaction was stirred at 35 °C for the reported amount of time. The vial was taken out

of the glovebox and quenched with 0.5 mL butyl vinyl ether. Solvents were removed *in vacuo*, and the product was purified with column chromatography on silica gel (1:49 Et$_2$O:pentane) to yield the product as a colorless oil (9.4 mg, 61% yield with **8.2**; 12.4 mg, 80% yield with **8.4**).

^{1}H NMR (400 MHz, Chloroform-d_1) δ 5.36 – 5.21 (m, 2H), 5.16 (dqd, J = 11.2, 6.3, 2.9 Hz, 1H), 2.37 (ddd, J = 14.1, 11.5, 4.0 Hz, 1H), 2.33 – 2.27 (m, 1H), 2.23 (ddd, J = 14.0, 5.5, 4.5 Hz, 1H), 2.20 – 2.06 (m, 2H), 2.03 – 1.91 (m, 1H), 1.88 – 1.75 (m, 1H), 1.57 – 1.46 (m, 3H), 1.46 – 1.32 (m, 2H), 1.24 (d, J = 6.3 Hz, 3H), 1.21 – 1.08 (m, 2H).

^{13}C NMR (101 MHz, CDCl$_3$) δ 173.58, 133.55, 127.16, 68.63, 41.09, 33.04, 30.34, 25.04, 24.74, 24.33, 23.27, 20.70.

HRMS (EI+): [M]$^+$ C$_{12}$H$_{20}$O$_2$ Calculated – 196.1463, Found – 196.1451.

Synthesis of (*E*)-oxacyclotridec-10-en-2-one (8.10)

In an N$_2$-filled glovebox, (*E*)-(*E*)-pent-3-en-1-yl undecen-9-enoate (22.6 mg, 89.7 μmol) and 17.0 mL THF were added to a vial charged with a stir bar. A solution of catalyst (6.7 μmol) in 1 mL of THF was then added to this mixture. The vial was loosely capped, and the reaction was stirred at 35 °C for the reported amount of time. The vial was taken out of the glovebox and quenched with 0.5 mL butyl vinyl ether. Solvents were removed *in vacuo*, and the product was purified with column chromatography on silica gel (1:49 Et$_2$O:pentane) to yield the product as a colorless oil (10.0 mg, 57% yield with **8.2**; 13.2 mg, 75% yield with **8.4**).

^{1}H NMR (400 MHz, Chloroform-d_1) δ 5.56 (dtt, J = 15.6, 7.1, 1.3 Hz, 1H), 5.34 (dtt, J = 15.1, 6.9, 1.3 Hz, 1H), 4.18 – 4.11 (m, 2H), 2.40 – 2.24 (m, 4H), 2.02 (dddd, J = 10.5,

5.9, 2.2, 1.1 Hz, 2H), 1.72 – 1.60 (m, 2H), 1.42 (dq, J = 5.7, 2.7 Hz, 2H), 1.38 – 1.23 (m, 6H).

13C NMR (101 MHz, CDCl$_3$) δ 174.24, 134.87, 126.58, 63.06, 34.08, 32.73, 32.14, 27.52, 27.51, 27.43, 27.09, 24.33.

HRMS (EI+): [M]$^+$ C$_{12}$H$_{20}$O$_2$ Calculated – 196.1463, Found – 196.1488.

Synthesis of (*E*)-oxacyclotetradec-11-en-2-one (8.6)

In an N$_2$-filled glovebox, (*E*)-(*E*)-pent-3-en-1-yl dodecen-10-enoate (20.8 mg, 78.1 μmol) and 14.6 mL THF were added to a vial charged with a stir bar. A solution of catalyst (5.8 μmol) in 1 mL of THF was then added to this mixture. The vial was loosely capped, and the reaction was stirred at 35 °C for the reported amount of time. The vial was taken out of the glovebox and quenched with 0.5 mL butyl vinyl ether. Solvents were removed *in vacuo*, and the product was purified with column chromatography on silica gel (1:49 Et$_2$O:pentane) to yield the product as a colorless oil (9.5 mg, 58% yield with **8.2**; 10.6 mg, 65% yield with **8.4**).

1H NMR (400 MHz, Chloroform-d_1) δ 5.55 – 5.27 (m, 2H), 4.16 – 4.07 (m, 2H), 2.41 – 2.31 (m, 4H), 2.05 – 1.95 (m, 2H), 1.65 – 1.53 (m, 2H), 1.45 – 1.17 (m, 10H).

13C NMR (101 MHz, CDCl$_3$) δ 174.22, 132.98, 127.93, 64.48, 35.25, 32.01, 31.42, 26.79, 26.29, 25.99, 25.77, 24.00, 23.92.

HRMS (EI+): [M]$^+$ C$_{13}$H$_{22}$O$_2$ Calculated – 210.1620, Found – 210.1592.

Synthesis of *(E)*-oxacyclotetradec-10-en-2-one (8.11)

In an N$_2$-filled glovebox, (*E*)-(*E*)-hex-4-en-1-yl undecen-9-enoate (24.4 mg, 91.6 μmol) and 17.3 mL THF were added to a vial charged with a stir bar. A solution of catalyst (6.9 μmol) in 1 mL of THF was then added to this mixture. The vial was loosely capped, and

the reaction was stirred at 35 °C for the reported amount of time. The vial was taken out of the glovebox and quenched with 0.5 mL butyl vinyl ether. Solvents were removed *in vacuo*, and the product was purified with column chromatography on silica gel (1:49 Et_2O:pentane) to yield the product as a colorless oil (11.5 mg, 60% yield with **8.2**; 12.9 mg, 67 % yield with **8.4**).

^{1}H NMR (400 MHz, Chloroform-d_1) δ 5.51 (dtt, *J* = 15.1, 7.0, 1.3 Hz, 1H), 5.37 (dtt, *J* = 15.2, 7.0, 1.3 Hz, 1H), 4.17 – 4.07 (m, 2H), 2.36 – 2.30 (m, 2H), 2.22 (dddd, *J* = 11.0, 5.8, 2.4, 1.2 Hz, 2H), 2.13 – 2.01 (m, 2H), 1.80 – 1.63 (m, 4H), 1.46 – 1.37 (m, 2H), 1.34 – 1.25 (m, 6H).

^{13}C NMR (101 MHz, $CDCl_3$) δ 174.41, 130.76, 130.54, 64.94, 33.14, 31.55, 31.05, 28.31, 27.19, 26.77, 26.66, 25.11, 24.22.

HRMS (EI+): [M]$^+$ $C_{13}H_{22}O_2$ Calculated – 210.1620, Found – 210.1614.

Synthesis of (*E*)-oxacyclopentadec-11-en-2-one (8.12)

In an N_2-filled glovebox, (*E*)-(*E*)-hex-4-en-1-yl dodecen-10-enoate (22.4 mg, 79.9 μmol) and 15.0 mL THF were added to a vial charged with a stir bar. A solution of catalyst (6.0 μmol) in 1 mL of THF was then added to this mixture. The vial was loosely capped, and the reaction was stirred at 35 °C for the reported amount of time. The vial was taken out of the glovebox and quenched with 0.5 mL butyl vinyl ether. Solvents were removed *in vacuo*, and the product was purified with column chromatography on silica gel (1:49 Et_2O:pentane) to yield the product as a colorless oil (11.3 mg, 63% yield with **8.2**; 12.5 mg, 70% yield with **8.4**).

¹H NMR (400 MHz, Chloroform-d_1) δ 5.51 – 5.32 (m, 2H), 4.18 – 4.09 (m, 2H), 2.38 – 2.29 (m, 2H), 2.25 – 2.15 (m, 2H), 2.08 – 1.99 (m, 2H), 1.81 – 1.73 (m, 2H), 1.67 – 1.58 (m, 2H), 1.39 – 1.22 (m, 10H).

¹³C NMR (101 MHz, CDCl₃) δ 174.49, 131.98, 129.88, 64.31, 35.02, 31.02, 30.33, 27.86, 27.57, 27.04, 26.83, 26.64, 25.04, 24.58.

HRMS (EI+): [M]⁺ $C_{14}H_{24}O_2$ Calculated – 224.1776, Found – 224.1791.

Synthesis of (*E*)-oxacyclohexadec-11-en-2-one (8.13)

In an N₂-filled glovebox, (*E*)-(*E*)-hept-5-en-1-yl dodecen-10-enoate (20.5 mg, 69.6 μmol) and 12.9 mL THF were added to a vial charged with a stir bar. A solution of catalyst (5.2 μmol) in 1 mL of THF was then added to this mixture. The vial was loosely capped, and the reaction was stirred at 35 °C for the reported amount of time. The vial was taken out of the glovebox and quenched with 0.5 mL butyl vinyl ether. Solvents were removed *in vacuo*, and the product was purified with column chromatography on silica gel (1:49 Et₂O:pentane) to yield the product as a colorless oil (11.0 mg, 66% yield with **8.2**; 11.6 mg, 70% yield with **8.4**).

¹H NMR (400 MHz, Chloroform-d_1) δ 5.37 – 5.23 (m, 2H), 4.12 (t, *J* = 7.2 Hz, 2H), 2.39 – 2.24 (m, 2H), 2.03 (dtd, *J* = 10.4, 5.8, 1.9 Hz, 4H), 1.70 – 1.55 (m, 4H), 1.42 – 1.21 (m, 12H).

¹³C NMR (101 MHz, CDCl₃) δ 174.09, 131.96, 130.47, 64.10, 34.91, 32.17, 32.13, 28.47, 28.42, 28.35, 28.15, 27.35, 26.69, 25.61, 25.31.

HRMS (EI+): [M]⁺ $C_{15}H_{26}O_2$ Calculated – 238.1933, Found – 238.1950.

Synthesis of (*E*)-oxacyclooctadec-11-en-2-one (8.14)

In an N_2-filled glovebox, (*E*)-(*E*)-non-7-en-1-yl dodecen-10-enoate (23.7 mg, 73.5 μmol) and 13.7 mL THF were added to a vial charged with a stir bar. A solution of catalyst (5.5 μmol) in 1 mL of THF was then added to this mixture. The vial was loosely capped, and the reaction was stirred at 35 °C for the reported amount of time. The vial was taken out of the glovebox and quenched with 0.5 mL butyl vinyl ether. Solvents were removed *in vacuo*, and the product was purified with column chromatography on silica gel (1:49 Et$_2$O:pentane) to yield the product as a colorless oil (12.5 mg, 64% yield with **8.2**; 12.3 mg, 63% yield with **8.4**).

^{1}H NMR (400 MHz, Chloroform-d_1) δ 5.43 – 5.20 (m, 2H), 4.11 (t, *J* = 5.9 Hz, 2H), 2.38 – 2.25 (m, 2H), 2.00 (p, *J* = 6.6 Hz, 4H), 1.71 – 1.56 (m, 4H), 1.47 – 1.15 (m, 16H).

^{13}C NMR (101 MHz, CDCl$_3$) δ 174.22, 130.95, 130.89, 63.85, 34.51, 31.96, 31.76, 29.32, 29.32, 28.87, 28.68, 28.46, 28.20, 27.39, 27.28, 25.65, 25.53.

HRMS (EI+): $[M]^+$ C$_{17}$H$_{30}$O$_2$ Calculated – 266.2246, Found – 266.2226.

GC Methods

HP-5 Agilent Column 30m × 0.25mm (ID) × 0.25μm film thickness; Injector temperature: 250 °C; Detector temperature: 350 °C; Oven temperature: Starting temperature: 50 °C, hold time: 1 min.; Ramp rate: 20 °C/min to 150 °C, hold time: 3 min., 10 °C/min to 210 °C hold time: 0 min., 35 °C/min to 300 °C, hold time: 3 min.; Carrier gas: He; Average velocity: 31 cm/s; Split ratio: 48.9:1

References

1. Grubbs, R. H., Wenzel, A. G., O'Leary, D. J., Khosravi, E., Eds. *Handbook of Metathesis*; Wiley−VCH: Weinheim, 2015.

2. (a) Michrowska, A.; Wawrzyniak, P.; Grela, K. *Eur. J. Org. Chem.* **2004**, 2053. (b) Rimkus, G. G. The Handbook of Environmental Chemistry; Springer: Berlin, 2004; Vol. 3X. (c) Rowe, D. J. Chemistry and Technology of Flavors and Fragrances; Blackwell: Oxford, U.K., 2005. (d) Gradillas, A.; Perez-Castells, J. *Angew. Chem., Int. Ed.* **2006**, *45*, 6086. (e) Ohloff, G.; Pickenhagen, W.; Kraft, P. Scent and Chemistry: The Molecular World of Odors; Verlag Helvetica Acta: Zürich, 2011. (f) Higman, C. S.; Lummiss, J. A. M.; Fogg, D. E. *Angew. Chem.*, *Int. Ed.* **2016**, *55*, 3552.

3. Marx, V. M.; Herbert, M. B.; Keitz, B. K.; Grubbs, R. H. *J. Am. Chem. Soc.* **2013**, 135, 94.

4. Yu, M.; Wang, C.; Kyle, A. F.; Jakubec, P.; Dixon, D. J.; Schrock, R. R.; Hoveyda, A. H. *Nature* **2011**, 479, 88.

5. Koh, M. J.; Khan, R. K. M.; Torker, S.; Yu, M.; Mikus, M. S.; Hoveyda, A. H. *Nature* **2015**, *517*, 181.

6. (a) Johns, A. M.; Ahmed, T. S.; Jackson, B. W.; Grubbs, R. H.; Pederson, R. L. *Org. Lett.* **2016**, *18*, 772. (b) Montgomery, T. P.; Ahmed, T. S.; Grubbs, R. H. *Angew. Chem. Int. Ed.* **2017**, *56*, 11024.

7. Nguyen, T. T.; Koh, M. J., Shen, X.; Romiti, F.; Shrock, R. R.; Hoveyda, A. H.; *Science* **2016**, *352,* 569.

8. Ahmed, T. S.; Grubbs, R. H. *J. Am. Chem. Soc.* **2017**, *139*, 1532.

9. Shen, X.; Nguyen, T. T; Koh, M. J.; Xu, D.; Speed, A. W. H.; Schrock, R. R.; Hoveyda, A. H. *Nature* **2017**, *541*, 380.

10. Ahmed, T. S.; Grubbs, R. H. *Angew. Chem. Int. Ed.* **2017**, *56*, 11213.

11. Xu, C.; Shen, X.; Hoveyda, A. H.; *J. Am. Chem. Soc.* **2017**, *139*, 10919.

12. Radkowski, K.; Sundararaju, B.; Fürstner, A. *Angew. Chem. Int. Ed.* **2013**, *52*, 355.

13. High catalyst loadings are often used in macrocyclization reactions because of the dilute conditions necessary for preventing oligomerization. For examples see ref. 3, 4, and 9.

14. This result was in agreement with previous studies showing that cross metathesis between *E*-olefins and terminal olefins using these catalysts is challenging (ref. 6 and 8)

15. Patel, H. H.; Sigman, M. S. *J. Am. Chem. Soc.* **2015**, *137*, 3462.

16. Denmark, S. E.; Forbes, D. C.; Hays, D. S.; DePue, J. S.; Wilde, R. G. *J. Org. Chem.* **1996**, 60, 1391.

17. Hotling, S.; Haberlag, B.; Tamm, M.; Collatz, J.; Mack, P.; Steidle, J. L. M.; Vences, M.; Schulz, S. *Chem. Eur. J.* **2014**, *20*, 3183.

18. De Medeiros, E. F.; Herbert, J. M.; Taylorw, R. J. K. *Tetrahedron Letters*. **1990**, *31*, 5843.

19. Robinson, J. A.; Flohr, H.; Kempe, U. M.; Panhorst, W.; Rétey, J. *Liebigs Annalen der Chemie*, **1983**, *2*, 181.

20. Cryle, M. J.; Hayes, P. Y.; De Voss, J. J. *Chem. Eur. J.* **2012**, *18*, 15994.